CARL VON OSSIETZKY universität OLDENBURG

Fakultät II - Informatik, Wirtschafts- und Rechtswissenschaften
Department für Informatik

Driver Modeling and Simulation of Lane Change Situations

Influence of Different Rear View Mirror Types on Gap Acceptance Behavior

Dissertation zur Erlangung des Grades eines
Doktors der Naturwissenschaften
(Dr. rer. nat.)

genehmigte Dissertation

von **Dipl. Inform. Lars Weber**

Gutachter:
Prof. Dr. Claus Möbus
Prof. Dr. Martin Fränzle

Tag der Disputation: 29.08.2017

Acknowledgements

At the very beginning of this thesis, I would like to thank everybody who helped me throughout the three and a half years to successfully finish this work. First and foremost I would like express my gratitude to my supervisors Prof. Dr. Claus Möbus and Prof. Dr. Martin Fränzle for their guidance and helpful advice. I also received valuable feedback during my defense and want to thank the additional members of the committee Prof. Dr. Susanne Boll and Dr. Sebastian Gerwinn.

A special thanks goes to Andreas Lüdtke: he already supervised my diploma thesis and offered me a position as a research staff in his group *Human Centered Design* at the OFFIS e.V. research institute in Oldenburg. After I worked already in two research projects he motivated me to write a doctoral thesis. Without his continuous support in many different ways I would not have finished this work.

I would also like to thank a number of further colleagues namely Jan-Patrick Osterloh, Sebastian Feuerstack, Bertram Wortelen and Florian Fortmann for the proofreading and the helpful advice to structure the text. I am also very thankful to my colleague Fei Yan, helping me out with regard to the discussions about the empirical studies in the driving simulator. I also want to thank Martin Baumann, who now is a professor for human factors at the university in Ulm. Although he was not directly involved in this thesis, we have been working together in different projects and I really enjoyed the interdisciplinary work with him.

Contents

1 Introduction

January 20th, 2013: two cars collided near Günzburg in southern Germany on the three-lane autobahn A8. A 35-year-old driver changed lane from the middle to the left and collided with a much faster car from behind. The damage was about 20K Euro. March 4th, 2013: on the A3 near Lohmar-Nord the driver of a car in the middle lane was overtaking a platoon of trucks. Suddenly one of the trucks changed to the middle lane, the car driver did not have enough time to react appropriately, resulting in a rear-end collision with the truck. The truck driver did not even recognize the crash and was stopped by the police about 50 km away near Solingen. October 20th, 2013: a 43-year-old motorcyclist was driving on the left lane of the A43 near Warendorf and crashed into a car that changed lane to the left. He did not have any chance to avoid the collision and died at the scene of accident.

The list of similar accidents is long and according to the German In-Depth Accident Study (GIDAS) seven percent of all autobahn accidents in 2003 fell into the category of overtaking maneuvers on the German autobahn. Compared to the timespan of 1985-1999 (five percent), this was an increase of two percent across all reported accidents. According to the reports of the "Statistische Bundesamt", most recent data for 2015 shows a reduction to 5.06%: 20113 accidents were counted on the Autobahn, and 2717 were classified as accidents with another vehicle that drives into the same direction on an adjacent lane: "Zusammenstoss mit einem anderen Fahrzeug, das seitlich in gleicher Richtung fährt" [DESTATIS2015, p. 73]. 4250 passengers were injured in these accidents and 23 people died.

But the Autobahn is not the only road category where these accidents happen. The same type of accidents happened on all other road types, too: "Bundesstrasse" (3164 accidents) "Landstrasse" (2456), "Kreisstrasse" (1040) and other roads (6074) [DESTATIS2015, p. 74-77].

In summary, 305659 traffic accidents were counted on all roads in Germany in 2015, and 15451 (5.055%) lead to collisions with vehicles that drove sideways into the same direction [DESTATIS2015, p. 72]).

The reasons for accidents during lane change maneuvers are diverse and some are mentioned in the examples above. In some situations drivers do not recognize an approaching vehicle from behind. This can be related to the blind-spot problem, if the approaching vehicle is already very close and no longer visible through the side mirror view. Further reasons are the underestimation of the speed difference or the overestimation of the available gap size. Common to all these problems is, that they are related to the use of exterior side mirrors.

The first available exterior driver side mirrors had a flat mirror surface (planar mirror) and a rather limited "field of view". According to [Bach2006] the *horizontal* field of view for this mirror category lays between 13-16 degree. As a consequence, they have a comparably large blind-spot region, which was the main reason for the development of other mirror types. The surface of the convex or spheric mirror has a constant curvature across the whole mirror surface.

This increases the horizontal field of view up to about 24 degrees already and reduces the size of the blind spot region. The third mirror type is the aspheric mirror which consist of two parts: from the inside to the outside, the first three quarter have a convex curvature, but for the outer / aspheric mirror part the horizontal curvature increases. This bipartite construction leads to an overall horizontal field of view of up to 37 degree.

The enlargement of the horizontal field of view reduces the blind-spot region, but there are also drawbacks associated with such curved mirror surfaces. One important property of a planar mirror is *unit magnification*: when directly looking towards an object at a given eye-object distance, its projection onto the retina has a certain size determined by the laws of optics. When viewing the same object through a planar mirror at the same distance (but now eye-mirror-object) the projected image is of the same size without any distortion. This unit magnification does no longer hold for spheric and aspheric mirrors which instead introduce an *image minification*, where the image of an object that is reflected by the mirror onto the retina is smaller. Unit magnification and image minification are the main reasons, why different countries have different regulations, which mirror types are allowed. According to the US regulations (Code of Federal Regulations (§571.111) a planar mirror with unit magnification is required on the driver side, while the European directive 2003/97/EC [EC2003] explicitly allows all three types of mirrors.

Research studies revealed that changes to the field of view can lead to problems for with regard to the estimation of distances and motion. [Caird1992] and [Groeger1988] conducted studies where participants had to observe approaching vehicles, and they reported that the underestimation of the time-to-contact increases significantly, if the field of view is decreased[1]. [Carstengerdes2005] conducted a series of field studies, where participants had to estimate distances as well as the time-to-contact. Three mirror types were tested: planar, spheric and aspheric. He found a dependency between strength of underestimation and the field of view of the mirrors: planar mirrors lead to relatively strong amount of underestimation of distances and the time-to-collision, while curved mirrors with a larger field of view in general lead to a smaller amount of underestimation.

Considering the lane change scenario the stronger underestimation of distances and the time to collision with the planar mirror is beneficial, because if a gap a is judged smaller or the time-to-collision is underestimated, it is less likely that a lane change is done. It seems plausible that the reduction of this underestimation (when curved mirrors are used) could result in acceptance of smaller gaps during a lane change. The published literature on this topic is split, some empirical evidence supports this hypothesis, but also rejecting findings were published.

Instead of using a curved mirrors to reduce the blind-spot region, [Platzer1995] proposed a *Blind Zone and Glare Elimination* (BGE) setting for planar mirrors, which reduces the blind spot to a minimum by adjusting the mirror towards the outside. With this setting the own vehicle is no longer visible from the drivers' normal seat / head position. Platzer admitted that „*When driving with the BGE setting, most drivers initially feel a sense of confusion with the outside mirrors. You are not sure where they are pointed.*“ Such an alternative mirror adjustment reduces the blind-spot region, but [Meyer2013] reported a significant impact of different mirror

[1] In the automotive domain time-to-collision is more often used than time-to-contact. Both have the same meaning and specify the amount of time until two objects collide, if the current direction of movement and the speed difference between the objects remains unchanged.

adjustments on the accuracy of distance estimations, especially if the visible portion of the own vehicle in the mirror is reduced to a minimum. Therefore, it is questionable if the BGE setting is advisable.

Summarizing the different aspects of mirror usage, there seems to be a trade-off between the reduction of the blind-spot region with the help of curved mirrors, or alternative mirror adjustments, and potential negative influences with regard to the estimation of distances and the time-to-collision.

Besides adjusting or changing the mirrors, modern technology offers another possibility to address the blind spot issue. Blind-spot detection systems are nowadays offered by most automobile manufacturers. Most of these systems use a visual warning (one or multiple color LED's), which is integrated into case of the side mirror. As soon as a vehicle is sensed within the blind-spot region, this is signaled to the driver. According to ISO 17387 about *lane change decision aid systems* (LCDAS), those blind-spot systems are classified as *Type I systems*. Systems which are developed according to higher specification levels (Type II and III) need to have the capability to detect vehicles within larger distances (time-to-collision up to 3 seconds). Nevertheless, also these higher level systems are still warning systems and they do not have sophisticated lane change assistance functionality. This likely changes in the future, because automated driving is probably the hottest topic in the automotive domain and considerable advancements in sensor technology and automated driving functions have already been made.

Regardless of the type of system, as long as the driver is in charge, it has to be investigated how such systems impact the overall behavior of the driver: if additional information about adjacent gaps towards approaching rear vehicles is presented, how does the driver integrate these information into his common lane change routine? Besides the intended functionality, does the system introduce any negative side-effects? It seems obvious that the decision making of the driver has to be understood in more detail. Consequently, if different mirror configurations (mirror type and adjustment) are critical for the perception and assessment of the traffic situation, this should also be considered during the development of such assistance systems.

There are a lot of different ways to consider human behavior during system development for example by involving potential end users during requirements engineering, by the integration of expert knowledge during system design, or later on during empirical evaluation in driving simulators and in real test vehicles. Involving human expertise at different stages of the development is important, and a systematic approach is necessary, for example the user-centered design method according to ISO 9241-210. A domain specific guideline for driver assistance system development is the *Code of Practice for Design and Evaluation of ADAS*[2] [CoP2006] (short CoP), which describes a wide spectrum of human-factors design analysis questions. These are categorized into 18 different issues, like for example perception, behavioral change, learning, safety / risk, workload or controllability.

The involvement of test drivers during the development of such systems is an important part of todays assistance system development. Empirical studies on test tracks, or in driving simulators can already be considered a standard approach to assess how well drivers interact with the functionality of a newly developed system, and how comfortably they feel when using the system. Unfortunately, the systematic testing of different system configurations, within a

[2] Advanced Driver Assistance Systems

number of different traffic situations very quickly leads to a huge number of test conditions. Therefore, such empirical tests are very time consuming. Additionally, such tests often require a fully functional prototype of the system, including a physical human-machine interaction interface. This limits the approach to later development and evaluation phases of the system, when such prototypes are already developed.

During earlier development phases, computer simulations offer a valuable alternative (pure software simulations, but also software-hardware co-simulations). Software models of the system under development can be integrated into vehicle dynamic simulations, and such vehicle models can be part of larger traffic simulation environments as well. If the objective is to evaluate *human-machine interaction* with the help of such a simulation platforms, a *human driver behavior model* is a necessary part of such a simulation-based approach. One requirement for such models is, that they are at least partially able to simulate the variability of human behavior. This allows to test the system under development with a wider range of potential driver behavior. Such behavior models should also implement limitations of human drivers which are relevant for the test scenarios, for example the mean or minimum reaction times or limitations of the visual field of view. With regard to the lane change scenario, it is of interest how drivers perceive and estimate distance gaps and speed differences and which gaps do they accept or reject.

Before the objectives for this work are outlined, a short summary of the previous argumentation is given: the number of accidents during lane change maneuvers remains at a relatively constant level between 5-7% within the last 20 years. Several safety relevant issues related to mirrors were mentioned above: the blind-spot problem, the image minification, and an appropriate mirror adjustment. Although curved mirrors reduce the size of the blind-spot region, research has also shown that these mirrors change the perception of approaching vehicles and it is questionable, if drivers are aware of effects like image minification. Upcoming lane change decision aid systems can support the driver during lane change maneuvers, but their impact on the overall driving behavior has to be assessed early during system design. Testing of early system prototypes can be done with the help of pure software simulation platforms, and driver behavior models are necessary, if the human-machine interaction needs to be investigated. If the system interacts with the driver on a decision making level (like lane changing), human behavior models need the ability to simulate such maneuver decisions similar to human drivers, and they should also be able to reproduce the individual behavior differences of human drivers.

Objectives and Research Approach Based on the previous argumentation, there is a need to develop individual driver behavior models, which can simulate the behavior of drivers especially for maneuvers that are prone to accidents. This work targets the overtaking scenario with a focus on the German Autobahn. More specifically, the work investigates the driver behavior with regard to the observation of the rearward traffic on the target lane using the left exterior side mirror, and the drivers' decision making whether a lane change can be done in the current situation. This behavior will be called "gap acceptance" in the following.

Objective 1: "This work will investigate the impact of different types of rear view mirrors (driver-side only) with regard to their influence on the driver's gap acceptance behavior.

The scenario of interest is the lane change left maneuver on a two-lane freeway (German Autobahn).“

Objective 2: “A behavior simulation model will be developed which is able to simulate the findings with regard to Objective 1. A previously developed and published gap acceptance model [Weber2013] will be reviewed, and if necessary, modifications will be implemented.“

To achieve the objectives, the work was split into several consecutive steps.

Literature Review The first step of the approach is a detailed literature review to motivate and justify the development of such a gap acceptance model. As a short summary, the following topics will be tackled by chapter 2:

1. The first section describes some technical background information about different types of rear view mirrors (section 2.1).

2. A review about existing driver models was done to identify what types of models already exist. It is investigated, whether and how these models simulate gap acceptance and also how the “look into the mirror“ is realized by these models. This part of the literature review will allow to classify the here developed model within the state of the art and clearly distinguish it from already existing models. Three different categories of models are reviewed: manual vehicle control models (section 2.2.1), traffic flow models (section 2.2.2) and cognitive driver models (section 2.2.3).

3. Psychophysical findings related to questions like “How do humans perceive size, distance and the time-to-collision between themselves and other objects?“ are presented in section 2.3.1 and 2.3.2

4. The last section 2.3.3 summarizes empirical studies which are directly concerned with the use of different types of rear view mirrors and questions like: “How do different mirror types impact the perception of distance, size, or the time-to-collision[3]?“ or “Does the mirror type impact the gap acceptance behavior?“

Simulation of Different Rear View Mirrors Types The literature review showed, that the published results do not provide a sufficient database to develop and parameterize a behavior simulation model for the gap acceptance task. Three alternative solutions were considered to gather additional empirical data: 1) field studies with real cars, which are equipped with different types of rear view mirror types. 2) driving simulator studies using real mirrors and 3) driving simulator studies using simulated rear view mirrors.

The realization of field studies with real cars was not possible with the available resources and infrastructure. Using the driving simulator of the C.v.O. University Oldenburg remained the preferred option, but again, due to the available resources, a simulation with real mirrors (solution 2) was not possible. Consequently, solution 3) was selected, but before the empirical

[3]time-to-collision (ttc), time in seconds until two vehicles collide if the current speed difference between them remains constant.

studies could be done, it was necessary to develop a software simulation for the different types of rear view mirrors and their specific characteristics. The invested efforts for the implementation and validation of the mirror simulation are explained in section 3.3.

Empirical Investigations After the mirror simulation was implemented in the driving simulator, this setup was used for two empirical studies which are described in chapter 4. Each of the studies had an effort of 45 hours of effective data recording. *Experiment 1* (see section 4.1) was necessary to validate the implemented mirror simulation in the driving simulator, because it was not known whether the simulation would be able to reproduce the published findings of the corresponding real mirror types. For this purpose, a distance estimation field study was replicated, which was previously conducted by [Carstengerdes2005] using real mirrors. Other researchers used similar setups, but the one of Carstengerdes was used as a reference. The success of this validation study was critical, before the *Experiment 2* could be conducted (section 4.2). The objective of this study was to investigate the impact of the different mirror types on the gap acceptance behavior of drivers. The results of the study are compared against already published literature findings and they also served as a database for the development of the gap acceptance model.

Developing the Gap Acceptance Model Chapter 5 describes the different steps of model development. As mentioned under Objective 2, a gap acceptance model for similar situations was developed previously in [Weber2013], but it has to be considered a rather simple one, and its empirical foundation is also quite limited. A brief description of this model is presented in the first section of the modeling chapter 5.2 and it served as a motivation to develop an improved gap acceptance model in this thesis based on the results of Experiment 2.

Section (5.3) of the modeling chapter contrasts two different categories of potential model variables. Measures like distance in meter, speed in m/s, acceleration in m/s^2 but also derived measures like the time-to-collision have been utilized a lot in the domain of driver modeling. Besides these measures, there is an alternative solution: from the drivers perspective, all objects within the field of view of his visual perception project an image onto the retinas of his eyes. The size of the projected images can be approximated using “visual angles“, a concept widely used in visual perception research for many years, and it will be introduced in detail in the literature review. Besides the size of objects, motion in certain directions can be described by the rate of change of angles (in terms of an angular velocity). Using the concept of visual angles for driver modeling is also not new, they were considered previously, for example by [Lee1976, Anderson2009]). But these models were developed for different driving scenarios, e.g. stopping in front of a traffic light / sign or behind a lead vehicle, or driving in a car-following situation. This work will investigate the use of angular measures within the context of the gap acceptance task. The decision, which of the two variable categories is used, is based on the results of the Experiment 2.

In 3D computer simulations, the relation between these two categories of variables is realized within graphic libraries like OpenGL or DirectX. Objects of the 3D world of such simulations are typically developed in a Cartesian world coordinate representation and a perspective projection transforms them into view coordinates, a representation from the viewpoint of the observer.

This perspective projection is also known as “camera analogy“. To differentiate the two different categories of variables, the terms *angular measures* and *metric measures* will be used[4].

The Experiment 2 chapter discusses the results based on the accumulated data across all subjects and the focus is put on the experiment hypotheses. Section 5.4 instead presents a more detailed view on the individual behavior data. It is expected that drivers approach the lane change situation in a variety of ways: some accept smaller gaps on average, while others are more defensive and reject significantly more gaps. This behavior is “hidden“ within the accumulated data, but as [Gray2005] point out, such individual behavior should be considered for the development of driver models. Considering individual behavior is also of practical interest, too: in recent years, the development of driver assistance systems heads into the direction of personalization and adaptation of systems. Therefore, if a driver model should be used as virtual test driver, it should be able to simulate at least parts of these individual behavior differences. Consequently, it was decided that “individual behavior models“ should be developed, which capture the differences of the observed gap acceptance behavior of the 14 subjects.

Section 5.5 presents how the basic concepts for the model were derived from the data of Experiment 2. The implementation of the model is described afterwards in detail in section 5.6. This comprises 1) how the model (visually) perceives the traffic situation, 2) how the model decides whether a gap is accepted or rejected, 3) how the interaction of the model with the driving simulator environment is realized, and specifically how the model interacts within the Experiment 2 scenario. Before the model can be used to simulate the behavior of each subject, the parameter were estimated from the data of Experiment 2. Afterwards the experiment was simulated multiple times. The results of the model runs are presented in section 5.7 and it is discussed, how well the model reproduces the behavior with regard to 1) the hypotheses of Experiment 2, and 2) how well the model can reproduce the behavior of each subject that participated in the experiment.

The final chapter of this thesis sums up the results that were achieved with regard to 1) the technical realization to simulate different mirror types, 2) the results of the two empirical driving simulator studies, and 3) the behavior modeling and simulation of the gap acceptance situations that were investigated in Experiment 2.

[4]While the term angular measures is rather intuitive, the search for an appropriate name for the other variable category led to different ideas, but none was really convincing, like “third-person“ variables contrasting the first-person term, but also Cartesian coordinate variables and a few others were considered. In the context of this work, these measures are all based on the metric length measure, which was the reason to call them metric measures here.

2 Literature Review

As mentioned in the introduction, the literature chapter is divided into a number of subsections. Section 2.1) gives a brief introduction about different mirror types. The main reference for the specification of "devices for indirect vision" is the European Directive 2003-EC-97 [EC2003].

The following second part 2.2 introduces to the domain of driver modeling and summarizes models according to three different categories: manual vehicle control models, microscopic traffic flow models and cognitive driver models. As stated in the objective for this thesis, this part is necessary to analyze what kind of driver models already exist, and how well the topics gap acceptance and lane changing, the *look into the mirror* and the impact of different mirror types on gap acceptance are already covered. This review serves as a motivation and justification for the model development.

The last part of the literature review is dedicated to empirical research which deals with the perception of size, distance (section 2.3.1). Afterwards, section 2.3.2 reviews research with regard to the time-to-collision. The last section focuses specifically on mirror related topics in the automotive domain (section 2.3.3). Here, researchers investigated, how different types of exterior mirrors impact the perception of size or distance, as well as dynamic measures like speed or the time-to-collision.

2.1 Rear View Mirrors: Devices for Indirect Vision

The aim of European Directive 2003/97/EC: „*is to harmonise rules relating to the type-approval of devices for indirect vision and of vehicles equipped with these devices.*" [EC2003, p. 3, Article 1]. The term devices tackles a broader scope, not only conventional mirrors: „*'Devices for indirect vision' means devices to observe the traffic area adjacent to the vehicle which cannot be observed by direct vision. These can be conventional mirrors, camera-monitors or other devices able to present information about the indirect field of vision to the driver.*" [EC2003, p. 8, §1.1]. The directive is effective for the following vehicle classes according to the *Consolidated Resolution on the Construction of Vehicles(R.E.3)* [UnitedNations2011]:

M1: passenger car $<= 9$ seats total (including driver).

M2: passenger car > 9 seats total and mass $<= 5$ tonnes.

M3: passenger car > 9 seats total and mass > 5 tonnes.

N1: cargo vehicle $<= 3.5$ tonnes.

N2: cargo vehicle $<= 12$ tonnes.

N3: cargo vehicle > 12 tonnes.

For these six vehicle classes, the directive defines six classes of mirrors [EC2003]. Following is a summary, which lists the mandatory mirrors:

Class I Interior rear-view mirror: mandatory for vehicle class M1, optionally mounted by the manufacturer on any other vehicle class. Typically not used in vehicles that have obstructed rear vision (M2, M3 and N1-N3).

Class II and III Main exterior rear-view mirror: mandatory for new vehicles: either a large sized class II (M2,3 and N2,3) or a small sized class III (M1, N1). The mirrors vary in the dimensioning of the field of view.

Class IV Wide angle exterior mirror: offers a larger field of vision compared to Class II and III. Mandatory for truck classes N2 and N3 if Class V mirror is also mandatory. This depends on country specific regulations.

Class V Close proximity exterior mirror: mandatory for N2, N3 only, used to observe the near side space left and right, optional for all other vehicle classes.

Class VI Front mirror: mandatory for trucks N2 and N3 >7.5 tonnes of mass, used to view the area in front of the driver cabin. Due to their high seat position, truck drivers have problems to see the gap in front of them, especially towards smaller passenger cars. The mirror type is also known as *cyclops* mirror.

For each mirror class, a specification is given, which includes (minimum) dimensions and shape of the mirror, as well as visual characteristics like the reflectivity of the surface and the visible field of view. Of special interest is the mirror surface requirement which „*must be either flat or spherically convex. Exterior mirrors may be equipped with an additional aspherical part [...].*“ [EC2003, p. 25, §3.1]

A spherical surface is defined as „*surface which has a constant and equal radius in all directions.*“ [EC2003, p. 8, §1.1.1.7]

Aspherical mirrors are defined as a composition „*of a spherical and an aspherical part, in which the transition of the reflecting surface from the spherical to the aspherical part has to be marked.*“ [EC2003, p. 8, §1.1.1.9] A simplified, schematic top view of the three mirror surfaces can be seen in Figure 2.1, visualizing the differences in the horizontal curvature.

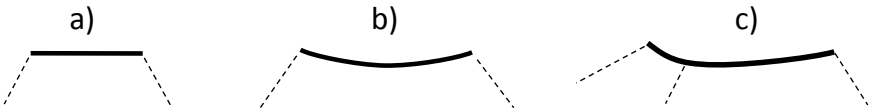

Figure 2.1: Schematic top view on three different mirror surfaces; a) flat mirror; b) spherical mirror; c) aspherical mirror with spherical part (right) and aspherical surface part(left)

When vehicles were first equipped with mirrors, their surfaces were flat. The characteristic property of flat mirrors is that the image of an object is reflected with its true size, and it it is not distorted in any direction. This is no longer fulfilled, if the mirror surface is curved, which leads to a *minification* effect: with increasing curvature (which is equivalent to a smaller radius of curvature) the projected image size on the retina gets smaller.

With regard to the amount of curvature which is allowed, the directive gives restrictions for a minimum radius (or maximum curvature) [EC2003]: for class I-III the minimum is 1200mm, for class IV it is 300mm and for class VI it is 200mm.

Review studies ([Bach2006,NHTSA2008]) show that spherical, as well as aspherical mirrors are used with 1400 and 2000mm radius for the spherical part. These mirror types are named C14, C20 (spherical) and A14, A20 (aspherical). The dimensioning of a mirror (width, height) has to fulfill the requirement that a minimum rectangular area must be enclosed, e.g. for the exterior driver side mirror this is 40 mm height, while the width is calculated according to $\frac{130}{1+\frac{1000}{r}}$. For a curvature r of 1400 and 2000 mm the minimum rectangular widths are 75.8 mm or 86.66 mm. Additionally, at one point the mirror must be at least 70 mm high.

Additionally to the dimension requirements, there is a requirement on the minimum field of view as seen in Figure 2.2. The field of view of different mirror types will be an important parameter for the simulation of different mirror types, which was developed in this thesis (chapter 3).

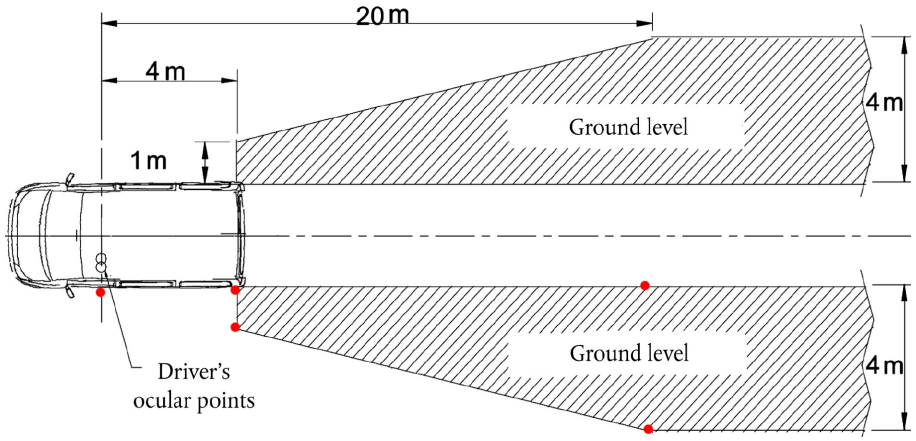

Figure 2.2: Figure taken from ([EC2003], Figure 8, p.42) Minimum field of view for the exterior mirrors class III for a passenger car (class M1)

Nowadays, most vehicle manufacturers (in Europe) offer spheric and aspheric driver side mirrors, at least as optional equipment. Passenger side mirrors are often spherically shaped. As reported before, at least two curvatures are used (1400 and 2000). Curved mirror surfaces are also allowed for the interior mirror, which makes the possible mix of different mirror types on a single car more complex. There is also no restriction on combining differently curved mirrors, which might lead to the situation that the driver has to deal with different optical impressions (and strength of minification) for each of the three mirrors (driver / passenger side and interior mirror). Statistic numbers about the distribution of mirrors are rare. One study was found only: [Bach2006] reported that in 2004 for the *city of Trier* 28.4% of the vehicles still had planar driver side mirrors, 22.1% were spherical mirrors and 49.5 had an aspherical driver side mirror.

Although the focus in this thesis is on passenger cars, the situation with regard to the number of mirrors is more complex for truck drivers: they do not only have one main exterior mirror on each side, but also additional wide angle mirrors. It would be interesting to investigate

which mirror truck drivers typically rely on in which driving situation. Do they use the main exterior mirrors for distance estimations and gap acceptance and are the wide mirrors used only to observe the blind-spot region? This question is out of scope of this work, but it would be interesting to find out which strategies are used.

It is concluded, that three basically different mirror types exist (planar, spheric / convex and aspheric) and for the curved mirror types at least two curvatures are manufactured. The main objective of this work is whether the different mirror types impact the gap acceptance behavior, but it is also of interest, what drivers really know about differences with regard to the mirrors.

2.2 Driver Models

The development of driver models began in the middle of the last century and first models were based on control-theory and they tackled *manual vehicle control*. These models try to emulate human steering behavior on straight and curvy roads (lateral control), as well as the speed selection (longitudinal control), which is appropriate for the current road curvature and road surface conditions. Because this work will not directly contribute to this model category, the first subsection 2.2.1 will give a short review only.

About twenty years ago, cognitive architectures were used for the first time as modeling framework for driver behavior. Vehicle control models were integrated into behaviorally more complex *cognitive driver models*, which incorporated more detailed models about human perception, goal-oriented behavior, multitasking, decision making and attention distribution. A review on cognitive driver models is given in section 2.2.3.

While the previous two model classes emphasize modeling the behavior of a single driver controlling his vehicle, *microscopic behavior models within traffic flow simulations* are concerned with multiple vehicles, multiple drivers and a broader traffic perspective. Although this is not the primary interest of this work, these models implement different types of driving maneuvers, e.g. overtaking and lane changing, which is of interest for this work. A brief view on some of these models is given in section 2.2.2.

2.2.1 Manual Vehicle Control

The first models for manual vehicle control were based on control theory, a mathematical approach to model dynamic systems, mostly based on linear, as well as non-linear differential equations. A short summary is given in the first subsection 2.2.1.1. Apart from this control-theory approach, manual vehicle control models were developed using fuzzy control, artificial neuronal network implementations and Bayesian programming. Some of these models are briefly reviewed in the second subsection 2.2.1.2.

2.2.1.1 Control Theoretic Models

In a comprehensive review report, McRuer and Krendel [McRuer1957] summed up previous research about manual control of machines since WWII. Based on their review, they proposed

the "quasi-linear human operator model"[1]. The model received its name, because observed operator behavior is split into two parts: a linear transfer function[2] and the "remnant" term which accounts for the non-linear parts of the observed operator response behavior.

Quasi-linearization of non-linear systems into separate linear and non-linear components goes back to the describing function method of Krylov and Bogoliubov published in 1930 [Krylov1930]. Previous practical experience with modeling of response functions of technical systems supported the idea that many non-linear system responses can be described / approximated well by equivalent linear system, at least for a certain range of the input values. In contrast to purely linear systems, which follow the superposition principle (changes to the forcing function lead to proportional changes at the output), non-linear systems can heavily react to small input changes which might lead to instabilities.

Adjustable parameters of the quasi-linear human operator model can be used to adjust the output behavior according to different human performance characteristics: lead delay times for example emulate processing delay of human senses, while lag delays can be used to simulate motor response time. The gain of a control circuit can be used to model subjective sensitivity to input values.

Although there are a number of parameters which can be used to adjust the model, McRuer and Krendel pointed out that their quasi-linear model should not be considered an explanatory psychological theory how the human mind "generates" behavior. Instead, the model gives an abstract, mathematical formulation which can reproduce observed human behavior.

The motivation to use such a system-theoretic approach originated from aircraft system design. Whenever a new flight system is developed, controllability needs to be investigated very carefully. A deeper understanding of the pilot - aircraft interaction, especially the pilot response characteristic, is necessary to build a flight system that can be easily handled by the pilot and supports him controlling the aircraft. During previous years, large amounts of pilot experience about system controllability were written down into catalogs. These experiences were a valuable source of information for designers, but they are descriptive, and subjective to a certain degree. McRuer and colleagues recognized that a mathematical model, which is able to capture the control behavior of the pilots could be very useful. Its use would even be higher, if it would be built from a database of observed real-time flight behavior. Such a model could be integrated within a more complex system-theoretic approach to analyze the overall dynamics of operator-machine interaction.

It was already known at that time that the quasi-linear model could not account for some important characteristics of human behavior. Mayne investigated motor responses, where persons had „*to follow with a pencil a line drawn on the paper of a standard recording instrument. The paper was driven at fixed speed and the position of the line [...] could be viewed through a narrow, transverse slot*" ([Mayne1951], p.207). Responses to discrete step changes of the line were always delayed by about 250 milliseconds and the drawn response was shaped similar to a steep sigmoid function.

Such behavior is easily reproducible by a linear approach, but if subjects had to follow a continuous sinus curve at a slow frequency of 1 Hz, the response was only initially delayed.

[1] Copies of the original report were not available for this thesis, but a later publication [McRuer1965] gives a very good overview about their early model development.

[2] system-theory term: describes the relation between system input and output by a linear differential equation

Subjects were able to compensate the initial delay within a short amount of time and adapted their initial response characteristics. Not only did they compensate delay times, they also used preview information (anticipatory control). Additionally, another important aspect of human performance is learning and the ability to recall complex response patterns.

Such adaptive behavior is not achievable by a linear closed-loop control function. Finally, most of the individual behavior variability remains inside the remnant term in form of noise. Because this first approach had a number of flaws, another control-theoretic model known as "McRuer's Law" or the *crossover model* was proposed which focused more on these adaptive capabilities. In contrast to the quasi linear model, the human operator and the system under investigation are both modeled together in this approach. [McRuer1967].

These different types of human performance models were first applied to model tracking tasks, like those of gun turret operators and manual control skills of aircraft pilots [McRuer1967]. Later on, McRuer and Weir transferred their approach of a *Theory of Manual Vehicular Control* to the domain of driver modeling [McRuer1969]. One of their main challenges was the identification of the perceived information that drivers use, which obviously is a lot different from the information that is used by aircraft pilots. During instrumented flight pilots must rely on the information presented by the machine, which has the advantage that it is well known, which kind of information is available to the pilot. On the other hand, the driver has to scan the surrounding traffic environment by himself to perceive the appropriate information.

McRuer and Weir were well aware of the fact that „*in driving the full visual field is available [...] this very diversity makes the definition of the cues used by the driver very difficult.*" ([McRuer1969], p.278). To systematically investigate this problem, they proposed to start with the synthesis of different control algorithms which are plausible candidates. Each of these candidate algorithms also demands specific input variables. Human driver behavior from specifically designed experiments should be gathered and used for each of the candidate algorithms. Their idea was to successively rule out the inappropriate control algorithms and come up with the best possible solution, which then also gives hints to the necessary input variables. Nevertheless, in a later publication, McRuer et al. said: „*Note that this driver response structure in no way implies the direct perception of either lateral position or heading angle as such, but only that the driver's output is, in part, some function of these variables.*" [McRuer1977, p. 383]

At the same time, when McRuer and Weir published their first driver model, Crossman and Szostak [Crossman1968] proposed a three level driver behavior model. They proposed a theory about the possible visual information that might be processed by the driver to accomplish the lateral control task. At the first level, their model used an „*open-loop curvature control using preview [...] driver scans the road ahead and detects points at which the highway changes curvature*" [Crossman1968, p. 181]. Based on the curvature estimation it is assumed that the driver mentally calculates an appropriate steering angle, which he translates into the appropriate muscle force to control the steering wheel. This open-loop control allows quick steering actions but it is expected to be imprecise due to curvature estimation inaccuracies and missing feedback.

Two consecutive closed-loop stages follow the open-loop control: a first order heading correction (using the angular change between vehicle heading and road orientation) and a second order lateral positional correction which could also deal with a driver specific, intended lateral position.

Crossman and Szostak speculated that the acquisition of lateral control skills might take

place in a reverse order to the stages: a novice driver would start with the level three basic driving skill (correction of lateral position error) and continuously develop level two heading correction skills. The learning of precise level one open-loop control skills would need the most experience with lots of exercise for all kinds of different curvatures and driving speeds. At the highest level of expertise, drivers might have learned highly sophisticated open-loop control programs. These require only very little correction by the slower feedback control processes.

Based on their initial driver model and the model of [Crossman1968], McRuer and colleagues successively improved their model for lateral control [Weir1973], and they finally published a three level control model [McRuer1977]: lateral control was achieved mainly by two *compensatory* closed control loops: 1) the outer loop which corrects deviations of the lateral position from the desired path and 2) the inner control loop which corrects vehicle heading errors.

In parallel to the compensatory control system, a *pursuit control system* is implemented as feed forward controller. Based on the assumption that perceived information about road curvature is accessible to the driver, he can predict a desired path. Similar to the proposal of [Crossman1968] a third control stage is proposed ("precognitive control") in form of specialized open loop motor programs which are learned with increasing driving expertise.

Similar to the compensatory and pursuit levels used by McRuer and Krendel, [Donges1978] proposed a two-level parallel steering model for stabilization and guidance (anticipation). He also proposed a more detailed theory about the visual perception of information which could be used for lateral vehicle control. Several three dimensional illustrations from the driver's perspective and his view ahead on the road (visual scene) can be found in his publication. For different combinations of lateral vehicle displacement and heading angle, these figures show, how the visual appearance of the road's vanishing point at the horizon, as well as location and orientation of the lane markings change within the driver's view.

Based on this visual scene analysis, Donges proposed a number of information that could be extracted by the driver from the visual scene for the stabilization task: „*1) Lateral deviation between driver's head position and road centerline. 2) Angle of tangents of desired and actual path [...], this quantity is called heading angle error. 3) Difference of the curvatures of the vehicle's actual and desired path[...].*" [Donges1978, p. 696]. He also described, how the characteristic road entities (vanishing point, road markings) are perceived during curvilinear motion.

Besides the question which information is probably perceived by the driver, Donges also discussed *where* this information could be extracted from the visual scene. The *near road* information should provide direct access to differences between the actual and the desired vehicle path, which can be used for the actual vehicle control (stabilization level). The *far road* information is processed in parallel and used for driving trajectory planning. Donges called the near and far road information „*the duality of information presented to the driver by the forward view of the road*" [Donges1978, p. 691].

The differentiation into far and near road information was based on previous research which suggests that „*the curve negotiation process perceptually starts well in advance of the curve itself*" [Donges1978, p. 696]. This anticipatory behavior could be a hint that the driver try to estimate the curvature of the road with a certain amount of preview time, and that he processes information from a far region. The stabilization information for maintaining the current trajectory supposedly comes from the near region.

With his detailed analysis of the visual scene and theory about the perceived information, Donges clearly goes beyond the proposal of McRuer and Krendel, who did not make such concrete assumptions about the perceivable information. Donges also proposed possible future applications for his driver model, for example the investigation of „*effects of vehicle dynamic parameters such as steering sensitivity, tire features, etc. on human steering behavior.*“ [Donges1978, p.707]. The ideas of Donges were also incorporated by Salvucci [Salvucci2001] into his driver model (described in section 2.2.3, p. 29).

Donges two-level approach was also the basis for two nowadays commercially sold and industrially used driver models - the DYNAware Driver [Fischer2008, Fischer2011] and the IPG Driver Model [Riedel1990, IPG2010]. Schick and colleagues [Schick2008] describe, how the IPG Driver model is used as component of a large scale real-time hardware/software in the loop simulation platform. The platform is used for testing of automotive assistance systems, simulating standardized driving scenarios developed in cooperation with TÜV Süd Automotive [Schick2007]. Albers and colleagues [Albers2010] explain the application of the IPGDriver within a car2x-in-the-loop-platform for virtual integration testing. The model was integrated into a MIL/HIL/SIL[3] simulation platform which was used to test cooperative assistance system functionality, including car2car as well as car2infrastructure system units.

Wurster and Schick [Wurster2010] present a good overview of about 20 possible application cases for assistance functionalities that can be tested with the IPGDriver model, e.g. simulation of reverse parking with assistance, hill-starting with parking brake or stop-and-go driving.

Interestingly, the mentioned application cases do not involve scenarios which need interaction with additional traffic participants, as it is necessary for the investigation of lane changing and overtaking maneuvers.

2.2.1.2 Further Modeling Approaches

Apart from the control-theoretic models, a number of alternative implementation techniques have been used for longitudinal and lateral control. [Juergensohn1997] evaluated fuzzy control and artificial neuronal networks for longitudinal and lateral vehicle control. Similar to most control-theoretic models, variables like acceleration, speed, road curvature, angular heading error or lateral position error were used as input. These measures were mapped onto linguistic fuzzy terms (fuzzification).

For the development of a compensatory lateral controller the majority of the work was invested for a manual fine tuning of 61 fuzzy rules. Unfortunately, this heuristic approach did not lead to successful (human like) steering behavior. Jürgensohn proposed a workaround, using a lateral controller based on the control-theoretic approach. He conducted simulation runs with this controller and used the input / output data for a reverse engineering of the characteristic field of the controller. This field was partitioned into smaller regions, which were then mapped onto linguistic terms of the fuzzy controller.

Jürgensohn described that the controller provided the “expert“ knowledge which was extracted and related to linguistic terms of the fuzzy approach. After manual fine-tuning, a comparison of driving data between the model and test driver for single and double lane change behavior showed, that the fit of the driving trajectory was good, but the analysis of the steering

[3] Model In the Loop, Hardware In the Loop, Software In the Loop

angle showed large differences between model and human driver. Although the overall result did not convince Jürgensohn, he mentioned that the strength of the fuzzy approach are its modularity and extensibility, because new behavioral features can be added by adding new fuzzy rules.

Nevertheless, it was questioned whether longitudinal and lateral control behavior is a good application domain for fuzzy control: more or less continuous steering actions have to be translated into a discrete set of linguistic terms and fuzzy rules. According to him, it seems unlikely that drivers can verbally explain how they accomplish *compensatory* steering or braking actions in detail (how they applied a certain amount of muscle force to do the steering). Because of these problems to assess the knowledge, the creation of the fuzzy knowledge base (linguistic terms, membership functions and rules) is a demanding task and at certain points an empirical derivation is complicated or hardly possible.

Along with the fuzzy controller, an artificial neuronal network classifier was developed by Jürgensohn, which allowed the driver model to detect different classes of road geometries. The basic idea behind the classifier was to use a set of 10 input neurons which sample the road ahead, longitudinally along its centerline. The trained network classified road segments into straight, curves and S-curves.

Jürgensohn also proposed that the classification of straights and curves has to be done within the context of the current speed. While at slow speed a large radius curve appears to be easy to drive, almost similar to a straight road, the same curve feels more demanding at high speed. To account for this difference, the (sampling) distance was related to the current speed which equals a the implementation of a preview distance.

Unfortunately, an evaluation of these different approaches against a larger empirical data base was not made in [Juergensohn1997], instead for each of his approaches a graphical comparison with the longitudinal and lateral driving trajectories of test drivers was presented. It is not known how many drivers were really used for the evaluation, because in most cases the diagrams were named “Test Driver“ or “Model Behavior“.

Recently, Bayesian programming has also been used to model longitudinal and lateral driving control. In one of their earlier publications Möbus and Eilers investigated gaze behavior of 21 drivers, while they were driving through curvy road sections [Moebus2009]. At a number of fixed road locations snapshots of the gaze behavior were analyzed. A small number of gazes were located at the tangent point of the curves, but lots of them were completely off-road, at the opposing lane, or at different lane locations other than the tangent point. These large variations seem to violate the assumptions of the two-point steering model published by [Salvucci2001]. This model proposed that drivers scan the curves along the tangent points of the curve’s inside, and these are used for anticipatory, lateral vehicle control.

It could be argued that the current on-road location and orientation of the vehicle might not have required any control action from the driver. This might have allowed the driver to direct his view towards other things which are not directly related to the vehicle control. Furthermore, fovea vision might not be needed all the time to accomplish steering. Instead, lots of information can probably be extracted from the periphery.

With regard to the vehicle control skills of the driver, [Moebus2009] proposed that machine learning and Bayesian programming can offer a reasonable alternative for the simulation of *percept-motor skills*. According to [Rasmussen1983], percept-motor skills describe human be-

havior that is performed with little conscious control only. These skills are learned by hundreds of repetitions, and this can be assumed for longitudinal and lateral control behavior of experienced drivers.

[Crossman1968] proposed specifically learned open-loop control programs (see above) to model such behavior. In contrast, the Bayesian programming approach uses machine learning to extract the most significant relations between a set of potential input variables (percepts) and the observed behavior (actions). This approach is strictly data driven and makes no assumptions about the underlying mechanisms that generate the behavior.

Subsequent improvements to the first model [Moebus2009] led to the "Bayesian Autonomous Driver Mixture of Behavior Model" (BAD-MoB) approach [Eilers2010]. Here, authors not only separate longitudinal and lateral control, they also separate behavior into smaller maneuver-based snippets like car-following, lane changing or even subparts of a driving maneuver. For each of these snippets a sufficient amount of empirical driving data is necessary to learn a specific "expert" action model. Each action model is accompanied by a behavior classifier model which evaluates the appropriateness of the action model in the current situation. Finally, the driver model output is generated by a gating model which mixes the output of the action models and the corresponding appropriateness as a weighted sum.

The latest work published on BAD-MoB models discusses the learning of appropriate perceptual input for longitudinal and lateral control model [Eilers2014]. Authors reviewed existing psychological literature and the proposed visual measures like for example bearing angles, splay angles or optic flow for lateral or time-to-collision and time-headway for longitudinal control. They proposed „*the use of structure-learning procedures to select hypothetically relevant percepts from the variety of possibilities based on their statistical relevance*" [Eilers2014, p. 19]. According to their classification, the bearing angle had the highest statistical relevance, while the far point proposed by [Salvucci2001] was ranked 114th only.

Beyond Manual Vehicle Control Models So far, the reviewed models were dedicated to the vehicle control actions (steering, accelerating and braking). In a very well known and often cited speech in 1985, John. A. Michon [Michon1985] talked about the current state of driver behavior research and the driver modeling community which, according to his impression, seemed to get stuck on the existing ideas at that time (mainly control theoretic models, risk models and task models). He concluded that driver models had failed to integrate research results from human factors and behavioral sciences.

Although empirical research on driver behavior and task analysis methods had accumulated a large amount of knowledge about the variety of driving tasks, ranging from navigation tasks, strategic and maneuver decision making to actual vehicle control level, the simulation approaches for driver behavior modeling mainly focused on manual vehicle control. Higher level cognitive abilities which are necessarily needed by a driver remained almost unconsidered. Michon also brought up the point that driver models completely lacked the integration of sophisticated models of human perception, for example how humans filter the required information for the driving task.

He had high hopes that cognitive architectures like ACT-R [Anderson2004, Anderson2009] would allow a better integration of human factors and psychological models of cognitive processes into the domain of driver models, e.g. by adding 1) models of human perception (visual

or acoustic perception) 2) memory models (working memory, long term memory) which store different representations of knowledge (declarative or procedural), 3) goal-oriented behavior using rule-based decision making and action selection and 4) execution of highly skilled actions like hand, finger, or eye movements.

It took an additional 10 years, before driver models were actually built within cognitive architectures, for example in Soar [Aasman1995], ACT-R [Salvucci2001], QN-MHP [Feyen2002] or in a driving domain specific architecture called COSMODRIVE [Bellet1999]. Besides the manual vehicle control skills, cognitive abilities like attention allocation, decision making and multitasking, problem solving and skill acquisition were investigated with these models.

Furthermore, in the middle of the nineties the *situation awareness* concept was introduced, especially in safety-critical domains like aeronautics or automotive. Mica Endsley was one of the main drivers in a quickly growing research community. Her conceptual model about three levels of situation awareness (perception, comprehension, projection) [Endsley1995] inspired the development of driver models which focused on the simulation of situation awareness related effects, for example distraction by mobile phones [Salvucci2002, Brumby2009], or in-vehicle information systems (IVIS) [Zhao2013]. Typical measures that were investigated are gaze distribution and glance durations, task execution times or impact on driving performance (mainly steering).

Due to the rapid development of technical devices like smart phones, but also automated driving features which come with more complex displays designs, this area of research is still growing and will be an application area for future driver models. Section 2.2.3 will provide a detailed review of cognitive driver models, but as mentioned at the beginning of this chapter, there is a third category of driver models which is reviewed briefly next, the *microscopic driver models in macroscopic traffic simulations*.

2.2.2 Microscopic Traffic Flow Models

The objective for which these models are developed, as well as their structure and the development approach are much different from manual vehicle control models (and also the cognitive driver models which are introduced in the next subsection). One of the main differences is that these models are not used to simulate the behavior of a single driver, or the detailed interaction with his vehicle, or an assistance system. Instead, these models are used to simulate the behavior of many drivers and their vehicles from a traffic flow perspective. Dependent on the scope of the simulation, a differentiation between driver and vehicle is not even necessary. The range of possible traffic scenarios varies from short road section with a few crossings and traffic lights only, to the investigation of a single highway ramp, up to large-scale urban traffic area simulations. Typical questions of interest are, if an alternative road layout or speed limitations result in a better, less congested traffic flow, or if a different synchronization of traffic light phases can improve traffic flow during rush hour.

But not only the use cases are different. Most developers of manual control models as well as cognitive driver models make extensive use of empirical investigations of smaller groups of individual drivers, either in driving simulators or in real vehicles. In contrast, the behavior for the microscopic behavior models is often extracted from traffic observation sites (e.g. video surveillance of highway sections or crossings). Measures like absolute and relative speed im m/s or

distances between vehicles are extracted from video data. Driver actions like braking, accelerating, turning, distance keeping or lane changing can be partially inferred from the externally observable behavior. Finally, the model structure itself is different: because such simulations often include a huge number of vehicles, complex vehicle dynamic models are rarely used and the output variables of the models are not individual driver actions, like controlling the steering wheel, or the accelerator position. Instead, the models generate the externally visible vehicle behavior, like current speed, acceleration or vehicle orientation.

A very detailed microscopic behavior model was presented in the dissertation of Ahmed [Ahmed1999]. The model was developed to simulate driver behavior on US motorways separated into different driving maneuvers: free-flow (lane following without a lead car), car-following, and lane change maneuver. Because the lane change model is of specific interest for this work, it has to be mentioned that driving on a US highway is a little different from driving on the German Autobahn. On US motorways with more than two lanes drivers can overtake other vehicles on any lane and the model of Ahmed was developed for this case. Therefore, lane selection has a strategic component with regard to which lane might offer the best possibility to travel at the preferred speed.

The lane change model is divided into two parts: 1) mandatory lane changes, for example entering a motorway through an access ramp, or because of a closed lane due to road work. 2) discretionary lane changes, where the driver is free to choose any lane according to his personal preferences, e.g. because he feels more comfortable on a certain lane, or wishes to drive at his usual travel speed. Because this work does not target mandatory lane changes only the discretionary part is briefly explained here, which is implemented in a two step step decision process:

1) Before a driver starts to search for another target lane, the current lane has to become unsatisfactory. Satisfaction with the current driving conditions is dependent on desired speed, speed of lead car, traffic density on the current lane, or if a heavy and slower vehicle is in front. If the driver is unsatisfied with the current lane, the evaluation of the adjacent lanes right and left is done in the same way. If the satisfaction level with another lane is above the satisfaction with the current lane plus a certain threshold value, a lane change maneuver is initiated, and the model starts to search for acceptable gaps in the second decision making step.

2) The gap acceptance procedure tests differential speed and gap size between the own vehicle and the lead and lag vehicle on the target lane (lead vehicle: first vehicle ahead on the target lane, lag vehicle: first approaching car from behind on the target lane). Each gap is considered individually and a gap (lead or lag) is considered acceptable, if it is larger than a critical gap size. Similar to the calculation of “being satisfied with a lane“ gap acceptance is a probabilistic decision.

Ahmed provides the option to include additional independent variables into the gap acceptance and makes suggestions (like for example driving style) but no specific model for the influence of such factors is derived. Obviously, it is complicated to derive such influences based on external observation of vehicles.

A significant improvement to this lane change model was made by [Toledo2003]. The situation in Figure 2.3 motivates his work: A is the vehicle under investigation, gaps BC and CD are considered acceptable, but the adjacent gap AC is rejected. The stateless decision making process implemented by Ahmed rejects a lane change, because it considers the adjacent gap only.

Consequently, the acceleration behavior is not changed, and the model can not systematically improve the adjacent gap situation to finally reach the acceptable gap CD.

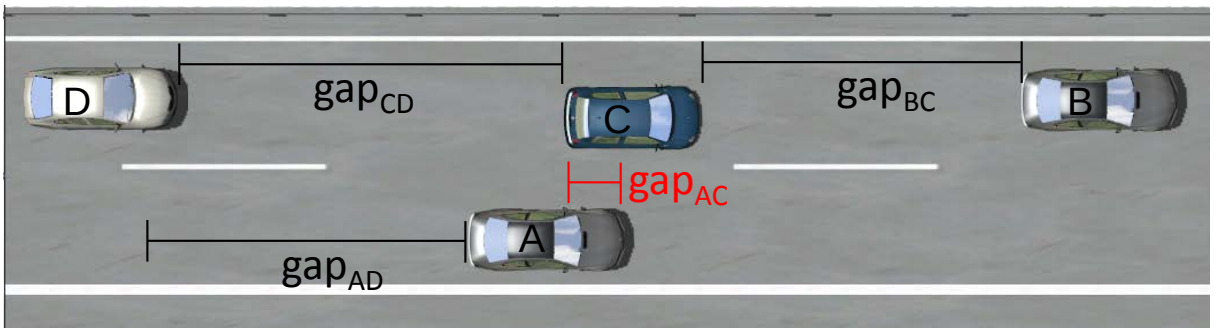

Figure 2.3: Adopted from [Toledo2003] Figure 2.5: A lane changing situation illustrating the limitations of existing models

A state-based process was integrated into the gap acceptance model that allows a sequential plan execution by selecting a target lane first, and afterwards the search for an acceptable gap is made (e.g. gap CD). During gap acceptance, the model considers whether acceleration or deceleration would be necessary to reach a gap. Additionally, not only the adjacent gap is considered, but all three gaps seen in Figure 2.3. The model of Toledo includes a prediction of the change of a gap over a short period of time. Therefore, even if a gap is too small at the moment, it might be chosen by the model, because the trend for that gap predicts that it will be adequate in a short period of time.

At TU Dresden, two different microscopic models were developed: a model for longitudinal control (Intelligent-Driver Model, IDM) [Treiber2002], and a lane-change model (Minimizing Overall Braking Induced by Lane Changes, MOBIL). MOBIL [Kesting2007] considers up to six different vehicles which potentially surround the ego vehicle: the nearest vehicle ahead and behind on its own as well as the adjacent left and right lane. It conducts a lane change, if an incentive criterion indicates a reasonable advantage (acceleration is possible above a minimum of 0.1 m/s^2), and if a deceleration safety criterion for the rear vehicle on the target lane is fulfilled: if the potential lane change would entail a braking maneuver of the rear vehicle, the allowed deceleration has to be below 4 m/s^2. Secondly, the model incorporates a "politeness" factor which allows to adjust behavior between a totally egoistic behavior (accept small gaps and higher deceleration of surrounding traffic) and cooperative behavior.

Although this model incorporates interesting subjective driver characteristics, the following citation shows that the model makes some drastic assumptions: „*by formulating the [safety] criterion in terms of safe braking decelerations of the longitudinal model, crashes due to lane changes are automatically excluded. [...] It should be noted that the maximum safe deceleration* b_{safe} *prevents accidents even in the case of totally selfish drivers as long as its value is not greater than the maximum possible deceleration* b_{max}" [Kesting2007, p. 87].

These assumptions certainly do not hold for a human driver. The behavior can be considered a normative, optimal driver behavior which does not consider limitations, or erroneous behavior of human drivers.

2.2.3 Cognitive Driver Models

Before the capabilities of different cognitive driver models are summarized, a few introductory explanations about basic concepts of cognitive architectures like Soar [Laird2015, Laird2012], ACT-R [Anderson2004, Anderson2009], or EPIC [Meyer1999] are given. [Langley2009] also provides a good review about the main concepts of cognitive architectures. Common to these architecture is a *production system*, which is the central component for the simulation of human behavior. Further components model human cognitive abilities with regard to short-term, long-term or working memory. To realize interaction with an external environment, visual or acoustic perception are integrated, as well as modules to execute motor actions, which simulate muscle movement for hand, finger or eye movements. The production system plays a central role in simulating *goal-oriented, rule-based* human-like behavior. While *goals* define the intention, or "what to do next", a *production rule* (short: rule) contains a conditional action plan which consists of a number of actions that need to be taken to achieve the goal.

The *cognitive cycle* of a cognitive architecture typically consists of two main steps: 1) select the next goal and 2) from a set of rules, which are related to this goal, select one rule with an appropriate action plan that fulfills the goal in the given situation. This second step contains a number of sub-steps which are now roughly explained.

Although cognitive architectures differ with regard to how the production system works at runtime, all architectures share a similar basic structure for the rules: they consist of two parts known as *if - then* or *boolean condition - action* parts. Within the boolean condition a number of variables can be specified which are tested by the production system. If the expression evaluates to true, the action part of the production is executed afterwards. Example: *If* current speed $>$ desired speed, *Then* reduce accelerator position. Before the condition part can be evaluated, production systems typically require to *retrieve* an actual set of values for the condition variables from a memory component or the perception (for the example: the current speed and the desired speed). Such a set of variables is bound within a compound data structure named *chunk*, which represents declarative or factual knowledge.

In case of successful retrieval and condition evaluation, the action part of the rule is executed next. Different actions can be specified 1) movements of extremities to interact with the environment (previous example: usage of accelerator pedal) 2) eye movements to visually observe a certain areas of interest. This is often necessary to sense information which is not available, or the necessary information is not up to date in the memory component. 3) Statements to manipulate and update declarative knowledge chunks which are then memorized. 4) If the successful execution of a rule lead to the completion of a goal, a new goal can be derived. This cyclic behavior is executed, until the model completes all tasks.

Besides this coarse description about the cognitive cycle, there are lots of details that vary between the cognitive architectures, but a detailed explanation of them is out of scope here. Instead, some remarks about the term *models* are given next, before different driver model implementations are introduced.

Cognitive Architectures and Model Implementations When speaking of a cognitive driver model, or in general a cognitive *operator model* implemented within a cognitive architecture, the architecture itself is only one part - it offers the cognitive modeler a framework of

inter-connected modules, which simulate aspects of certain cognitive functions that are characteristic for human behavior. Architectures also include some (physiological) limitations, like a visual field of view (divided into fovea and periphery), duration calculations for motor actions as well as capacity limits of information processing or reaction times.

Besides these architecture components, the second part of each operator model is the *knowledge base*, which has to be loaded into the architecture before a behavior simulation can be started. A knowledge base consists of *procedural knowledge* (the rules), which define learned behavior and memorized action plans, how a certain goal can be achieved with a number of dedicated actions. In contrast *declarative knowledge facts* in form of memory chunks, represent already learned knowledge about objects, their characteristic properties and also relations between them. The architecture can be considered task and domain independent, while the knowledge contains general as well as task an domain specific parts.

In the context of cognitive models which are used to simulate human-machine interaction (like pilot, driver, machine / plant operator models), the term *mental model* is often used to represent the operator's knowledge related to the use of technical equipment. Examples are the pilots' knowledge about the autopilot system of the aircraft, or the drivers' knowledge about technical details of his vehicle. But mental models can also be extended to include more of the environmental situation in which a certain task has to be accomplished. In this case, a mental model of the situation is often called *situation representation*, which in turn is directly related to *situation awareness*. For the implementation of a mental model, declarative knowledge facts as well as procedural knowledge can be used.

A main difficulty to develop adequate mental models is, that such knowledge is heavily influenced by learning and experience, which makes a mental model highly individual. Identifying a common core amongst a representative group of persons is a very complex task. In a professional work environment, where tasks have to be accomplished according to fixed procedures, it is likely that the variations are smaller. Pilots for example are operating in a rather restricted way, how to adjust the flight parameters. Instead, driving maneuvers are highly individual and depend a lot on the preferred style of driving. Such individual behavior differences will be tackled also by the gap acceptance model developed in this thesis.

Soar The first driver model implemented within a cognitive architecture was published by Jannes Aasman [Aasman1995] in his PhD thesis. He implemented the model in the cognitive architecture Soar, a production system, based on the ideas of the *Problem Space* hypothesis by Newell and Simon [Newell1972]. Problem solving in Soar starts with an initial problem state and a desired target state, which equals the goal that should be achieved. In general, a problem solver (human as well as a human model) needs to find a way to transform the problem state into the desired target state by 1) applying existing knowledge or 2) by gathering new information which helps to accomplish the task. One of the driving tasks which Aasman modeled was *manual gear shifting*.

The model was initially fed with some basic knowledge about the function of the clutch, the accelerator pedal as well as the gear lever (for example the accelerator can be pressed or released, the gear lever can be put from neutral into gear X, or from gear Y into neutral). Additionally, a couple of constraints were given: 1) before pressing the clutch, release the accelerator and 2) use gear lever only, when clutch is pressed. Furthermore, the model also

incorporated knowledge which extremity (right or left foot / hand) should be used, and how it to use it to manipulate the two pedals and the lever. At runtime, the model was then confronted with different traffic situations that demanded, for example, to shift the gear from second to third. By exploration of the problem space (explore the applicable knowledge and possible actions), the model learned the appropriate action sequence for accelerator pedal, clutch and gear lever, and it accomplished the goal of gear shifting. The successful action sequence was memorized, and from there on it was available as learned, procedural action plan.

The implementation of problem solving in Soar mimics the process of successive learning and refinement of behavior from novice to expert behavior. Such behavioral learning enables humans to deal with unfamiliar situations by applying existing knowledge to new problems. Because learning is not considered in this thesis, the SOAR model is not described in more detail.

Integrated Driver Model In a very detailed technical report, Levison and Cramer [Levison1995] described their efforts to integrate a „*driver / vehicle model*“ [Levison1989] and a „*procedural model*“ [Corker1990] into a two layered driver model, according to the skill-/ and rule-based behavior stages proposed by [Rasmussen1983]. The driver / vehicle model is responsible for the actual vehicle control tasks and is similar to implementations of other control-theoretic modeling approaches based on *optimal control*. Using the approach of optimal control implies that the simulated human driver „*is sufficiently well-trained and motivated to perform in a near-optimal manner subject to system goals and limitations*“ [Levison1995, p. 4].

The procedural model instead is used as „*supervisor of the integrated driver model.*“ [Levison1995, p. 19]. It schedules and executes all driving tasks which are specified as the model's procedural knowledge base in a rule-based format. It executes already existing action plans, but does not derive new plans through problem solving. Besides task scheduling, the model also cares about the allocation of visual, motor and cognitive resources. Each task competes for a number of necessary cognitive resources, and the selection of tasks is done according to the multiple-resource theory of [Wickens1988]. This theory defines a number of cognitive resource bottlenecks and interaction effects, for example only one task at a time can access fovea vision, process auditory input, or produce speech output. If multiple of these cognitive resources are used simultaneously, performance penalties on task execution time or accuracy can be expected.

Additionally to the resource model, a task priority scheduling algorithm was implemented based on task specific penalty functions. Such a penalty function decreases the likelihood that the current task is continued over and over again, which would completely block other tasks. [Levison1995] implemented specific penalty functions for each task, and the more tasks are waiting, the higher the chance for interruption. Besides the vehicle control and procedural model, a number of additional *human modeling parameters* were included to improve the execution times of the model, for example a time-delay for different perceptual processes (visual, auditory), or the response lag of hand, leg, eye movements or speech. [Levison1995] contains very detailed information about the mathematical model formulas for both vehicle and procedural model, the parameterization of all model components, as well as calibration and validation results compared to driving simulator and real driving data.

Simulation results of the model lead to predictions for driving performance, attention sharing

and task scheduling. The model was capable to simulate performance degradations of the driving control task when additional tasks were introduced, and secondly, when the driving task's difficulty was increased, the model distributed more attention to that task, while also a decrease in steering performance was measurable. These two effects were also found in empirical data of human drivers. Furthermore, the model predicted differences in attention sharing between voice-based or manual use of a cell-phone during driving, but the impact on driving performance in the manual condition was predicted significantly smaller, compared to the empirical data.

Conceptual Model of Driving with an ACC Boer and Hoedemaeker [Boer1998] published a conceptual driver model which was also based on the three layers of [Rasmussen1983], as well as [Michon1985]. Their work outlined an approach, how to model the impact of an adaptive cruise control (ACC) on driver behavior. The knowledge-based, or strategic level used a decision making process which was guided by the ideas of Simon's satisficing decision making [Simon1959]. Basic driving needs form a set of constraints which guide the decision making process, e.g. time until destination is reached, risk and safety, economic driving, current driving speed limitations, lane choice according to desired speed or traffic density.

One important task which was guided by these constraints, is lane selection. Whenever the current lane becomes unsatisfying, alternative lanes are evaluated which can lead to initiation of overtaking maneuvers or adaptation of the selected target route in case of closed roads. Feedback about the current driving situation from lower levels of the model is continuously evaluated. If the situation is not satisficing anymore, this leads to an evaluation of alternative lane possibilities. Below the strategic layer, a task scheduler allocates resources to initiate the appropriate driving actions.

According to the ideas of Boer and Hoedemaeker, the integration of human machine interaction with an ACC into the driver model could be realized by adding extra knowledge about the system's use, as well as technical details like sensor range, or system accuracy and limits. Authors explained that the ACC has an impact on the traditional driving task itself: whenever the system is operating under normal conditions, the longitudinal control task can be be skipped by the driver. This frees up some cognitive resources which could be used for additional tasks. Consequently, the ACC has a direct impact on the decision making of the driver. The authors also tackle issues like trust in automation, handover procedures between driver and system for different levels of automation or aspects of ecological interface design. But all of these aspects remain rather vague and it remained unclear, how this can be integrated into an executable simulation model.

ACT-R The conceptual work of Boer and Hoedemaeker, as well as the previously explained simulation model of Levison and Cramer inspired the development of a model published by Salvucci, Boer and Liu [Salvucci2001] named "Toward an Integrated Model of Driver Behavior in a Cognitive Architecture". The model is implemented in the cognitive architecture ART-R and realizes driving on a highway with a focus on vehicle control, and the two maneuvers car-following and lane changing. The knowledge base of the model consists of three main tasks for 1) vehicle control (observe road geometry and adjust controls), 2) monitoring the surrounding road for other vehicles and 3) decide if a lane change is necessary and possible based on the

model's intention, information about the lead vehicle in front and (if present) a rear car on the target lane.

For the *lateral control task* and the calculation of an appropriate steering wheel angle two preview points are used, a near and a far point. This two point strategy is based on the earlier work of [Donges1978]. The near point is always positioned at the center of the ego lane in a distance of 0.5 seconds time headway. Whenever the vehicle has a lateral deviation from the lane's center, this leads to a horizontal visual angle between the near point and the orientation of the vehicle on the road. The far point is used in a similar way to calculate a horizontal visual angle, but its positioning is variable. On a straight road the far point is located at a preview / lookahead distance of two seconds time headway at the center of the ego lane. Whenever the point reaches a curved road section, it is no longer positioned at the lane's center. Instead it moves at „*the tangent point of a curved road segment*" ([Salvucci2001], p. 10). This means, the far point travels along the intersection point of a straight line which originates from the eye of the observer (the driver model) and intersects the inner border of the ego lane at the tangential point.

The far point behavior is inspired by the work of Land and Lee [Land1994] and provides the model with a preview / lookahead to observe oncoming changes to the road curvature. Instead, the near point angle is used to maintain the position of the vehicle close to the middle of the road. At runtime, both points are scanned sequentially by the visual perception. The resulting two visual angles and their first derivatives are used as input (lead value) of a PD-control formula which is specified within the action part of a production rule. The output of the controller is used to manipulate the current steering wheel angle. Finally, to conduct a lane change maneuver the two points are moved from the ego lane to the target lane which automatically results in an increase of the two angles that is compensated by the controller with a steering action towards that lane.

Besides the lateral control task the model also maintains a certain speed. As soon as the model approaches a lead vehicle, the time headway between ego and lead vehicle is computed, and the difference between this value and a desired time headway is used for the adjustment of the accelerator pedal. The adjustment itself is again realized by a second control formula which is embedded in the action part of another production rule.

The second task of the model is monitoring, and the production system selects from a set of rules which trigger visual percept actions to scan the road around for upcoming traffic participants. Each of these "percept" rules updates certain memory chunks of the model's internal representation of surrounding traffic (situation awareness).

The third task of the model implements the decision making with regard to a lane change (either left or right): when driving on the right lane and the distance to the lead vehicle falls below a time headway of two seconds, the model intends a lane change left maneuver. If no vehicle can be perceived on the target lane withing a safety distance of 30 meters, a lane change left command is triggered. Even if no vehicle is perceived within the safety distance, the model also has the capability to *remember* vehicles that were seen immediately before, but might now be hidden within the blind spot of the mirror. Authors mention, that the model uses a rear-view mirror to observe traffic from behind, but no specific details about the implementation are given.

A year after their first publication, Salvucci and Liu published detailed results from an empir-

ical simulator study with human drivers [Salvucci2002]. The scenario was a two-lane highway with medium traffic density. The speed of the surrounding traffic varied between 22.35 and 31.29 m/s (50-70 mph). Unfortunately, the target speed of the drivers was not given, therefore speed differences within the scenario remain unclear. Similar to the previous modeling paper, the focus of the study was put on longitudinal and lateral vehicle control, the timing of the turn signal, and the gaze behavior during the course of the lane change. A more detailed analysis of the perception of traffic during lane change preparation is not found.

The model is also described later on in [Salvucci2006] with more details and the lane changing behavior was evaluated by comparing „*lane position, steering wheel angle and proportion gaze time*“ [Salvucci2006, p. 375] with human driver data. Instead, gap acceptance behavior was not the focus of the modeling efforts. According to the list of parameters (see TABLE 1 [Salvucci2006]) the minimum distance threshold for gap acceptance was increased to 40 meters. Similar to some other parameter this one was „*simply set to reasonable values based on informal observation of the model driving as well as approximations derived from available empirical literature*“ [Salvucci2006, p. 371].

Over the past ten years, this driver model was used for research with regard to multitasking, mainly to evaluate distraction effects by in-vehicle information systems (IVIS), or nomadic devices like mobile phones [Salvucci2002a, Brumby2007, Brumby2009]. A recent publication investigated multi-modal interface technology similar to mp3 players [Zhao2013]. Gunzelmann investigated fatigue during driving [Gunzelmann2011] and another publication dealt with impact of memory rehearsal tasks on driving performance [Salvucci2008].

Salvucci also developed the tool Distract-R [Salvucci2005], which offers the possibility to model secondary tasks by implementing the interaction of the driver model with a number of graphical components (for example buttons, displays, dials) that can be arranged to a GUI. In a later publication about Distract-R, Salvucci summarizes a number of different model applications to simulate interaction with the GUI of a radio, a cell phone, but also in-vehicle systems like heating or air condition [Salvucci2009].

Based on the implementation of the driver model, Salvucci and colleagues developed a real-time lane-change recognition system [Salvucci2007]. This system can be seen as a “Co-Driver“ which gets the input from the simulation while a driver steers the vehicle. The model is not connected to the vehicle controls, but it receives input from the simulator and calculates its own driving behavior in parallel (for example the vehicle steering based on near and far point). It uses its own lane change behavior to predict the lane change behavior of the human driver. To be able to match human data and model predictions at runtime a lane-change was defined as „*a segment in which the vehicle starts moving towards another lane and continues without reversal through that lane*“ [Salvucci2007, p. 537]. With this definition the model was able to predict 82% of all lane-changes half a second after the maneuver was started and 93% of all lane changes one second after maneuver initiation.

QN-MHP The Queuing Network - Model Human Processor is clearly different from production system frameworks ACT-R or Soar, because it defines each cognitive function as a processing node within a queuing network. Each of the nodes is related to a specific area in the brain [Liu1996]. Connections between the nodes are made according to neurophysiological findings about pathways in the human brain, for example the dorsal or ventral pathway in the

visual processing path[4]. In contrast to other cognitive architectures, QN-MHP is implemented within a commercially sold, discrete event simulation framework ProModel.

Tsimhoni and Liu published a steering model [Tsimhoni2003] which, similarly to the model of Salvucci, is based on ideas of the quasi-linear human operator model [McRuer1957] as well as the two level model of Donges [Donges1978]. Both models were briefly explained before. This basic model was later on extended for research on multitasking and workload prediction according to the six categories defined in the NASA-TLX workload index by [Wu2007]. Another contribution was made by [Bi2009], who published an extension for longitudinal control during car-following.

Lately, the thesis of Fuller dealt with implementation and simulation of multitasking behavior in QN-MHP [Fuller2010]. Her goal was to simulate the impact of a secondary distraction task (touch screen interaction) on longitudinal and lateral vehicle control. Model extensions for lane changing and gap acceptance were not found in the published literature for this model.

COSMODRIVE Although, the first journal article about COSMODRIVE (COgnitive Simulation MOdel of the DRIVEr) [Bellet1999] was already published in 1999, the implementation as simulation model was done in recent years [Bellet2011]. The model shares many similarities from a theoretical point of view with previous models, using a three-layered behavior model approach, again inspired by [Rasmussen1983] and [Michon1985]. It also has modules which implement a perception-cognition-action cycle. Bellet focused his research on how the driver represent the surrounding environment (*mental model* or *situation representation*). He introduced the concept *driving schema*, which binds a couple of elements from four categories into a compound declarative representation: characteristic properties of road infrastructure, driver intention, vehicle state and a set of zones. Similar to a production rule the schema is also bound to a specific goal. However, in contrast to a production, the driving schema is domain specific and demands specific links that characterize traffic and road conditions. The zone category for example contains a specification of specific parts of the oncoming road where the driver either seeks information or simply parts of the road where he intends to drive through. The schema can be seen as a pattern which (partially) matches specific driving situations and multiple schema may interfere with each other based on the input of the model at runtime. With regard to lane changing and gap acceptance no publication could be found for COSMODRIVE.

2.2.4 Summary

This section reviewed driver models which were developed for three different application areas: manual vehicle control models, microscopic traffic flow models and cognitive driver models. The focus was put on models which can be used to simulate driver behavior within a traffic simulation or within a third / first-person driving simulator software. It is known that this categorization is not exhaustive, for example risk models [Naeaetaenen1974, Wilde1982, Fuller1984], or purely descriptive models were not considered here.

[4] [Ungerleider1982] proposed that the visual pathway following the primary visual cortex is split into two streams, the *ventral* stream, which is supposed to be responsible for the identification of objects (“what“ path), while the *dorsal* stream or “where“ path, is likely involved in spatial processing of object locations and motion.

Manual vehicle control models have the longest history of these three model categories, and their objective is to model and simulate the longitudinal and lateral control behavior. Throughout the years, a number of different techniques have been used to implement such vehicle control models. Most common are the controller models (based on control-theory), which typically incorporate multiple control loops. Alternative implementation techniques like fuzzy control, artificial neuronal networks and Bayesian programming were also used.

From a driving maneuver point of view, most manual vehicle control models have been developed for lane-following and car-following which needs interaction with only one traffic participant - a lead vehicle. But their are also models which simulate the vehicle control behavior within a more complex maneuver situation like lane changing, for example the model by [Moebus2009, Eilers2014]. They extended their driver model with a probabilistic decision making component, which allowed to dynamically switch between different basic driving skills, and enabled the model to interact within more complex traffic scenarios with multiple surrounding vehicles.

With regard to lane changing, several models can be found in the microscopic traffic flow model category. The intended use of these models is different from the manual vehicle control models, but vehicle control is nevertheless an integral part. Nevertheless, their main focus lies on the simulation of macroscopic traffic flow effects, simulated by a large number of microscopic driver-vehicle models. To simulate such traffic flow effects, it is not necessary to model fine granular driver actions like eye and head movements to perceive information from different locations. In most cases, it is already sufficient to simulate the observable driver-vehicle behavior. To represent the variability of individual driver behavior, these models include certain human performance parameters, like a distribution function for reaction times. The lane change model by [Toledo2003] extended the model of [Ahmed1999] by a state-based decision making approach, which allows a continuous evaluation of multiple surrounding gaps, and the initiation of planned actions to systematically reach a specific target gap.

The last category of models which was reviewed are the cognitive driver models, which specify behavioral action sequences on a fine granular level, like for example eye and head movements. Most of the cognitive driver models realize the vehicle control tasks similar to the manual vehicle control models in form of control formulas. [Salvucci2001] integrated such control formulas into the action part of the rule-based behavior model specification.

Because cognitive architectures allow to model the behavior on such a fine level of detail, the generated output behavior can also be compared against a finer sequence of human behavior actions. The drawback of this detailed modeling approach is, that it very quickly leads to a high complexity of the model, including a large amount of behavioral rules and (domain specific) knowledge facts. The validation of such models is a very challenging task, especially if empirical evidence needs to be found for the integrated mental models (rules and factual knowledge). In most cases it is possible only, to validate the observable output behavior, which does not imply that the knowledge base itself is valid.

From the reviewed cognitive driver models, only the model of Salvucci was developed with the purpose to interact with surrounding traffic in a lane change situation. But his model dealed with the maneuver in a rather simplified way, and used a fixed distance threshold for gap acceptance (30 meter, later on 40 meter). Interestingly, Salvucci mentioned that a mirror view was implemented, but no details were published and it is assumed that this view is used to perceive

the distance in meter.

From what has been found in the literature, there seems to be no model which offers a more detailed approach to implement the *look in the mirror* during lane changing and gap acceptance.

2.3 Psychophysics: Size, Distance and Motion Perception

Psychophysical research tries to explain human behavior based on empirical behavior investigation, ranging from high-level, application oriented research within a more realistic, natural setting, down to very specific psychological questions about perception, which are typically investigated under highly controlled laboratory conditions. The next subsections will give an overview about different directions of psychophysical research on the perception of size and distance, while section 2.3.3 summarizes research results related to rear view mirrors.

2.3.1 Theories on Size and Distance Perception

Around 300 BC the Greek mathematician *Euclid* published a mathematical theory about how objects appear to our vision[5]. His approach was based on geometry, and he defined the visible field of view as a cone. Objects (or parts of them) which intersect this cone can be seen (unless they are obstructed by other objects).

2.3.1.1 Law of Visual Angle, Emmert's Law, Size Constancy

Euclid specified 58 geometrical definitions, each of them consisted of an example figure and a textural explanation. Figure 2.4 and it's subscript explain one of them.

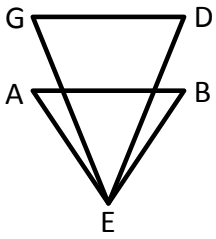

Figure 2.4: Figure according to [Burton1945] (Fig. 5): the eye is located at point E, looking towards the equally sized lines (objects) AB and GD. „*Objects of equal size unequally distant appear unequal and the one lying nearer to the eye always appears larger.*“ [Burton1945, p. 358].

Euclid also defined relations for the size of objects (objects appear longer, shorter if ...), distance (objects appear closer or farther) and also relative positioning between objects (left,

[5]The original manuscript was translated by Harry Edwin Burton and published in the Journal of the Optical Society of America [Burton1945]

right, upper, lower). In Euclid's theory, the common measure to relate objects to each other is the angle / angular size, or in the context of vision known as *visual angle*: „*[...] things seen within greater angles appear larger, [...]*" [Burton1945, p. 358]. The visual angle offers a simple way to represent the image size that an object casts onto the retina. The geometric view that Euclid already formulated can be found also in the *law of visual angle*: „*The apparent size of any object or image seen by the eye depends upon the size of the retinal image [...]. Objects which subtend the same visual angle will have the same apparent size, although their actual sizes may be very different if they are at different distances from the eye*" [Fincham1945, p. 160]. Although the wording is a little different, the main assumption stays the same. According to this theory, the appearance of object size depends on the size of the visual angle which represents the retinal image size.

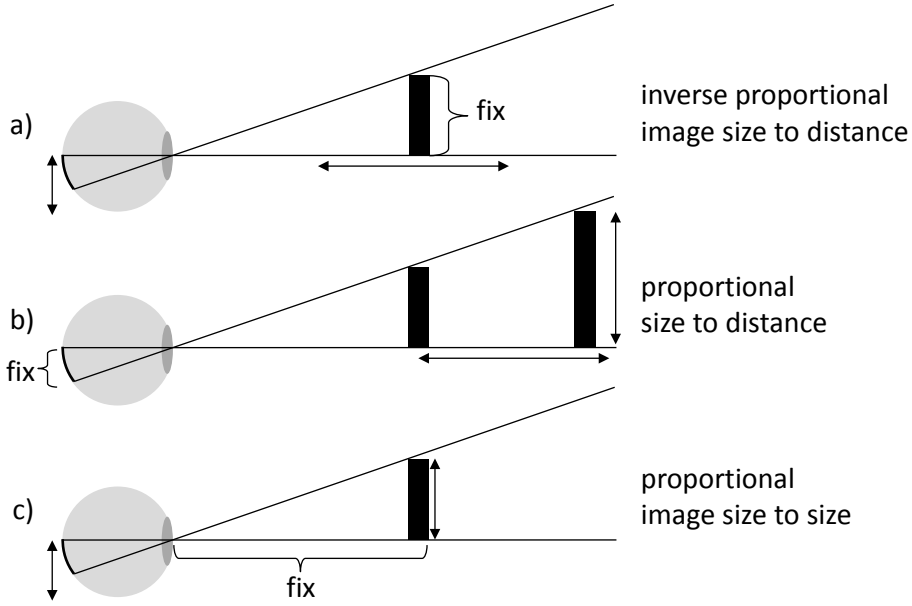

Figure 2.5: Relations between the distance observer - object, object size and retinal image size. If one measure is held constant the other two vary proportionally.

Figure 2.5 shows three basic relations between distance, size and retinal image. The law of visual angle assumes: in case of a) and c) the perceived object size varies, because the visual angle varies. In case of b) the perceived object size remains the same, because the visual angle is held constant. But is the visual angle / retinal image size the only variable which determines our perception of size? Some serious doubts on the general validity of the law of visual angle can be raised, based on finding of Emil Emmert[6]. In 1881 he was experimenting with the appearance of afterimages and reported [Emmert1881] that an afterimage appears to increase in size, when looking on more distant walls.

This finding suggests that distance plays an important role in our size judgment. If we would simply judge the size of an afterimage by its visual angle (retinal size), the result should always be the same, because the afterimage does not change its size on the retina anymore. Looking

[6]Swiss ophthalmologist (1844 - 1911)

at Figure 2.5, the situation of the afterimage can be compared to b) where the two bars can be considered the two walls in different distances against which the observer compares the afterimage. But in contrast to the law of visual angle, the afterimage at the more distant wall is perceived larger and not equally sized. This finding is also known as Emmert's law: the *perceived object size* has a proportional relation to the *product of visual angle and distance*.

The experiment of Holway and Boring [Holway1941] is one of the most often cited experiments. They found more evidence that the perceived object size could be related to distance: subjects had to sit on a chair located in the corner of two orthogonal hallways. A canvas was positioned in each of the hallways and a light circle was projected on each of them. One canvas was located at a fixed distance of 10 foot and the projected light circle had a constant size. In each trial the second canvas in the orthogonal hallway was located at a variable distance between 10-120 foot and the experimenter adjusted the size of the corresponding light circle projected on this canvas, until the subject reported that it looks equally sized to the reference / standard light circle.

In one experiment condition, the hallways were almost completely dark and subjects could use monocular vision only. In this case, they adjusted the size according to the law of visual angle. But with the availability of more depth cues, distance estimation changed and subjects increasingly started to match the linear size of the light circle and not the angular size. This effect is called *size constancy*. The difference between size constancy and Emmert's law can be explained with the help of Figure 2.5: while Emmert's law considers changes in object size and distance (described by b) size constancy deals with the situation shown in a). The fixed size stimulus was positioned at different distances, but unlike visualized a) it is still perceived at the same size, which is *not* what the geometrical relations would predict. In this case, the linear object size is perceived.

As main result of their experiment, [Holway1941] concluded that human perception can not simply be described by one of the two laws alone: „*For all that has been said by Gestalt psychologists against the validity of the law of the visual angle, it would nevertheless appear that, when no relevant datum other than retinal size is available, then the perception of size will after all vary solely with the visual angle. [...] Size constancy can be the law of size, therefore, only when determination is complex.*“ [Holway1941, p. 36].

Ten years later [Gilinsky1951] made an approach to integrate the observations made by Holway and Boring into a common model of perception. She published a mathematical approach which integrates the law of visual angle and size constancy. Furthermore, one additional parameter (A) is used to interpolate between the two extremes. Her definition of perceived size s is based on the specification of the ratio s/S:

$$\frac{s}{S} = \frac{A + \delta}{A + D}$$

The variable of interest, which balances between the law of visual angle and size constancy, is A. The effect of different values is illustrated in Figure 2.6. According to Gilinski, it is a subjective parameter which defines „*the maximum limit of perceived distance for an O*[7] *under given conditions.*“ It depends on the amount of depth cues available in a certain experimental setting

[7] O abbreviates observer

and needs to be estimated for each observer and situation. Parameter A can be considered a rough abstraction of the amount of available depth cues within a scenery, and the way how they are subjectively used by the person to infer size and distance of objects. Referring to the experiment of [Holway1941] above, it has different values for each of the different conditions (e.g. dark, bright light, monocular).

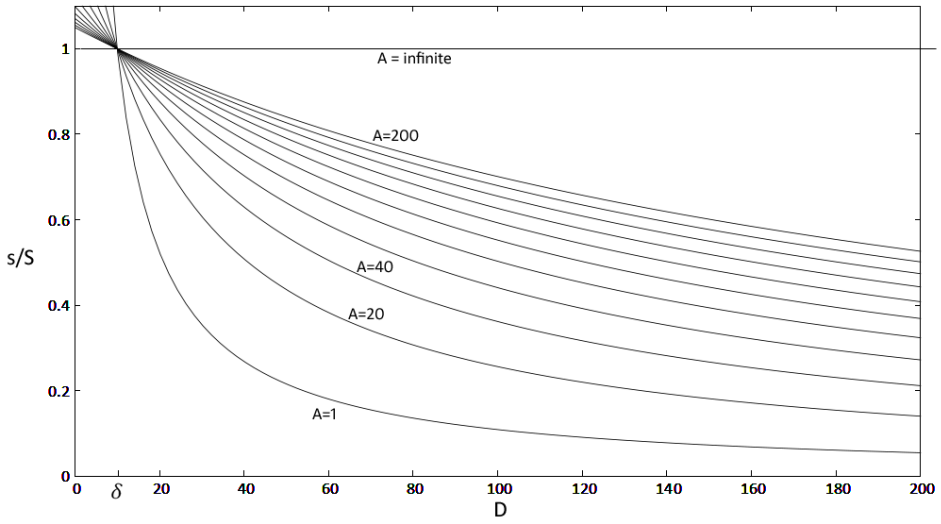

Figure 2.6: According to [Gilinsky1951, Fig. 2] x-axis: distance D between object and observer; y-axis: perceived size defined as ratio s/S; Parameter δ was chosen 10 here to demonstrate its effect: ratio s/S equals one which means perceived size equals subjective true size at subjective distance δ. Each curve shows a variation of parameter A between 1 (towards law of visual angle) and infinity (towards size constancy).

Figure 2.6 illustrates how A mediates between law of visual angle and size constancy. With D the distance between observer and object and s/S the perceived size: if A converges to infinity $\frac{s}{S}$ equals $1 \rightarrow$ at all distances which reflects size constancy. For smaller A converging to 0, the curve shapes into a hyperbole. In this case, the same object is perceived successively smaller with increasing distance and the drop off is comparable to the non-linear change of the angular size with distance (law of visual angle). In accordance with [Thouless1931], the variable A can also be considered a measure for *phenomenal regression*.

2.3.1.2 Size Distance Invariance Hypothesis (SDIH)

The SDIH formulated by [Kilpatrick1953] assumes: „*a retinal projection or visual angle of given size determines a unique ratio of* apparent size *to* apparent distance“. In a mathematical formula this can be written as $\tan(\alpha) = S'/D'$, with $\tan(\alpha)$ being the angular size, S' the apparent (or perceived) size and D' the apparent (or perceived) distance. This is a reformulation of the law of optics and it can explain both, the effect explained by the law of visual angle and the effect of size constancy. Considering a situation where no cues to depth are given, and the observer sees a geometrical figure in an otherwise black environment. Surely, the perceived distance D' is not 0, because an object can not be seen at zero distance. Since no further cues to

distance exist (perceived distance D' is constant), adding a second object with a larger angular size $\tan(\alpha)$ leads to an increased perceived size S' for that object: the perceived size S' varies with the angular size $\tan(\alpha)$. In case of size constancy, the interpretation is different: if cues to distance exist, the perceived distance D' is no longer constant, instead it varies with the angular size $\tan(\alpha)$ and the perceived size S' remains constant. But there are also situations which can not be explained with SDIH and visual size illusions, for example the Titchener Circles / Ebbinghaus Illusion see Figure 2.7 can be used to illustrate such situations.

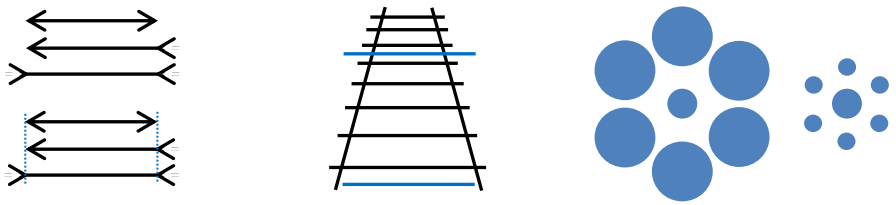

Figure 2.7: Size assessment of a target object depends on surrounding elements as demonstrated by a number of size illusion effects; Left: Müller-Lyer Illusion; Center: Ponzo Illusion; Right: Ebbinghaus Illusion (Titchener Circles)

The central circle has the same extent in both cases, thus its retinal image size is the same. Nevertheless, most observers perceive their size differently, but not their distance which would be suggested by SDIH. SDIH proposes that two mental representations exist for size and distance (perceived size and perceived distance). Based on the observations with regard to the illusions, it was proposed that the visual angle probably also has a mental representation, the perceived visual angle. The resulting formula $\tan(\alpha') = S'/D'$ would allow to explain the illusion: if the perceived distance remains unchanged, the perceived size can nevertheless change proportionally with the perceived angular size.

Support for the concept of a perceived visual angle concept comes from [Murray2006], who investigated whether the strength of size illusion can be measured by a difference in the cortical activation in the visual cortex V1. They used a variation of the original Ponzo illusion: in a computer experiment, subjects looked into a virtual hallway receding straight away from the observers viewing direction. Within the hallway two spheres were put with equal angular size, but at two different virtual distances. As expected from the Ponzo illusion subjects reported different angular sizes for the spheres. Murray and colleagues found a correlation between the difference in the perceived angular size and the activation in the primary visual cortex: „*the retinotopic representation of an object changes in accordance with its perceived angular size.*"

A further conclusion of [Murray2006] was: „*the ultimate goal of the visual system is clearly not to precisely measure the size of an image projected onto the retina. A more behaviorally critical property of an object is its size relative to the environment, which helps determine its identity and how one should interact with the object*". Results of this study indicated, that illusion effects lead to measurable differences in V1 activity, but only five participants were investigated in that study. In a recent article, Schwarzkopf and Rees [Schwarzkopf2013] published results of another fMRI study. They investigated cortical activity with regard to the Ebbinghaus illusion, and found that a smaller distance between the inner circle and the outer

circles have a considerable impact on the illusion strength and this can also be measured in the V1 brain activity.

Alternative formulations of SDIH were also discussed: according to [Epstein1961] SDIH is an: „*[...] the apparent size of an object is uniquely determined by an interaction of visual angle and apparent distance*“. A mathematical formulation would be $S' = D' * \tan(\alpha)$ with the interaction of visual angle and apparent distance on the right hand side of the equation. From a mathematical point of view this is a transformation of [Kilpatrick1953]: „*a retinal projection or visual angle of given size determines a unique ratio of* apparent size *to* apparent distance“, or $\tan(\alpha') = S'/D'$. However, if the right hand side of the equation is considered a description of an underlying cognitive process, different underlying processes are assumed. In this regard, different formulations of SDIH assume different perceptual processes and coding sequences of the involved measures.

To investigate potential coding sequences, the precision of judgments near the perceptual limits, also termed “just noticeable differences“ or JND, can be investigated.

JND: About 200 years ago Ernst Heinrich Weber was the first to constitute the idea of a JND, which specifies a threshold value above which a change in stimulus intensity is perceived and recognized. According to his empirical findings, a stimuli I and an intensity change ΔI of that stimuli, have a proportional relation to each other which is known as:

$$K = \frac{\Delta I}{I} \tag{2.1}$$

For each stimulus class (e.g. brightness, loudness ...) the threshold value for ΔI has to be empirically quantified. The JND is considered a statistical quantity, thus the threshold is typically set to the value where subjects have a chance of at least 50% to detect a stimulus change ΔI for a given I. Typically, the 50% JND is reported, but in principle any value above 50% can also be reported. This proportional relation is today known as *Weber's law*

According to McKee and Welch: „*The precision of psychophysical thresholds is usually limited by noise in the neural pathways coding the stimulus dimensions*“ [McKee1992, p. 1447], and such noise typically influences the standard deviation of the judgments. If there is a dependency of coding sequences, the noise of a dependent measures should increase by subsequent processing steps. Authors conducted an experiment where subjects had to judge small incremental changes in vertical spacing between two horizontal lines. The two lines were presented through a stereoscope which allowed the manipulation of perceived depth by variations to the binocular disparity. McKee and Welch found that for small changes below 10 arc min[8] size judgments were considerably worse compared to angular size judgment, while for larger changes both judgments were almost equally good.

For small and large changes two quite different neural mechanisms were proposed: For small changes subtle differences in local contrast can be perceived and offer a direct basis for angular judgments. In case of larger changes, local contrast differences are no longer available,

[8] equals $0.1\overline{6}^{\circ}$

instead each object is supposed to be represented separately as a sign in visual memory associated with spatial coordinates. Angular judgment can now be done using the distance between these coordinates. That distance processing is done before angular size judgment is also supported by [Kaufman2006], who compared noise between depth discrimination and objective size discrimination and found the same dependency.

[McKee1992] also concluded, it is „*unlikely that information about angular subtense or retinal location is preserved beyond the binocular confluence occurring at striate cortex. The first primitive map of location may be generated at the striate level, but it already represents a transformation of the retinal coordinates*“. For the objective size judgment condition [McKee1992] assume an additional process in parallel to the angular size judgment which transforms the spatial coordinates with the help of additional depth cues. In case of small changes the spatial representation is already subject to some noise and a second transformation based on depth information seems to lead to an overall impaired objective size judgment compared to the angular size judgment. In case of larger differences the impact of the noise is less strong and compared to angular judgments almost equally good results seem to be possible.

Several theories were presented so far, how the perception of size and distance are probably related to each other, and it was also mentioned a couple of times that distance is “derived from depth cues“. The next section will summarize different types of depth cues.

2.3.1.3 Depth Cues

Depth cues are of specific interest for this work, because there are several differences between simulated mirror views in a driving simulator and real mirrors (see section 3.5), which lead to differences with regard to some of the cues.

Criteria	Explanation
Accommodation	Adjustment of lense curvature by ciliary muscle
Vergence	To focus an object with foveal vision the viewing direction of both eyes must point straight towards the object. The rotation of the eyeballs is called vergence and if an object moves towards the observer the eyes converge each other and if it moves away the eye diverge from each other.
Binocular disparity	Only the focused object projects onto corresponding retinal locations in both eyes (the center of the fovea). For all other objects the retinal image has an offset from the fovea but at a different amount for both eyes, the disparity. The amount of disparity depends on distance of the object compared to the focused object
Occlusion	Objects can be partially / fully hidden by those located in front of them
Perspective	Relation between size distance and angular size based on optics, see Figure 2.5
Texture	Geometrically regular surface patterns help us to recognize the orientation of an object. With increasing distance such regular patterns continuously decrease in size. With increasing distance more and more surface details also fall below the visual acuity and are no longer recognized. For groundplane textures an additional foreshortening effect exists: drawing a circle on a piece of paper and putting it on the floor in different distances, it can be seen that with increasing distance the circle appears more and more like an ellipsoid. The vertical size (in the direction away from the observer) shrinks faster than the horizontal size.
Lighting, Shadows, Shading	Directional lighting causes objects to cast shadows onto other objects. Shading is a term used in computer graphics and describes how an object surface appears to our vision. It depends on the roughness of a surface how much light is reflected towards our eyes.
Atmosphere	Dust, rain, snow or also smog particles impact our vision, the farther away an object the more particles will be between the object and the observer. They impact brightness, contrast and color perception.
Familiarity	Knowledge about size of objects; if an object of known size appears smaller it is typically concludes that its more far away.
Motion parallax	see Figure 2.8 below.

Table 2.1: Different depth cues gathered from [Goldstein1997] and [Bruce2003].

When focusing an object, vergence and accommodation (physiological cues) are necessary to 1) orient the eyeballs towards the target object which is achieved by the contraction / relaxation of the six extraocular muscles (vergence) and 2) to adjust the lens to focus the object by contraction / relaxation of the ciliary eye muscle which adjusts the shape of the lens (accommodation). Effects of accommodation and vergence are considered to be relevant in a near range up to 10 meters.

Binocular disparity is the difference between the two angles α and β shown in Figure 2.9 and is the main cue for stereo vision. Similar to the previous two physiological cues the effect of disparity is most effective in the near field. Because disparity decreases with squared distance, it quickly looses its power with increasing distance.

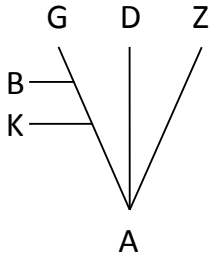

Figure 2.8: Figure according to [Burton1945] (Fig. 54). Motion parallax was already known to Euclid. The observer is located at A and the lines B and K are moved from left to right through the visual field at equal speed. Euclid's assumption was: „*When objects move at equal speed, those more remote seem to move more slowly.*"

Besides the last two cues, all other cues are considered pictorial cues[9] and most of them work on much longer distance than the physiological cues and disparity.

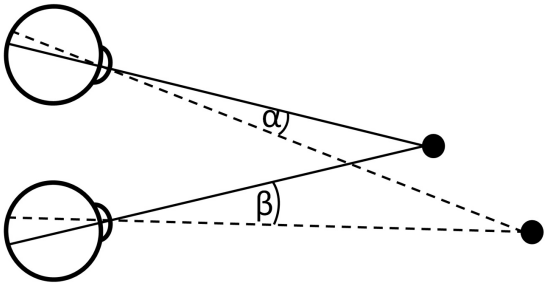

Figure 2.9: Calculation of binocular disparity (angle $\alpha - \beta$)

Occlusion can be considered twofolds: for each of the two eyes the same object occludes a slightly different part of the visual field due to the different viewing direction towards the object. Therefore occlusion has a meaning for stereo vision, but at the same time it works for monocular vision also.

Most of the effects of perspective (here linear perspective) are based on the relation which is described by the law of visual angle: objects more far away cast a smaller image on the retina. When two parallel lines recede towards the horizon the visual angle between them also reduces which gives the impression that they converge to each other with increasing distance, although the real distance between them remains the same. Similarly, a surface texture pattern reduces in size with distance. Figure 2.10 shows the specific effect of foreshortening, related to textures and the effect of perspective.

[9] pictorial, because they are used by painters to give the observer of an image the impression of depth and a three dimensional scene

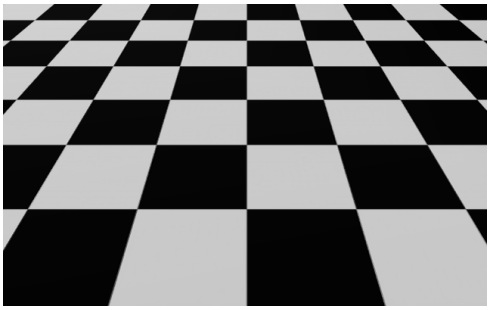

Figure 2.10: Effect of foreshortening: height decreases at a higher rate than width.

"Familiarity with objects" is often mentioned as a cue to depth, but it can be questioned „*what should be considered perception, and where do further cognitive processes start, which associate additional knowledge to support the estimation of the size of an object or distance*"? The knowledge that an object is x cm in height is certainly not directly given in the optical array, therefore an absolute size estimation always requires either the recognition of an object and remembering of associated knowledge about it, or learned knowledge about a unit of measurement (for example how large looks a meter in a given distance) which can be used to make an estimation for an unknown object.

The concept of a "visual yardstick" (a mental measurement reference) was already used by [Gilinsky1951]. Similarly, size estimations of an object can be done, by comparing it to another object, e.g. "This tree looks twice as large as the one next to my house". The remembered information about the tree next to "my house" was once perceived within the optical array. Such familiarity cues are often used, and they provide a cue to depth because a certain object size is assumed at a certain distance. Nevertheless, this information is not directly given in the optical array, instead it is associated knowledge.

Besides the different types of cues, it is of interest, which one is probably more effective and how do the different cues actually work together. Attempts which try to investigate this topic face a huge combinatorics problem and this question is still far from being solved. A systematic empirical investigation would need to test hundreds of combinations of cue pairs, triples, quadruples and so on. Furthermore, the magnitude of many cues can be varied on a continuous scale and the interaction between cues might not simply be a linear function.

Despite these problems, there are many published results about small subsets of cue combinations. Cutting and Vishton [Cutting1995] reviewed and gathered such information and proposed a hierarchy of cues (Figure 2.11).

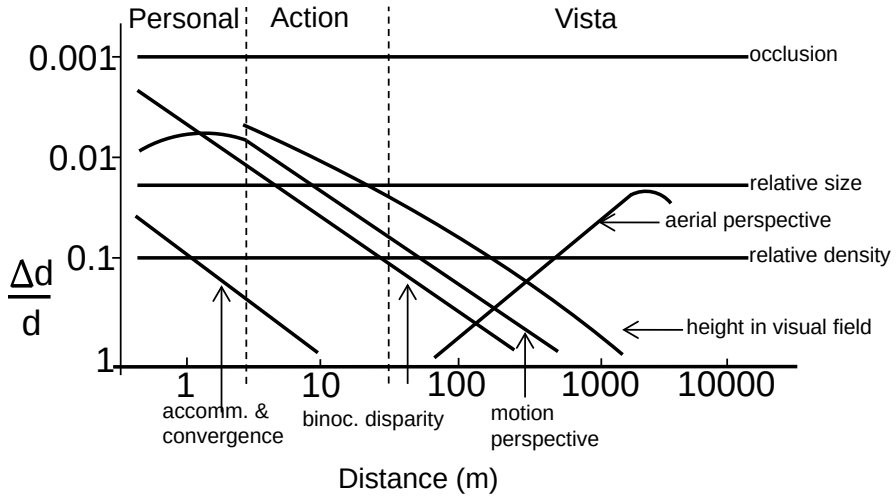

Figure 2.11: Figure is drawn according to Figure 1 from [Cutting1995], please see original article; x-axis distance in m; y-axis ($\Delta d/d$), depth discrimination threshold; Different depth cues with proposed precision values, smaller value = more precise

For each cue they assigned a level of precision or, in other words, how well a cue serves our visual system to extract information about depth from a visual scene. Precision was expressed by the a JND for depth. According to this classification, a cue is likely more relevant, if the discrimination threshold is small across a higher range of perceived distances. Occlusion offers the strongest cue to depth with a proposed constant precision of 0.1% (one millimeter per meter distance). But occlusion is a binary cue, and does not give information about the actual distance between objects. Nevertheless, if occlusion is available, it is probably the best available depth cue, and it is equally good across a wide range of distances.

Relative size and density are also available across a large range with almost constant precision. Aerial perspective effects (haze, fog, rain) work just the opposite way and get more effective at larger ranges when they start to cover objects with increasing fog / rain density. Accommodation and vergence offer only weak cues at distances above a couple of meters, and they are dominated by other cues if distances are $>=$10 meter.

In summary, there are many different possible sources which provide information about depth and spatial layout of a scene, but they vary with regard to their effectiveness. The general ability of our visual perception to extract multiple of these depth cues makes it very flexible. This is necessary, because the effectiveness of specific depth cues varies not only with distance (as depicted in Figure 2.11). Instead, environmental circumstances also influence how effective certain depth cues are, e.g. the effect of the "height in visual field" changes, if the observer moves from a flat to a mountainous environment, motion perspective cues change between walking around or driving a car and finally the effectiveness of accommodation and vergence are largely reduced with increasing age.

Additionally, certain depth cues can be perceived only, if at least two objects are considered: occlusion requires that one object is (partly) hidden by another one. Similarly, it needs an object which casts a shadow, and another object or surface where the shadow is seen. Walter Gogel was one of the main drivers behind the idea that relations between objects should be incorpo-

rated into theories of size and distance perception. He proposed the "adjacency principle" that „*perceived size and distance or position of an object is determined by whatever size or distance cues are present between it and adjacent objects.*" [Gogel1964, p. 1].

It is furthermore very likely, that our visual system uses a combination of different depth cues to reduce and balance between different flaws of the individual cues. [Cutting1995] argue that our visual system has probably evolved this capability to be able to deal with many different situations.

The theories mentioned in this section (e.g. law of visual angle, size constancy and SDIH) were also evaluated within a dynamic context but a further review on these theories goes beyond the scope of this thesis. Findings with regard to speed constancy were made by [Rock1968, Wist1976,Noguchi1981,Regan1986]. With regard to SDIH, [Gogel1997] reported, that it failed to explain the relation between perceived object size and perceived sagittal motion in depth[10].

Apart from size and distance, a further measure is of specific interest in the context of driving: the time-to-collision. The next section will present a brief introduction to this research topic and several findings inspired the modeling work with regard to gap acceptance in this thesis.

2.3.2 Perception of the Time-To-Collision

Research about the perception of the time-to-collision (also called time-to-contact, or ttc) is a broad research topic, and empirical findings were made in basic laboratory studies, as well as application specific studies in sports, e.g. catch a basketball pass, the receives has to coordinate his arm and hands which is presumably done using the time-to-collision. In the automotive domain, for example during overtaking on a rural road, the driver has to estimate, whether the gap towards the oncoming traffic is sufficient. A good overview on the time-to-collision research is provided by [Hecht2004].

[Lee1976] presented a mathematical derivation of the time-to-collision (ttc) which led to the specification of the optical variable τ. This variable is defined as Θ/Θ', with Θ the angular separation of two retinal image points, divided by Θ', the rate of change of the angular separation. In other words, the visual angle divided by its angular velocity. According to the mathematical derivation from the optical flow field, the visual perception should be able to directly perceive this measure. The critical part for a "correct" perception of τ is the detection threshold for the perception of the angular velocity. This publication of Lee inspired many authors to apply the ttc in scenarios where an observer approaches towards an object or vice versa.

In section 2.3.1.2 it was mentioned that the precision of visual processing near the detection and discrimination thresholds is an important measure, because noise at these threshold levels can be used to distinguish between different neural mechanisms for such processes[11]. Measuring thresholds is a difficult task, because the ttc is an aggregated measure, and if the empirical paradigm is not adequate, it is not possible to differentiate, if subjects rely on variations of 1) Θ' or 2) Θ/Θ' or 3) an absolute change of Θ during a single experimental condition.

[Regan1993] conducted a set of five experiments, where an isotropically expanding bright rectangle was presented on a monitor within an otherwise dark environment. No further cues

[10] sagittal motion = movement towards or away from the observer

[11] Note: the threshold for the "detection" of an angular velocity is different from a threshold for the "discrimination" between two angular velocities or ttc's.

to distance were available, the monitor itself was not visible, and viewing conditions were monocular with one eye being patched. It was systematically controlled which of the three mentioned cues (or combinations) were available to the subjects[12]. A set of moving stimuli was shown, before the actual target was presented, and subjects had to indicate whether the target was either "expanding faster / slower" or would "arrive sooner / later" than the mean of the stimuli set. Expanding faster or slower tests the angular velocity (Θ'), while arrive sooner / later targets the estimation of the ttc. Based on their results [Regan1993] proposed a number of different mechanisms:

1. „*There is psychophysical evidence that the human visual pathway contains a mechanism sensitive to the angular size* Θ *of a stimulus*" (p. 458)

2. „*Human visual pathway contains a mechanism that encodes the ratio* Θ/Θ' *rather independently of the absolute values of* Θ *and* Θ'" (p. 459)

3. Some restrictions have to be made: „*A necessary condition is that the value of* Θ/Θ' *in the object's retinal image does not vary with azimuth*" (p. 459), meaning there is no sideways movement. Additional limitations for this mechanism are *isotropically-expanding retinal images* and that the object is rigid / solid and non-rotating.

4. „*There is psychophysical evidence that the human visual pathway contains channels selectively sensitive to positive and to negative values of* Θ'*, [...] channels are important [...] in judging time to collision in aviation and driving.*" (p. 458)

5. „*When rate of expansion and time to contact were both available as cues, discrimination threshold was on average lower than when only one of the two cues was present. We conclude that there is some summation of the two cues.*" (p. 447)

6. „*However, evidence that the visual pathway is separately sensitive to* Θ *and to* Θ' *does not necessarily imply that subjects base judgments of time to contact on estimates of the ratio* Θ/Θ'" (p. 458)

7. Concerning discrimination thresholds they found for a range of ttc from one to four seconds, [Regan1993] report that the "discrimination" thresholds for Θ/Θ' was between 0.07-0.13 and discrimination threshold for Θ' was between 0.09 and 0.12.

It has to be considered that the experiments were conducted with few subjects only, therefore one should be careful at least with the actual values for the discrimination thresholds. The concluded mechanisms can be assumed only in case of isotropically expanding solid, non-rotating objects, but isotropic expansion and contraction can occur at any position on the retina.

Regan and Vincent [Regan1995] tested whether the previously proposed mechanisms vary, if motion is seen at different eccentricities in the visual field. The same empirical paradigm was used as previously by [Regan1993], but the expanding rectangles were also varied in their location, and they were shown at different eccentricities between 0 and 32 degree in all 4 major directions (left-right, up-down). For fovea vision it was found that, depending on the instruction

[12] see [Regan1995, p. 1847] for a description of the experiment setup

(expanding sooner/faster, arriving sooner/later than mean of stimulus set), participants made their decisions based on the task relevant variable, either angular velocity (Θ') or ttc (Θ/Θ') and they ignored the other information. Authors proposed that fovea vision might feed two parallel, separate pathways for Θ' and ttc which supports the previous finding.

For peripheral vision this strict separation did not hold: if the ttc was held constant between different conditions, variations to the rate of change influenced the ttc perception with increasing eccentricity. The discrimination threshold at 20 degree eccentricity was about factor 2.2 of fovea vision for ttc and 1.8 for Θ'. Compared to the much stronger drop-off for the visual acuity (factor six already at eight degree eccentricity) the motion detection is much less impacted with increasing eccentricity.

[Gray1999] reviewed the debate whether vision "calculates" the ttc based on the division Θ/Θ' (constructivism), or the ttc can be perceived directly (ecological approach). Although, their own experiments supported the ecological approach, they also remarked that it depends on the situation, which measures are actually used. They argue that human vision has a number of different potential alternatives to infer the ttc, and it depends on the situation: „*weighting of different sources of time-to-collision information has the effect of favoring the more unequivocal and reliable information.*" This is similar to the observation that was made with regard to depth cues [Cutting1995], our visual system has multiple options, which is necessary to adapt to various environmental conditions. Therefore, the search for one ultimate measure seems not to be useful.

How well people can actually perceive and judge the ttc is not only a question of discrimination thresholds (how well can differences be detected). The ability to perceive small differences does not automatically imply that estimations are correct, there can be underestimation or overestimation. Therefore, both parts need to be investigated to get a more clearer picture.

[Regan1993] published discrimination threshold for Θ/Θ' at about 7-13%, and for Θ' the threshold was about 9-12%. Both results were obtained with monocular vision, and no cues to absolute distance existed. [Gray1998] reported, if binocular disparity is the sole cue to depth, it allows discrimination thresholds of about 5.1-9.8%. No significant change was found when the target size was reduced from $0.7°$ to $0.03°$. For monocular vision, the threshold was between 2-12% for the larger target, but significantly larger for the smaller target (17-32%). With regard to the absolute estimation quality, the ttc was overestimated (3-10%), if binocular disparity was the sole cue. Instead, for monocular vision ttc was underestimated.

In a study of Hoffmann and Mortimer [Hoffmann1994], participants had to view short film snippets taken from the driver's perspective in a car-following situation. After a variable viewing time of the approach scenery (between 0.68 and 2.74 seconds) the presentation screen got black. Subjects had to wait and press a button when they thought they would have collided with the lead vehicle (they estimated the ttc towards the lead vehicle B in real time). Hoffmann and Mortimer varied the initial distance (18.9/31.4/43.9 m) and differential speed (1.04/2.27/2.78/5.20 m/s) to the lead vehicle B which lead to actual ttc values between 3.63 and 42.23 seconds.

On average, drivers underestimated the ttc by 20% with higher estimations for smaller viewing times. Hoffmann and Mortimer mentioned earlier studies, where underestimations of about 40% were found. They argued that in those previous studies either the observer, or the opposing object was stationary and absolute velocity was available, whereas in their experiment relative

motion between themselves and the lead vehicle was available: „*The only source of information for estimating ttc would appear to be the visual expansion of the lead vehicle. Thus with the elimination of absolute speed information, the estimation of the ttc is improved.*“ [Hoffmann1994, p. 519].

Besides the underestimation Hoffmann and Mortimer also reported a detection threshold for the angular velocity Θ', below which the ttc perception was drastically reduced:

- Above an angular velocity Θ' threshold of 0.003 rad/s, participants were able to estimate the ttc irrespective of the viewing time with similar accuracy.
- For angular velocities below the threshold of 0.003 rad/s, a shorter viewing time reduced the accuracy of the estimation.

They concluded that, above the threshold, a short viewing time (here 700ms) already provides sufficient information to estimate the ttc, even if the absolute change of the visual angle is quite small. Such a mechanism was previously proposed by [Regan1993]. Below the threshold, Hoffmann and Mortimer suggest that „*information about spacing changes of the lead vehicle during the viewing time may be used to infer the relative speed hence the time to collision.*“ [Hoffmann1994, p. 517].

Besides the average amount of underestimation (20%) and the detection threshold finding of $\Theta' = 0.003\ rad/s$, Hoffmann and Mortimer also reported that a number of participants *overestimated* the ttc, and the overestimation grows proportional with absolute value for the ttc: for a ttc of 3 seconds 2.3% of the drivers overestimated, for 5s 20% of the drivers and for 10s 38% of the drivers overestimated.

This study by [Hoffmann1994] inspired colleagues and myself to conduct a driving simulator experiment [Steenken2011]. It was tested, whether the observation with regard to the detection threshold still holds, when a driver observes traffic with the help of a rear view mirror, instead of directly observing a vehicle ahead. Participants were sitting in a driving simulator and a highway entering scenario onto the right lane of a German Autobahn was shown: the ego vehicle was driven by an automation and participants had to observe an approaching rear vehicle through the left exterior mirror. Compared to Hoffmann and Mortimer, the viewing time was considerably shorter in this experiment 200 - 600 ms instead of 690 ms - 2,7 seconds. The results supported the detection threshold in general, but at a significantly smaller level of $\Delta = 0.002\ rad/s$ or $0.171°/s$ instead of $0.003\ rad/s$. Similarly to Hoffmann and Mortimer, estimations above this threshold were significantly better compared to those below. In contrast, longer viewing times improved the accuracy of the estimation for situations above the threshold, but not for below threshold situations.

The results can also be interpreted in the context of the different mechanisms proposed by [Regan1993, Regan1995, Hoffmann1994]: above the threshold the ttc can be directly perceived by a dedicated mechanism and only very short viewing times below 600 ms probably impact its accuracy. The much longer viewing times used by Hoffmann and Mortimer (690 ms - 2,7 seconds) are probably not necessary for this mechanism to achieve better results. In contrast, for below threshold scenes, Hoffmann and Mortimer proposed that another mechanism might be in operation, which could rely on detection of changes in the absolute spacing. In this case, longer viewing times automatically result in a larger overall change of spacing, which probably

increases the accuracy of the estimation. In contrast, the very short viewing times in our setting (<600ms) might have been too short to measure a positive impact for this mechanism.

In the paper „*Perceptual Processes Used by Drivers During Overtaking in a Driving Simulator*“, [Gray2005] investigated two objectives 1) which driving strategies are applied during approach and lead car following before an overtaking maneuver, and 2) which strategies are applied for the decision making to overtake on rural roads with oncoming traffic.

As proposed by other researchers before, two different strategies for approaching / car-following were compared: constant distance and constant time-headway (TH). Constant distance strategy means, the driver approaches and then follows the lead vehicle at an individually different, but constant distance before he initiates an overtaking maneuver. For the time-headway strategy[13] the distance varies with the actual driving speed. The scenario was approaching towards and overtaking of a slower lead vehicle in regular intervals on a straight rural road. Drivers should consider the possibility that opposing traffic could emerge. The lead vehicle speed was constant but varied between situations (14 - 20 m/s). Subjects were explicitly instructed to drive as they would normally do in such a situation.

8 of 18 drivers used a constant TH strategy during approach, but variation between drivers was large (1.3 - 4.9 s, mean 2.2 s). 3 of 18 drivers used a constant distance strategy, and the distance between drivers varied between 50 and 60 meters. The remaining seven drivers used a mixed strategic approach, preferring a constant distance strategy for lower speeds, and a constant TH strategy at higher speeds. The threshold value when strategies were switched varied between 18 - 24 m/s.

In a second experiment the procedure was slightly changed: drivers were advised to approach the lead vehicle and follow it for a short amount of time. After 5 seconds of car-following, an acoustic signal was given, and an overtaking maneuver should be done, if possible. In this scenario opposing traffic occurred. Each of the 18 participants conducted 50 overtaking maneuvers. The lead car speed was varied between 9 - 18 m/s, and the speed of the opposing traffic was varied between 20 - 31 m/s. The initial distance of the opposing car was 200 - 400 m at the point in time when the acoustic signal was given. Figure 2.12 visualizes the measures, that were used to classify overtaking maneuvers as safe or not. A positive difference of the TTC - TRO was considered a safe overtaking maneuver. Actual overtaking maneuvers ranged between 4.9 s and 7.9 s difference with a mean of 2.6 s. 425 maneuvers were classified safe, 84 unsafe.

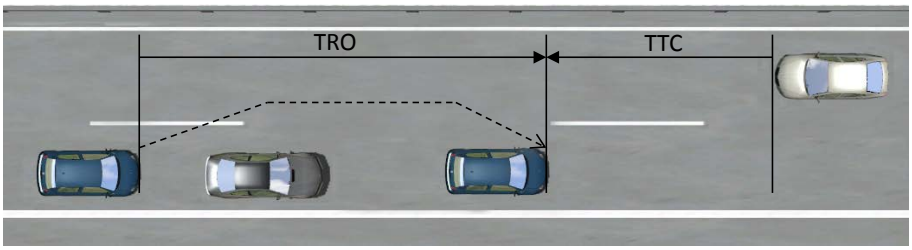

Figure 2.12: Situation is according to Figure 8a from [Gray2005], showing the *time required for overtaking* (TRO) and the time-to-collision (TTC) for the opposing vehicle to reach the same point.

[13]time-headway: time until a specific location is reached, if the current velocity remains constant.

Authors evaluated three potential strategies, which drivers probably used to decide whether an overtaking maneuver was feasible or not: 1) 11% of the drivers relied on an absolute distance strategy, 2) 33% of the drivers relied on the rate of expansion of the oncoming vehicle, 3) 56% of the drivers relied on the temporal margin strategy: a positive value for TTC - TRO.

Authors investigated whether there was a significant impact on the strategies, if the rate of expansion of the oncoming vehicle was above or below the threshold of $\Theta' = 0.003\ rad/s$ reported by [Hoffmann1994]. For drivers with the constant distance strategy, this threshold did not have any relevance, which seemed plausible, because they did not consider the dynamic of the situation. The drivers which applied the temporal margin strategy conducted only few overtaking maneuver for below threshold situations. For the drivers, who relied on the rate of expansion, there was a significant impact of the threshold: below, they used a constant distance strategy and above they used the temporal margin strategy.

2.3.3 Perception and Rear View Mirrors

Section 2.3.1 presented a review about basic research about the perception of object size and distance. The next subsection (2.3.3.1) summarizes the results of several studies which were interested in the question, how different types of rear view mirrors (planar, spheric or aspheric) change the distance perception of car drivers. The situations that were tested in these studies motivated the setup of the first driving simulator experiment of this thesis (Experiment 1, section 4.1).

It was already concluded by [Gray2005] that research on lane changing and overtaking has received much less attention, compared to the amount of research that was done on car-following, or driving skills (manual vehicle control). With regard to the topic of this work: "Influence of Different Rear View Mirror Types on Gap Acceptance Behavior", the number of studies is small. A reason for this is probably the high amount of effort for such studies. To systematically test gap acceptance behavior in field studies needs a test track, which allows to create and test reproducible traffic situations without the risk of traffic accidents. Section 2.3.3.2 describes the results of studies which investigated the impact of different mirror types on the perception of the time-to-collision, as well as gap acceptance.

2.3.3.1 Distance Estimation

[Flannagan1996] investigated the impact of different mirror types on the accuracy of distance estimations. Three mirror types were tested: a planar mirror, a spherical mirror with 1000 mm curve radius, and an aspheric A14 mirror with 1400 mm curve radius for the interior spherical part, which reduces to 175 mm for the aspheric outer part. Study participants were sitting in a stand-still car on the driver seat. An anchor car was located at 20 meter distance ahead of them (measured from subject's eye position) and a rear car to the left behind of them visible was located at distances of 5,10,20,30 and 40 meter (distance was measured between mirror and front of the rear vehicle). The mirrors were adjusted horizontally, until each subject could see the same section of their own vehicle. Authors explicitly noted that in the 5 and 10 meter condition the rear vehicle was only partially visible in the planar mirror.

Participants were informed that the study was about an „*innovative rear view mirror*", but no

further information about the mirror characteristics were given. The task of the subjects was to give distance estimations of the rear car, relative to the anchor vehicle (100% if rear seemed to be at equal distance, <100% in case it seemed to be closer and >100% if it seemed to be farther away). The experiment consisted of three phases, a pre test, a training and a post test phase. During the pre test, as well as the post test, subjects had to give estimations only. During the training, they first gave an estimation and afterwards they could to take a direct look at the rear vehicle.

Accumulated across all five distances, results showed that the planar mirror lead to strong underestimation of distances (about 35%), while the curved mirrors lead to less underestimation. During the pre test, the estimations for the two curved mirrors were significantly different from each other, while this was no longer the case in the post test. For the spherical mirror (which had the strongest curvature) estimations were initially higher compared to the aspheric, but after some trials the estimations were at similar compared to the aspheric mirror. Compared to the planar mirror, the curved mirror types lead to significantly higher estimations (less underestimation). This was the case in all three phases. For the first phase, authors also tested, whether the strength of underestimation caused by each mirror types is correlated with the visual angle subtended by the rear vehicle seen. The predicted underestimation by the visual angle was larger for both curved mirrors but the relative difference between the mirror types was correctly predicted.

In a second study a year later, [Flannagan1997] compared distance estimations with an identical spherical mirror on the driver side and the passenger side. Compared to the spherical mirrors on the driver side the same mirror on the passenger side led to even more underestimation. Authors concluded that the eye-mirror distance significantly contributes to the difference between driver side and passenger side mirror. Authors also argue that a simple model which uses the visual angle of an approaching vehicle qualitatively predicts the effect of decreasing underestimation with increasing convexity, but the quantitative predictions significantly differ from most of the published results. Authors again tested how well the visual angle subtended by the vehicle could be used as a predictor for the strength of the underestimation effect. Similar to the driver side mirror the qualitative prediction was correct, but the quantitative prediction exceeded the actual effect size for the passenger side.

In a third study, [Flannagan1998] tested spherical mirrors with very large radii up to 8900 mm. Their goal was to evaluate, whether the quite small minification effect of such a large radius convex mirror would fall below the JND. A slight but still significant difference of 8% was found, and the conclusion was that even such large radii still impact the distance perception.

Carstengerdes compared planar, spherical and aspheric mirrors in his doctoral thesis [Carstengerdes2005]. His point of emphasis was on testing the aspherical mirror portion more explicitly. Therefore the interior spherical / convex part of the aspheric mirror was completely covered with tape. Similarly, the same portion of the other two mirrors was covered with tape. Similar to the study of [Flannagan1996] a magnitude estimation paradigm was used for a distance estimation experiment. The distance to the rear car was manipulated between 4 and 20 meter, measured between mirror location and the front bumper of the rear car. In contrast to [Flannagan1996], the reference object ahead was a pylon at a distance of 12 meter. Similar to the experiment of Flannagan, subjects had to give relative distance estimations in percent. The results of his study supported the findings that were previously made by [Flannagan1996]

with regard to the difference between planar and both curved mirror surfaces.

According the the author, the study setup had some drawbacks and constraints: Carstengerdes instructed participants to estimate the distance from themselves towards the opposing car, but he admitted that some may have estimated the distance between the rear end of their own behicle and the front of the opposing car. Several participants also criticized the low degree of reality, because only a small portion of the mirrors was visible.

The findings which were consistently reported by all studies are: distances are underestimated with planar mirrors and curved mirrors lead to a lesser amount of underestimation. From a perspective of traffic safety, underestimation is positive, because the underestimation of gaps should lead to lesser acceptance of small gaps. The magnitude of the underestimation effect is highly subjective and it varied between the studies. But a comparison of the effect size is problematic, because the conditions and setting of the studies are different, too.

Apart from the investigation of different mirror types, Meyer and Skottke [Meyer2013] investigated, how different mirror adjustments impact the perception of distances. Participants of their study had to look at photos, which showed the left exterior mirror view from the position of the driver. The ego car was located an the right of a two-lane road, and a rear car was standing on either the right or the left lane at a distance of 12.5m, 25m or 50m behind the ego car. The left exterior mirror was adjusted at three different horizontal positions and two vertical positions, which lead to different views at the rear scene. As a consequence of the horizontal adjustments, the visibility of the ego car in the mirror ranged between "not visible" and "ego car covered $1/3$rd or $2/3$rd" of the horizontal mirror space. Authors also varied the vertical adjustment, aligning the horizon to the center or to the upper part of the mirror. In general, distances were underestimated when using a rear mirror. All three variables (distance, mirror adjustment as well as lane position of the rear car) had a significant impact on the accuracy of the distance estimation.

2.3.3.2 Time-to-collision Estimation and Gap Acceptance

[Carstengerdes2005] also conducted an experiment, where subjects had to estimate the ttc towards an approaching rear car. Similar to his distance estimation study, subjects had to use three different mirror types (planar, spheric and aspheric). To conduct such an experiment within a normal driving scenario, a large test track would be required. Because such a track was not available, the experiment was conducted with a stand-still ego vehicle, while the rear vehicle approached at a speed of either 20, 30 or 40 km/h. A hydraulic shutter mechanism was installed in front of the mirror, and by opening and closing it, it was possible to control how long subjects could use the mirror view. When the approaching rear car passed a first light barrier, the shutter was opened, and the mirror view got visible. Passing a second barrier closed the shutter, and afterwards the approaching vehicle stopped. The second barrier was located at five different distances (20-60 meter) behind the ego vehicle, thus not only the approaching speed but also the overall distance to the ego vehicle was manipulated.

The ttc was underestimated with all three mirror types, but the effect strength varied between the mirror types: planar mirror (51.9%), spheric (47.3%) and aspheric mirror (48.3%). No significant difference was found between the spherical and aspherical mirrors, but a significant difference was found between the curved mirror and the planar mirror. The influence of

both, speed and distance was significant, but independent of the mirror type the distance had a stronger influence compared to the speed.

With regard to gap acceptance, Walraven and Michon [Walraven1969] conducted a study with a planar and two spherical mirrors. The spherical mirrors had curvatures of 1200 and 600 mm radius. Six experienced and six unexperienced drivers drove within a DAF YA 314 truck at 50 km/h on the right lane of a two lane highway[14] A rear vehicle approached from behind on the left lane with a speed difference of 0, 13, 30 or 40 km/h. The left mirror was put in a box which had a shutter mechanism that opened as soon as a certain distance between approaching and subject's car was reached. The distance was varied in steps of five meter up to a total distance of 100m. Subject's task was to accept or reject a lane change. The response was given with the indicator lever.

The results were 1) at higher speeds larger distances were required for an overtaking decision, but generally experienced drivers accepted shorter gaps. 2) Experienced drivers accepted smaller gaps with spherical mirrors, although this effect was small. In contrast, the accepted distances increased for the inexperienced drivers. It was argued, that inexperienced drivers are probably more cautious, especially at the higher speed differences. This probably negates the minification effect of the spheric mirror. 3) Spherical mirrors did not lead to a change in the reaction time. Their overall conclusion was that spherical mirrors with a radius of at least 1200 mm can be mounted, because "serious effects on driver behavior is to be expected not even in the conservatism of youthful car owners."

[deVos2000] conducted a last safe gap experiment, and investigated the impact of different mirror types on gap acceptance. They used a planar mirror, a spherical convex mirror with 1400mm curve radius (C14), and two different aspheric mirrors with 1400 mm (A14) and 2000mm curve radius (A20). Participants drove on the right lane of a closed two-lane highway with a speed of 30 km/h, while a vehicle from behind on the left lane approached at either 50, or 80 km/h. Participants were instructed to indicate a lane change at the last possible moment, equaling the last safe gap they would accept.

Independent of the mirror type, it was found that the last safe time gap reduced with higher speed differences (on average from 5.1 seconds for 20 km/h speed difference to 2.9 seconds for 50 km/h speed difference). With regard to the different mirror types, the last safe time gap reduced from 4.4 seconds for the planar mirror, to 4.0 seconds for the A20, 3.8 seconds for C14 and 3.7 seconds for the A14. Compensation effects amongst drivers who had experience with spherical mirrors were found, but not for drivers who had experience with aspheric mirrors only. Authors mentioned, that aspheric mirrors were only recently mounted, and driving experience in general was smaller for these subjects, compared to those who had more years of experience with spheric mirrors. According to the authors it can be questioned, „*if it is acceptable that drivers are only able to compensate after many years of experience.*" [deVos2000, p.76].

Another interesting result was found in the explanatory questionnaire: „*The extent to which drivers turn their head reduces with increasing mirror convexity*" [deVos2000, p.78]. This can be considered a safety risk, because a wrong adjustment of the mirror does not reduce the blind-spot region as much as probably expected.

Apart from the investigation with real mirrors, another study was conducted by [Flanna-

[14]Experienced drivers were professional truck drivers who were also familiar with spherical mirrors.

gan2003] which investigated whether a camera-based rear vision system impacts gap acceptance behavior. The synthetic vision system emulated two conditions: a planar mirror view and a view with an image minification of 0.5. The latter one approximates the minification of a convex mirror with 1400 mm radius (C14). The LCD display was mounted on top of the middle console, at a comparable distance to the left mirror. The ego vehicle was driven by the participant at a speed of 40 km/h on the right lane of a closed two lane road. A vehicle from behind on the left lane approached at 56 km/h. Subjects were instructed to indicate the last safe gap for a lane change and the results were surprising.

The shortest accepted average distance was observed for the conventional planar mirror (27.2 meter). For the vision system with a minification of 0.5 almost the same gap size was accepted (27.5). For the simulated planar mirror view gaps were actually larger by about 25 %. It was expected that the accepted gap size would be equal for the planar mirror and its simulated counterpart, and that smaller gaps would be accepted for the simulation which had a minification of 0.5. They concluded, that drivers might have been more conservative with the new vision system, and this probably led to the overall larger accepted gap size for this system. Authors admitted, that more research is necessary and the results should be considered preliminary.

In comparably complex study was done by the US highway administration [NHTSA2008] and the impact of different mirror types on gap acceptance was investigated within a couple of different overtaking scenarios. The investigated normal planar, spherical and aspherical mirrors, but also some new mirror designs called “Elongated“, which were available for planar and convex surfaces. Those mirrors had a larger vertical size, comparable to mirrors which are mounted on trucks. Compared to all previous studies, the main difference of this experiment was that drivers were allowed to use the interior mirror. In this study, no effect of the mirror type could be found for any of the tested lane change situations. The explanation was, that drivers do not rely on the exterior mirror and use the interior mirror instead. This might be true, but makes the experiment setting ineffective with regard to an explanation about the effect of the different mirror types. Also, no consequences can be drawn for those drivers which do not have the possibility to use an interior mirror, e.g. drivers of vans with closed cabins, truck drivers or motorcycle drivers.

2.3.4 Summary

Within this section an overview was given about different theories on size and distance perception (section 2.3.1), including a discussion of different depth cues (section 2.3.1.3). Afterwards, studies with regard to the perception of the time-to-collision were summarized (section 2.3.2). Finally, literature was reviewed, which dealt with the impact of different types of rear view mirrors on the perception of distance and time-to-collision, as well as the impact on gap acceptance and lane changing (section 2.3.3).

Size Distance Perception Early writings about optics by Euclid describe the relation between real object size, distance between an observer and an object, and the projected image size on the retina. The visual angle can be used to describe the image size that an objects casts onto the retina, and is an important measure used by all theories. It was found that the visual angle is a good predictor for the estimation of the size of an object in situations where

depth cues are reduced. This led to the formulation of the law of visual angle. The opposing concept is size constancy, which describes a different situation: with additional cues to depth, size estimations continuously shift towards the estimation of the linear object size (cmp. [Holway1941]. The strongest cue which leads to size constancy is probably familiarity, but it can be discussed whether the association of learned knowledge about the size of an object still remains perception only.

The size-distance invariance hypothesis (SDIH) proposed that „*a retinal projection or visual angle of given size determines a unique ratio of* apparent size *to* apparent distance“ [Kilpatrick1953]. This theory can be used to describe the effects of both, law of visual angle and size constancy (section 2.3.1.2). However, SDIH fails to explain certain visual illusion effects, for example the Titchener circles or the Ebbinghaus illusion (see Figure 2.7). In this regard, fMRI studies have provided some evidence that our visual system transforms the retinal size of an object, and that additional contextual information influence the estimation of the angular size. The influence of contextual information or relative measures between objects (relative distances, relative height) on perception of size and distance was already expressed in the adjacency principle by Gogel in the 1960's.

Psychophysical experiments were also conducted to unravel the processing order between angular size, perceived distance and perceived object size. It was proposed by [McKee1992] that a coordinate representation is created very early from the retinal image, and that the distance information between these coordinates is later on transformed by depth cues. It was proposed that separate processes exist for the estimation of angular size and linear size but both are based on the coordinate representation.

Time-to-Collision The question, if and how the ttc is perceived, has drawn the attention of lots of researchers. The ttc can be formulated as the quotient of the distance in meter, divided by the speed difference in m/s. It has been questioned whether these measures can be perceived, and whether these mental calculations are necessary. [Lee1976] proposed that the ttc can be perceived directly from the optical array. According to the τ theory, the time-to-collision can be calculated by Θ/Θ', the angular size as well as its rate of change are available on the retina.

Further psychophysical research by [Regan1993] supported this assumption, and they proposed that the visual system has separate mechanisms or channels, which are sensitive to different measures: 1) the visual system is sensitive to the angular stimulus size Θ'. 2) the visual system is sensitive to Θ/Θ' with a discrimination threshold of 0.07-0.13. This channel is rather independent of the absolute values of Θ and Θ'). 3) Separate channels were also proposed for positive and negative Θ' with a discrimination threshold between 0.09-0.12. This latter observation supported previous work by [Noguchi1981, Regan1986].

The work of [Regan1995] extended these findings and proposed that these channels work relatively independent for fovea vision, but with increasing eccentricity, there is an increasing interference. At 20 degree of eccentricity, the discrimination threshold for the channels Θ/Θ' and Θ' is already about twice as high, compared to fovea vision. However, the threshold is still considerably lower as the decrease of visual acuity would suggest (which is about factor 6 to 8 degree). [Gray1998] reported that with binocular vision (and disparity as solely cue) discrimination thresholds for ttc do not change if the object size is manipulated (between $0.7°$ to $0.03°$). For monocular vision instead, the threshold was about three times larger for the

smaller target.

[Hoffmann1994] reported that the ttc can be estimated irrespective of the viewing time (0.68 - 2.74 seconds), as long as the angular velocity Θ' remains above a threshold of 0.003 rad/s. Below the threshold, shorter viewing times led to a considerably reduced accuracy. It was proposed that the channel which is sensitive to the ttc (Θ/Θ') operates only above the threshold, while below the threshold, subjects probably have to rely on absolute changes of Θ and Θ'. Longer viewing times increase the overall larger changes, which could be an explanation why performance was improved in below threshold situations.

Hoffmann and Mortimer also reported that with increasing ttc, an increasing number of participants began to *overestimate* the time-to-collision (for ttc of 3 seconds, 2.3% overestimated, and for ttc = 10 seconds already 38% overestimated). This finding challenged the assumption that the channel for Θ/Θ' is completely independent of the absolute values of Θ and Θ' as it was proposed by [Regan1993].

In another experiment by [Steenken2011] it was observed, that the accuracy of the ttc perception reduces even above the threshold of 0.003 rad/s, if the viewing time is reduced to values between 200-600 ms. It was proposed, that 600 ms are already the maximum necessary time for the channel, which is sensitive to the ttc (Θ/Θ') and a negative impact on the accuracy can only be found for shorter viewing times. Because Hoffman and Mortimer did not test shorter viewing times (shortest was 680 ms), this effect was not observed previously.

Impact of Different Mirror Types The last part of this chapter summarized empirical findings with regard to the use of exterior rear view mirrors. In most studies, distances with flat mirror types were underestimated on average by 20-40% [Flannagan1996,Flannagan1997,Carstengerdes2005]. With increasing surface curvature (smaller radius), the amount of underestimation was reduced, and for the most strongly curved mirror surfaces there was already a significant amount of overestimation reported. It was proposed that the minification effect could be used to explain the effects but according to [Flannagan1997, p. 1]: „*The effect of convex mirrors on distance judgments is not well understood [...]. No quantitative model has been proposed that is even approximately accurate in predicting the magnitude of the overestimation effect*“.

Similarly to the underestimation of distances, the ttc is also underestimated if planar mirrors are used. Furthermore, the underestimation of the ttc decreases with increasing mirror curvature. With regard to the lane change, the results are indecisive. The overall number of studies on this topic is comparably small, but it was found that drivers actually accept smaller time gaps with increasing mirror curvature [deVos2000]. But authors also concluded that the changes are not big enough to cause serious problems. However, studies have not directly investigated critical situations (in dense traffic, when gaps are smaller in general).

It was also argued that the benefit of reducing the blind spot region outweighs the negative effect of smaller accepted time gaps. On the other hand, accepting smaller gaps might not directly lead to more accidents, but certainly leads to frustration for those drivers who are forced to initiate stronger braking maneuvers, which could force more aggressive driving.

The results of the reviewed gap acceptance studies were limited with regard to the level of detail. Different traffic situations were tested, but as a result, single characteristic number were reported, e.g. an average reduction of the time-gap, the distance gap or the amount of

underestimation. Objective 2 of this work targets a behavior simulation model which requires a more detailed database. Therefore, the second experiment in this thesis (section 4.2) tested 3 different mirror types and 26 traffic situations. The results of this study are presented in the experiment chapter (section 4.2). A more detailed investigation of the individual behavior differences is given in the modeling chapter (section 5.4).

3 Simulation of Different Mirror Types in a Driving Simulator

The driving simulator and it's software SILAB[1] are used for two different aspects of this work: two empirical studies are conducted in the simulator (chapter 4), and the developed driver model (chapter 5) is also connected to the software and interacts within the same driving scenario as the subjects in Experiment 2.

This chapter describes the effort that was necessary to upgrade the simulator with additional hardware and software to be able to conduct the studies as well as to feed the driver model with the required data. The first subsection describes the technical equipment (3.1) while the following subsections describe, how the simulation of the different mirror types was accomplished. Afterwards a brief summary is given about the differences between the real mirrors and the simulated ones, and whether these differences can have an impact on the expected quality of the simulation results. The last subsection provides some technical details on the calculation of *visual angles* in the simulator, which is important for the driver model.

3.1 Hardware Platform and Software

The first version of the driving simulator was build at the start of a 3-years, nationally funded project (named IMoST, Integrated Modeling for Safe Transportation) in the middle of 2010. All of the hardware assembling, the electrical work and the low-level software development was done by colleagues from the DLR Institute of Transportation Systems, Brunswick which whom we worked together in close cooperation. Figure 3.1 shows the first installation of the simulator back in 2010. Although this small mockup was successfully used in a number of experiments, it was found that drivers had a tendency to stay very close to the right side of their actual driving lane.

The first assumption of an incorrect calibration of the simulator perspective has been rejected. In some dedicated tests, drivers where advised to stay in the center of their lane, but instead they were driving about 40 cm to the right. The feedback of the drivers indicated that the physical extent of the simulator (which was the front left quarter of a real car at that time, see Figure 3.1) might be responsible for this problem. Subjects did not have a good feel for their own position on the road and because the passenger side was completely missing they could also directly watch the road to the right.

Because the objective of this work is to investigate and model the estimation of distances, relative speed and also gap acceptance this was a serious problem: the fact that people don't have a good idea about their own location on the road and also the boundaries of their vehicle

[1] www.wivw.de/silab

seemed to bear the risk that the empirical results might suffer because of an inappropriate simulator design.

Figure 3.1: First installation of the driving simulator in 2010

To improve the simulator, a number of components had to be added, before the studies could be conducted (engine hood, left mudguard, passenger side / door and dashboard). The revised simulator can be seen in Figure 3.2. It has the dimensions of the front of a real vehicle until B-pillar, and gives the driver a more realistic feeling inside the simulator.

Figure 3.2: Driving simulator lab since middle of 2014.

Section 3.2 gives a brief overview of the hardware and software components that are currently installed in the simulator. The implementation of the different mirror types investigated in this thesis is covered within section 3.3. Besides the implementation details and calibration issues, differences between properties of real mirrors and simulated mirrors with a focus on depth perception are discussed in paragraph 3.5.

3.2 Technical Specification

The physical dimensions of the simulator correspond to the front half of a middle class vehicle (until B pillar). It is surrounded by 3 video walls, each 240 x 240 cm in size. The following listing briefly describes the main components of the simulator:

Main visualization: The 3-beamer configuration (Canon XEED SX6, 1400*1050) offers a maximum field of view of 150 degree. Each beamer is connected to a workstation (Core2Duo, 3.0Ghz) equipped with a Nvidia 9800GTX graphics card.

Side Mirrors: Two additional displays with a resolution of 1024*768 are used for the simulation of left and right exterior mirror powered by an identical workstation as used for the beamer.

Cockpit: The software to simulate the cockpit instrument view is installed on a windows tablet pc with a screen resolution of 1024*600.

Audio: A Teufel 5.1 speaker system is integrated and the audio simulation for ego vehicle sounds and surrounding traffic participants uses OpenAL. The software allows the integration of additional acoustic stimuli that can be triggered as timed events which is often needed for specific experimental paradigms.

Haptic Feedback: Three Lexium Schneider CAN bus servo drives (LXM05A) apply force feedback and vibration signals with adjustable amplitude and frequency on the steering wheel as well as accelerator and brake pedal.

Peripheral Hardware: To integrate additional hardware devices a WAGO CANopen fieldbus controller (750-337) is connected which can control up to 64 different A/D converter modules.

The software basis for the driving simulator is SILAB, which is commercially sold by the WIVW[2]. It offers the basic functionality to create traffic scenarios, including landscape simulation, complex road network design, vehicle dynamic simulation, simulation of additional traffic participants and lots more. Additional functionality can be integrated in form of .dll plug-in libraries.

3.3 Mirror View Simulation

In Figure 3.2 the two exterior mirrors which show the rearward scenery can already be seen in their final state as used during the two studies. Unfortunately, smaller displays which would

[2] www.wivw.de

have fitted inside the mirror case did not have an acceptable resolution, or were not available for end customers in small quantities. Therefore the available LCD displays had to be mounted on top of the original mirror case. To give their visible front surface a more realistic, mirror-like appearance, a cover was cut according to the mirror surface dimensions and shape of a VW Passat Variant, model generation 2013.

To simulate a corresponding mirror view, a separate instance of an OpenGL[3] window has to be opened by the simulator software and needs to be configured appropriately. For this purpose, a specific SILAB DPU is instantiated multiple times on different computers to generate all the views (three beamer views and the two mirror displays). Each view implements an OpenGL camera which shows a *planar* projection of the 3D scenery. Parameters like camera orientation, height above ground and positioning in 3D space have to be adjusted to fit with the needs of the respective view. The SILAB implementation of the camera view also allows to render a "mirrored" 3D scene which is important to realize the correct visualization. Furthermore, the DPU has two configurable parameters for the *vertical* field of view angle in degree (FovY° or "Field of view in Y / vertical / upwards direction") and the aspect ratio. Because the LCD displays have a screen resolution of 1024*768, the aspect ratio parameter is 4:3. In contrast, the field of views of real mirrors is typically specified by the *horizontal* field of view in degree. Calculation from horizontal into vertical field of view can be done using the aspect ratio parameter, for example FovY° = horizontal field of view / 4 * 3.

[Bach2006] reported horizontal field of view ranges for each mirror types: 16.3° - 24.9° for planar, 24.2° - 32.2° for convex and 29.4° - 40.4° for aspheric mirrors. Table 3.3 shows actually measured values for different mirror types reported by the NHTSA[4].

Table 7. Angular coverage, direct view limit, and blind angle as a function of mirror type.

	Average Actual	Projected					
Mirror Type	Flat	C20	C14	A20 Convex Part	A20 Overall	A14 Convex Part	A14 Overall
Coverage in Deg *	12.6	22.6	28.4	15.8	41.1	19.0	39.0
Direct View Limit * in Deg	58.8	58.8	58.8		58.8		58.8
Blind Angle in Deg	46.2	36.2	30.4		17.7		19.8

** Measured from rear longitudinal axis*

Figure 3.3: Measured field of view of different mirror types, according to [NHTSA2008, Table 7].

Each mirror reported in Figure 3.3 has a dedicated ID which start either with a *C* or an *A*. The letters abbreviate convex (spheric) or aspheric and the number (20, resp. 14) is a short term for the radius of curvature with values of 2000 or 1400 mm. For the convex (C) mirrors the whole surface is equally curved, therefore the field of view can be reported as a single value.

[3] https://www.opengl.org/

[4] National Highway Traffic Safety Administration

For the aspheric mirror types, the outer portion has an increasing curvature. Therefore two field of view values are given for A20 and A14, one for the inner convex (spheric) part and one value for the total mirror including the outer aspheric part too.

3.3.1 Planar Mirror Simulation

In the introduction and the literature section (see 2.3.3) it was already mentioned, that a planar mirror reflects the environment without any distortion or minification. The visible size of an object remains the same, as if it would be seen directly by the observer. This demands a proper adjustment of the field of view angle for each OpenGL view (each of the three front views, but also each mirror view). The correct angle can be calculated using the distance between the driver and the mirror display in the simulator and the size of the visible mirror display surface. The measured width of the visible portion of the mirror display was 17.5 cm and for the eye - left exterior mirror distance a value of 65 cm was measured.

> **Remark**: It has to be considered that the 65 cm are an average value and vary from subject to subject. During the two studies (next chapter) a fixed position of the back rest was used and subjects were allowed to adjust the seat on the track only within a limited range of 15 cm. To measure the average position, the seat was centered on the track. A medium sized test person (1.76 m) had to sit in the simulator and put his head against the head cushion, looking towards the mirror. A distance of 65 cm was measured between the test person's nose and the center point of the left side mirror.

For these two values the tangent formula can be used to calculate the horizontal field of view in degree: $atan(\frac{17.5°/2}{65.0}) * 2 = 15.33°$. This value is within the range of the published numbers [Bach2006, NHTSA2008] and for the calculated angle, objects are displayed at their original size. This is true at least for the reference / average seat location. As long as no real-time head measurement can be done to adapt the field of view of all displays during simulation, the movement of the subjects can not be compensated. Based on the horizontal field of view the SILAB parameter FovY° can be calculated $15.33°/4 * 3 = 11.5°$.

Horizontal and Vertical Adjustment After the adjustment of the field of view was done, the next step is the horizontal adjustment. Directive 2003/97/EG from the European Commission [EC2003] can be used as a guideline for this. Figure 3.4 shows the minimum horizontal range that a driver must be able to observe.

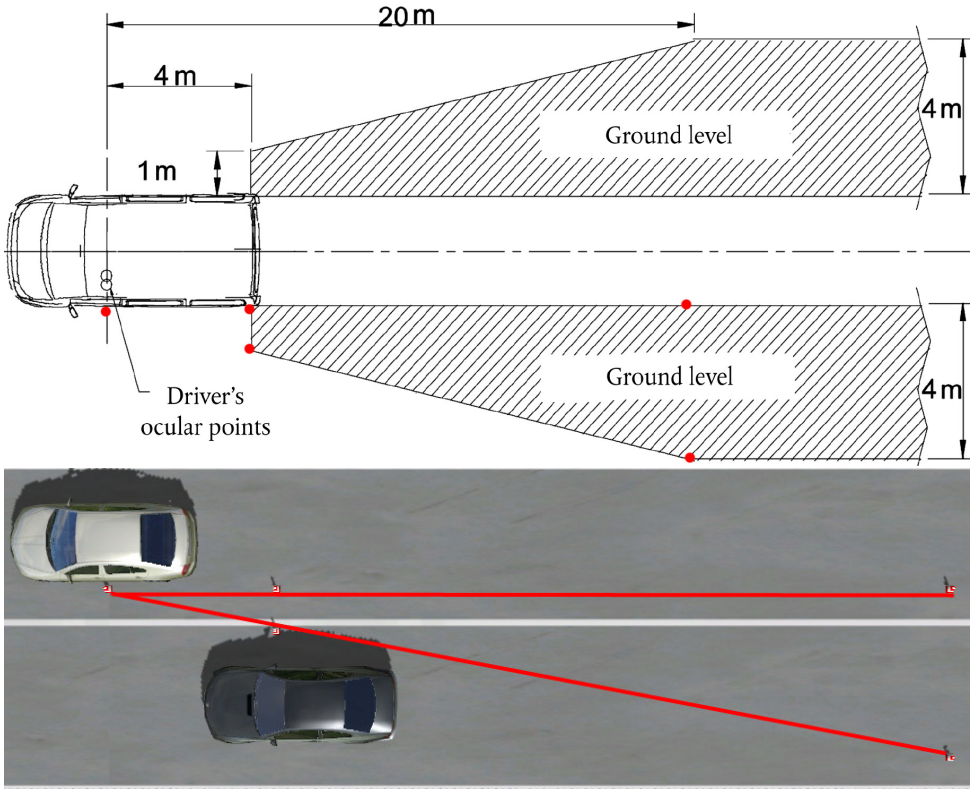

Figure 3.4: *Top*: Figure taken from [EC2003, Figure 8], shows the proposed visible range of the exterior side mirrors. Remark: the distances 1m, 4m and 20m are not scaled properly! *Bottom*: bird's eye view in the driving simulator, visualizing the area from the picture above. The five small pylons on the road are located at the five reference locations indicated by the additional small dots that were added to the top figure.

The small red dots were added to the figure to visualize some calibration points. In the lower part of the figure a simulated bird's eye view can be seen which shows the ego vehicle on the right lane and a rear vehicle on the left lane. 5 small pylons were located in the simulation, corresponding to the positions marked by the red dots in the figure above. Remark: the upper figure is not scaled correctly, but the given numbers in meter were used to position the pylons.

Figure 3.5 shows the result of the horizontal adjustment. Eight screenshots were taken from four situations, a bird's eye view and the corresponding mirror view. The top left figure shows the rear vehicle at zero distance and the car is completely hidden in the blind spot. This situation can also be seen in Figure 3.4. The figures also show the visibility of the 4 pylons as demanded by the Directive and the subsequent situations show the vehicle in 1.6, 6 and 12 meter distance. So far, the mirror is not finally adjusted in the vertical direction. After the curved mirror views were also created (see next subsection) the horizon was vertically aligned to the middle of the view for all mirror types.

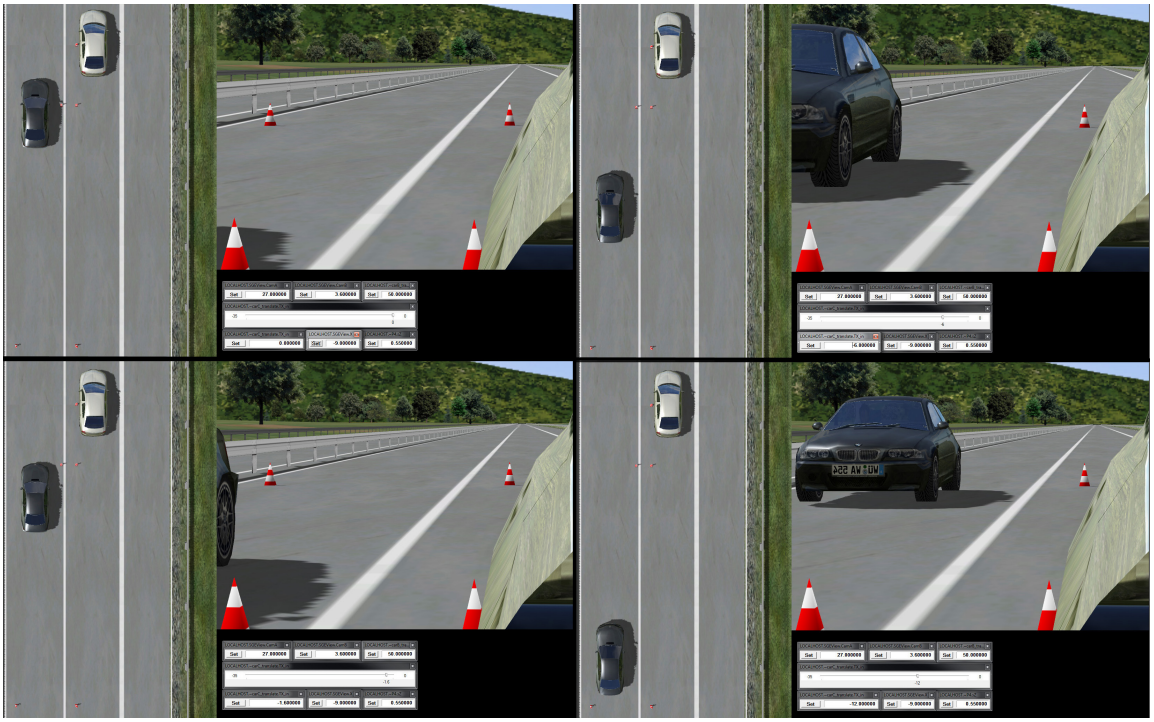

Figure 3.5: Adjustment of the planar mirror: as seen in the figure above, the pylons are located at the reference points. The horizontal mirror adjustment was done according to the pylons. The rear car is located at 4 different bumper to bumper distance: 0m, 1.6m (on the left), 6m and 12m (on the right). Top left figure: a vehicle can fully hide in the blind spot region of the planar mirror.

.

3.3.2 Simulation of Spheric and Aspheric Mirror Surfaces

Based on the planar mirror settings, the simulation of a spheric mirror type can be done with relatively small changes to the OpenGL camera parameters: the important characteristic of spheric or convex mirrors is the minification effect. Due to the equally curved surface the viewing angle is widened and a larger area is seen by the observer with basically the same surface area compared to the planar mirror. As a consequence, all visible objects are minified and the stronger the curvature (Planar $\rightarrow$ C20 $\rightarrow$ C14) the stronger the minification. This effect can be reproduced in the simulation by increasing the field of view (adjusting the FovY° parameter in SILAB). [Bach2006] gives a larger angular range measured for different spheric mirror surfaces (24.2° - 32.2°), but these numbers are not directly related to certain spheric mirror types. In contrast, [NHTSA2008] published values for different specific mirror types (e.g. C20 and C14, see Figure 3.3) and more importantly the amount of minification for these types was also published. The *minification factor* can be used as a test to compare and validate the different simulated mirrors (see next subsection). Therefore it was decided to start with the 22.6° field of view for the C20 type.

Besides the planar and the C20 spheric / convex mirror it was planned to use an aspheric

mirror for this work, similarly to the study of [Carstengerdes2005]. As explained in section 2.1 the aspheric mirror has an increasing mirror curvature towards the outer mirror region. Simply changing the field of view is not sufficient in this case. SILAB offers a separate DPU which allows to distort an OpenGL view based on a 5*5 control point bezier patch. The control points are equally spread across the view and can be moved to manipulate the distortion in horizontal and vertical direction. It was tested, if the distortion could be used to achieve a view similar to a real aspheric mirror. For this purpose, the aspheric mirror of the aforementioned VW Passat model generation 2013 was used, and a series of photos was taken, which showed the mirror image of specific reference object that were positioned around the side of the vehicle. The reference objects were also located in the driving simulation at the same locations and the bezier matrix for the mirror view was adjusted, until the simulated view looked as similar as possible compared to the photos.

Remark: the empirical procedure which was used to create the aspheric mirror type is documented in Annex 7, p. 221.

But there was a technically unresolvable problem which prevented to use the aspheric mirror for this work: for both, the empirical studies and the driver modeling, it was required that the visual size of objects on the mirror display can be calculated. For this purpose, SILAB has a plug-in which transforms 3D world coordinates into 2D screen coordinates. Because the bezier matrix was applied on the finally rendered image, the coordinate transformation can not consider this distortion effect.

Although this finding was quite disappointing, it was not a huge problem for this work. The aspheric portion of the mirror is mainly useful to reduce the size of the blind-spot region. Figure 7.12, p. 225 in the Annex shows, that the aspheric mirror portion is no longer effective at distances of 12 meter and beyond. The typical distances during a lane change on the Autobahn are much bigger, and these distances are observed with the spheric part of the aspheric mirror. Therefore it was decided that, instead of the aspheric mirror, a second spheric / convex mirror might be of higher interest for this scenario. [NHTSA2008] provides the field of view parameters for a C20 and a C14 spheric mirror type: $C20 = 22.6°, C14 = 28.4°$. Using two spheric mirrors allows to test the impact of the magnitude of the mirror curvature in more detail.

The next section describes how the minification effect can be used to calibrate the simulated C20 and C14 mirror types in the driving simulator.

3.4 Evaluating the Image Minification Effect

According to [NHTSA2008, Chapter 7], the minification factor is the „*ratio of image size as it appears with the convex mirror compared with the image size as it appears with a corresponding flat mirror. This ratio, which is always less than unity, provides an indication of how much smaller an image is when the convex mirror is used.*“. A value of one equals “no minification“, while smaller values indicate a minification effect. Figure 3.6 shows that the minification factor (y axis) for the real mirrors increases slightly at smaller distances, especially around 10 feet. With regard to the investigated scenario in this work, this non-linearity at close distances can be ignored.

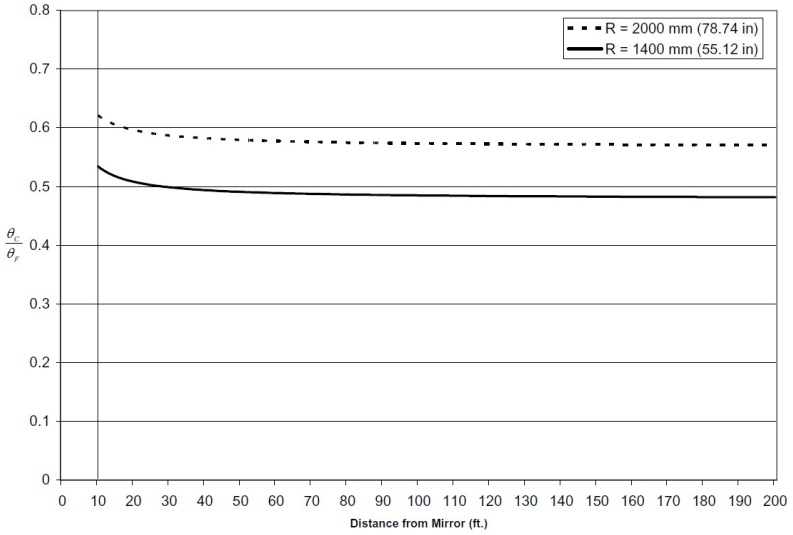

Figure 3.6: Figure taken from [NHTSA2008, p. 44]

To validate the models of the curved mirrors C20 and C14, it was tested, if the minification factor can be compared to the real mirrors. To calculate the minification factor across a larger range of distances, a small computer experiment with the driving simulator software was done: the software allows to gather data from all simulated vehicles. For each of these vehicles the current state in 3D space is also accessible (x,y,z coordinates and yaw, pitch and roll angles), as well as the vehicle dimensions and many other specific attributes. For this test procedure the coordinates are of interest only which were converted from 3D world coordinates into 2D screen coordinates. The procedure to gather data for the calculation of minification was the following: a vehicle was positioned 150 meter behind the ego vehicle (bumper to bumper distance). At this early stage of the work it was not decided how far the distances in the experiments would be, but 150 meters was considered a sufficient range at that stage. The largest distance that was finally used was 88 meter.

The ego vehicle was centered on the right lane, while the approaching vehicle was centered on the left lane. Both lanes had a width of 3.75 meter. The vehicle from behind was moved automatically towards the standstill ego vehicle with a differential speed of 1 km/h (0.278 m/s). The front left and front right corner points of the approaching vehicles were transformed into 2D screen / view coordinates of the mirror and used to calculate the vehicle width. This procedure was done for the planar mirror as well as for the C20 and C14 mirrors. The minification for the mirrors equals the ratio of the two measured vehicle width's $\frac{width_{C20}}{width_{planar}}$, or $\frac{width_{C14}}{width_{planar}}$. Figure 3.7 shows the results of the measurement.

As expected, the minification factor gets smaller with increasing field of view. This is similar to an increasing curvature of real mirrors (where the radius gets smaller). It can be seen that for both curved mirrors the minification is slightly smaller, about 0.04 for the C20 and 0.06 for the C14. This effect is likely caused by the larger field of view for the planar mirror, which was necessary to achieve a projection which projects objects at their true, undistorted size. To achieve a better match with the minification factor, the field of view for the curved mirrors was finally adjusted to 23.6° for the C20 and 30.9° for the C14. With these settings the minification

factor was matched to an average level of 0.49 and 0.58 respectively.

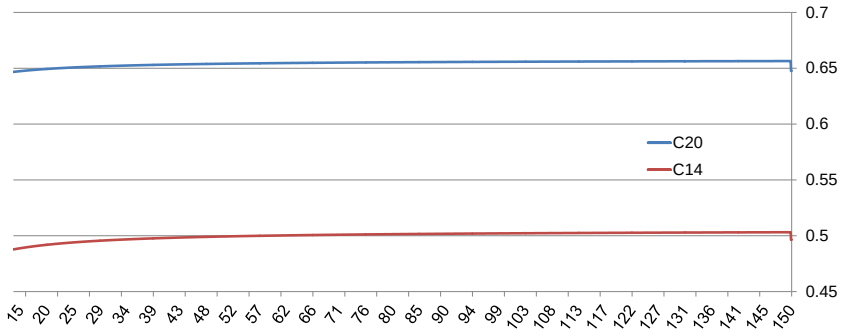

Figure 3.7: Minification measurement for the simulated mirror with 15.33 field of view for planar mirror, 22.6 for C20 and 28.4 for C14; x-axis is distance in meter between ego and rear vehicle. These settings do not excatly fit with the results in 3.6. Therefore the field of view was corrected to the finally used settings of 23.6° for the C20 and 30.9° for the C14.

A slight difference to the NHTSA study can be seen at shorter distances. While the minification raises slightly for the real mirrors in the NHTSA study, it falls slightly for the simulated mirrors. The reason for this difference can be found in the implementation: the OpenGL camera is placed at the location of the exterior mirror and does not correctly simulate the exact distance between the observer (the driver) and the mirror. This leads to a slight error with regard to the minification and is responsible for the difference between reality and simulation. It can be questioned whether this will impact the investigations of the two empirical studies described in the next chapter. According to [NHTSA2008] the slight changes of the minification factor for larger distances (above 30 foot) are too small to impact the driver. If this argument is true, the slightly falling minification factor should also be negligible. With regard to the shorter distances (below 30 foot): as argued above, the focus of both experiments was put on larger distances and the investigation of the near range and the blind spot region was explicitly not considered for the lane change scenario.

3.5 Further Differences between Simulated and Real Mirrors

Viewing objects through a simulated mirror changes the depth perception which potentially impacts the estimation of distances or speed of approaching vehicles. There are a number of different criteria which have an impact on our depth perception and they were briefly presented in section 2.3.1.3. It is commonly agreed that depth perception relies on a combination of the available criteria. This conclusion can be drawn from all the findings that were cited in the discussion about law of visual angle and size constancy (see section 2.3.1). But depth criteria can not simply be weighted against each other (like four of seven available equals a reduction of X%), some operate in a limited range of distance (convergence, accommodation), while for example coverage has no impact if the target is not obstructed by any other objects (a single

tree on a grassfield). Pictorial depth cues like texture or shadows and knowledge about size of familiar objects are typically available to us in the real world, while they are often taken away in specific laboratory conditions which often work with simple geometric forms only. Table 2.1 in section 2.3.1.3 already summed up different depth cues. The following table gives an overview on the same set of depth cues and if they are covered by the SILAB driving simulation or not.

Criteria	**Availability**	**Comment**
Accommodation	no	Incorrect cue in simulator, distance of screen is focused instead of real object distance
Vergence	no	same as accommodation
Binocular disparity	no	No stereovision used in simulator
Motion parallax	yes	Simulated by OpenGL camera, , but in this scenario movement was always towards the observer.
Occlusion	yes	Simulated by OpenGL z-buffering
Perspective	yes	Property of the OpenGL camera view
Texture	yes	Simulated by OpenGL texture mapping and mipmaps
Lighting, Shadows, Shading	yes	Diffuse OpenGL lighting was used during simulation, plus 12 o' clock directional sunlight
Atmosphere	yes	Available, but not used
Familiarity	yes	Realistic 3D simulation and models for vehicles, the road geometry and surrounding environment

Table 3.1: Comparison of available depth criteria in the driving simulator environment. A brief explanation of the cues can be found in section.

The simulator does not provide a stereoscopic vision, therefore binocular disparity and motion parallax are not available. The absence of these cues can be a problem for distance estimations, but it is also known that these cues are dominated by the pictorial cues. A little more complicated are accommodation and vergence, which deliver incorrect cues in the simulator: fixating an object through a real mirror leads to vergence and accommodation according to the true distance. If for example a vehicle is observed through a mirror in a distance of 20 m behind, the eyes vergence and accommodation are adjusted according to the absolute distance *eye - mirror - vehicle behind*. In case of a simulated mirror, the vergence and accommodation distance is *eye - mirror* (TFT display) only, irrespective of the real distance to the vehicle. Thus, the contraction state of extraocular and ciliary muscles is the same for each distance of a vehicle that is being observed. Both of these cues do not match the other pictorial depth cues of the simulated 3D world. This might lead to an overall changed perception of depth of objects compared to what people have learned from driving in a real vehicle.

Effects of accommodation and convergence are considered to be relevant in a near range up to 3-6 meters. While the smallest distances of the observed vehicles in the real world examples are often above this minimum, vergence and accommodation might not be important for the impact of mirror types on perception. On the other hand, the actual distances for vergence and accommodation in the simulator are a lot below these thresholds (*eye - mirror* distance is about 65 cm, while the distance *eye - front projection wall* is about 2.7 meters). Because of that, both effects could very well lead to changes in the depth perception and change the distance estimations. Because of these differences, it was decided that a validation study is necessary

to test the overall setup of the simulator and check if the simulated mirrors lead to similar effects compared to their real world equivalents. For this purpose, a replication of the distance estimation field study of [Carstengerdes2005] was done in the simulator (section 4.1).

It should be mentioned here that the simulated mirrors also do not reproduce the changed reflectivity properties of real curved mirrors. With increasing curvature these mirrors produce less glare, which is an advantage especially during night drive. Because light does not play a major role for the experiments, this difference seems to be less relevant in this context.

3.6 Measuring Visual Angles in SILAB

In the reviewed psychophysical literature (see section 2.3.2, p. 45, or summary 2.3.4), the concept of visual angles was widely used by researchers, who investigated the perception of size and distance as well as motion of objects. Visual angles will also play an important role for the driver model development in chapter 5, and they are also of partial interest for the two experiments. Because the technical information how these angles can be calculated should not be spread across different chapters, a short description is given here already.

In the previous section it was already mentioned, that SILAB offers a module which allows the transformation of 3D world coordinates into 2D screen coordinates. Based on these visible screen coordinates and the resolution of the mirror display (pixel / mm) it is possible to calculate the visible size of objects on the mirror display (see Figure 3.8).

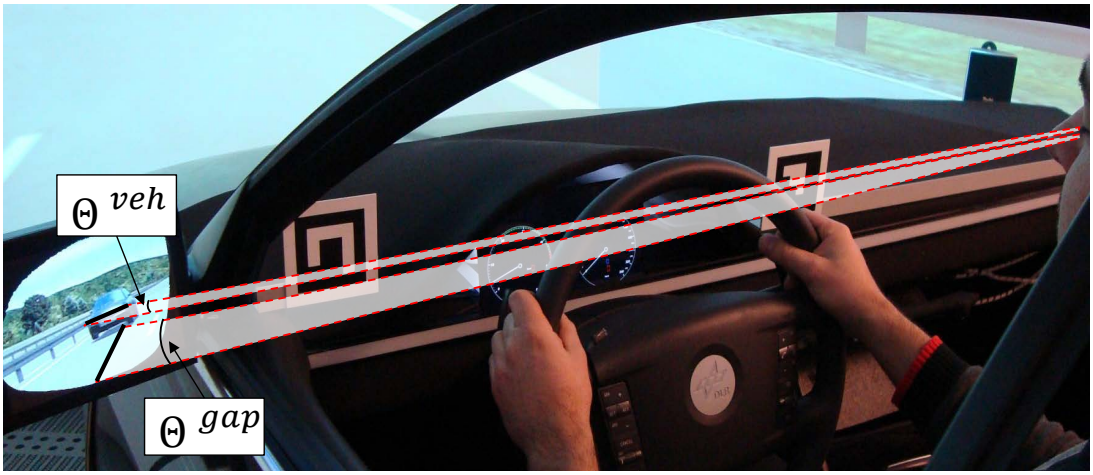

Figure 3.8: Calculation of visual angles: thick, black lines illustrate the *visible gap size* between ego car and rear car, and the *visible vehicle width*, measured across the front width of the rear vehicle. Pixel information about the both sizes is available from the simulator, and transformed into a length in millimeter using the pixel resolution of the mirror display. The length in millimeter is used to calculate the corresponding angles: *angular gap size* Θ^{gap} and *angular vehicle width* Θ_{veh}.

For the calculation of the visual angles the visible object size / length in millimeter is one prerequisite, but also the distance between the driver and the mirror display (or the front projection surface) is necessary. Because subjects were allowed to slightly adjust the seat position

in the simulator, it was originally planned to calculate the angles for each individual separately, to achieve a higher accuracy. But already during pre-tests this procedure seemed not to be feasible, because even if the seating position would have been measured, subjects also slightly moved their body and head position forth and back or sideways during an experiment session. The best way would have been a head tracker to measure the distance continuously during the experiments and calculate visual angles based on this information. Because such a device was not available in the simulator, the attempt to use an individual head position was abandoned.

Instead, an average distance for all observers was assumed later on for the analysis of the experiment data, knowing that the exact visual angles for each subject varies from this value. How was the average distance measured? During the experiments a fixed position of the back rest and the head cushion were used to limit the variability. Furthermore, the seat adjustment on the track was limited to a range of 15 cm. For the measurement of the average head position the seat position was centered on the track and a test person had to put his head against the head cushion, while looking towards the mirror. A distance of 0.65 meter was measured between the driver's nose and the center point of the left side mirror. Looking towards the from projection surface of the beamer the distance between driver and the front beamer wall was 2.80 meters. These measured length's were used for the trigonometric calculations to receive the visual angle measures. A small plug-in module was implemented and integrated into the simulation which conducts these calculations at runtime. This module also receives the current simulation time in milliseconds which allows a calculation of the rate of change for each angle (the angular velocity). These values were recorded during both experiments and they are also used by the driver model at runtime.

4 Driving Simulator Studies

Introductory remark: Whenever in this chapter the mirror types "planar, C20 or C14" are mentioned, this refers to the simulated mirror types in the driving simulator. Please, see section 3.3 for details how these different mirror types were implemented. Only in the discussion section of each experiment, the results are compared against published studies that were done with the real mirrors.

This chapter presents two driving simulator studies that have been conducted to a) validate the implementation of the three simulated mirror types (planar, C20 and C14) and b) to gather data about the impact of those simulated mirror types on gap acceptance behavior during a simulated lane change scenario.

To validate the implementation of the simulated mirrors, it was decided to replicate the distance estimation experiment done by [Carstengerdes2005]. The goal of *Experiment 1* was to show that the main effects reported by [Carstengerdes2005] and [Flannagan1996], can be replicated with this driving simulator setup. To improve comparability with the existing findings, the magnitude estimation paradigm of their experiments was reused, and very similar hypotheses were derived. The second experiment investigated the impact of the different mirror types on gap acceptance in a simulated lane change task. It was argued at the very end of the literature chapter (section 2.3.4), that the published data with regard to this topic is not very detailed. Therefore, Experiment 2 tested 26 different traffic situations, and the results of the experiment were then used for the driver model development, which is described in the next chapter.

For both studies, a call for participants was posted online at the webportal of the C.v.O. University of Oldenburg[1]. For the first study (Experiment 1) a valid driving license was the only requirement, while for the second study (Experiment 2, gap acceptance) at least three years of driving experience were demanded. Participants of the first study were not allowed to take part in the second study. For both studies each participant received a detailed description of the experiment and also had to fill out an informed consent, which explained what type of data was recorded and it would be used. Money was given in cash (10 Euro / hour), which removed the necessity to collect any additional private data. The participant's email addresses were stored for the period of time of the experiment for contact purposes. They were deleted afterwards. To match the recorded driving simulator data of each participant with the results of a short questionnaire, each participant received an abstract identifier.

[1] "Stud.IP", https://www.uni-oldenburg.de/studium/studip/

4.1 Experiment 1: Distance Estimation

As described in the introduction this study was based on the experimental paradigm used by [Carstengerdes2005] as well as [Flannagan1996]. The scenario for this experiment can be seen in Figure 4.1 and is explained in the following paragraph. Afterwards, the hypotheses for the experiment are explained, followed by the procedure and the results part. Finally, a discussion on the findings includes a comparison of the similarities and differences between this study and the presented studies in the literature review.

4.1.1 Scenario and Task

Figure 4.1 illustrates the scenario with the ego vehicle (A) on the right lane of a two-lane Autobahn. The ego vehicle was not moving and subjects did not have to drive. In each trial of the experiment, a standstill lead vehicle (B) was set up at one of three distances $d_{AB} =$ 20, 40 or 60 meter distance (bumper to bumper) on the right lane. Additionally, a standstill rear vehicle (C) was positioned on the left lane behind at relative distances of $d_{AC} = d_{AB} * \{70, 85, 100, 115, 130\}\%$. In summary, the experiment design was: 15 distance combinations (3 lead car distances * 5 rear car distances) * 12 repetitions = 180 trials per experiment sessions. The 12 repetitions were divided into 3 blocks, each with 4 repetitions of the 15 conditions which equals 3 blocks of 60 trials in one experiment session.

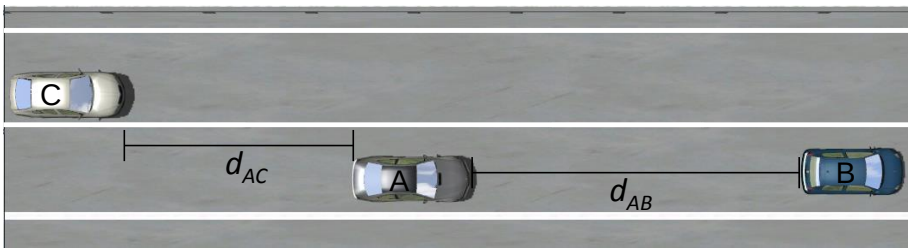

Figure 4.1: Ego vehicle (A), with a lead car (B) located at different distances $d_{AB} = 20$, 40 or 60 meter; The rear vehicle (C) which was set up at one of five relative distances $d_{AC} = d_{AB} * \{70, 85, 100, 115, 130\}\%$ to (B).

The task of the participants was to estimate the rear car distance d_{AC} in relation to the lead car distance d_{AB}. Estimations had to be given in percent, e.g. 100%, if they thought distances were equal. If it appeared to them that $d_{AC} < d_{AB}$, estimations should be $< 100\%$. Vice versa, if d_{AC} appeared to be larger than d_{AB}, estimations should be $> 100\%$. It was also explained that the magnitude of the percent estimations should equal the perceived distance difference, for example if d_{AC} appears to be at half the distance of d_{AB}, the answer should be 50%. The estimation in percent had to be entered into a key pad and the result was recorded by the simulator.

Subjects were not informed about any of the absolute distances and they also did not know how many different combinations were used in the experiment. Each participant was invited for three experiment sessions and in each of them a different mirror type was used. To not give additional hints to distance, some typical characteristic elements were removed from the traffic

scenario: a continuous lane marking between right and left lane was used, because stippled lane markings offer a hint to the distance. Additional posts behind the guardrail are typically positioned every 50 meter on a German Autobahn which could also be used to compare distances.

An advantage over the field study of [Carstengerdes2005] was that the positioning of the lead and rear vehicles at the appropriate distances for each trial does not consume any time in the simulator. This offered the opportunity to test more conditions in the same amount of time, which allowed to vary the lead vehicle's distance d_{AB}. Carstengerdes used 12 meter distance for the object ahead (a pylon in his study) and the rear car distance was varied in 5 steps between 4 - 20 meter. To test short distances of 4 meter, Carstengerdes had to adjust the mirror vertically towards the outside which led to an unusual mirror view. This was necessary, because the front of the rear vehicle would not have been visible in the mirror, instead the vehicle would have been located in the blind-spot region of the mirrors. Because the scenario of interest in this thesis is lane changing on the German Autobahn, it was decided to use a distance range that is more common for this scenario. Very short distances < 10 meter do not only interfere with the blind spot of the mirrors, but with regard to lane changing, they would also drastically violate German traffic laws. For this reason, the lead vehicle was located at 20, 40 and 60 meter which automatically resulted in much larger relative distances for the rear vehicle (shortest distance was 14 meter: 70% at 20 meter lead car distance). As a result of these distances, the mirror adjustment was comparable to normal driving conditions.

4.1.2 Hypotheses

Because Experiment 1 is very closely related to the one of [Carstengerdes2005], my hypotheses are also very similar. The following list cites the first three of his four hypotheses [Carstengerdes2005, p. 66,67] in German (English translations in brackets):

Hypothesis 1.1: „*Mit gekrümmten Spiegeln werden Distanzen (im Vergleich zu planen Spiegeln) überschätzt*“ (In comparison to planar mirrors distances will be overestimated with curved mirrors.)

Hypothesis 1.2: „*Mit planen Spiegeln werden Distanzen unterschätzt*“ (With planar mirrors, distances will be underestimated)

Hypothesis 1.3: „*Mit zunehmendem Krümmungsradius nähern sich die Distanzschätzungen mit gekrümmten Spiegeln den Schätzungen mit planen Spiegeln an.*“ (With increasing curve radius the estimations with the curved mirrors converge to those of the planar mirror.)

Hypothesis 1.2 of Carstengerdes can be considered the “baseline“ behavior when a planar mirror is used. Therefore a similar formulation is used for this experiment in Hypothesis 1 (see below). Hypothesis 1.1 and 1.3 of Carstengerdes capture the changes with regard to distance estimation, when curved mirror surfaces are used instead. The assumptions of these two hypotheses are put together into a single Hypothesis 2 here. Because the overall distances of both vehicles was varied using three distances for the lead vehicle a third hypothesis was added to investigate, if the underestimation of the distances decreases at overall larger distances of both

vehicles. It is expected that the ability to detect differences in the distance between the two vehicles is reduced, if the overall distance is increased, and it is assumed that the underestimation effect is also reduced.

Hypothesis 1: Drivers underestimate the distance of the rear vehicle (C) when using a simulated, planar mirror.

Hypothesis 2: Increasing the field of view of the simulated mirrors (from Planar to C20 to C14) successively reduces the amount of underestimation compared to the planar mirror.

Hypothesis 3: Increasing the distance of the reference / lead vehicle (d_{AB}) and the dependent rear car distances (d_{AC}) reduces the amount of underestimation.

4.1.3 Procedure

15 Participants were invited for Experiment 1 (9 male, 6 female). They were between 20 and 32 years of age with an average age of 24.7. Driving experience was between 3 and 14 years (average of 7.2 years), between 100 - 22500 km/year (average 5370) and 50-12000 km/year (average 2860) on the Autobahn. All participants were invited for three experiment sessions, each at a different day and at least one day off in between was required. In each session one of the three mirror types was used and the order of mirror type per session was randomized between participants. In contrast to Carstengerdes, subjects were not informed that different mirror types were used and the mirrors were also not changed during a session. Subjects should not actively think about differences between the mirror types which might have influenced their perception of the situation.

At the beginning of each trial, subjects were instructed to look at the lead vehicle which was randomly positioned at one of the three distances d_{AB}. After four seconds an acoustic signal was given from the front left side near to the exterior mirror which signaled that subjects should now look into the left mirror to observe the rear vehicle at one of the five possible relative distances d_{AC}. The four seconds initial delay before the acoustic signal were used, because subjects should get accustomed to a possibly changed distance of the lead vehicle. After 4.5 seconds of viewing time the left mirror view was blackened. Participants had to type their estimation about the relative distance into a keypad. After pressing “enter“ the next trial began. The 4.5 seconds that subjects were given to observe the rear vehicle in the mirror was derived from the study of Carstengerdes. In his experiment, a shutter in front of the mirror was opened two times for two seconds each, which simulated two short mirror glances. Such a restriction on the viewing behavior was not used in this study, instead subjects were free to move their gaze to observe both, front and rear vehicle. Therefore the overall viewing time was also slightly increased to 4.5 seconds. Figure 4.2 gives an impression, how the experiment looked from the viewpoint of the subjects.

Figure 4.2: Experiment 1 scenario from the perspective of the subjects.

Before the 3 blocks of the experiment were tested, 10 randomized test trials were shown. This was done in each of the three experiment sessions, and allowed the subjects to get familiar with the procedure. Subjects were also informed, that further help can be given or some additional test trials can be done if they experience any trouble with the procedure. None of the participants asked for such additional help. After the third session each participant had to fill out a short questionnaire, and the objectives of the experiment were explained in detail.

4.1.4 Data Recording and Preprocessing

The recorded data from the simulator was formatted as a large table of time stamped values, stored in a comma separated value file. The sampling frequency of the recording was 120 Hz (a value for each variable every 6 ms). The data file contained columns for time stamp, the current trial and block number, variables for the two bumper to bumper distances (between ego and lead / rear vehicle) and a variable which contained the last estimation value that was typed into the keypad.

The recorded real-time data required some preprocessing steps before a statistic analysis can be done, because the relevant points in time have to be identified and removed. A manual processing of the data is impossible for the total amount of 8100 trials. To simplify such automatic preprocessing and cutting, a marker variable was recorded during the simulation which had different values to identify the start (when the lead vehicle was relocated at one of the three

distances) and the end of each trial (when the number was entered). It was also necessary to detect trials where subjects pressed the “Enter“ button multiple times, because this would have led to faulty detections of start-end combinations.

After the data was cut, inappropriate trials had to be removed or manually corrected: in some cases subjects reported during the experiment that a wrong value was entered. Because trial and block numbers were always recorded and visible in the data file, a note was made and these cases were corrected manually. Another small amount of trials was marked as faulty because subjects typed in percentage values like ’777’ or ’0’ which obviously seemed to be wrong. The first case could not be corrected, because it could be either 7 or 77, while the zero appeared when subjects pressed enter before typing their answer. Unfortunately, such missing values lead to imbalances in the design which impacts the statistical analysis approach. Fortunately, such faulty values were rare (25 of 8100) and not more than one was found per condition / subject / mirror, thus at least eleven of twelve ratings were always correctly recorded. R package ezANOVA (type=2) can be used for unbalanced designs.

4.1.5 Results

The result section is split into several parts. Hypothesis 1 and 2 are discussed together in the first part 4.1.5.1, because tables and figures which are useful for an analysis are very similar. Afterwards results are investigated with regard to Hypothesis 3 in section 4.1.5.2. Some additional findings were made for which no hypothesis was defined, these are explained in subsection 4.1.5.3. The results of the short questionnaire are explained in 4.1.5.4.

4.1.5.1 Hypothesis 1 & 2

Hypothesis 1 postulates an underestimation of distances using planar mirrors while Hypothesis 2 formulates a decreasing underestimation with increasing mirror curvature. The first step is a comparison of the mean value and the standard deviation of the subject’s estimations for each of the three mirror types which was done with the help of the statistic software R[2]. Boxplots were drawn using gnuplot[3]. For this first analysis no difference was made between the 5 different rear car distances. Because these distances were equally distributed around the 100% distance (70% vs. 130%, 85% vs. 115% and a 100% condition) the overall sum of all estimations should result in 100%, if either 1) estimations were always correct without any overestimation or underestimation or 2) if both (overestimation and underestimation) equal themselves out. The result can be seen in the table on the right side of Figure 4.3. Those numbers already give a first indication that the planar mirror leads to the largest underestimation compared to both C20 and C14. For the planar mirror, the real distances were underestimated with an average of 25.48% (100% - 74.52%), while for the C20 the average underestimation was 8.18% and for the C14 the average estimations were almost equal to the real distances. The standard deviations on the other hand decreases with increasing mirror curvature.

[2] version 3.2.3 was used, webpage: https://www.r-project.org/
[3] version 5.0 was used, http://www.gnuplot.info/

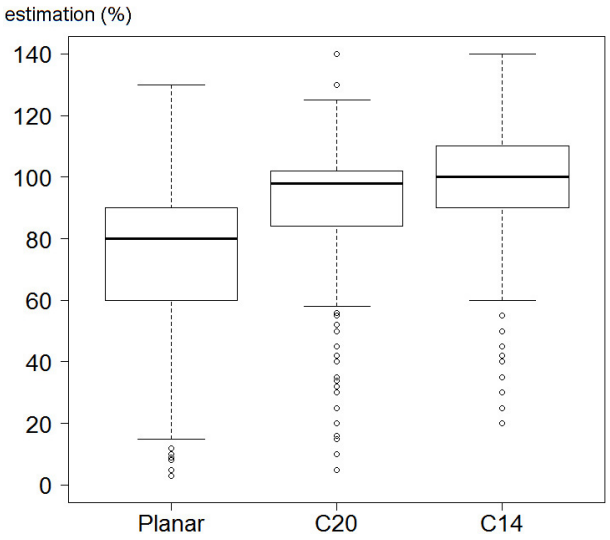

Estimation (%)			
Mirror	Planar	C20	C14
Mean	74.52	91.82	99.96
St.-dev.	23.94	19.03	17.13

Figure 4.3: Left side: boxplot visualizing the estimation results for the three mirror types; Right side: table shows mean values and standard deviation of the subject's estimations for each of the three mirror types.

The boxplot on the side left of Figure 4.3 visualizes the distribution of the estimations and shows a number of outliers below the lower whisker. These outliers might impact an ANOVA, and a more detailed view was taken at the data of the 15 subjects. An overview on the data of all 15 subject is given in Figure 4.4 (For better readability, refer to full page figure in Annex 7.1, p. 214). The data for each subject is presented in a column and each of the three rows contains the results for one of the three mirrors: planar mirror (top row), C20 (center row) and C14 (bottom row). Along the x-axis, the 5 rear car distances are denoted in percent (70, 85, 100, 115, 130). The y-axis of the bars shows the corresponding estimations of the subjects in percent. A horizontal line is drawn at the estimation value of 100%. In this graphic the data of the three lead car distance is accumulated (20, 40, 60 m). The A separate investigation of the three distances is subject to Hypothesis 3 and is discussed later.

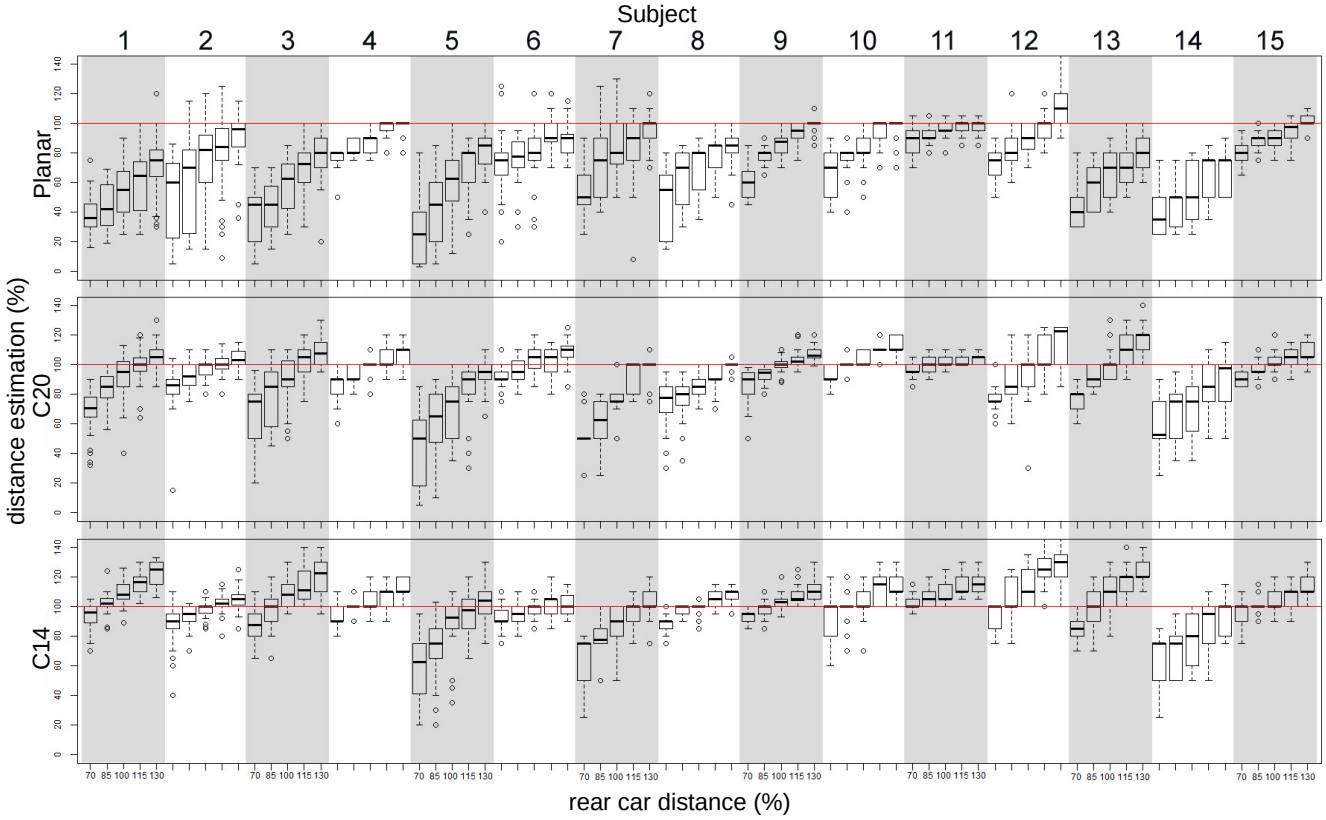

Figure 4.4: Results for all 15 subjects; Full page figure, Annex 7.1, p. 214; x-axis: five distances to rear vehicle in %; y-axis: distance estimation in %; top row: planar mirror, center row: C20, bottom row: C14

The following four observations on the basis of the illustration in Figure 4.4:

1) The relative estimations for the five rear car distances from 70% up to 130% increase accordingly for almost all conditions across all participants. This can be seen by comparing the increase of the median values of the bar plots from left to right (from 70% to 130% rear car distance)

2) For several subjects a quite high amount of variance was observed across all mirror types and conditions, especially for the subjects 5 and 14. In comparison to other subjects, the upper and lower quartiles are much wider here. More stable estimations with a smaller amount of variability was observed for subjects 4, 6, 11 or 15.

3) With regard to the five rear car distances distances: if a virtual line is drawn from the left bar median (the 70%) to the right bar median (the 130%), the steepness of this diagonal line represents the total average percent range that a subject used across the five conditions. The actual range was 60% (from 70% up to 130%). A lot of subjects used a considerably smaller overall percentage range about 25-40% (for example subjects 4, 9, 11, 15). For those four subjects this small range was consistently used across all mirrors. Other subjects used a much larger range, especially subject 5.

4) As explained in the procedure section, each mirror type was measured in a separate experiment session on a different day. This might explain why some subjects showed more variation

for a specific mirror condition (for example subject 2 for the planar mirror).

After the descriptive and visual inspection of the data the next step is to conduct a one-way repeated-measures ANOVA to check, if the differences between the three mirror types are statistically significant. For this analysis, the ez library (ezANOVA) of the statistic software R was used. The ANOVA results showed that the differences between the three mirror types were significant with $F(2, 28) = 42.64, p < 0.001$. Similar to the distance experiment of Carstengerdes, Mauchly's test of sphericity was violated in this Experiment with $p < 0.001$ and $\epsilon = 0.503$. According to [Girden1992] the Greenhouse-Geisser correction should be applied for $\epsilon < 0.75$, while Huynh-Feldt is used in case of $\epsilon > 0.75$. The Greenhouse-Geisser correction delivers the corrected values $\epsilon = 0.668, p < 0.001$ and the effect remains significant. In addition to the ANOVA, a pairwise t-test was significant for all 3 possible mirror comparisons with ($p < 0.001$) using both, Holm and Bonferroni methods. It can be concluded that the differences between the mirrors are statistically significant.

Furthermore, it is of interest, if the differences between the mirrors have a similar magnitude. The underestimation was strongest for the planar mirror which was suggested by Hypothesis 1 and it significantly decreases with increasing mirror curvature (Hypothesis 2). Additionally, a comparison of the incremental changes between the mirror types from 1) planar to C20 and 2) C20 to C14 can be used to compare the absolute differences between the mirrors. These changes will be referred to as first and second transition. Table 4.1 shows a comparison of the relative changes of the field of view and the minification factor as well as the changes to the mean estimations and their standard deviation.

Relative Change between Mirrors (%)		
	Planar to C20	C20 to C14
Field of view	47.4	25.7
Minification	35	23.1
Estimation mean	20.3	8.14
Estimation std.-dev.	-21.51	-9.98

Table 4.1: Relative changes in % between the mirror types for the physical properties field of view and minification factor in comparison to the changes of the estimations with those mirrors.

For the first transition (from planar to C20) the field of view increases by 47.4% and by another 25.7% for the second transition (from C20 to C14). Changes to the minification factor behave similar (first transition larger than second), but at a smaller absolute magnitude. It may not be surprising that mean and standard deviation of the estimations also have a similar tendency which might indicate a correlation between estimations and these properties.

The results of the ANOVA and the pairwise t-test can be used to conclude that there is a significant change in the magnitude of the estimations from first to second transition. On the other hand, if the absolute percentages of the physical properties and the estimations are compared, the estimations are a lot smaller as it would be suggested by the physical properties.

4.1.5.2 Hypothesis 3

So far, the results have not been split into the different lead car distances. This is the objective of Hypothesis 3 which states that an increase of the lead car distance leads to decreasing underestimation.

	Estimation Mean(%)								
	Planar			C20			C14		
d_{AB} (m)	20	40	60	20	40	60	20	40	60
d_{AC} (%)									
70	44.89	61.64	65.17	67.15	79.57	81.20	79.35	88.65	90.29
85	56.93	69.23	75.72	77.46	87.01	91.59	88.65	93.97	99.55
100	62.58	78.69	84.61	85.57	93.53	97.75	94.58	101.54	104.92
115	76.61	85.10	88.95	94.97	99.89	104.93	102.54	107.06	112.40
130	82.75	91.56	94.39	101.14	106.18	109.43	106.40	111.82	117.39

Table 4.2: Mean estimations of the subjects for each of the three lead car distances $d_{AB} = (20, 40, 60)$ meter and each of the dependent / relative rear car distances $d_{AC} = (70\% - 130\%)$. Results are presented separately for the three simulated mirror types.

Table 4.2 shows the mean values for all three mirror types. A corresponding visualization can be found in Figure 4.5. Considering the planar mirror first, it can be concluded from the data that the underestimation effect is found for all 15 conditions. Across the three lead car distances (from column to column) the mean values continuously increase from 20 to 40 and finally 60 meters, which supports the assumption of Hypothesis 3, that the underestimation reduces with increasing lead car distance. The same characteristics for the mean estimations can be found similarly for the C20 and C14 mirrors, but the effects have a continuously smaller magnitude (from Planar to C20 to C14).

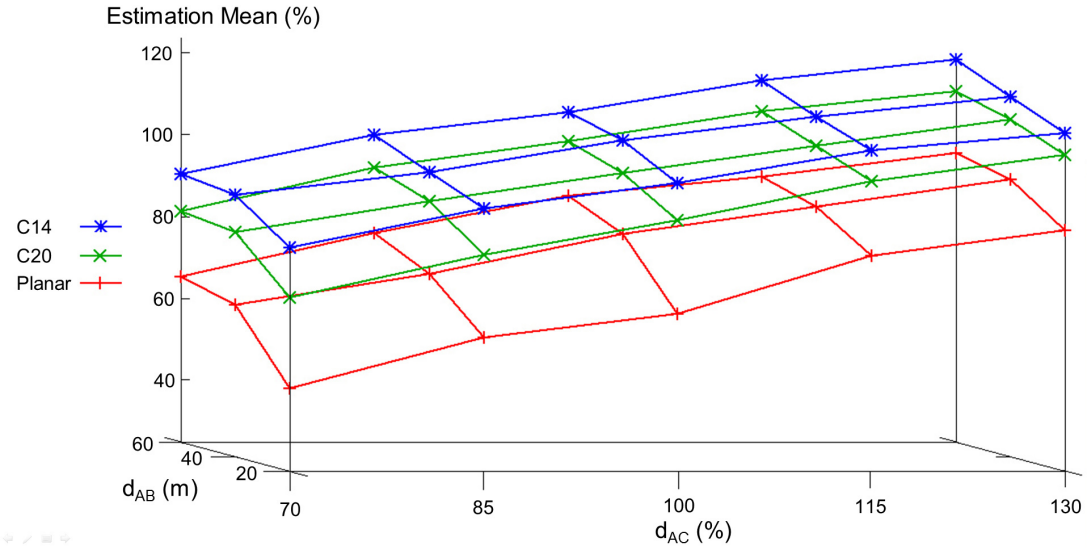

Figure 4.5: Visualization of the mean values from Table 4.2

A two-way ANOVA was conducted to test the significance of the lead car distance on the estimation. For the main factor "mirror" the p and F values were only very slightly different from the previously reported one-way ANOVA $F(2.28) = 42.75, p < 0.001$ and the lead car distance had a significant effect $F(2, 28) = 20.99, p < 0.001$. Again Mauchly's sphericity assumption was violated ($\epsilon = 0.51$), but the Greenhouse-Geisser corrected p-value was still significant $p < 0.001$. The interaction effect between mirror and lead car distance was significant with $F(4, 56) = 3.33, p = 0.016$, but due to the violation of the sphericity assumption it was no longer significant after the Greenhouse Geisser correction was applied: $p = 0.063 > 0.05$.

It can be concluded that a significant effect of the lead car distance on the estimation of distances was found and Hypothesis 3 is accepted

4.1.5.3 Additional Observations

After the experiment was assessed against the three hypotheses, two additional observations were made in the data. Figure 4.6 visualizes the estimations of the subjects, separated into the five rear car distances for each mirror type. If estimations would have been exact, each of the boxes would have been centered on the diagonal line.

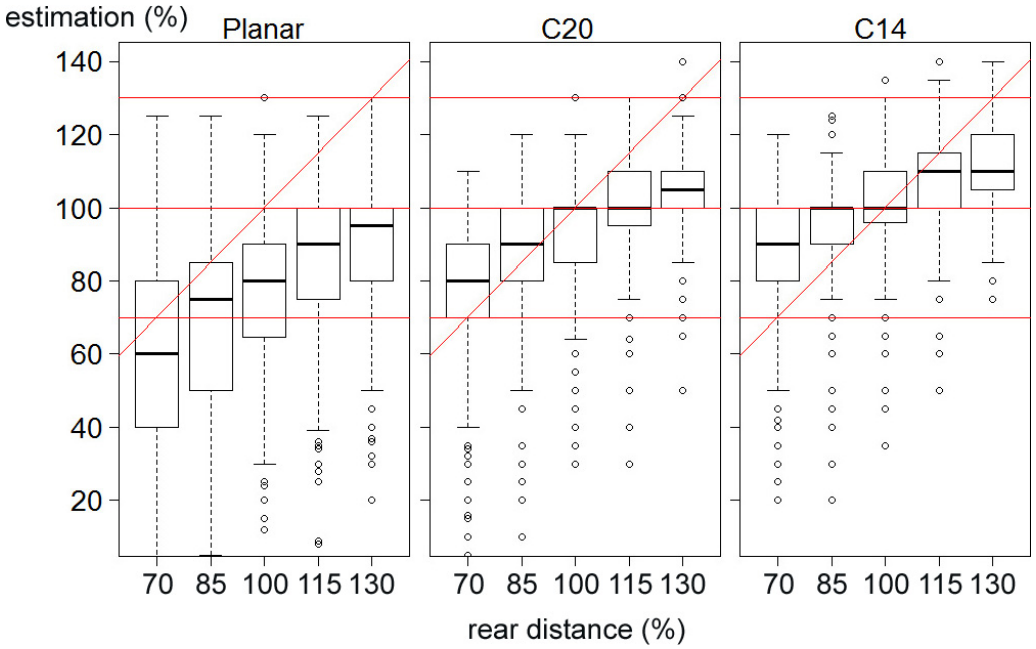

Figure 4.6: y-axis: subject estimations in % , x-axis: rear car distances. Horizontal lines (in red) mark the 70%, 100% and 130% estimation. If estimations would have been perfect, the boxes would have been aligned along the diagonal line, which is drawn through each of the three plots.

The observation in the figure is that across all mirror types, the smaller rear car distances were less strongly underestimated. Because of the already reported decreasing underestimation with increasing mirror curvature (Hypothesis 2), the smaller rear car distances are already overestimated with the C20 mirror type. This trend continues for the C14 mirror and reveals

a safety relevant problem: generally, shorter distances have a higher potential for more critical situations and if these situations are overestimated there is a higher risk if a lane change is considered by the driver. To test if this finding was significant, it was tested if the amount of underestimation significantly varies between the five rear car distances. Instead of using the estimations as input for an ANOVA, the estimation error is used, which equals the under- / overestimation of the subjects. Therefore, from each estimation in % the actual rear car distance in % was subtracted (the result is the subject's deviation in each trial). Based on this data, an ANOVA showed that the rear distance has a significant impact on the amount of underestimation ($F(4, 56) = 110.53, p < 0.001$).

The second observation is made for the standard deviations, which are shown in Table 4.3. They decrease with a) increasing rear car distance (top-down within a column) as well as with increasing lead car distance (from column to column). Similarly to the mean values, this effect is strong for the planar mirror and reduces successively for the curved mirrors C20 and C14.

	Estimation std.-dev.(%)								
	Planar			C20			C14		
d_{AB} (m)	20	40	60	20	40	60	20	40	60
d_{AC} (%)									
70	29.54	20.52	15.91	25.66	16.08	13.24	21.06	13.91	10.70
85	29.61	17.70	17.58	23.49	13.14	10.95	19.19	11.66	11.54
100	25.59	15.92	13.58	21.25	11.03	11.13	18.15	9.37	10.85
115	23.72	15.48	13.96	16.45	9.14	11.93	14.41	9.61	12.51
130	20.72	15.00	13.21	12.87	10.13	10.36	12.91	12.67	11.88

Table 4.3: Standard deviations for the estimations of all subjects for each of the three lead car distances $d_{AB} = (20, 40, 60)$ meter and each of the dependent / relative rear car distances $d_{AC} = (70\% - 130\%)$. Results are presented separately for the three simulated mirror types.

4.1.5.4 Questionnaire

The main objective of the questionnaire was to gather additional background information, if the invited drivers have any knowledge about different mirror types. It was assumed that most drivers might know about the blind spot of a side mirror, but they might not be aware of the more subtle minification issue.

Two questions were asked, the first was "Which type of driver side mirror does your own vehicle have or, if you do not own a car personally, the vehicle that you usually drive?"[4] Subjects should decide between four different answers: "planar", "spherical", "aspherical" or don't know. 12 of 15 subjects answered the first question with *don't know* while two answered "planar" and one "aspherical". While trying to answer this first question, the two subjects who answered *planar* explained, their mirror does not have some kind of blind spot feature and seems to be just a normal mirror, therefore they concluded it should be the planar one.

The second question asked for more details on the mirror types: "Can you describe some characteristic properties of the mirror?" Here, only the subject who answered "aspherical" for

[4]The questions were originally asked in German

the first question made a statement: “Hat keine starke Vergrösserung“, engl.: “has no strong magnification“. This answer is not correct, because the aspherical mirror does just the opposite, it minifies the object’s image compared to the planar mirror. The two other subjects who answered “planar“, did not know something about specific properties of such a mirror. At least for the 15 drivers that were involved in this study, the majority is not aware about what kind of mirror type they use and none had specific knowledge with regard to the specific characteristics.

Besides the mirror related issue another question asked about the strategy used during the experiment to solve the distance estimation task. The following list contains the answers of all 15 subjects:

1: Tried to put myself into the driver position of the rear vehicle and tried to compare both distances.

2: 1. Guardrail length, 2. length street (front my car to back front car, my back to front rear car)

3: 1. Guardrail, 2. is distance about half or third, or doubled? (distance on street)

4: I mainly orientated myself by using the size of the vehicle, using relative as well as absolute size

5: Size of the vehicle and distance of the side lane / guardrail (length).

6: First I tried to use readability of the number plates, later the guardrail

7: For the very short distance I tried to use the guardrail.

8: Distance (street), size of vehicle

9: Number plates of the vehicles / tried to find out how many vehicles might fit between me and the other cars.

10: Size of vehicles, direct comparison (similarity)

11: Guard rail, traffic signs

12: 1. Size of the vehicle (relative to mirror), 2. Guardrail

13: Compared to previous distance

14: Length of street, Guardrail

15: I have tried, as well as possible, to orientate myself using the rear end of my vehicle in the mirror and used that for the estimation. I tried to build a spatial image (overtaking scenario)

6 subjects mentioned the “distance“ along either the road or the lane marking[5] or the visible length of guardrail. On the other hand, the “size“ of the vehicles was mentioned 5 times also. Although the task was clearly to estimate and compare distances, the latter five subjects used the size to infer distance. This is not surprising with the background knowledge presented in the literature review (section 2.3): a major part of the scientific discussion and the models that are used to explain size and distance perception deal with the question how the perception of size and distance are related to each other.

[5] lane marking was a continuous and not a stippled white line

Besides the vehicle size and distance, it is interesting that the “guardrail“ was mentioned 8 times. A couple of subjects admitted verbally, that they initially tried to count the number of the guardrail posts, but this strategy was not feasible within the short amount of time, especially because the reference distance (lead car) changed almost every time from trial to trial. It seems possible that for the lead car distance of 20 meter the guardrails actually offer a potential cue, but at 40 and 60 meters lead car distance there are too many of them (the guardrail posts are located at every 1.5 meter), and counting them is no longer possible.

If this “counting“ strategy was applied by all eight subjects is not known. Instead, it could also be possible that subjects mentioned the guardrail, because it offered an additional cue with regard to the central perspective. While the orientation of the road and also the lane markings proceed along the same plane (from the bottom of the viewing field towards the central point), the guardrail offers an orthogonal cue (from the left or right side towards the central point). It could be tested in a future experiment whether such orthogonal cues change the distance perception: the guardrail could be shown in two versions, either with posts visible, or without posts. As a third condition the guardrail could be completely removed. With regard to the setting in the current experiment, no definite answer can be given on this topic.

It was surprising, that two subjects actually tried to use the size / readability of the “number plates“. Due to the pixel resolution these are almost unreadable already at the medium distances of 20-25 meter. Nevertheless, the number plates should also be removed in further studies. Finally, it remains unknown, why one subject mentioned a “traffic sign“, because a speed limit sign was visible only in about 60 meter ahead, but none was located behind the ego vehicle. In summary, six subjects answered that they tried to estimate and compare the distances directly (f.e. length of street), while five mentioned they tried to infer the distance from size cues like the vehicle size or the readability of number plates. Nine subjects did not name only one measure, but two or even more of them. This supports the view that, as soon as available, multiple visual cues are used and potentially integrated based on the individual strategy / approach.

4.1.6 Summary and Discussion

The main objective of this experiment was to validate the simulation of different types of driver-side mirrors and to assess their impact on the driver’s estimation of distances. Based on the study of [Carstengerdes2005], a distance estimation experiment was conducted and three hypotheses were evaluated. The first two of these hypotheses were already investigated in field studies by other researchers. According to *Hypothesis 1*, the simulation of a planar mirror lead to a significant amount of distance underestimation for all conditions. *Hypothesis 2* investigated the differences between the planar reference mirror and two spherical mirror types (C20 and C14). Such mirror types (in reality and in this simulation) offer a wider field of view without increasing the overall mirror dimensions. As a drawback, this leads to image minification. Both mirror types were simulated by adjusting the field of view accordingly to published values for these mirror types (see section 3.3.2). The amount of underestimation successively and significantly decreased with increasing field of view which supports Hypothesis 2. Hypothesis 1 and 2 were derived from the distance experiment of [Carstengerdes2005], and the reproduction of his main results (strong underestimation with planar mirror, lesser underestimation with increasing mirror curvature) indicates, that the parameterization of the simulated mirrors leads

to a comparable perception of distances in the simulator. These effects were also previously reported by [Flannagan1996].

For *Hypothesis 3* the lead car distance was varied between 20, 40 and 60 meter and two findings were made: increasing the distance of the reference stimuli (lead car) leads to an overall lesser amount of underestimation. Secondly, a reduction of the standard deviation with increasing distance was observed. Both findings were consistently observed for all three mirror types, but their magnitude reduces successively with increasing mirror curvature (from Planar to C20 to C14). Based on the reviewed literature, such a systematic variation of the reference stimuli and the findings of Hypothesis 3 was not reported before and the simulator study contributes to the state of the art. A probable reason, why no further literature was found for this topic, is that this setting triples the amount of experiment conditions, which leads to a huge amount of effort for a field study. In contrast, this is a much smaller problem in the simulator, because the positioning of the vehicles for each trial does not consume any time.

The proper adjustment of the field of view of the simulated mirrors as well as the minification effect were tested and reported before (section 3.3). Therefore it can be concluded that the pictorial depth cues (e.g. absolute size of objects, relative size between them) lead to a realistic perception of the objects (lead vehicle, rear vehicle). But section 3.5 also explained that there are differences with regard to the physiological depth cues which probably lead to a different perception of distances in the simulator (accommodation, vergence and disparity deliver inappropriate information). From section 2.3.1.3 and the hierarchy of depth cues by [Cutting1995] it is known that these physiological cues are no longer reliable at distances > 10 meter. But in the simulator, these distances are much smaller and accommodation and vergence give wrong distance informations: the eye - mirror distance is approximately 0.65 meter, and the eye - front beamer wall is approximately 2.8 meter. These distances are fix, regardless of the shown distances for the two vehicles. The mismatch between pictorial and physiological depth cues was one of the main reasons, why this study was done. Because the main findings of the field study of [Carstengerdes2005] and also [Flannagan1996] were reproduced and the average magnitude of the underestimation was at a similar amount, it can be assumed that the misleading physiological cues were not the primary source of information for the subjects.

Nevertheless, it has to be considered, that there are a few subjects which showed a much stronger underestimation of distances across all mirror types (subjects 5 and 14, see Figure 4.4, p. 80). It is imaginable, that in these cases the physiological cues still play a role for the distance estimation: the eye-mirror distance is four times smaller compared to the eye-front screen distance which would support this assumption (0.65m vs. 2.8m). For a further more detailed investigation of this topic, a different driving simulator setup would be useful, where the front beamer view is replaced by a monitor, which is located at the same distance as the mirror. In this case, the physiological cues to distance would still remain faulty (they do not relate to the real distance) but less underestimation would be expected, because physical distance between mirror and front view would not be the same.

As said before, the setting of this experiment was derived from the distance estimation study conducted by [Carstengerdes2005], but the distances that subjects had to estimate were adapted. In this study, distances were used which are more common for a lane change scenario on a German Autobahn. Nevertheless, there are some rear car distances which were shown in both

studies: in the study of Carstengerdes, the largest rear car distance that subject had to estimate was 20 meter and in this simulator study the same rear car distance was also tested. Unfortunately, Carstengerdes did not publish the exact numbers for the estimated distances, therefore a comparison can only be done on a visual basis with the help of Figure 4.7.

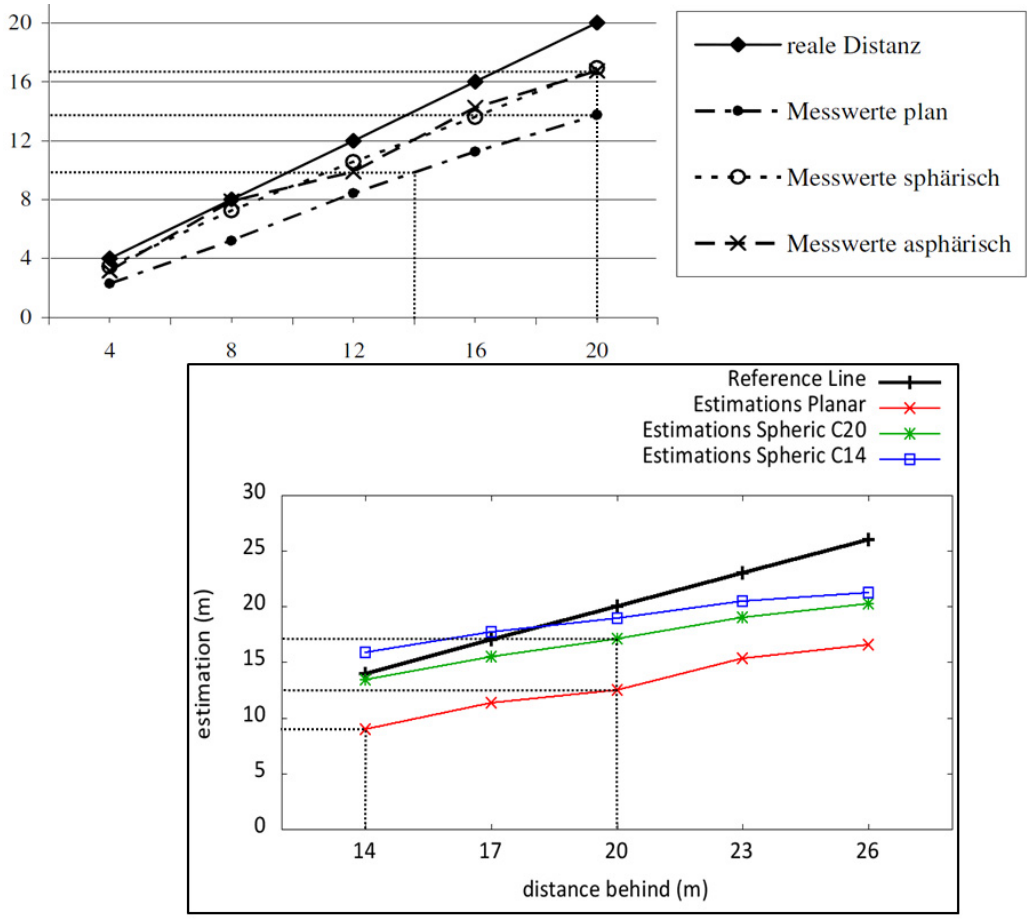

Figure 4.7: Top: original figure taken from [Carstengerdes2005, p.75, Abbildung 4]); Bottom: results of this study for the 20 meter lead car distance. Comparison of 14 meter and 20 meter real distance (x-axis) and corresponding estimations (y-axis).

As a prerequisite, the relative estimations in percent that were given by the subjects in this study were transformed into distances in meter. With regard to the planar mirror, and the 20 meter rear car distance, both studies lead to similar average values for the estimated distances in meter: 12.50 meter in this study vs. approximately 13.5 meter for Carstengerdes. For the same rear car distance of 20 meter, the spherical mirror in the study of Carstengerdes lead to an average estimated distance of approximately 16.5 meter. The comparable mirror type in this study is the C20 which led to an average estimated value of 16.49 meter. For the smallest rear car distance of 14 meters in this study, the average estimated distance is 9.51 meter. The value for the study of Carstengerdes can be derived from the linear regression line in the graphic, and is approximately 10.0 meter. Although this procedure is not exact, the few possible visual comparisons provide a further indication, that the chosen parameterization of the simulated

mirror types delivers acceptable results compared to the used mirror types in the field study of Carstengerdes.

Two further differences between the study of Carstengerdes and this simulator study existed. 1) In this study, a lead car was used as reference object (similar to the distance estimation study by [Flannagan1996]). Instead, Carstengerdes used a pylon as an abstract reference object. This abstract object removes the possibility to use the object (vehicle) size as a cue to distance. Because a car was used as reference object in this study, it was not surprising that 5 subjects mentioned in the questionnaire, that they used the vehicle size as a cue to estimate the relative distance. 2) Another slight change was made with regard to the amount of viewing time: subjects in the experiment of Carstengerdes could see the rear vehicle in the mirror for two short periods of time (2 * 2 seconds, with a short pause in between). This was used to emulate two separate mirror glances. Instead, my intention was not to force subjects into a certain gaze pattern which might not be common for them. Instead, subjects were allowed to freely move their gaze within the period of time of 4.5 seconds. These two differences did not change the main results with regard to the Hypotheses 1 and 2.

Apart from the comparability with the study of Carstengerdes, a comparison with further studies is possible only in a limited way. The general effect of a strong distance underestimation with the planar mirror and lesser underestimation with increasing mirror curvature is comparable on the basis of an average amount of underestimation. Nevertheless, such comparisons are problematic, because the experiment conditions and the procedures are different. One problem is that the used mirror types vary, and especially the visible field of view is not exactly known. The mirror simulation used in this thesis used an empirical approach to calibrate the mirror view according according to some key parameters for the three different mirror types: field of view, horizontal and vertical adjustment, physical dimensions and minification strength, but such a procedure is not found in every study. Even if the mirror type is given ([Flannagan1996] for example used a spherical mirror with 1000mm curvature radius and an aspheric A14 mirror), the physical dimensions of these mirrors vary from vendor to vendor and from vehicle to vehicle. Such variations in the mirror dimensions also change the field of view. Without these numbers a more detailed quantitative comparison of the studies is hardly possible.

4.2 Experiment 2: Gap Acceptance and Lane Change Behavior

The objective of the second experiment is to investigate whether the different simulated mirror types have an impact on the gap acceptance behavior during a simulated lane change task. The results of the first experiment showed, that the planar mirror leads to a stronger amount of underestimation of distances, while this effect is reduced with increasing mirror curvature. If drivers use the distance as a cue to decide if a gap is acceptable or not, it can be assumed, that drivers also accept more gaps with increasing mirror curvature. Based on the literature findings in section 2.3.3.2 it is also expected that there is a reduction of the accepted time-gaps with increasing mirror curvature (from Planar to C20 to C14). It is the objective of this experiment to investigate these assumptions and to gather a database that can be used for the gap acceptance

model development which is described in the next chapter.

4.2.1 Scenario and Task

Figure 4.8 shows the basic setting of the traffic scenario that was used for this experiment. In each condition, subject's vehicle A was approaching with a speed of 130 km/h towards the slower lead vehicle B. After 4.5 seconds of approach an acoustic signal was given and subjects should now look into the left exterior mirror. At this point in time, the vehicle from behind (C) was set up at various distances d_{AC}, and approached the ego vehicle with one of three higher speed differences Δv_{CA}={+10, +15, +20 km/h}.

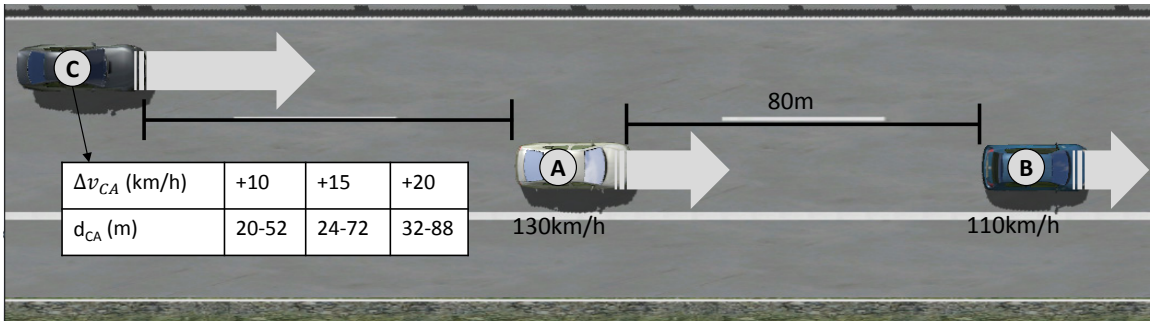

Figure 4.8: Different scenario configurations at each trial start; Ego / subject vehicle (A) drove with 130 km/h; slower lead car (B) located 80 meter ahead, driving 110 km/h; faster rear vehicle (C) was set up with a higher speed difference Δv_{CA} = {+10, +15, +20} km/h. For each speed difference, (C) was set up at different distances d_{CA}. See text for details on combinations.

The task of the subject was to either signal a lane change decision ahead of vehicle C, by turning the steering wheel left (by 30 degrees), or to press the brake pedal (by about 20%) to signal a braking action to let vehicle C pass and stay behind lead car B.

The two action responses (braking or steering) were not fed into the vehicle dynamics of the simulator, instead the vehicle was driven by an automation which controlled the steering as well as the speed of the ego vehicle. It was not required to actually drive the vehicle, instead, the action response was recorded and afterwards the next situation was started. Because drivers did not need to drive, and the steering wheel was decoupled from the vehicle dynamics, it was necessary to strengthen the force feedback compared to a normal driving simulation. This allowed the subjects to rest the foot on the brake pedal and also ensured, that the steering wheel always turned back to a centered steering wheel position. In both cases, the stronger force feedback prevented that already slight movements of the pedal or the steering wheel were recorded as action responses.

Table 4.4 gives a detailed overview about all 26 *experiment conditions* (combinations of distance and speed difference for the approaching rear vehicle (C)). The experiment conditions are sorted according to the initial value of the time-to-collision (ttc_{init}) which can be calculated by the division of distance / speed difference.

Δv_{CA} (km/h)	+10	+15	+20
ttc_{init} (s)	d_{CA} (m)		
5.76	-	24	32
7.19	20	30	40
8.63	24	36	48
10.07	38	42	56
11.51	32	48	64
12.95	36	54	72
14.39	40	60	80
15.83	44	66	88
17.27	48	72	-
18.71	52	-	-

Table 4.4: Overview on the 26 experiment conditions for the approaching vehicle C. Each table entry shows the distance d_{CA} in meter, which results from the combination of ttc_{init} and speed difference Δv_{CA}.

The ttc_{init} conditions which are marked bold were presented in all three speed differences Δv_{CA}. The ttc_{init} conditions were chosen based on a previous study in the same simulator ([Yan2015]). In that study subjects used a planar mirror and conducted 87% lane changes at 15.83 s and 97% braking actions at 7.19 s which sufficiently covers the behavioral range. With the description of the basic traffic scenario, the hypotheses for the experiment can be defined. Why additional ttc_{init} conditions were added is explained in the hypotheses section below.

4.2.2 Hypotheses

As mentioned in the introduction, the hypotheses of this experiment are derived from the results of the distance estimation study and the findings that were previously reported in the literature.

Hypothesis 2.1: The planar mirror leads to the smallest number of lane changes. Increasing the field of view of the simulated mirrors (from Planar to C20 to C14) leads to an increased number of lane changes.

Hypothesis 2.2: With increasing speed difference Δv_{CA}, the number of accepted gaps for situations with equal ttc_{init} will increase.

Hypothesis 2.1 is derived from the results of the first experiment, which showed, that the planar mirror leads to a stronger amount of underestimation of distances, while this effect is reduced with increasing mirror curvature. Due to the minification the gap not only appears larger, but at the same time the same relative speed (in m/s) is also perceived smaller, because the angular change is smaller if the image is minified. It is assumed that drivers use these two effects as cues to decide whether a gap is acceptable or not. As a consequence of the minification, Hypothesis 2.1 postulates that drivers accept more gaps with increasing mirror curvature.

Hypothesis 2.2 is motivated by the following idea: if the subjects would rely on the time-to-collision to make their lane change decision, the number of accepted gaps should be the same for situation with equal ttc_{init} (a row in Table 4.4). But, if ttc_{init} is constant, the increasing

speed difference automatically leads to an increased distance, because the time-to-collision is calculated by $d_{CA}/\Delta v_{CA}$. It is proposed, that the effect of Hypothesis 2.2 is caused by the increasing distance, which is coupled with the increasing speed. This proposal is based on the finding [Carstengerdes2005], who tested the impact of different mirror types on the perception of the time-to-collision. He manipulated speed and distance and found that the influence of both, speed and distance was significant, but independent of the mirror type the distance had a stronger influence compared to the speed.

After Hypothesis 2.2 is described, it can be explained, why the number of the experiment conditions in Table 4.4 is not equal for each speed difference. As said above the seven ttc_{init} which are marked bold were derived from a previous experiment. Based on these 21 conditions, the calculation of the total experiment time was done (with a maximum of 60 minutes per experiment session). Because a short amount of time was left, a few more conditions could be added.

The minimum number of lane changes is certainly reached at a small ttc_{init} condition, while the maximum possible number of lane change will be reached at a certain large ttc_{init} condition. With the assumption that Hypothesis 2.2 is correct: if the maximum number of lane changes is reached at a certain large ttc_{init} condition and a small speed difference (e.g. 10 km/h), the same maximum number of lane changes should be reached for a smaller ttc_{init} condition already at a higher speed difference.

Therefore, the table was diagonally extended by two larger ttc_{init} conditions (17.27 s and 18.71 s) which are tested for the smaller speeds. Vice versa, an additional smaller ttc_{init} condition of 5.76 s was added for the larger speed differences. Because these additional conditions were not shown in all speed difference conditions they were not used for the testing of the hypotheses. These conditions were added, because it is expected, that for some conservative subjects, the $ttc_{init} = 15.83$ seconds might not be sufficient to already see the maximum number of lane changes, while some more risk seeking drivers might conduct lane changes at $ttc_{init} = 7.19$ seconds. Although, this is not a problem for the hypotheses testing it could be beneficial for the model development if the full behavioral range is covered and these additional condition increase the chance that this is achieved.

4.2.3 Procedure

14 Participants were invited for the experiment (7 male, 7 female), aged between 22 and 36 with an average of 26.4 years. Driving experience was between 4 and 18 years (average 8.4), estimated driving kilometers per year 700-15000 (average 6130) and for the Autobahn 500-12000 km/year (average 3960). All participants had not participated in the first experiment and were invited for three sessions, each at a different day and at least one day off in between was required. In each session one of the three mirror types was used and the order of mirror type per session was randomized between participants. Similar to the Experiment 1, subjects were not informed about the different mirror types. Similar to the first experiment, the reason was again that subjects should not actively think about potential differences between the mirror types because this might have led to compensation effect and adaptation of the usual decision making behavior.

At the beginning of the trial, subjects were instructed to look at the lead vehicle. After four

seconds an acoustic signal was given from the front speaker of the simulator near to the exterior mirror. This signaled the subjects to shift their gaze towards the left mirror and observe the rear vehicle, which was set up randomly at one of the 26 speed / distance combinations. They were instructed to conduct an overtaking maneuver if possible. Furthermore, they were told to behave like they would normally do in a real Autobahn situation. Besides the approach towards the front vehicle no time pressure was given and subjects should decide as they would normally do. At each of the three days 10 randomized test trials were shown before the three blocks were done. This should allow the subjects to get familiar with the procedure. It was also said that, in case of having trouble with the task, further help can be given or some additional test trials can be done. None of the participants asked for such additional help. After the third session each participant had to fill out a short questionnaire and the goals of the experiment were explained in detail. Similar to the first experiment, money was given in cash after the third trial (10 Euro / hour). The collected contact email addresses were deleted after the experiment was finished. Each participant was given a number to match questionnaire results and recorded simulator data later on.
In summary, the total experiment design was: 26 ttc_{init} conditions based on a combination of d_{CA} and Δv_{CA}. Each of these conditions was repeated 12 times. Similar to the distance experiment, the repetitions were divided into three blocks with four repetitions. This resulted in 312 trials per mirror ($3 * 4 * 26$), a total amount of 936 trials per subject and overall 13104 actions for the 14 subjects. The number of ttc_{init} conditions used for hypotheses testing was 21 (those marked bold in Table 4.4) which resulted in 252 trials per mirror/subject, 756 total trials per subject and 10584 total trials. For each experiment condition, 168 action responses were recorded. (12 repetitions, 14 subjects).

4.2.4 Data Recording and Preprocessing

The data recording was also similar to Experiment 1 and the main difference was the recorded action response. Instead of typing on a keypad, subjects had to use the steering wheel and the brake pedal. Both analog signals were recorded individually in the data files and a third variable was used to store an integer signal. Whenever the subjects turned the steering wheel left or pushed the brake pedal above a threshold (30° steering left, or 20% brake) the variable was either one or a two. If both action responses would have been used at the same time a three would have been recorded, which would have indicated a faulty response. Such a case did not appear, reactions were always steering or braking. Participants also conducted each maneuver "in-time". meaning no collisions with the lead or the rear vehicle were detected. Therefore, the data set for the analysis was complete and no trials were missing.

4.2.5 Results

The first analysis can be done on the overall number of lane changes with a separate view for the different mirror types (Hypothesis 2.1) and the three speed differences (Hypothesis 2.2). For this purpose, data was accumulated across all 14 subjects. Table 4.5 shows the total number of lane changes and the probability for a lane change in the respective condition (mirror type, Δv_{CA}).

Important Remark: the table below uses the data of the experiment conditions $ttc_{init} = [7.19 - 15.83]$ seconds, because they were available for all three speed differences and are used for the hypotheses testing.

Δv_{CA} (km/h)	+10	+15	+20
mirror	lane changes, total / %		
planar	146 / 12.4	438 / 37.2	651 / 55.4
C20	330 / 28.1	656 / 55.8	**856** / 72.6
C14	406 / 34.5	701 / 59.4	**833** / 70.7

Table 4.5: Summary Table, total number of lane changes (max. 756 per entry) and relative number of lane changes in %; Violation against Hypothesis 2.1 is marked bold.

Considering Hypothesis 2.2 first, the number of lane changes continuously increases with increasing speed difference Δv_{CA}. This effect is also consistently found across all mirror types, thus Hypothesis 2.2 is supported by this first comparison of data. Concerning Hypothesis 2.1, there is a big increase from planar to C20, and a much smaller increase from C20 to C14. Considering the results of the first experiment, the smaller difference between the curved mirrors was expected, because the differences of the mirror attributes field of view and minification are much smaller between C20 and C14, compared to the relation between planar and C20 or planar and C14 (please see 4.1 Experiment 1). At Δv_{CA} = 20 km/h the number of lane change is larger for C20 compared to the C14 mirror. This is a *violation* of Hypothesis 2.1 and the next paragraph investigates this in more detail.

Hypothesis 2.1 Table 4.6 provides a more detailed view on the data of the summary Table 4.5 and the violation against Hypothesis 2.1 is seen for the colorized entries.

Number of Lane Changes									
	10 kmh			15kmh			20kmh		
ttc_{init}	pl.	C20	C14	pl.	C20	C14	pl.	C20	C14
7.19	0	0	0	0	2	12	2	15	17
8.63	0	0	3	2	13	31	22	62	56
10.07	0	6	25	25	55	73	66	139	127
11.51	12	23	50	58	119	117	106	146	144
12.95	24	62	75	88	144	144	133	160	157
14.39	46	109	122	124	158	159	155	167	166
15.83	64	130	131	141	165	165	167	167	166
Sum	146	330	406	438	656	701	651	856	833

Table 4.6: Detailed overview on the summary data. Violation against Hypothesis 2.1 at $\Delta v_{CA} = 20$ km/h marked. One further violation is seen at 15 km/h. Colors indicate different magnitudes of the violation: yellow (violation <=3 lane changes) or red (violation >3 lane changes).

It can be seen that the violation is observed across multiple ttc_{init} conditions and it is the strongest for $ttc_{init} = 10.07$. To explore the nature of this violation, a brief review of the

individual behavior data showed, that one subject behaved quite unexpected during the C14 session. The total number of lane changes for this subject was 92 for the planar, 108 for C20 but only 68 for the C14, which is a huge reduction from 108 to 68 (-40) lane changes against Hypothesis 2.1. Considering the total magnitude of the violation on the accumulated data level (856 - 823 = 23 lane changes) the huge reduction for this subject is almost twice as high.

It remains speculative what might have caused this behavior, probably the subject behaved a lot more conservative on that specific day. Although this behavior might be considered an outlier which impacts the significance of the results, one can not simply remove the subject from the overall results, because there is no reason to assume that the subject behaved actively against any instructions. It is assumed that the empirical paradigm is at the root of this problem: each mirror type was tested on a different day and uncontrolled variations in the behavior are more likely in this case. But there was also a good reason to use this empirical paradigm, because the days in between the three sessions should prevent active compensation effects.

After the violation of Hypothesis 2.1 for the C20 and C14 was explored first, the scope is broadened to discuss the results of Hypothesis 2.1 for all three mirrors. Figure 4.9 shows the number of lane changes for $\Delta v_{CA} = 10$ km/h and all ttc_{init} conditions (not only within the range of 7.19 - 15.83 seconds).

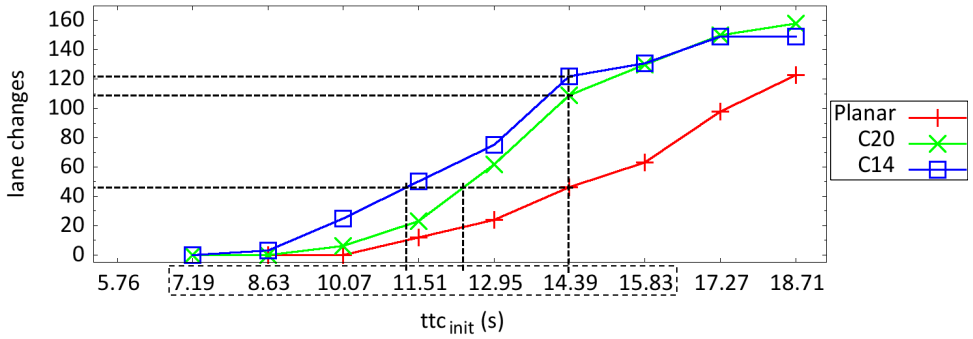

Figure 4.9: Number of lane changes for all subjects at $\Delta v_{CA} = 10$ km/h; Dashed rectangle marks the data range used in the result tables; y-axis: maximum number of lane changes is 168 per ttc_{init} condition; Vertical line at $ttc_{init} = 14.39$ seconds illustrates effect of Hypothesis 2.1: number of lane changes increases from planar (46) to C20 (109) to C14 (122); Additionally, 46 lane changes are reached at smaller ttc_{init} for C20 and C14.

The vertical line at $ttc_{init} = 14.39$ illustrated the effect of Hypothesis 2.1. But the effect can also be interpreted in a different way: considering the 46 lane changes for the planar mirror, the two short vertical lines in the figure indicate where the same number of lane changes could be expected for the C20 and C14 respectively. For the C20, 46 lane changes would approximately be reached at approximately $ttc_{init} = 12.4$ seconds already, which is about 2 seconds less, compared to the planar mirror. For the C14, the same number of lane changes can be expected already at $ttc_{init} = 11.39$ seconds. This reduction of the ttc_{init} for a certain number of lane changes can be observed for all ttc_{init} conditions between $11.51-17.27$ seconds but the strength of this effect diminishes towards the smallest and largest ttc_{init} conditions.

For the speed difference $\Delta v_{CA} = 10$ km/h, no violations were observed in the two tables

above, but it can be seen, that for the increased range another small violation is observed between C20 and C14 at $ttc_{init} = 18.28$ with the magnitude of 6 lane changes.

For the planar mirror condition $ttc_{init} = 15.83$ seconds, it was surprising that only 64 out of 168 lane changes (38.1%) were observed, because in a previous study [Yan2015] there were already 87% lane changes recorded. This high amount of lane changes is not even reached at $ttc_{init} = 18.19$ seconds, where only 123 of 168 or 73.2% lane changes were recorded. It is likely that the instructions led to smaller number of lane changes, because in the experiment of Yan, subjects were advised to react as quickly as possible, while in this experiment, subjects were instructed to behave, as if it was a usual lane change situation on the Autobahn. With this instruction, subjects probably took more time to observe the traffic. During this time the approaching vehicle came closer, which could explain why less lane change actions were observed. Although this difference in the number of lane changes was not foreseen, it still is no problem for the hypotheses which are tested here, because the instruction was the same in all experiment sessions.

Hypothesis 2.2 The next step is to compare the number of lane changes between the three different Δv_{CA} conditions with regard to Hypothesis 2.2: "with increasing speed difference Δv_{CA} the number of accepted gaps for situations with equal ttc_{init} will increase." Figure 4.10 can be used to explain the effect of Hypothesis 2.2 in two ways, similarly to Hypothesis 2.1.

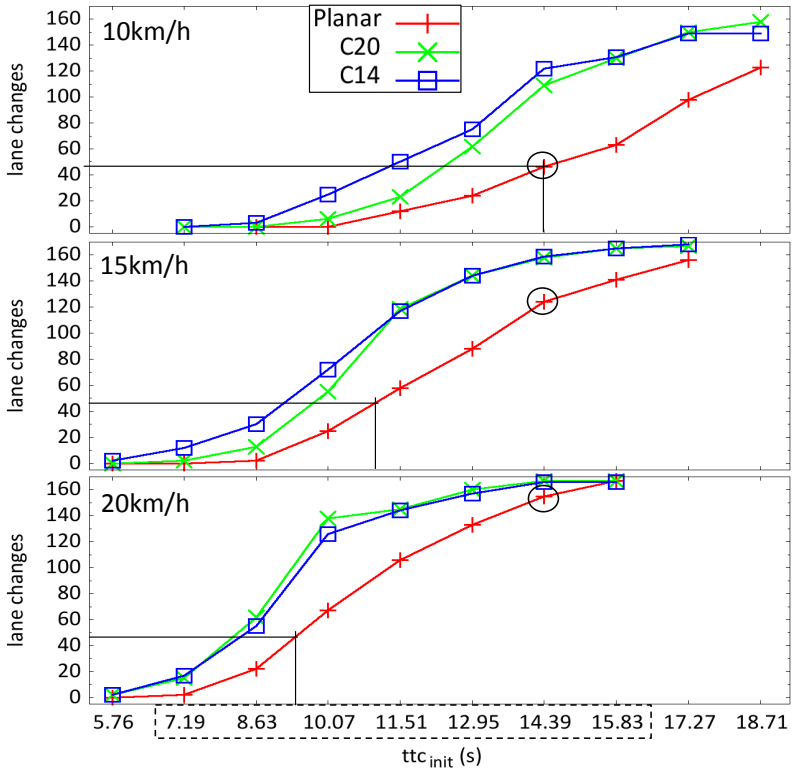

Figure 4.10: Number of lane changes for all three Δv_{CA}; Effect of Hypothesis 2.2 is illustrated at $ttc_{init} = 14.39$ seconds (small circles). Violation of Hypothesis 2.1 at 20 km/h.

1) similar to the previous Figure 4.9, 46 lane changes for the planar mirror at $\Delta v_{CA} = 10$ km/h and $ttc_{init} = 14.39$ seconds are marked in Figure 4.10. For this ttc_{init} condition, the number of lane changes increases from 46 to 124 at 15 km/h speed difference and increases again to 155 lane changes at 20 km/h speed difference.

2) If the number of lane changes increases with Δv_{CA}, the same number of 46 lane changes for the same mirror type can be found at smaller ttc_{init} conditions. The three horizontal lines for the 46 lane changes in the other two speed conditions (+15 , +20 km/h) show that this is also the case.

Generally, the number of lane changes for all three mirror types at all three speed differences converges towards zero for the smallest ttc_{init} conditions, and it converges towards the maximum of 168 for the largest ttc_{init} conditions. Differences between the mirrors can be observed for those ttc_{init} conditions in between (especially these conditions "in between" will be of interest later on in the modeling section). Geometrically speaking, the area which is embraced between the number of lane change curves reduces with increasing speed difference. This interaction describes why Hypothesis 2.1 supposedly failed at the largest speed difference condition of $\Delta v_{CA} = 20$ km/h.

Comparison of both hypotheses Both hypotheses can be discussed from a safety point of view: the situations with small ttc_{init} are of specific interest here, because the risk for accidents increases in these situations. For 10 km/h, there is no difference between the mirrors at $ttc_{init} = 7.19$ seconds. The number of lane changes is 0 for all mirror types. At 15 km/h the number remains 0 for planar, but already increases to two for the C20 and 12 for the C14. At 20 km/h the number of lane changes increases to 2, 15 and 17 for the three mirrors. With these numbers it can be argued that at the smaller ttc_{init} the combination of mirror type and increased speed difference should not be ignored. Although not tested in this experiment, typical speed differences on the German Autobahn are usually much higher and if this trend continues at higher speed differences, it could be expected that even smaller time-to-collision gaps are accepted at higher speeds. Although a value of $ttc_{init} = 7.19$ might not cause accidents, it has to be considered that this value is set at the beginning of the trial and the time-to-collision is smaller when the response action was given and is even smaller when the lane is finally changed.

The reduction of the time-to-collision for both hypotheses can be underpinned by the calculation of the *mean accepted* ttc_{init}. Each entry in Table 4.7 is calculated by multiplying the value of each $ttc_{init} = [7.19 - 15.83]$ condition, e.g. 7.19 or 12.95 with the number of lane changes that was observed for that condition. Summing up the these results for all ttc_{init} conditions, and afterwards dividing the sum by the total number of lane changes of all conditions $ttc_{init} = [7.19 - 15.83]$.

Δv_{CA} (km/h)	+10	+15	+20
mirror	mean accepted ttc_{init} (s)		
planar	14.28	13.89	13.33
C20	14.19	13.36	12.66
C14	13.83	13.16	12.72

Table 4.7: Mean accepted ttc_{init} in seconds. Violation against Hypothesis 2.1 is propagated.

Apart from one exception, the mean accepted ttc_{init} continuously reduces with increasing speed difference, as well as with increasing mirror curvature and also the violation against Hypothesis 2.1 is now also observed for the mean accepted ttc_{init}.

The next table compares the strength of the reduction caused by the different mirrors with the reduction caused by the speed differences. Table 4.8 summarizes the average difference of the mean accepted ttc_{init} for the three possible mirror combinations and the three possible speed difference combination.

Reduction of the mean accepted ttc_{init}			
	Transition between Mirror Types		
	Planar - C20	C20 - C14	Planar - C14
$\Delta\phi$ (s)	0.43	0.167	0.597
	Δv_{CA} transition		
	10 - 15 km/h	15 - 20 km/h	10 - 20 km/h
$\Delta\phi$ (s)	0.63	0.566	1.197

Table 4.8: Difference between the mean accepted ttc_{init} for the transitions between the mirror types and the speed differences.

From 10 to 20 km/h the mean accepted ttc_{init} reduces by 1.197 second on average. In contrast, the reduction from planar to C14 is only about 0.597 seconds on average. With regard to the mean accepted ttc_{init} in seconds, the speed difference has a stronger effect compared to difference between the mirrors. It can also be remarked, that reduction of the mean accepted ttc_{init} by 0.597 seconds between planar mirror and C14 is similar to the results of [deVos2000], although they used a different experimental paradigm.

Statistical Tests After the visual inspection of the results, additional statistical tests were conducted. For this purpose, a couple of two-way ANOVAs and t-tests were calculated to test, if the differences between the mirror types and between the three speed differences are statistically significant or not. For the ANOVAs the dependent variable was the number of lane changes. Subsequent tests were conducted for the independent variables mirror type + ttc_{init}, and for mirror type + speed difference. The accumulated results of both two-way ANOVAs can be seen in Table 4.9 below.

	F	p	p[GG][6]	p
mirror	F(2,26) = 32.02	< 0.001	< 0.001	*
ttc_{init}	F(6,78) = 178.93	< 0.001	< 0.001	*
Δv_{CA}	F(2,26) = 114.04	< 0.001	< 0.001	*
mirror:ttc_{init}	F(12:156) = 5.03	< 0.001	0.002	*
mirror:Δv_{CA}	F(4:52) = 1.31	0.275	0.283	

Table 4.9: Results of the two-way ANOVA's to test if the impact of the mirror type, speed difference Δv_{CA} or ttc_{init} on the number of lane changes is significant. Two interaction effects were also tested.

All three variables (mirror, ttc_{init}, speed difference) had a significant effect on the number of lane changes and also the interaction effect between mirror and ttc_{init} was significant. The interaction effect mirror - Δv_{CA} was not significant. Similarly to the distance estimation experiment, Mauchly's sphericity test was violated and the Greenhouse-Geisser correction has to be used, because ϵ was < 0.75. The ANOVA results support Hypothesis 2.1 (variable mirror is significant) and also Hypothesis 2.2 (variable speed difference is significant). But, a violation of Hypothesis 2.1 was also observed between C20 and C14. A paired t-tests was calculated for each of the three speed differences, results are given in Table 4.10.

Δv_{CA}	10 km/h		15 km/h		20 km/h	
	planar	C20	planar	C20	planar	C20
C20	< 0.001	-	0.0011	-	< 0.001	-
C14	< 0.001	0.155	< 0.001	0.39	0.0011	0.7

Table 4.10: Hypothesis 2.1: p values for paired t-tests (Holm) separately done for each of the three Δv_{CA} conditions. Significant difference between the planar and both curved mirror types, but no significant difference between the curved mirrors.

As expected, the t-tests show a significant difference between the planar and both curved mirror types C20 and C14 for all three speed differences. The differences between C20 and C14 were not significant.

With regard to Hypothesis 2.2, a paired t-test was calculated across all three mirror types. The results in Table 4.11 show that this hypothesis is fully accepted and the number of lane changes is difference for all three speed differences.

Δv_{CA}	10 km/h	15 km/h
15 km/h	< 0.001	-
20 km/h	< 0.001	< 0.001

Table 4.11: Hypothesis 2.2: p values for paired t-tests for the three speed differences, tested for the data of all mirror types.

Conclusion The paired t-tests support the results that were presented already in the summary table at the beginning of this section (see Table 4.5). The violation against Hypothesis 2.1

at the highest speed difference was already observed there and the t-test showed, that Hypothesis 2.1 holds for the relation between the planar mirror and both curved mirrors C20 and C14, but Hypothesis 2.1 is not significant for the comparison of the two curved mirrors. With regard to Hypothesis 2.2, the observation in the summary table already showed, that the number of lane changes increases with increasing speed difference for all three mirror types. The t-test supports this and Hypothesis 2.2 is accepted for all three speed differences.

4.2.6 Questionnaire

Similar to Experiment 1, a short questionnaire had to be filled out and again, the main objective was to find out, if people have any knowledge about what type of mirror they have on their car. The two questions were the same as in Experiment 1: “Which type of driver side mirror does your own vehicle have or, if you do not own a car personally, the vehicle that you usually drive?“ The potential answers were “planar“, “spherical“, “aspherical“ and “don’t know“. The second question asked: “Can you describe some characteristic properties of the mirror?“. Results were quite similar to Experiment 1: only two of fourteen subjects answered they have an aspherical mirror, knowing that it reduces the size of the blind spot region. The other twelve subjects had no idea which mirror type their vehicle had and they were also not aware about different characteristics. None of the fourteen subjects made any comments about a distortion effect (minification) that comes with the curved mirror types.

Subjects were also asked what situation characteristics (variables) they used to make their decision: “Please revisualize the situations and try to describe how you made the decision for a gap. Which situation characteristics were used?“

Concerning the characteristic properties of the traffic situation, four subjects named only one criteria: rear vehicle speed (1 subject), the comparison of the speed between rear and lead vehicle (1 subject) and the rear vehicle distance (2 subjects). The other ten subjects mentioned both, distance and speed of the rear vehicle speed, while one of them additionally mentioned the speed difference to the front vehicle. One of the ten subjects also described that it was difficult to estimate if the speed of the rear vehicle in the near and far conditions was different from each other. From all fourteen subjects, thirteen did not write more details about how they actually made the decision or if different situation dependent strategies were used.

Similar to Experiment 1, the questionnaire was mainly used to ask about the mirror types and the result in this case was the same as in the previous experiment. None of the subjects knew anything about a minification effect, while the blind-spot problem is known by a couple of subjects. With these results it can be assumed that no compensation effects can be found in the data.

4.2.7 Summary

This driving simulator experiment investigated three different hypotheses with regard to potential changes of gap acceptance and lane change behavior, which might be caused by three different simulated driver side mirror types. The previous Experiment 1 had already shown that distance underestimation decreased with increasing mirror curvature (from Planar to C20 to

C14). Because of that, Hypothesis 2.1 proposed that more gaps will be accepted with increasing mirror curvature. Hypothesis 2.2 tested whether more lane changes will be accepted with increasing speed difference although the time-to-collision is kept constant.

In contrast to the reviewed field studies (literature review, section 2.3.3.2), the participants of this simulator study were not informed about the use of different mirror types. The result of the questionnaire showed, that participants had no idea what type of mirror is mounted on their own vehicle, and they did not know anything about the minification effect of curved mirrors. Therefore, it is relatively safe to say that no compensation effects exist in the data.

Hypothesis 2.1 was partially confirmed: the smallest number of gaps was accepted with the planar mirror, and a significantly larger number of accepted gaps was observed for both curved mirrors (C20 and C14). The gaps were also significantly smaller with regard to the mean accepted ttc_{init}. In contrast, the number of lane changes was not significantly different between the C20 and the C14 mirrors. A separation of the data into the three speed differences showed that there was a slight difference in the number of lane changes between C20 and C14 according to Hypothesis 2.1, but this difference successively diminished with increasing speed difference. However, a t-test resulted in a non-significant difference for all three speed difference conditions.

With regard to the violation of Hypothesis 2.1 between C20 and C14: it was found that the total number of lane changes for one subject largely violated Hypothesis 2.1: for this subject 108 out of 168 possible lane changes were observed for the C20 but only 68 for the C14 (a difference of 40). On the level of the accumulated data of all 14 subjects, the strength of the violation was even smaller (only 23 lane changes). Interestingly, the subject behaved according to the hypothesis with regard to the relation planar - C20, because here the number of lane changes increased from 92 to 108. It is assumed that the experiment design caused this violation, because subjects were using each mirror type at a different day, which bears the risk, that potential behavior variations have an impact on the experiment. Nevertheless, it was not considered to exclude this subject from the analysis, because there was no indication that the subject behaved actively against any of the instructions. Furthermore, the behavior of the subject did not fully violate Hypothesis 2.1.

Hypothesis 2.2 was fully accepted, the number of lane changes increased significantly with increasing speed difference. A paired t-test showed that all three speed differences were are significantly different from each other and the effect was also consistently found across all three mirror types. The original idea behind this hypothesis was confirmed and this is important also for the development of the gap acceptance model: if subjects accept smaller gaps for the same ttc_{init} condition, the time-to-collision is supposedly not used by the subjects to make their decision. The higher speed difference does not not offer a plausible explanation, because this should lead to fewer lane changes. But speed difference and distance were linked to each other and if the speed difference was increased, the distance was also increased (because $ttc_{init} =$ distance / speed difference). Consequently, the increased distance can be considered the explanation for the effect of Hypothesis 2.2. It is concluded that the time-to-collision seems not to be the dominant cue for the decision making with regard to gap acceptance (at least in this study).

A comparison of the results of this simulator study with previously conducted field studies (section 2.3.3.2) is limited. The finding of [deVos2000] with regard to a reduction in the accepted time gap was also observed in Experiment 2, but the experiments used different de-

signs. [deVos2000] asked subjects to accept the gap at the latest possible point in time, while subjects in this study were free to decide, whether and when they wanted to do a lane change. An interesting aspect was found in the results of their questionnaire: „*Half the respondents accurately knew what type of mirror they had, a quarter said they did not know, a quarter thought they had a planar driver's side mirror, while in fact it was convex and only a very small proportion thought the mirror was convex while it was flat.*“ [deVos2000, p.78]. In the questionnaires for Experiment 1 and 2, the results were completely different: from the 29 participants, only 5 had knowledge about the mirror type of their own vehicle, and no participant knew about image minification. Another study by the NHTSA did not find an impact of different mirror types on gap acceptance, but drivers were allowed to use the interior mirror, which might have completely negated the effect [NHTSA2008].

The results of this driving simulator study offer a detailed database for the development of the gap acceptance model and the next chapter will describe the modeling efforts that were made in this thesis.

5 Modeling Gap Acceptance Behavior

The development of the gap acceptance model in this thesis is inspired by previous driver modeling efforts, which were published in [Weber2013]. The main concepts behind that model are briefly summarized in the first section 5.1.

Afterwards, the modeling objectives for this work are derived (section 5.2). The question, which variables are used for the gap acceptance model is discussed in section 5.3, and two alternative approaches are compared. Based on the results of Experiment 2, it is explained why visual angles are preferred over variables like distance in meter, speed in km/h or the time-to-collision.

The fact that Hypothesis 2.1 of Experiment 2 was only partially accepted was explained with a behavior variation of one specific subject (see summary section 4.2.7). A more detailed investigation of the individual behavior of all subjects was not done in the experiment chapter, because the focus was to test the significance of the two hypotheses of the experiment, which was done using the accumulated data of all subjects. With regard to the gap acceptance model, this is not sufficient: the introduction of this thesis explained that the industry has a practical interest in driver models which are able to simulate individual behavior differences, in this case the variability that can be observed during gap acceptance situations. For this purpose, it is necessary to take a closer look at the individual behavior data, and section 5.4 presents a more detailed view on the 14 subjects.

Afterwards, section 5.5 presents the basic ideas of the gap acceptance model, which are derived from the individual behavior data of Experiment 2. In this section, the concepts of the previously developed model in [Weber2013] are assessed and revised (5.6.1). A visual approach (called visual mapping) is used to demonstrate, how behavioral differences of the subjects can be integrated into the gap acceptance model (section 5.5.2).

Section 5.6 describes the implementation details of the model, how it interacts in real-time with the Experiment 2 scenario (5.6.1), how it perceives its input (5.6.2), and how the decision making process is implemented and parameterized (5.6.3).

The implemented model was used to simulate the behavior of all subjects of Experiment 2 and the full experiment was simulated multiple times. The results of the model simulations are presented in section 5.7. First, they are analyzed with regard to the hypotheses of Experiment 2 (5.7.1), and afterwards the quality of the individual behavior models is assessed in more detail (5.7.2). The last section of this chapter summarizes the modeling efforts and gives an outlook on future extensions of the model.

5.1 Previous Driver Modeling Work

The driver model described in [Weber2013] was developed in the three year research project IMoST2[1]. One project objective was to explore the potential use of an integrated simulation platform (driver behavior model integrated into a driving simulation environment) as a tool to support the development of driver assistance systems. Due to the scope of the project, the model development was not focused on a single maneuver like gap acceptance. Instead, it was intended that it can handle "typical" driving maneuvers on a German Autobahn in a real-time 3D driving simulation, e.g. lane following, car-following, lane change left / right. Additionally, the model served as a common framework to integrate different research interests of the project: longitudinal and lateral vehicle control [Eilers2011, Eilers2014], TWIN model which tackles multi-modal stimuli integration, e.g. visual and acoustic cues [Steenken2014], Situation Awareness and task modeling to create an adequate situation representation for the driver model [Baumann2010, Baumann2009].

My personal responsibility in that project was the integration of the different research topics into the common driver model which interacted within the real-time 3D driving simulation. Furthermore, I was also involved in the task modeling, and implemented the decision making process which enabled the model to execute the different driving maneuvers.

The idea to use angular measures as input variables for the model already emerged in this project, because the model was designed as a first-person driver model. Figure 5.1 illustrates, how the *angular vehicle width* Θ^{veh} was calculated, based on 3D coordinates that were available at runtime in the driving simulation. The *angular vehicle width* Θ^{veh} was previously used in driver models by other researchers (e.g. [Lee1976, Anderson2009]), but not in the context of lane changing, where the model uses the mirror view to observe an approaching rear vehicle.

Terminology: In the literature review, Θ was also used as a symbol for a visual angle. Additionally, Θ' was used to specify its rate of change (angular velocity). To improve readability, the symbol Θ' for the angular velocity is replaced by Δ.

Based on the angular vehicle width Θ^{veh}, its rate of change Δ^{veh} can be calculated during the simulation. Both were used as input variables for the decision making process of the model whether a lane change left can be done or not. It was assumed that drivers would assess the dynamics of the situation, in other words the approaching speed, or how fast vehicle C closes the gap. Therefore, the angular velocity Δ^{veh} was considered the main decision criteria and a single threshold value was assumed: if the rear vehicle approaches slower than the threshold, a lane change is done. Vice versa, the model rejects a lane change, if the approaching speed is above the threshold. Due to the hyperbolic characteristic of the angular velocity Δ^{veh} with decreasing distance, the model accepts larger approach speeds at higher distances.

[1] Integrated Modeling for Safe Transportation 2

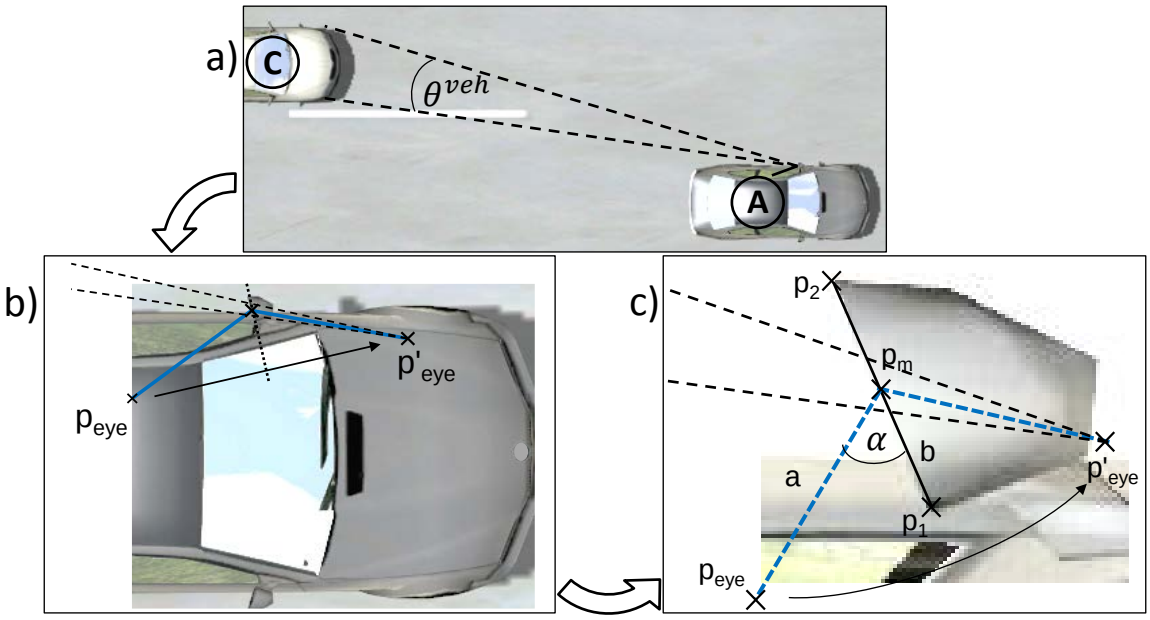

Figure 5.1: a) Driver model in vehicle (A) considers a lane change in front of a faster vehicle (C). Angular vehicle width Θ^{veh} perceived by the model; b) the assumed location of the driver p_{eye} is mirrored at the horizontal mirror axis; c) p_1, p_2 specify the horizontal mirror axis. It was assumed that the driver looks at the center of the mirror p_m. Distances a, b and the angle α were defined for the model, which allows to calculate point p'_{eye}. *Important*: approach is valid only, if a planar mirror surface is assumed.

If the model would exclusively rely on the angular velocity Δ^{veh}, it would accept even the smallest gaps, if the speed difference to the approaching vehicle is very small or even zero. To consider a minimum safety distance, a second decision criterion was implemented, which tested the current angular vehicle width Θ^{veh} against a fixed threshold value (a minimum safety distance). With these two threshold comparisons, the decision making process was twofolds: first, the minimum safety distance was tested, and if the approaching vehicle C was not inside this range, the current angular velocity Δ^{veh} was assessed. If both tests were successful, the model initiated a lane change maneuver.

Unfortunately, this model implementation could not be validated, because no dedicated experiment was conducted, which systematically assessed different gap acceptance situations. Instead, driver behavior data for the parameterization of the model was available only from a simulator study where a free-driving scenario was investigated. In this two-lane Autobahn scenario the participants were advised to obey speed restrictions of 100 and 130 km/h. Otherwise they could freely drive within moderate traffic, which consisted of slower trucks (driving between 80-90 km/h) and passenger cars (100 - 140 km/h). This scenario was also the target scenario for the IMoST model[2]. With the available data of this study, the two threshold values for the gap acceptance decision were manually adjusted: the Θ^{veh} threshold was adjusted, until no near range accidents occurred any more. Afterwards, the threshold for the angular velocity

[2]https://hcd.offis.de/wordpress/?page_id=16 offers a video download which demonstrates how the IMoST model drives within the Autobahn scenario.

Δ^{veh} was adjusted, until the accepted, average time-to-collision between the ego vehicle driven by the model and the approaching vehicle C was comparable to the subject data of the free driving scenario. It needs to be mentioned that in the study only 35 lane changes were observed, where a faster approaching vehicle C was within a distance of at least 100 meter when the lane change was done. This shows how small the available database was.

In contrast to the free driving scenario, the results of Experiment 2 offer a much better starting point for a systematic assessment of the gap acceptance concept that was implemented in the IMoST model, and this will be done throughout this modeling chapter.

5.2 Modeling Objectives

The gap acceptance model developed in this thesis will follow the approach of a "first-person" driver behavior model, which was already used for the development of the IMoST driver model. Instead of using empirical data of a free driving scenario, Experiment 2 now offers the possibility to develop such a model with the help of a more elaborated database, and this is expressed by the main objective for the development, Objective 1:

Objective 1: The model shall be able to simulate the observed findings of Experiment 2 with regard to the experiment hypotheses:

- **Hypothesis 2.1**: The planar mirror leads to the smallest number of lane changes. Increasing the field of view of the simulated mirrors leads to an increased overall number of lane changes (from Planar to C20 to C14).
- **Hypothesis 2.2**: With increasing speed difference Δv_{CA}, the number of accepted gaps for situations with equal ttc_{init} will increase.

To achieve this main objective, the model needs different capabilities, which are specified in the next three objectives.

Objective 2: The model needs to be able to perceive the different traffic situations of Experiment 2. It shall perceive its visual input via the implemented mirror simulation (described in section 3.3 realizing the "look into the mirror", from a first-person driver perspective.

Objective 3: The model needs a decision making process to solve the gap acceptance task of the subjects in Experiment 2. The basic threshold concepts of the IMoST model shall be evaluated with regard to its appropriateness and, if necessary, revisions shall be done.

Objective 4: The model shall interact within the Experiment 2 scenario similar to the human participants. In this regard, it can be considered a "real-time" behavior simulation model.

5.3 Discussion about Model Variables

While the use of angular measures in the IMoST model was based on plausible assumptions only, this section argues on the basis of the results of Experiment 2, why angular measures like

the angular vehicle width Θ^{veh} or the angular velocity Δ^{veh} should be preferred for the gap acceptance model.

The first section 5.3.1 explains, why variables like distance in meter or the speed in km/h can not be used, before section 5.3.2 discusses the angular measures.

5.3.1 Metric Measures

As explained in the driver model review (section 2.2), measures like distances in meter, absolute or relative velocities in m/s or km/h, or derived measures like the time-to-collision in seconds have been used a lot as variables and parameters in driver modeling. Most of the lane change models that were reviewed relied exclusively on these measures.

These variables are also typically used in the context of empirical studies to specify controlled traffic situations, like it was done for Experiment 2 in the previous chapter:

- distance d_{CA} between ego and rear vehicle measured in meter from bumper to bumper.
- speed difference Δv_{CA} between ego and rear vehicle in m/s (or km/h).
- the 26 experiment conditions (Table 5.1 below) were specified and categorized according to the time-to-collision: $ttc_{init} = \frac{d_{CA}}{\Delta v_{CA}}$.

Δv_{CA} (km/h)	+10	+15	+20
ttc_{init} (s)	d_{CA} (m)		
5.76	-	24	32
7.19	20	30	40
8.63	24	36	48
10.07	38	42	56
11.51	32	48	64
12.95	36	54	72
14.39	40	60	80
15.83	44	66	88
17.27	48	72	-
18.71	52	-	-

Table 5.1: All 26 experiment conditions of Experiment 2, reprint of Table 4.4, p. 91.

According to the experiment description, all of the 26 experiment conditions were shown in each of the three experiment sessions, and in each of these three sessions one of the three mirror types was used (planar, C20, C14). If the same situations were shown in each session, and the values for the three measures d_{CA}, Δv_{CA} as well as the ttc_{init} were identical, they can not be used to explain the effects that were observed with regard to Hypothesis 2.1. It follows, that a model which would rely exclusively on these measures, would not be able to reproduce the results with regard to that hypothesis. If they should nevertheless be used by a model, a further variable or function would be necessary, which captures the effect of Hypothesis 2.1 (increasing number of lane changes with increasing mirror curvature).

The minification effect was mentioned as a potential explanation for the mirror related findings in the literature review (see section 2.3.3). Therefore, a minification factor (or a function) could be used as additional model variable. This variable could act as a transformation function and manipulate the perception of the metric variables. But including the minification factor explicitly into the model has some drawbacks that need to be discussed: the minification itself is a characteristic property of the mirror. It belongs to the environment, and it is not part of the perception or the cognition of the driver. Instead, what the driver perceives, is the *result* of this minification process. From a perceptual point of view of a first-person driver model the inclusion of a minification variable / factor is not preferred.

But, minification could probably be included into the model on a knowledge-based level: in several of the reviewed studies in section 2.3.3, drivers were informed that different mirrors were tested. In this case subjects had at least some explicit knowledge, which could be part of a model. But, there was a reason why such explicit mirror related information was not given to the subjects in Experiment 2 (and also Experiment 1): it was expected, that subjects might have used this information to actively compensate the visual differences between the mirrors. But how such a compensation actually works, and to what degree it would have happened, is a completely different topic, presumably related to knowledge processing, learning or other cognitive abilities. These issues should be investigated separately with dedicated experiments and are not part of this work. Consequently, in the context of Experiment 2, the minification factor should not be included as factual knowledge into the model either. The questionnaire revealed also, that only two subjects actually noticed which type of mirror is mounted on their own vehicle, and even those two had no idea about a mirror related minification effect. This is interpreted as an indicator that the awareness (the knowledge) for the characteristic properties of mirrors should not be assumed and should not be part of the model.

From the perception point of view of a first-person driver model, and also from a knowledge based perspective, this approach is not preferred.

5.3.2 Angular Measures

As mentioned in the previous section, the driver perceives the outcome of the minification process, which means he perceives an altered visual image of the environment. The natural way for a driver model, which interacts from the perspective of the driver within the scenario, is to rely on variables which can be derived, or are directly related to the visible content of the mirror image. As mentioned in the introduction of this thesis, the perspective projection of the size of objects onto the retina can be approximated by (visual) angles. The angular vehicle width Θ^{veh} and its angular velocity Δ^{veh} were already introduced in the previous driver modeling work (see Figure 5.2).

A lot of psychophysical research was already dedicated to the investigation of such angular measures, and parts of this research was summarized in the literature sections 2.3.1 and 2.3.2. It was proposed by [Regan1993, Hoffmann1994], that different *channels* exist in the visual perception, which are sensitive to the angular size of an object (e.g. Θ^{veh}), the rate of change of such angles (e.g the angular velocities Δ^{veh}) as well as the time-to-collision.

In „*A theory of visual control of braking based on information about time-to-collision*“ [Lee1976], Lee proposed that drivers should be able to perceive the time-to-collision based

on the available visual information in the optic array. He derived a *visual representation of the time-to-collision*, called τ, which equals the quotient of the visual angle that an object subtends on the retina, divided by the rate of change of this angle, e.g. $\tau = \frac{\Theta^{veh}}{\Delta^{veh}}$. Figure 5.2 shows an example for the calculation of τ in case of a car following scenario.

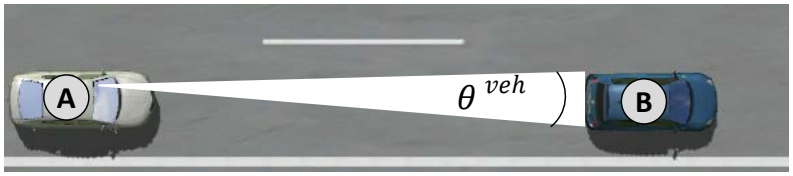

Figure 5.2: *Angular vehicle width* Θ^{veh} in a car-following situation. With Δ^{veh}, the rate of change of Θ^{veh}, τ can be calculated by $\frac{\Theta^{veh}}{\Delta^{veh}}$.

According to Lee, drivers do not even need to do any "mental calculations" (the quotient) to receive τ, instead the information should be directly accessible from the retinal image. Lee proposed that τ is utilized by drivers during braking maneuvers, to stop their vehicle right in front of an object. Further empirical studies by [Regan1995] supported the assumption that τ can be utilized directly by the visual system: they proposed, that the fovea vision is sensitive to both, the angular velocity as well as τ, while in peripheral vision this separation reduces with increasing eccentricity (increasing distance from the fovea).

Other researchers argue that τ is probably not the best available information in every traffic situation: [Anderson2007] explain that τ is less useful during car-following (see scenario in Figure 5.2), because the objective of the following driver (A) is to reduce the speed difference between himself and the vehicle ahead (B) to a minimum or zero. Especially for very small speed differences, τ (the time-to-collision) quickly grows towards infinity, because the speed difference gets very small. If the speed difference between ego and lead vehicle oscillate slightly around zero (sometimes A drives a bit slower or a bit faster), τ oscillates between very large negative and very large positive values. Such a strong oscillation should not provide a good cue for the driver to control small differential speeds. Instead of using τ, the *driving by visual angle model* (DVA) car-following model [Anderson2007] relies on the *angular vehicle width* Θ^{veh} of the lead car and the corresponding rate of change of this angle Δ^{veh}.

But, using the angular vehicle width Θ^{veh} in the car-following situation has a drawback: the distance (or gap) between ego and lead vehicle is not directly perceived by the model, and to realize distance keeping, an extra parameter was used, the "desired angular vehicle width". The control formula of the DVA car-following model tries to maintain the current angular vehicle width Θ^{veh} at a certain constant value (the desired angular vehicle width). This enables the model to hold a certain distance. An open issue is, how the driver selects the appropriate desired angular vehicle width, especially if the size of the lead vehicle varies, e.g. a truck, a car or a motorcycle?

With regard to the specific context of gap acceptance in this work, there is another issue: for a car-following model the control strategy is to maintain a constant distance. For the gap acceptance task of Experiment 2, a constantly *changing gap* needs to be assessed. It is questionable, why the driver should assess the size of the gap with the help of complex mental arithmetics, which involve a desired angular vehicle width for an approaching rear vehicle. Instead, it seems

plausible, to directly consider the angular representation of the gap size, the *angular gap size* Θ^{gap}, see Figure 5.3.

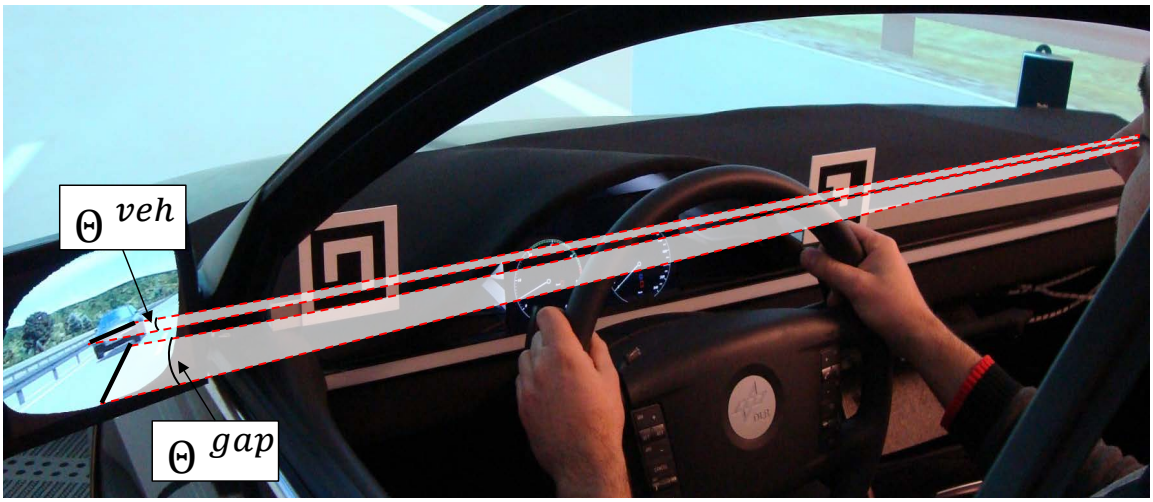

Figure 5.3: *Angular gap size* Θ^{gap} and *angular vehicle width* Θ^{veh} of the approaching rear vehicle. For each angle the rate of change can be calculated: Δ^{gap}, respectively Δ^{veh}. The time-to-collision can be perceived by the driver according to the τ theory of [Lee1976]: $\tau = \frac{\Theta^{veh}}{\Delta^{veh}}$.

If it is assumed that the driver uses the angular gap size Θ^{gap}, he can also use its rate of change (the angular velocity Δ^{gap}) to assess how quickly the rear vehicle approaches towards himself.

A further hint, why the angular gap size Θ^{gap} is preferred over the angular vehicle width Θ^{veh} for the lane change scenario, can be derived from the questionnaire results of Experiment 1 and 2: both questionnaires asked subjects which situational characteristics (or cues) they used to make their decision. In the magnitude estimation paradigm of Experiment 1, subjects had to compare the distance of a rear car, which was visible in the mirror, against the distance to a lead car ahead of them. Their task was to give a *relative distance estimation*. For that experiment, the size of the vehicles was mentioned by 5 subjects as a cue, while the distance between themselves and the vehicles was mentioned 6 times (see section 4.1.5.4). Indeed, both of those cues offer the possibility to conduct a relative distance estimation between the two vehicles. In contrast, not a single subject mentioned the size of the approaching vehicle as a cue for Experiment 2 (the gap acceptance study). Instead 13 out of 14 subjects answered, they used either the distance (or gap size) or the closing speed or both. Because the task of the subjects was to decide, if a lane change left can be done (gap acceptance), they seem to focus on the gap itself and how quickly its size changes.

Finally, one open issue remains to be discussed: although [Anderson2007] rejected τ ($\frac{\Theta^{veh}}{\Delta^{veh}}$) as a potential cue for car-following, it could probably deliver a useful information for the driver in the gap acceptance situation, because the approaching vehicle constantly closes the gap. It was already explained in the previous section, that the time-to-collision (based on d_{CA} (m) and Δv_{CA} (m/s)) can not explain the findings of Experiment 2 with regard to Hypothesis 2.1, because the 26 experiment conditions remained identical, regardless of the mirror type that

was used. But the curved mirrors C20 and C14 manipulate the angular vehicle width Θ^{veh}, because the minification effect reduces the visible size of the objects. Because Θ^{veh} and Δ^{veh} are manipulated by the same minification factor, this factor is eliminated from the quotient of τ. Therefore, τ remains unchanged which can also be seen in the actual measurements of τ from the simulator (see Figure 5.4).

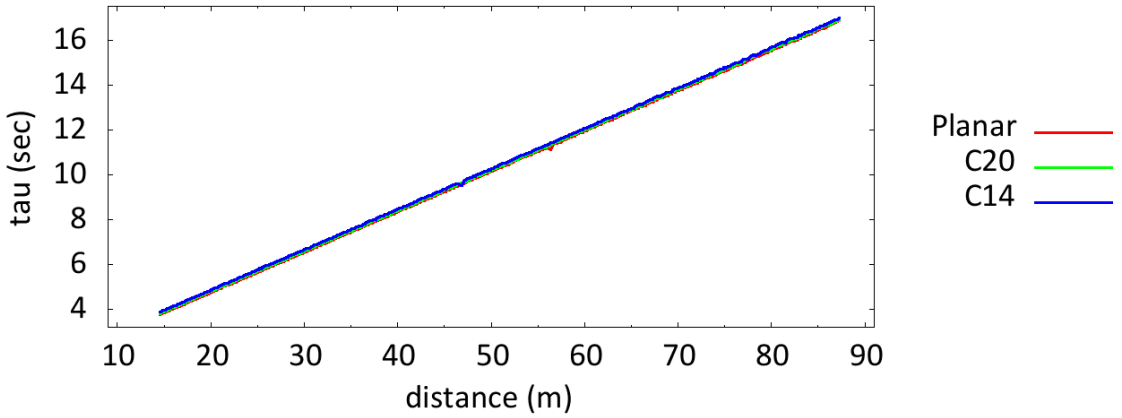

Figure 5.4: τ is unchanged by the different mirror types; recording of a single approach of the rear vehicle starting at 88 meter distance behind (maximum distance used in Experiment 2) with 20 km/h speed difference. τ was calculated using the quotient angular vehicle width divided by its angular velocity.

Remark: Based on the speed difference of 20 km/h (or 5.56 m/s) and the distance in meter on the x-axis, it can be observed that τ has a constant offset. According to the data, τ is 1.19 seconds larger, which equals 6.6 meter distance. Explanation: the angular vehicle width is measured from the perspective of the driver, while the time-to-collision is measured from bumper to bumper between the two vehicles. Distance rear bumper - mirror is 3.7 meter, lateral displacement to center of rear vehicle is 2.9 meter: $\sqrt{3.7^2 + 2.9^2} = 4.70$ meter. The distance driver - mirror adds 0.75 meter, which explains 5.45 meter or 0.98 seconds. For the remainder of 0.2 seconds implementation details have to be considered: the angular measurement has a time delay of 3 steps which equals 50 ms. Consequently, older values are used as the current values. This delay is even larger for the angular velocity, because it differentiates between two such "delayed" angle measurements. Larger delay implies, the a smaller angular velocity is measured, because the vehicle was farther away at that time. Because the angular velocity is the divisor in the τ calculation, the resulting value for τ increases.

It can be concluded, that neither the time-to-collision nor τ offer an explanation for the results of Experiment 2 with regard to Hypothesis 2.1. A possible reason, why the time-to-collision was less useful for the subjects in this experiment can be given based on the proposal of [Hoffmann1994]: according to the authors the perceptual mechanism which is sensitive to τ seems to work properly for angular velocities above 0.003 rad/s. For angular velocities below this threshold, the preciseness of the τ estimations was largely reduced in their experiment. It was

proposed that in these "below threshold situations" subjects probably have to rely on the mental calculation of τ, e.g. $\frac{\Theta^{veh}}{\Delta^{veh}}$. It was also proposed that subjects could use the absolute change of the angular size measured for the period of time that an object is observed.

With regard to Experiment 2 and the gap acceptance scenario, Figure 5.5 shows the angular velocity Δ^{gap} for each of the three speed differences and mirror types.

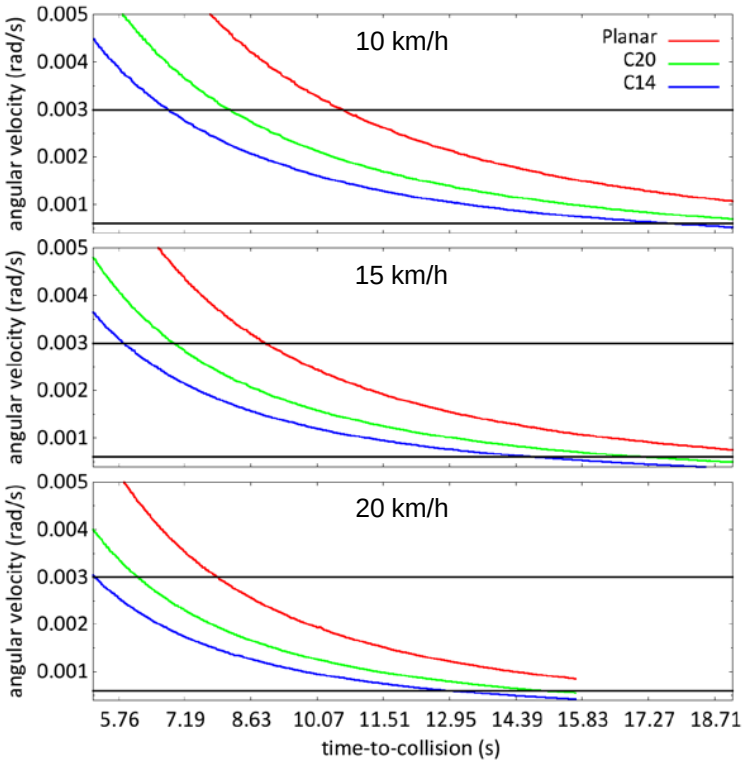

Figure 5.5: Angular velocity Δ^{gap} of the angular gap size Θ^{gap}, measured for a full approach of the rear vehicle from 88 meter distance until 14 meter distance. Threshold values reported by [Hoffmann1994] (0.003 rad /s) and [Michaels1963, Brackstone1999] (0.0006 rad /s) are marked.

For the planar mirror, 18 of the 26 experiment conditions start below the angular velocity threshold of 0.003 rad/s: for 10 km/h six conditions $ttc_{init} = [11.51 - 18.71]$, for 15 km/h seven conditions $ttc_{init} = [10.07 - 18.71]$ and for 20 km/h six conditions $ttc_{init} = [8.63 - 15.83]$. It has to be considered that the angular velocity values measured at the ttc_{init} conditions are the values when the experiment trial starts. The angular velocity Δ^{gap} successively increases, until the subject makes its decision (the reaction time analysis follows in section 5.5.3, in advance, for 13 of 14 subjects the average reaction time was about two seconds or below). Even after a reaction time of two seconds, 10 of the previously identified 18 experiment conditions still remain below the angular velocity threshold of 0.003 rad/s.

For the curved mirror types, the number of experiment conditions below the threshold is even greater, because with increasing mirror curvature, the angular velocity values continuously decrease. With the assumption that the perceptual mechanism for τ is sensitive only above

0.003 rad/s, the availability of adequate time-to-collision information is questionable for most of the experiment conditions of Experiment 2.

Based on the preceding argumentation, the angular gap size Θ^{gap} and its rate of change (angular velocity Δ^{gap}) are the preferred measures for the gap acceptance model developed in this work. With regard to the angular velocity, [Brackstone1999] mentioned a further perceptual threshold (originally published by [Michaels1963], but this source was not available). During car-following, drivers responded to a lead car deceleration if the angular velocity was above 0.0006 rad/s. If a similar threshold would be assumed for the detection of the speed difference in Experiment 2, most of the experiment conditions would already start above this threshold (compare Figure 5.5). Because the rear vehicle approaches, the angular velocity also increases. It can be concluded that the angular velocity Δ^{gap} should be perceivable for the study participants and can be utilized for the gap acceptance decision.

To close this discussion, the *accepted* angular gap size Θ^{gap} and the *accepted* angular velocity Δ^{gap} will be investigated with regard to the open issue of Hypothesis 2.1 (no significant difference in the number of lane changes between the C20 and the C14). Accepted means, these values were measured at the point in time, when the actions of the subjects were recorded (steering or braking).

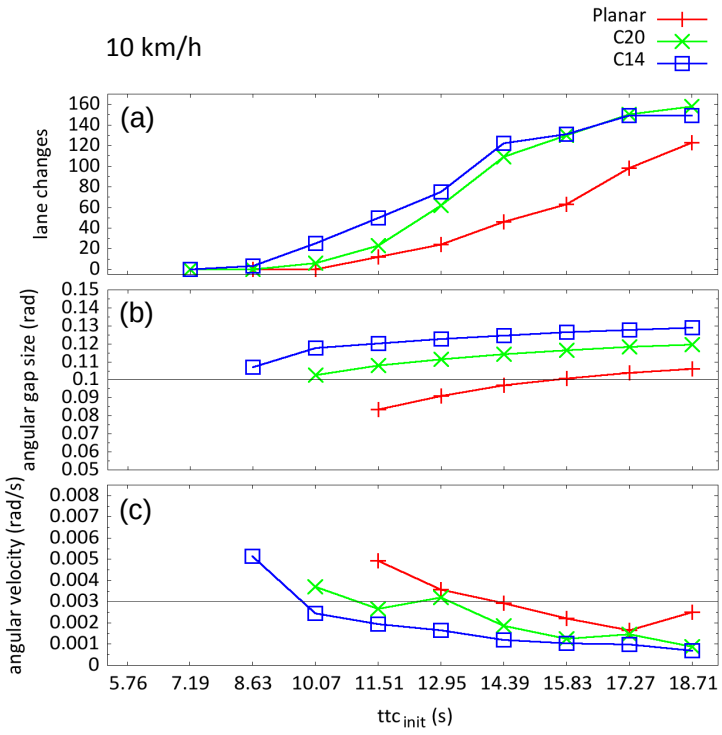

Figure 5.6: (a): number of lane changes of all drivers of Experiment 2; (b): the mean values of the corresponding *accepted* angular gap size Θ^{gap}; (c): the *accepted* angular velocity Δ^{gap}. Remark: for experiment conditions where no lane changes occurred, no values were recorded for (b) / (c), for example $ttc_{init} = 7.19$ seconds.

Figure 5.6 (a) shows the accumulated number of lane changes of all drivers for all experiment conditions at the speed difference $\Delta v_{CA} = 10$ km/h. (b) and (c) show the corresponding mean

values for the accepted angular gap size / accepted angular velocity. With respect to the accepted angular gap size in Figure 5.6 (b), the values increase with increasing mirror curvature (from planar to C20 to C14), which is in line with Hypothesis 2.1. For the accepted angular velocity (Figure 5.6 (c)) the values increase with increasing mirror curvature, but the curves are less smooth and no clear tendency for the relative separation between them can be observed, at least for the 10 km/h speed difference.

For the 15 and 20 km/h speed differences (Figure 5.7), the separation between the three mirrors remains similar for the accepted angular gap size compared to the 10 km/h situation. The curves for the accepted angular velocity are smoother compared to 10 km/h and the difference between C20 and C14 remains below the 0.0006 rad/s velocity threshold for all ttc_{init} conditions between 10.07-15.83 seconds. This could be an indication why the curved mirrors were not significantly different. Instead, the number of lane changes at 20 km/h speed difference and $ttc_{init} = 10.07$ seconds is smaller for the C14 compared to the C20 (violates the assumption of Hypothesis 2.1), but the accepted angular velocity values for the C20 are still above those of the C14. This violation can not be explained on the basis of the accepted angular velocity. But, the difference between the angular velocity values for the two C20 and C14 is close to the perceptual threshold of 0.0006 rad/s which is an indication that it might not be possible for the subjects to detect any differences.

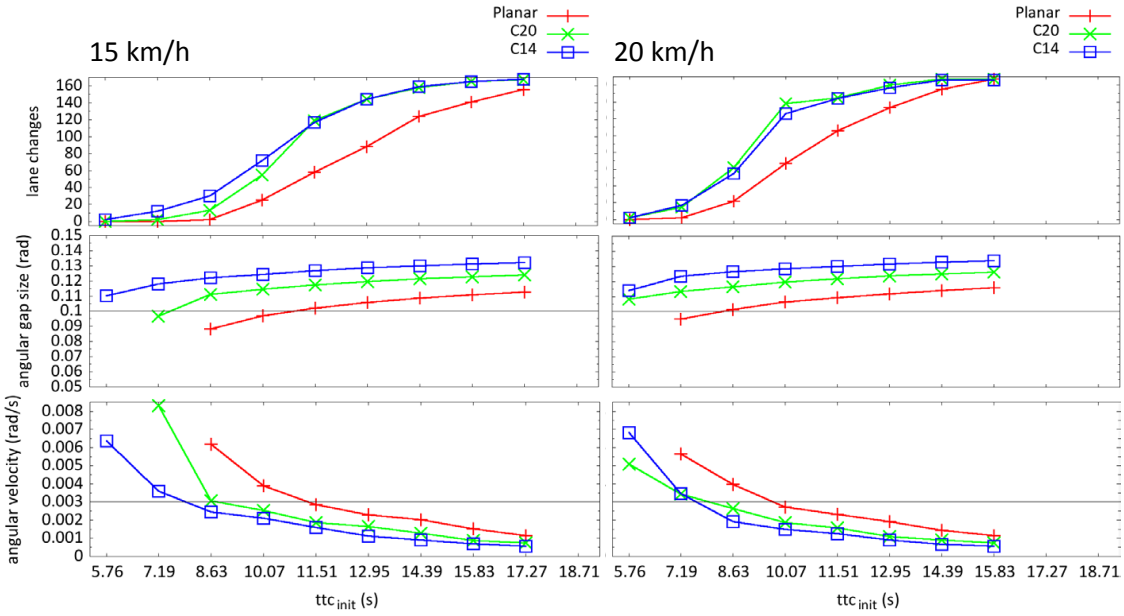

Figure 5.7: Equivalent to Figure 5.6, shows the mean values of the accepted angular gap size and accepted angular velocity for the two speed differences 15 and 20 km/h, equivalent to Figure 5.6.

5.3.3 Conclusion

The analysis of the two categories of variables (metric measures vs. angular measures) lead to the following argumentation: the metric variables distance (m), speed difference (m/s) and

time-to-collision (m/(m/s)) alone can not explain the observed differences with regard to Hypothesis 2.1, because the same 26 experimental conditions were shown, regardless of the mirror type that was used. If the model would nevertheless use these measures, an additional variable would be necessary, which incorporates the mirror related differences. The minification factor would be a possible candidate for such a variable. This approach was rejected, because 1) the minification is a property of the mirror and not the drivers' perception, and 2) knowledge about the minification should also not be included into the model explicitly, because throughout Experiment 2, subjects did not receive such information. The questionnaire showed that subjects did not have knowledge about minification effects in general.

The alternative proposal here is to use the angular gap size Θ^{gap} and its angular velocity Δ^{gap}. These are directly related to the visual image of the scenery as it was perceived by the subjects (Figure 5.3, p. 110). The appropriateness of two different measures was discussed with regard to the specific scenario of this thesis (gap acceptance), and the angular gap size Θ^{gap} was preferred over the angular vehicle width Θ^{veh}. It was also shown that τ (according to [Lee1976]) is not manipulated by the different mirror types and behaves similar to the time-to-collision. Therefore τ can also be excluded from the model variables.

With regard to Hypothesis 2.1 (the number of lane changes increases with increasing mirror curvature, from Planar to C20 to C14): the values of the accepted angular gap size and the accepted angular velocity would suggest that this hypothesis is fulfilled for the relation between all three mirrors. The analysis of Experiment 2 instead showed that the relation between C20 and C14 was not significant. Especially for the 15 and 20 km/h situations, the difference in the accepted angular velocities between C20 and C14 is very close or even below the discrimination threshold of 0.0006 rad/s. If subjects would rely on the angular velocity Δ^{gap} as decision criteria, this would be a reasonable explanation why the mirrors were not significantly different with regard to the number of lane changes. But even the angular velocity does not deliver a very good explanation why the number of lane changes for the C14 was actually smaller for some ttc_{init} conditions compared to the C20.

It was already explained in the Experiment 2 chapter that at least one subject was found, were the number of lane changes for the C14 was way below the number of lane changes for the C20. The individual behavior analysis in the next section will show, that not only one subject violated Hypothesis 2.1, instead a number of violations were identified for different subjects.

5.4 Individual Gap Acceptance Behavior

The objective of this analysis was motivated in the previous section: the inspection of the accepted angular gap size respectively the accepted angular velocity on the accumulated data level gave some indications, why Hypothesis 2.1 failed with regard to the two curved mirrors (number of lane changes was actually smaller for C14 than for the C20), but the investigation of the individual behavior is necessary to provide a clearer picture on this issue.

A quick overview on the data is provided in the first subsection 5.4.1 and a number of violations against Hypothesis 2.1 are identified here. Afterwards, section 5.4.2 shows the most detailed view on all these violations, using detailed figures which show the number of lane change data for each of the 26 experiment condition. Afterwards, a final conclusion is drawn in

subsection 5.4.3, and it is explained, how the further model development will deal with these violations. It will also be explained, why the Experiment 2 setting was not optimal and what should be improved in a future study.

5.4.1 Data Overview

With regard to the number of lane changes, the empirical data of Experiment 2 can be broken down systematically into different levels of detail:

Level 1: for each mirror the data of all subjects is accumulated.

Level 2: for each mirror the data is separated into individual subject data

Level 3: for each mirror and subject the data is split according to the speed difference Δv_{CA}

Level 4: for each mirror and subject the data is split according to speed difference Δv_{CA} and the corresponding ttc_{init} conditions.

The data at Level 1 was discussed in the Experiment chapter and will not be presented here anymore. Level 2 and 3 are summarized in form of two tables in this section, which provides an overview on the number of violations that occurred against Hypothesis 2.1. The following section 5.4.2 presents the detailed view at Level 4.

Important Remark: the two tables in this section compare the data of all subjects, the three speed differences and mirror types. Remember that only the data of the ttc_{init} conditions within $[7.19 - 15.83]$ seconds is available for all three speed differences. The Level 4 data in the next section instead shows all ttc_{init} conditions that were presented for each speed difference. The comparable range used in the tables ($[7.19 - 15.83]$ seconds) is marked in the Level 4 data by a dashed rectangle around the ttc_{init} conditions in those figures.

Table 5.2 below summarizes the Level 2 and 3 data for each of the 14 subjects of the experiment. *Violations* with regard to Hypothesis 2.1 are highlighted.

Group	VP	Number of Lane Changes											
		Level 2			Level 3								
					+10 km/h			+15 km/h			+20 km/h		
		pl.	C20	C14	pl.	C20	C14	pl.	C20	C14	pl.	C20	C14
G1	14	51	83	111	1	12	24	17	30	40	33	41	47
	6	98	145	180	3	20	36	37	54	66	58	71	78
	7	114	141	159	22	36	45	42	49	54	50	56	60
	12	120	173	212	7	46	61	48	61	78	65	66	73
G2	5	32	103	114	1	6	17	7	40	46	24	57	51
	4	86	147	152	1	22	22	30	55	58	55	70	72
	10	124	138	145	23	36	33	45	45	51	56	57	61
	2	127	128	148	39	35	40	45	43	51	43	50	57
	8	168	182	211	40	39	59	60	64	74	68	79	78
G3	9	15	67	63	0	0	2	0	23	20	15	44	41
	13	51	133	114	0	18	12	16	49	44	35	66	58
	3	78	149	135	1	26	26	28	53	48	49	70	61
	11	79	145	128	2	27	28	33	52	47	44	66	53
	1	92	108	68	6	7	1	30	38	24	56	63	43

Table 5.2: Number of lane changes for each subject; VP: German abbreviation for subject Versuchsperson; VP's grouped and sorted according to the occurrence and magnitude of the violations; Level 2 data: max. number per entry is 252 (7 $ttc_{init} = [7.19 - 15.83]$ conditions, 3 speed differences Δv_{CA}, 12 repetitions); Level 3 (Level 2 data split up according to Δv_{CA}): max. number per entry is 84 (252 / 3); Violations against Hypothesis 2.1 are highlighted at both levels, colors indicate different magnitudes: green (number of lane changes between two mirrors is equal), yellow (violation <=3 lane changes) or red (violation >3 lane changes).

With regard to Level 2, the 9 subjects of group G1 and G2 behaved according to Hypothesis 2.1. For the subjects of group G3 violations are already found at this level. For subject VP9 (first in G3) the magnitude of the violation is comparably small (3 lane changes only) while for VP13, 3 and 11, it is already between 14-19 lane changes. The violation with the strongest magnitude is observed for VP1 with 40 lane changes. The data of Level 2 already reveals, that the reason for the non-significant difference between C20 and C14 should be found mainly in the behavior of the last four subjects in G3, because the violations have the strongest magnitude here. In the Experiment chapter it was speculated that the strong violation of VP1 might already be responsible for this observation, but there are at least three more subjects which have a considerable impact, too (VP13, 3, 11).

Considering data Level 3, the situation changes and more violations can be observed for more subjects: for G3, where violations were already found at Level 2, these are now consistently seen at almost every speed difference. In addition to the subjects of G3, there are now also violations observed for the participants in G2. Because these violations have a less stronger magnitude, they are not visible on Level 2. With regard to G3 it can be observed, that the magnitude of the violations at Level 3 increases with increasing speed difference. At 10 km/h there even two subjects (VP9 and VP11) without a violation (although, the difference between C20 and C14 is very small). The strength increases especially from the 15 to 20 km/h transition.

This effect will be discussed later on in the next section in more detail when Level 4 is inspected.

The Level 3 data in the table can be quickly reorganized to investigate Hypothesis 2.2 (With increasing speed difference Δv_{CA}, the number of accepted gaps for situations with equal ttc_{init} will increase).

	Number of Lane Changes								
	Planar			C20			C14		
VP	+10	+15	+20	+10	+15	+20	+10	+15	+20
14	1	17	33	12	30	41	24	40	47
6	3	37	58	20	54	71	36	66	78
7	22	42	50	36	49	56	45	54	60
12	7	48	65	46	61	66	61	78	73
5	1	7	24	6	40	57	17	46	51
4	1	30	55	22	55	70	22	58	72
10	23	45	56	36	45	57	33	51	61
2	39	45	43	35	43	50	40	51	57
8	40	60	68	39	64	79	59	74	78
9	0	0	15	0	23	44	2	20	41
13	0	16	35	18	49	66	12	44	58
3	1	28	49	26	53	70	26	48	61
11	2	33	44	27	52	66	28	47	53
1	6	30	56	7	38	63	1	24	43

Table 5.3: Level 3 data reorganized to assess Hypothesis 2.2 of the experiment.

Table 5.3 shows that only two violations of a comparably small magnitude can be found, which means that the effect of Hypothesis 2.2 is much more consistently found compared to Hypothesis 2.1. A likely reason for this observation is, that Hypothesis 2.1 can only be analyzed across the three study days, which potentially involves more individual behavior variations, while Hypothesis 2.3 can be analyzed per session individually, which reduces such influences. At this point, the experiment design seems to be a two-bladed sword. The original intention was, to not inform subjects about the mirror types, which should prevent subjects to think about mirror differences. It should be avoided that they compensate these differences by actively changing their behavior. For this purpose, it was also necessary to split the mirror sessions and have at least a couple of days off in between. This reduces the possibilities for the subjects to draw a direct comparison, but: additional behavior variations are also likely introduced. At least for the four subjects of G3 which had stronger violations against Hypothesis 2.1, it can be assumed, that these additional influences were strong enough, to fully compensate / overshadow the expected effect postulated by Hypothesis 2.1.

5.4.2 Detailed View on Violations of Hypothesis 2.1

After the tables presented a good overview on the individual data and the violations, this section provides the most detailed perspective on the data of the subjects from the groups G2 and G3.

From the analysis of Hypothesis 2.2 in the experiment chapter it is known, that the difference in the number of lane changes between the three mirrors reduces with increasing speed difference (see Figure 4.10, p. 96, smaller separation between the curves). In the previous section it was mentioned, that the magnitude of the violations for G3 increases with increasing speed difference and this can be considered the very same effect. But this effect can be observed already for subjects in group G2.

Naturally, if the difference in the number of lane changes between two mirrors is already quite small at a smaller speed difference, the chances increase that a violation occurs at a higher speed difference. This is observed for the violation of VP5 at the Level 3 data in Table 5.4.

	Number of Lane Changes											
	Level 2			Level 3								
				+10 km/h			+15 km/h			+20 km/h		
VP	pl.	C20	C14	pl.	C20	C14	pl.	C20	C14	pl.	C20	C14
5	32	103	114	1	6	17	7	40	46	24	57	51
4	86	147	152	1	22	22	30	55	58	55	70	72

Table 5.4: Violations of VP5 and VP4 against Hypothesis 2.1.

VP5 The difference in the number of lane changes between C20 and C14 is already small at the 15 km/h speed difference (40 vs. 46), and it can be expected that it will get even smaller at 20 km/h. In fact the C14 has considerable less lane changes than the C20: from +6 at 15 km/h to -6 at 20 km/h). Figure 5.8 a) below shows this violation of VP5 in detail (only the ttc_{init} conditions within $[7.19 - 15.83]$ can be compared between tables and figures, see remark at p. 116).

In addition, the figures 5.8 a) and b) point to another aspect. At this level of detail, the curves which represent the number of lane changes, do no longer behave strictly monotonously, as it was observed for the accumulated data across all subjects in the Experiment chapter (Figure 4.10, p. 96). Instead, there are larger ttc_{init} conditions which have a smaller number of lane changes compared to their predecessor conditions, e.g. $ttc_{init} = 11.51$. It can be concluded that violations can already be observed at the highest level of detail and dependent on their strength and number they subsequently propagate towards higher levels of detail.

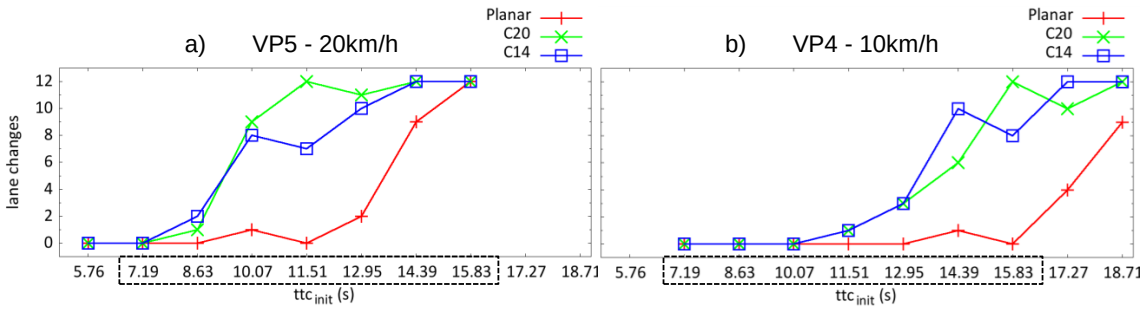

Figure 5.8: Details on the violations that were found for the subjects VP5 and VP4. Dashed rectangle around ttc_{init} conditions, see remark, p. 116.

These non-monotonous points in the number of lane change curves can not be explained on the basis of the angular measures, because the angular gap size Θ^{gap} and also the angular velocity Δ^{gap} have a strict monotonous behavior, not only over the course of a trial, but also from the smaller towards the larger ttc_{init} conditions. It was also investigated, if the accepted angular measures showed some noticeable values at these locations, but this was not observed for neither VP5, nor VP4. It has to be considered, that only 12 repetitions for each ttc_{init} condition were measured per subject, and the magnitude of these non-monotonous occurrences is rather small (a few more or less accepted gaps). The experiment design made with the objective to test, if the hypotheses can be shown for the accumulated data of all subjects. The number of subjects and repetitions per experiment condition were chosen, to fit the needs of the experiment on that level. It is assumed, that these noise effects should diminish, if more repetitions would have been available.

Because the *accepted* angular gap size Θ^{gap} and the *accepted* angular velocity Δ^{gap} were mentioned earlier, Figure 5.9 shows these values for VP5. Similar to the accumulated data, the difference in the accepted angular velocity values between C20 and C14 are close to the perceptual threshold of 0.0006 rad/s, but the C14 still has smaller values compared to the C20. This observation was made for all of the following violations that are reported below, and consequently, also on the individual behavior level, the *accepted* angular gap size Θ^{gap} as well as the *accepted* angular velocity Δ^{gap} do not provide a conclusive answer why Hypothesis 2.1 was violated.

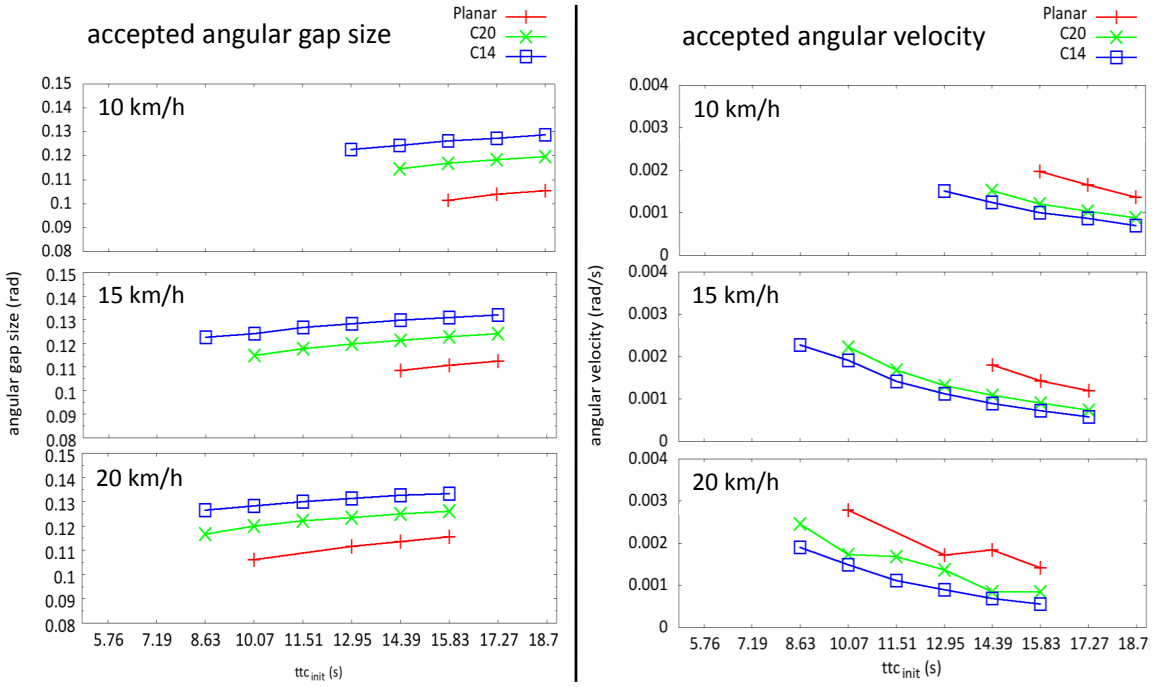

Figure 5.9: *Accepted* angular gap size Θ^{gap} and *accepted* angular velocity Δ^{gap} for VP5. Values are shown only for those ttc_{init} conditions, where lane changes were conducted: planar mirror at 20 km/h, no lane change at $ttc_{init} = 11.51$s, compare Figure 5.8 a) above. Dashed rectangle around ttc_{init} conditions, see remark, p. 116.

Besides VP5 and 4, there are 3 more subjects in group G2 (VP10, 2 and 8) and for each of them, two violations can be found at the different speed differences. But, what really separates these subjects from all other participants of the study is the fact, that the relation Planar mirror C20 mirror is affected, too.

	Number of Lane Changes											
	Level 2			Level 3								
				+10 km/h			+15 km/h			+20 km/h		
VP	pl.	C20	C14	pl.	C20	C14	pl.	C20	C14	pl.	C20	C14
10	124	138	145	23	36	33	45	45	51	56	57	61
2	127	128	148	39	35	40	45	43	51	43	50	57
8	168	182	211	40	39	59	60	64	74	68	79	78

Table 5.5: Violations of VP10, 2 and 8 against Hypothesis 2.1. On the basis of the accumulated data the planar mirror had significantly less lane changes compared to both curved mirrors, but for these three subjects, violations were found on the individual behavior level.

VP10 For this subject, the difference in the number of lane changes between C20 and C14 is very small, only 7 lane changes in total at Level 2, and consequently even smaller when separated into the three speed differences. In contrast to VP5, the violation happened at the smallest speed difference and not the largest.

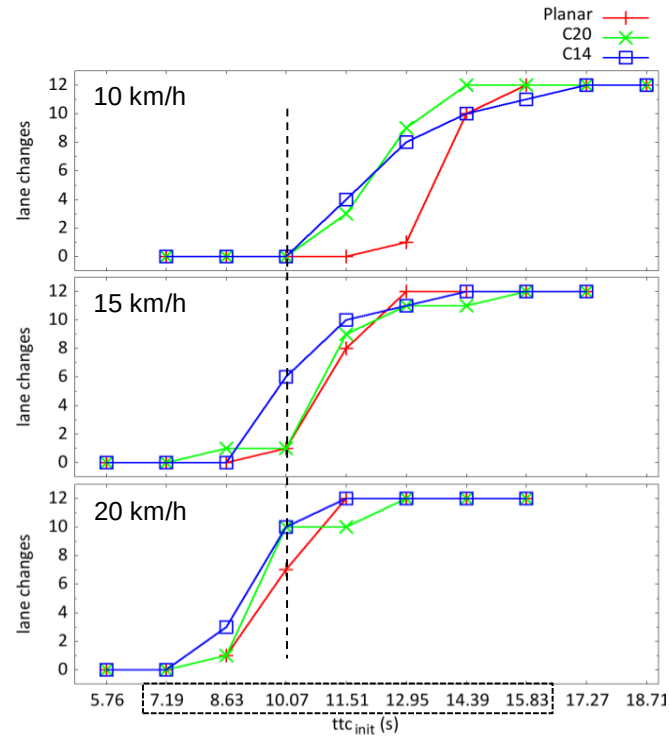

Figure 5.10: Number of lane changes for subject VP10 and the three speed differences; Vertical line illustrates effect of Hypothesis 2.2: more lane changes with increasing speed difference. Dashed rectangle ttc_{init} conditions, see remark, p. 116.

Looking at Figure 5.10, and especially at the 15 and 20 km/h speed differences, it could be assumed that the time-to-collision (or τ) could be a good predictor, because the number of lane changes is very similar for all three mirrors. But this changes for the 10 km/h speed difference, where the planar mirror has considerably fewer lane changes. Furthermore, the vertical line shows, that Hypothesis 2.2 still holds for this subject: smaller ttc_{init} conditions are accepted with increasing speed difference. This also speaks against τ.

VP2 Examining the data of VP2 in the following Figure 5.11 shows, that VP2 has some general similarities with VP10. For two of the three speed differences, the number of lane changes is very similar for all three mirrors, but in contrast to VP10, these are the 10 and 15 km/h speed differences and not 15 and 20 km/h.

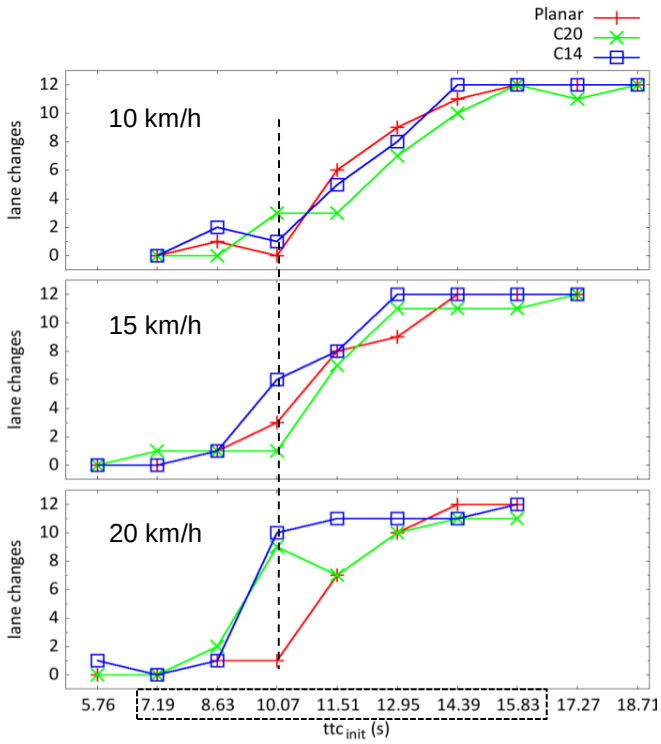

Figure 5.11: Number of lane changes for subject VP2. Dashed rectangle around ttc_{init} conditions, see remark, p. 116.

Additionally, one of two violations against Hypothesis 2.2 was recorded for VP2, observed for the planar mirror. Taking the vertical line as a comparator, the number of lane changes increases with increasing speed difference only for the C20 and C14, but not for the planar mirror. While for VP10 the time-to-collision was rejected as explanatory variable, because Hypothesis 2.2 held for all three mirrors types, the situation is different for VP2: considering the fact that each mirror was tested in a separate session (and on a different study day), at least the data for the planar mirror might be explained by τ, because Hypothesis 2.2 failed in that particular session and the number of lane changes is almost equal if the three speed differences are compared.

This observation is a first hint, that the data of each session might have to be considered separately during model development, because it could be difficult to consistently explain the observed behavior of all subjects, if the data is compared across three different sessions.

VP8 The data of VP8 in Figure 5.12 gives a further indication that the violations are probably related to variability of the behavior across the three sessions. Hypothesis 2.1 holds for the relation between planar and C14, but for the C20, especially at 10 km/h, the number of lane changes is smaller compared to the planar mirror and violates Hypothesis 2.1. The occurrence of violations seems to be fostered by the following fact: the physical difference between the mirrors (minification, field of view, see Table 4.1 at p. 81) is smaller between the curved mirrors C20 and C14, compared to the relation between planar and C20.

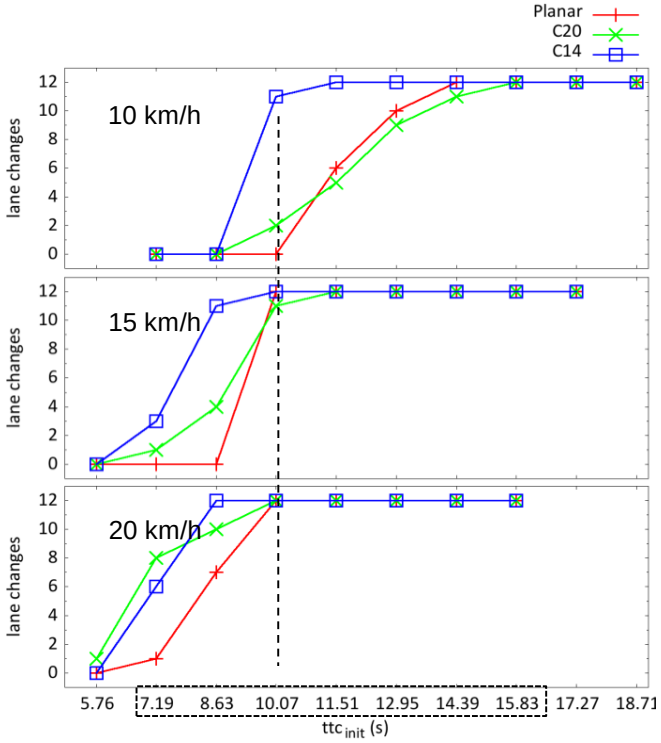

Figure 5.12: Number of lane changes for subject VP8. Dashed rectangle around ttc_{init} conditions, see remark, p. 116.

Apart from one exception (VP1, shown below), no violations of Hypothesis 2.1 are found between planar - C14 (where the physical difference is the largest), three violations for different subjects are found for the relation planar - C20 (VP10, 2, 8), but the most violations are observed between C20 and C14, where the physical difference between the mirrors is the smallest. A more detailed discussion and conclusion how to deal with the individual behavior variations with regard to the modeling is given in the conclusion section below, but beforehand, the data of the subjects of group G3 is presented here. For these subjects, violations against Hypothesis 2.1 were already visible at Level 2 of the data hierarchy.

VP9 An interesting observation is made for subject VP9: zero lane changes were found for the planar and the C20 mirrors at 10 km/h in the overview table. But as mentioned before, the data in the table only compares the conditions $ttc_{init} = [7.19 - 15.83]]$ which were available for all three speed differences.

	Number of Lane Changes											
	Level 2			Level 3								
				+10 km/h			+15 km/h			+20 km/h		
VP	pl.	C20	C14	pl.	C20	C14	pl.	C20	C14	pl.	C20	C14
9	15	67	63	0	0	2	0	23	20	15	44	41

Table 5.6: VP9 is the subject with the most conservative lane change behavior; few lane changes especially for the planar mirror.

Figure 5.13 instead shows the number of lane changes for the whole range of all ttc_{init} conditions. It can be seen that there are still zero lane changes for the planar mirror in the 10 km/h speed difference, but a small number of seven lane changes are recorded for the C20 at ttc_{init} of 17.27 and 18.71 seconds.

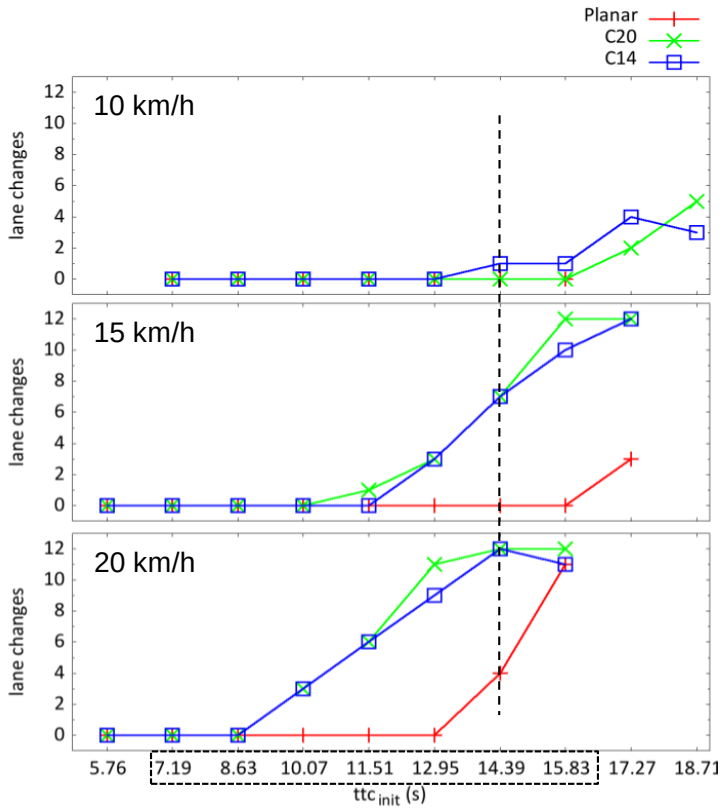

Figure 5.13: Number of lane changes for subject VP9. Subject with the most conservative lane change behavior. Dashed rectangle around ttc_{init} conditions, see remark, p. 116.

Similarly, the number of lane changes rises for the C14 and these two experiment conditions. In the experiment chapter it was argued, that the additional ttc_{init} conditions were used to offer

a wider data range, because this might be useful for the modeling, but they were tested only for certain speed differences (see Table 4.4, p.91). Here, these ttc_{init} conditions captured a relevant part of the behavior of VP9, which would not have been observed otherwise.

Generally, VP9 is the subject with the fewest number of lane changes across all three mirror sessions, or in other words the most conservative lane change behavior of all 14 subjects. It can also be observed, that Hypothesis 2.2 had a strong impact, especially for the C20 and C14 mirrors: the number of lane changes largely increases from 10 to 15 and also 20 km/h (compare Table 5.3, p. 118). Instead, for the planar mirror, a considerable increase is only observed at 20 km/h. The explanation for this is the following: it was proposed earlier in the Experiment 2 chapter, that at higher speed differences the distance automatically increases for each ttc_{init} condition, and is considered the main reason for the Hypothesis 2.2 effect. For the planar mirror configuration, the majority of the distances of all ttc_{init} conditions was too small, even at the higher speed differences. The minification effect of the curved mirrors C20 and C14 visually increases the gap size, and in those sessions the subject started to accept considerably more gaps (Hypothesis 2.1).

VP1 The subject which had the strongest violation of Hypothesis 2.1 is VP1, and in this case the number of lane changes for the C14 is even way below the numbers for the planar mirror (see Figure 5.14). On the other hand, the relation planar - C14 is according to Hypothesis 2.1, meaning again, there is one session (the C14 session) where the individual behavior variability supposedly causes the hypothesis to fail, while on the other side, Hypothesis 2.2 is not violated and the number of lane changes clearly rises with increasing speed difference (and increasing distance).

	Number of Lane Changes											
	Level 2			Level 3								
				+10 km/h			+15 km/h			+20 km/h		
VP	pl.	C20	C14	pl.	C20	C14	pl.	C20	C14	pl.	C20	C14
1	92	108	68	6	7	1	30	38	24	56	63	43

Table 5.7: The magnitude of the violation of subjects VP1 was extraordinarily high.

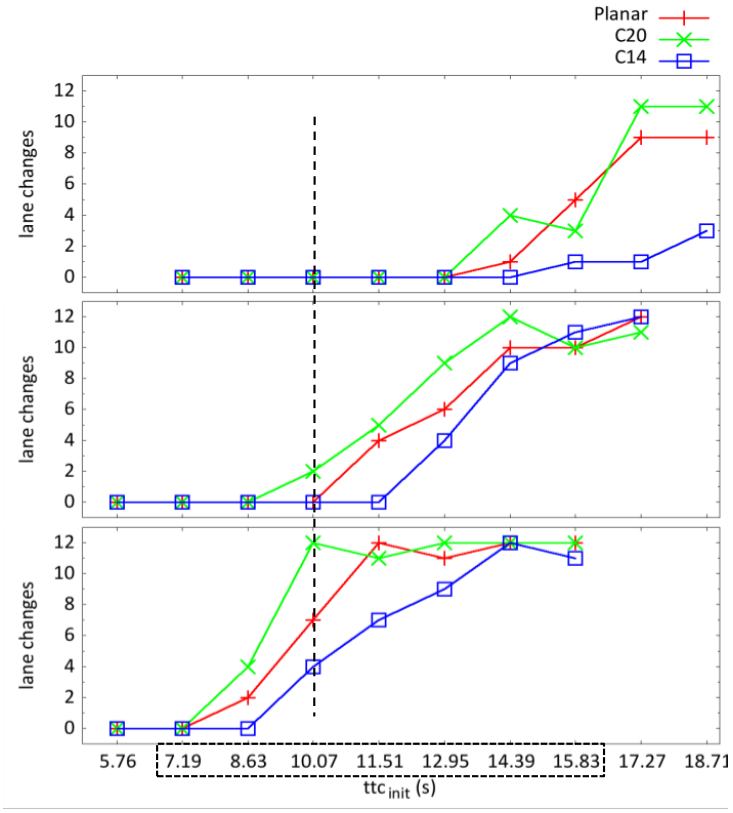

Figure 5.14: Number of lane changes for subject VP1. This subject had the strongest violations against Hypothesis 2.1. Dashed rectangle ttc_{init} conditions, see remark, p. 116.

VP13, 3, 11 Finally, for the last three subjects of group G3, violations of Hypothesis 2.1 were also observed at Level 2. Table 5.8 again shows these subjects. It can also be seen, that the magnitude of the violations increases with increasing speed difference. A similar observation was already made for VP5 at the beginning of this section. It was argued that with higher speed differences the difference in the number of lane changes between the mirrors decreases and the chances for violations increase. This argumentation can be extended in the way that violations not only occur but also their strength increases.

	Number of Lane Changes											
	Level 2			Level 3								
				+10 km/h			+15 km/h			+20 km/h		
VP	pl.	C20	C14	pl.	C20	C14	pl.	C20	C14	pl.	C20	C14
13	51	133	114	0	18	12	16	49	44	35	66	58
3	78	149	135	1	26	26	28	53	48	49	70	61
11	79	145	128	2	27	28	33	52	47	44	66	53

Table 5.8: Three more subjects with stronger violations against Hypothesis 2.1.

The detailed figures for these subjects can be found below, however no new observations were made which were not reported before.

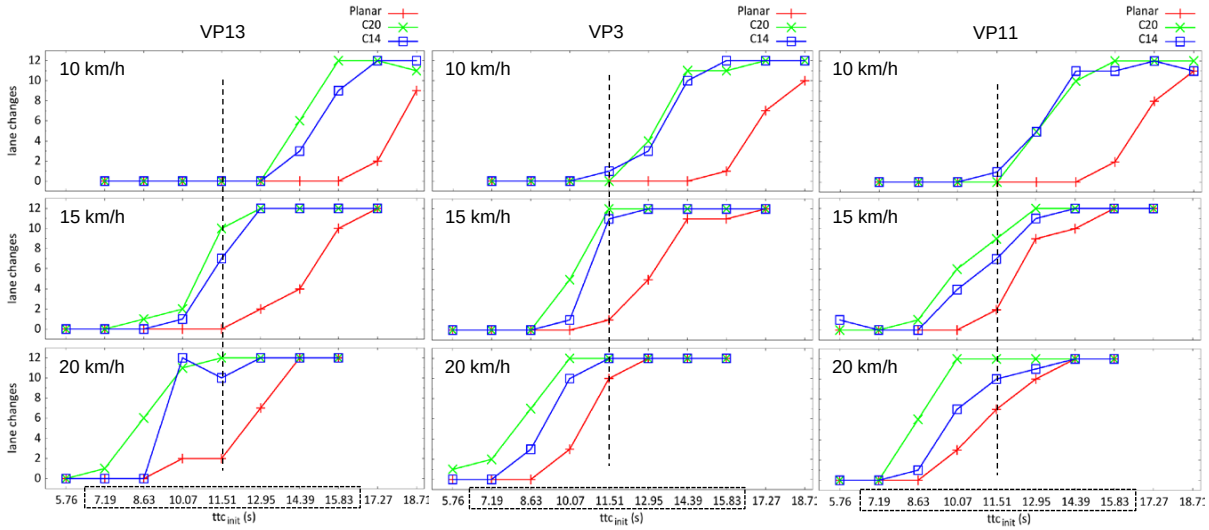

Figure 5.15: From left to right: number of lane changes for subject VP13, 3 and 11; Hypothesis 2.1: for all subjects, the planar mirror is very well separated across all ttc_{init} conditions for all subjects, while the C14 and C20 order is consistently violated especially at the higher speed differences; Hypothesis 2.2 is fulfilled for all subjects, the number of lane changes increases with increasing speed difference. Dashed rectangle around ttc_{init} conditions, see remark, p. 116.

5.4.3 Conclusion

The objective of this section was to report the individual gap acceptance behavior for each of the 14 subjects and try to find answers, why there was no significant difference between the two curved mirrors C20 and C14. As a reminder, Hypothesis 2.1 postulated: „*The planar mirror leads to the smallest number of lane changes. Increasing the field of view of the simulated mirrors (from Planar over C20 to C14) leads to an increased overall number of lane changes*“.

For the analysis of the Experiment 2 hypotheses in the previous chapter, the individual behavior data was only very briefly consulted, mainly because the hypotheses were not formulated to investigate individual behavior. Because the individual behavior should be considered by the gap acceptance model, this was not sufficient. At the end of this section, a clearer picture is available why the number of lane changes was not significantly different between the curved mirrors C20 and C14 and Hypothesis 2.1 was not fulfilled.

On a more detailed level (Level 3, Table 5.2, p. 117), the data was investigated for each of the three speed differences and all 14 subjects ($3 * 14 = 42$ comparisons possible). With regard to the curved mirrors C20 and C14, 17 violations were marked in Table 5.2, and four additional violations were found, where even the planar mirror was involved (VP10, VP2, VP8). The violations can be distinguished by different characteristics: 1) different magnitudes were observed (group G2 vs. G3, Table 5.2) 2) in general, all speed differences are affected. For group G2 the violations were found sporadically for only one or two speed differences, while they were observed more consistently across at all speed differences for group G3. This leads to the difference in the observed magnitude. 3) observations of non-monotonous behavior of the number of lane change curves at specific ttc_{init} conditions were found (e.g. VP4, VP5), and

it was concluded that this likely happens, because the number of repetitions is rather small (12 repetitions per ttc_{init} condition), and already a couple of lane changes more or less cause such violations.

It can be concluded, that none of the violations can be explained on the basis of the angular measures alone. Figure 5.5, p. 112 showed the values of the angular velocity Δ^{gap}. Based on these values it could be assumed, that the number of lane changes increases with increasing mirror curvature, according to Hypothesis 2.1, because for the planar mirror the angular velocity is consistently larger compared to the C20 and for the C14 the values are larger compared to the C20.

The *accepted* angular velocity Δ^{gap} did provide an indicator, why the C20 and the C14 are less well distinguishable (Figures 5.6, 5.7, pp. 113), because the separation between their values is close or even below the perceptual threshold of 0.0006 rad/s. Although the difference is close to this threshold, the value of the *accepted* angular velocity Δ^{gap} for the C20 is still larger compared to the C14. Instead, the violations of group G3 (Table 5.2) showed that the number of lane changes is consistently smaller for the C14 compared to the C20. Additionally, the accepted angular gap size and accepted angular velocity did not provide a conclusive explanation on the individual behavior level, an example was given for VP5, Figure 5.9, p. 120, but this was observed for the other violations, too.

During the discussion of VP2 and VP8 it was mentioned, that behavioral variations between the different experiment sessions likely occurred, and that they could have prevented a significant difference between C20 and C14 with regard to Hypothesis 2.1. It was proposed, that the occurrence of violations increases specifically for these two mirrors, because the difference with regard to the physical attributes (field of view and minification) is the smallest for these two (see Table 5.9 below).

Relative Change between Mirrors		
	Planar - C20	C20 - C14
Field of view	47.4%	25.7%
Minification	35.0%	23.1%

Table 5.9: Relative changes in % between the mirror types for the physical properties field of view and minification factor. Table was shown already at p.81 in the Experiment 1 chapter.

A smaller difference in the physical attributes also reduces the expected effect size for Hypothesis 2.1. This makes the C20 - C14 relation more prone to behavioral variability. In fact, the number of violations increased with decreasing difference in the physical attributes. Only VP1 violated the planar - C14 relation and the largest difference with regard to the physical attributes is found between these two mirrors. Additional three subjects (VP10, 2, 8) violated the planar - C20 relation, were a medium difference is observed with regard to the physical attributes. An additional number of five more subjects (group G3, Table 5.2) violated the C20 - C14, and here the difference is the smallest.

Generally, behavior variations are typically observed in empirical studies with human subjects, but the study design of Experiment 2 should be reviewed, to identify possible reasons, why such behavior variations caused the fail of Hypothesis 2.1 for the relation between the mirrors C20 and C14. Looking back at both experiments, a problem can be reported in transferring

the study design from Experiment 1 to Experiment 2: in the first study, the distance estimation experiment, subjects were invited for three sessions and one mirror was used per session. The original idea behind this was, to not inform subjects about the mirror types, so they do not have the possibility to consciously adapt their behavior.

The questionnaire revealed, that subjects indeed did not recognize that different mirrors were tested, and the differences between all three mirrors with regard to the hypotheses were significant. Because this experiment paradigm worked pretty well in the first study, the same procedure was also applied for the lane change study. But their is a difference between the two experiments: Experiment 1 used a magnitude estimation paradigm, where two stimuli had to be compared against each other (relative distance estimation between lead and rear vehicle). Both of these stimuli were well controlled: the rear car, which was visible in the left side mirror and also the lead vehicle, which was the cue against which the rear vehicle was compared.

In Experiment 2, there was no well controlled reference cue like the lead car, against which the rear vehicle could be compared. Instead, subjects compared the approach situation with their *subjective* gap acceptance criteria. The variability of this criteria could not be controlled, especially between the three sessions on different study days. This problem was known, therefore subjects were instructed to not change their driving style actively. The idea for this instruction was, that subjects should not consciously consider a sports-like driving style on one day, while driving very conservatively on another day. Nevertheless, this does not not guarantee, that a change of the driving style did not happened, consciously or unconsciously. Furthermore, variability in the subjective gap acceptance criteria is likely a part of the usual driving behavior.

Unfortunately, the results with regard to Hypothesis 2.1 are mixed with such behavioral variability and they likely caused the fail of Hypothesis 2.1 with regard to the relation between the curved mirrors C20 and C14. To be able to separate this mix of two effects (differences between the mirrors versus the potential variability of the subjective gap acceptance criteria), it would be necessary to conduct a follow-up study and repeat each mirror session multiple times. This would allow to calculate the variability of the subjective gap acceptance criteria for each mirror type individually, and afterwards the impact of the mirrors could be assessed much better. For Experiment 2, only one session exists per mirror and the variability of the gap acceptance criteria can not be assessed, without mixing it with the mirror related effects. Nevertheless, the required time for such a much more complex and time consuming follow-up study was not available during this thesis and this to be considered future work.

What are the consequences for the further model development? It was already concluded that the violations can not be explained on the basis of the angular measures. Additional model variable(s) or model functionality would be necessary to capture the characteristic properties of the violations and allow their simulation. It was argued above, that behavioral variability between the sessions likely caused the violations, and in this regard this additional model functionality would somehow capture the variability of the subjects.

Having in mind the diverse characteristic of the violations, it seems unlikely that a single parameter setting would be sufficient to simulate 1) the different magnitudes of the violations, 2) their occurrence at one specific or at all speed differences and finally 3) to simulate violations which occurred between different types of mirrors (e.g. planar - C20, C20 - C14, and even

planar - C14). As a consequence, it seems likely that a model concept would be necessary, which is differently parameterized to simulate all of the observed behavior variations. But this approach nevertheless has one major issue: because the effect of the mirrors can not be precisely separated from the behavioral inter-session variability, the model would also not be able to clearly separate the effects. This jeopardizes its predictive power. The "additional functionality" would capture all of the observed behavior which is not fully in line with the predictions of the angular measures. This approach is not pursued in this work.

Which alternatives exist? Focusing on those subjects who behaved according to Hypothesis 2.1 (group G1) is certainly not possible, because Hypothesis 2.1 was fully accepted for four subjects only. Hypothetically, some noise generation mechanism might be sufficient to simulate the subjects of group G2, too, but this is also not preferred and at least the five subjects of group G3 would be completely lost for the model. Another option would be, to focus on the significant relation between planar mirror and the curved mirrors (planar - C20, planar - C14), and to skip the C20 - C14 relation. In this case, the data of almost all subjects could be used (besides the four violations reported on data level 3 which involved the planar mirror), but the model concept would then also completely fail to deal with the relation between the C20 and the C14.

It was decided, to reject these alternatives for two reasons: 1) skipping large amount of the data seemed not to be appropriate, because it reduces the database for the model, and it would also look like "the unpleasant part of the experiment was simply ignored", which should be clearly avoided. 2) Even these approaches would incorporate the inter-session variability, which is still mixed with the mirror related effects postulated in Hypothesis 2.1. Unless a follow-up study will be conducted which is able to separate these two effects, this situation can not be changed.

But there still remains the possibility to consider all the data for the model development, if all 42 sessions are considered individually. What has been left out of this whole discussion so far, is the fact that Hypothesis 2.2 was significant too, and in this case, only 2 violations of a very small magnitude were found (see Table 5.3, p. 118). Furthermore, the effect of Hypothesis 2.2 is not affected by the inter-session variability. If a common model approach could be derived, which allows the simulation of all 42 sessions, it would still be possible to accumulate the results (in the same way as it was done for the subjects), and to compare them with regard to Hypothesis 2.1. Furthermore, if the development of the model will focus on Hypothesis 2.2 first, it is still not guaranteed that the model can reproduce the results of Hypothesis 2.1. Therefore, this approach is still challenging.

If the model development will focus on Hypothesis 2.2, does this cause problems with regard to the selection of the model variables, and the argumentation from the beginning of this chapter (especially the conclusions drawn in section 5.3.3, p.114)? This question can be answered with "No", because on the basis of the metric measures, there should have been no significant effect at all for Hypothesis 2.1 in the experiment, but as explained above, the first part of Hypothesis 2.1 was accepted: for the planar mirror, a significantly smaller number of lane changes was observed, compared to both curved mirrors, the C20 as well as the C14 and this significant relation can be explained by the angular measures, but not by the metric measures. Therefore, it is proposed, that in general the choice of these variables is still adequate.

5.5 Gap Acceptance Model I: Basic Ideas

After the decision was made that the model development will focus on Hypothesis 2.2, this section now explains the basic ideas behind the gap acceptance model. The development of the model starts with an assessment of the previously developed IMoST model. With the help of the data of Experiment 2 it is explained, why the concepts that were used for the IMoST model are not sufficient to deal with the behavior of all subjects of Experiment 2.

It was explained in section 5.1 that a sound empirical validation of the gap acceptance model could not be accomplished for the IMoST model. There was no empirical data available, where a systematic variation of gap situations was done. With the Experiment 2 results at hand, this is possible, and an evaluation of the basic concepts of the IMoST model will be done in the first subsection (5.5.1). Afterwards, the angular measures are investigated whether they can be used to predict the behavior that was observed with regard to Hypothesis 2.2. For this purpose, a visual approach is used to demonstrate that the angular gap size Θ^{gap} and its angular velocity Δ^{gap} can be used to explain different magnitudes of the effect which is described in Hypothesis 2.2. Afterwards, the *mean reaction time* of the subjects of Experiment 2 is briefly analyzed, because this will be an important parameter for the real-time implementation of the gap acceptance model.

Afterwards, section 5.6 "Gap Acceptance Model II: Implementation" describes the implementation of the model and how it is parameterized.

5.5.1 Assessment of the Threshold Concept

The decision making process of the IMoST model (described in section 5.1), was based on two tests: 1) a comparison of the angular vehicle width Θ^{veh} against a fixed threshold value (minimum safety distance). If the approaching vehicle was outside of the safety distance, the approaching speed was assessed by a comparison of the angular velocity Δ^{veh} against a second threshold value. Due to the non-linear relation between the distance to the rear vehicle and the angular velocity Δ^{veh}, the model accepts larger speed differences (in m/s) at larger distances.

Instead of using the angular vehicle width Θ^{veh} and its angular velocity Δ^{veh}, it was proposed that the angular gap size Θ^{gap}, and the corresponding angular velocity Δ^{gap} are more appropriate for the lane change scenario (section 5.3.2). Nevertheless, the same principle with regard to the angular velocity apply here, too: if an approaching vehicle from behind approaches at a constant speed difference (in m/s) the angular velocity Δ^{gap} will increase with decreasing distance in meter (the angular gap size Θ^{gap} reduces quicker at short distances). If, similar to the IMoST model, a fixed threshold for the angular velocity Δ^{gap} is used, the model will still accept larger speed differences at larger distances. The next step is to evaluate whether the threshold concept of the IMoST model is sufficient to deal with the observed behavior of Experiment 2.

One conclusion from the previous investigations of Experiment 2 is the following: the number of lane changes does not switch at a single ttc_{init} condition from "no lane changes" to "only lane changes". Figure 5.16 below shows the number of lane changes for the 14 experiment sessions (one per subject) where the planar mirror was used. The following observation can be made: "there is a certain region along the ttc_{init} conditions (x-axis in the figure), where the number of lane change decisions continually rises, from braking only (at a smaller ttc_{init} con-

dition), towards lane changes only (at a larger ttc_{init} condition)“. In the following, this region will be referred to as the *transition region*.

The concept of the transition region can be used for a first assessment of the threshold concept of the IMoST model: already at the time when that model was developed, it was assumed that a fixed, crisp transition might not reflect the real driver behavior. It would have been a small implementation detail to just add some noise to the threshold concept, however, the available empirical data did not allow to systematically assess the behavior that is observed in the transition region.

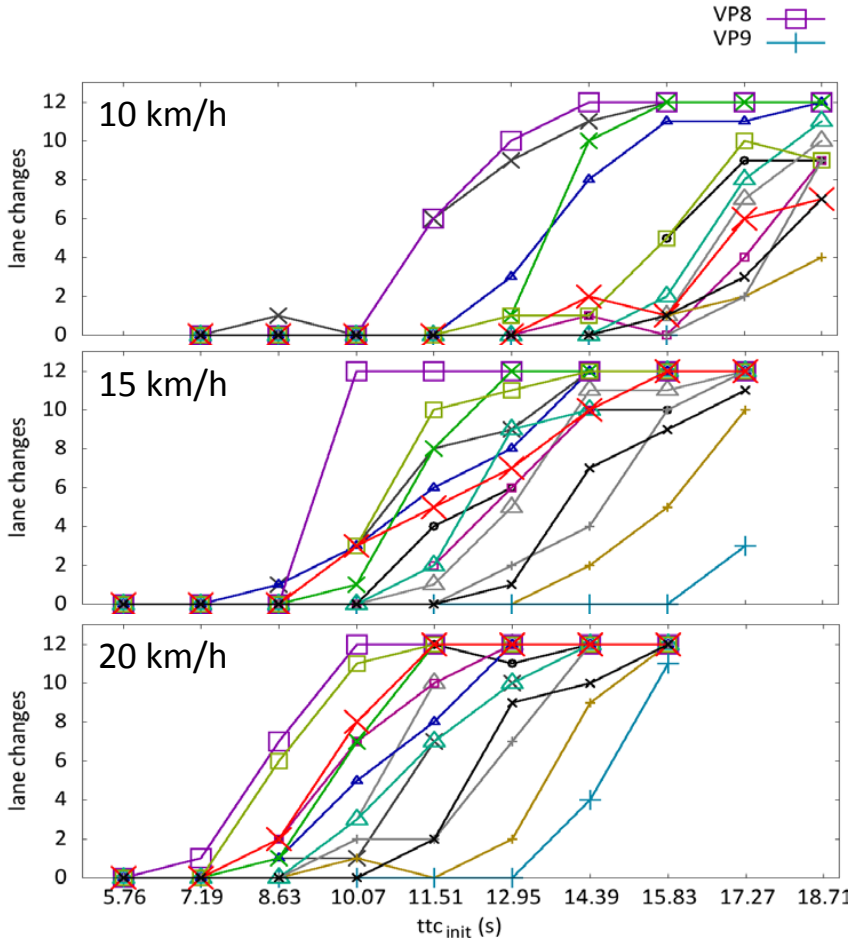

Figure 5.16: Planar mirror sessions: number of lane change data for all subjects; VP9 accepted only the largest ttc_{init} conditions, while VP8 accepted the most gaps.

Figure 5.16 shows all 14 experiment sessions for the planar mirror, separated into the three speed differences. Similar figures for the C20 and C14 sessions can be found in the Annex (Figures 7.2 and 7.3, p. 215). Figure 5.16 visualizes, how individually different the 14 participants dealt with the same situations, and two characteristic properties are of interest for the assessment of the threshold concept:

1) For each speed differences, the transition regions of all 14 subjects cover a range of approximately 6-7 ttc_{init} conditions, which roughly equals a range of 9 seconds time-to-collision.

Compared across all three speed differences, this range increases to about 11 seconds, and only the two smallest ttc_{init} conditions are barely reached (for 5.76 seconds no lane changes were recorded for the planar mirror).

In the introduction of this work it was argued that there is a need for individual driver models, because upcoming driver assistance systems should be able to adapt to individual driver behavior, and individual driver behavior models can be used to test these systems. Figure 5.16 gives a good impression about the individual behavior differences with regard to the gap acceptance task (as observed in Experiment 2). Consequently, this variability needs to be considered by the gap acceptance model.

2) If the transition regions for each subjects is investigated individually, the large majority of them spans a range of up to four ttc_{init} conditions, which equals a time-to-collision range of approximately 1.5 - 5 seconds. A single, fixed threshold, as it was used in the IMoST model, is inadequate to cover this range, because it always decides at a single point along the ttc_{init} conditions.

Instead, a less strict decision making criterion is necessary and a probabilistic approach is proposed here, which utilizes the transition region concept: "within each transition region, from smaller towards larger ttc_{init} conditions, the *probability for a lane change* continuously rises with increasing time-to-collision". To consider the behavioral differences between subjects, the location of the transition regions along the ttc_{init} conditions needs to be considered by the model. Furthermore, their size (how many ttc_{init} conditions they embrace) has to be incorporated into the model, too. These characteristic properties have to be estimated from the data of Experiment 2, for each subject and session. As a result, the gap acceptance model will be individually parameterized to simulate the behavior of a each subject in a specific experiment session.

Finally, Figure 5.16 also shows the effect that is postulated by Hypothesis 2.2: *With increasing speed difference Δv_{CA}, the number of accepted gaps for situations with equal ttc_{init} will increase.* VP8 can be used as an example for this effect. As a consequence, the location of the transition region seems to be dependent on the increasing speed difference. It could be concluded, that the speed difference is a necessary variable for the model, but the next section shows that the angular gap size Θ^{gap} and its angular velocity Δ^{gap} can be used to simulate different effect strengths of Hypothesis 2.2.

5.5.2 Θ^{gap} and Δ^{gap} as Model Input

According to the argumentation from the previous section, the transition regions for each subject vary with increasing speed difference. If a transition region is specified for each speed difference, and the three transition regions for an experiment session can be mapped onto a similar value range of the angular gap size Θ^{gap}, or the angular velocity Δ^{gap}, such a common value range can be used as a predictor for the observed behavior with regard to all three speed differences.

A visual approach is used in this section to *demonstrate* how a decision can be made, which of the two angular measures (Θ^{gap} and Δ^{gap}) should be used to simulate the observed behavior of a certain subject and experiment session. This approach will be referred to as *visual mapping*. Later on, this approach will be implemented, and the decision between the angular measures

can be made on the basis of numeric values (Implementation section 5.6.3.2).

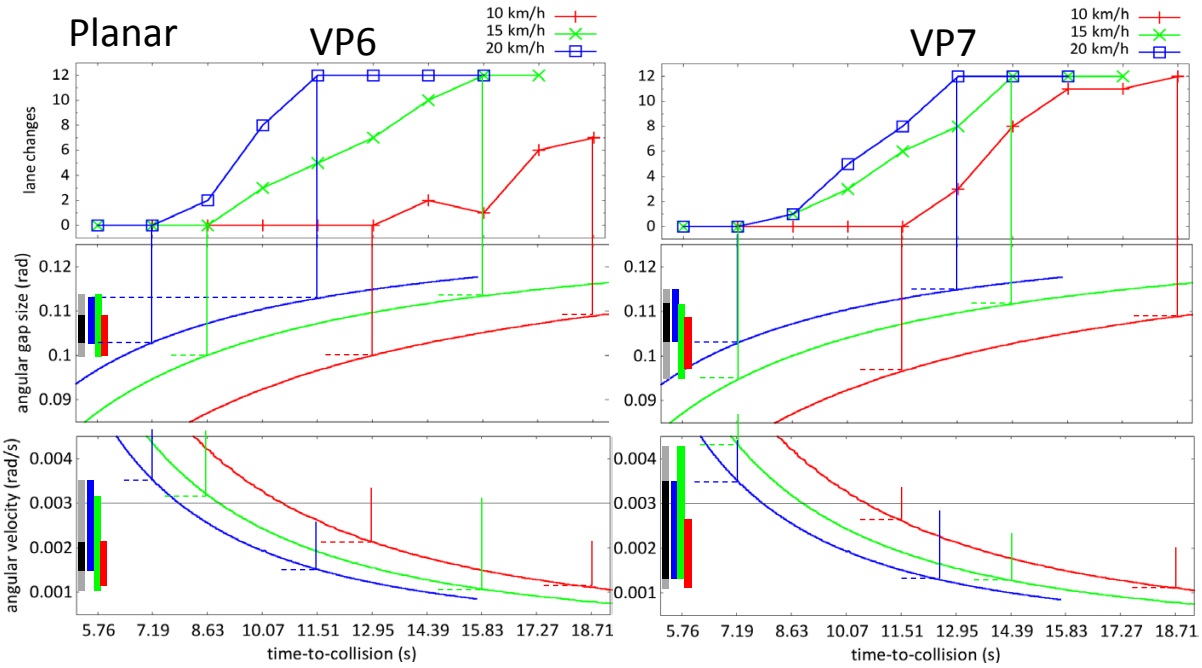

Figure 5.17: Two planar mirror sessions (VP6 and VP7); Mapping of the transition regions onto the angular measures; Please refer to the text below for a description.

First of all, the color coding of Figure 5.17 is different from all previous figures, because the data of one session per subject is analyzed here, and each color represents one of the three speed differences.

Looking at the number of lane changes first (top row for both subjects), it can be observed that the increasing speed difference had a bigger impact for subject VP6 compared to VP7: the three curves have a larger separation for VP6 compared to VP7. It was explained earlier that the increased speed difference is likely not the cause for the increased number of lane changes (Summary Hypothesis 2.2, section 4.2.7). Instead, with increasing speed difference, the distance between ego and the approaching vehicle automatically increases, because $ttc_{init} = \frac{d_{CA}}{\Delta v_{CA}}$. In the experiment chapter, the proposed explanation for the Hypothesis 2.2 effect was: the increased gap size at higher speed differences leads to an increased number of lane changes.

The two graphics below the number of lane change diagrams show values for the angular gap size Θ^{gap} (middle row) and its angular velocity Δ^{gap} (bottom row). The curves were printed from actual data recordings of the simulator.

Considering VP6 first, the boundaries of the three transition regions in the number of lane change diagram (top) are embraced by vertical lines of the same color. These vertical lines also mark the corresponding values for the angular gap size (Θ^{gap}, middle row). To the left of the angular gap size diagram, the associated *value range* for each of the three transition regions is illustrated by a bar of the same color (e.g. a red bar for the transition region of the 10 km/h speed difference).

At the beginning of this section it was said that a common value range is of interest because this could be used as a predictor for the behavior of all three transition regions: the *overlap* O between the three colored bars is indicated by the black bar. Additionally, the *total range* R, which is covered by the three colored bars is illustrated by the gray bar. The same procedure is also applied for the angular velocity (Δ^{gap}, bottom diagram). Afterwards, the relation between O and R is investigated for each angular measure: the quotient O/R denotes, how well the overlap O covers the total range R. This quotient will be called the *score* $S = O/R$. The exact numbers will be calculated later when the implementation of the approach is explained. For the explanations here, a rough visual inspection of $S = O/R$ is sufficient.

For VP6, the resulting S value is larger for the angular gap size Θ^{gap}, compared to the angular velocity Δ^{gap}, in other words the overlap O covers a larger part of the total range R. For VP7, the situation is different: here, the overlap O covers the total range R better for the angular velocity Δ^{gap}.

What is the interpretation of this observation: it was mentioned above that the magnitude of the Hypothesis 2.2 effect is larger for VP6, while it is smaller for VP7. It was also explained, that the *increased distance* with increasing speed difference causes the Hypothesis 2.2 effect.

This explanation is supported by the results for $S = O/R$: the mapping of the three transition regions for VP6 produces a better result for S for the angular gap size Θ^{gap}, and this subject showed a much stronger effect size for Hypothesis 2.2. It can be concluded that VP6 might rely more on a distance based approach for decision making. In contrast, VP7 has a smaller Hypothesis 2.2 effect size, which produces a better S for the angular velocity Δ^{gap}.

It is proposed, that the $S = O/R$ quotient can be used to decide which angular measure should be used for the simulation of the behavior of a certain subject, in a specific experiment session and the selection of either Θ^{gap} or Δ^{gap} corresponds to the observed effect strength of Hypothesis 2.2.

[Gray2005] reported a similar observation with regard to different strategies. They investigated overtaking on rural roads with oncoming traffic. Authors conducted a detailed individual behavior analysis, and as a result, drivers used either a distance-based strategy, a strategy according to the rate of expansion (angular velocity) of the oncoming vehicle, or a temporal margin strategy (see p. 49 and Figure 2.12). The visual mapping approach above demonstrates that similar behavioral differences can also be identified in Experiment 2.

The two following figures 5.18 and 5.19 show the application of the same procedure. It can be seen that the same behavioral difference is observed consistently throughout all three sessions for both of these subjects.

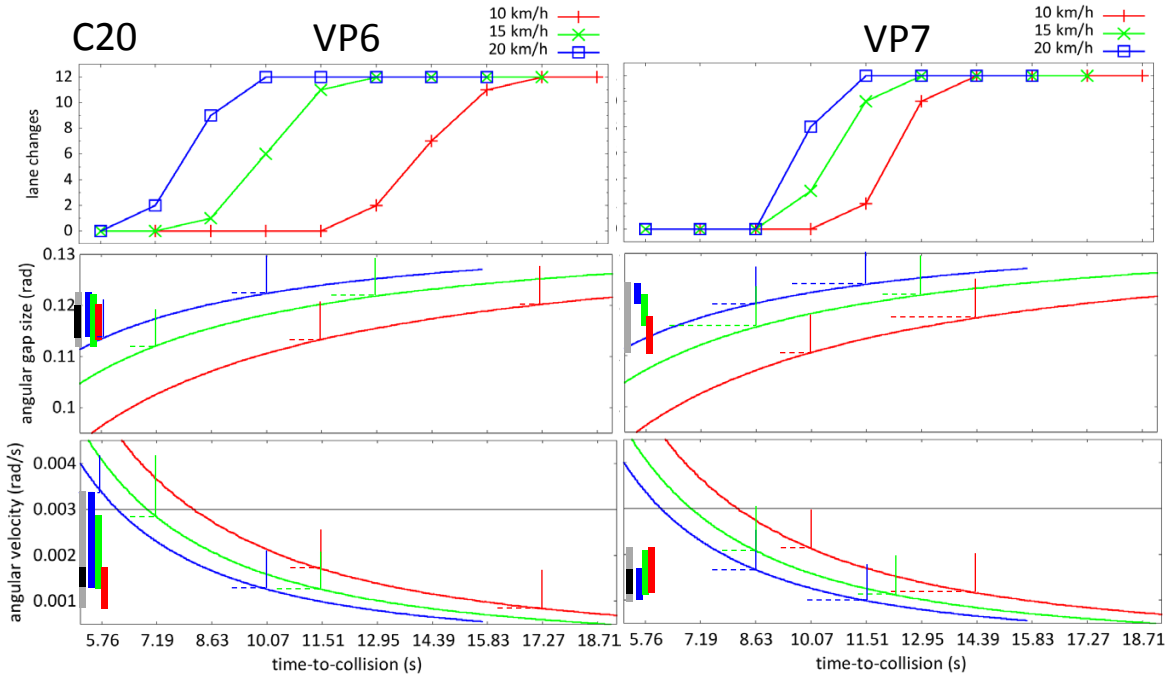

Figure 5.18: C20 sessions for VP6 and VP7.

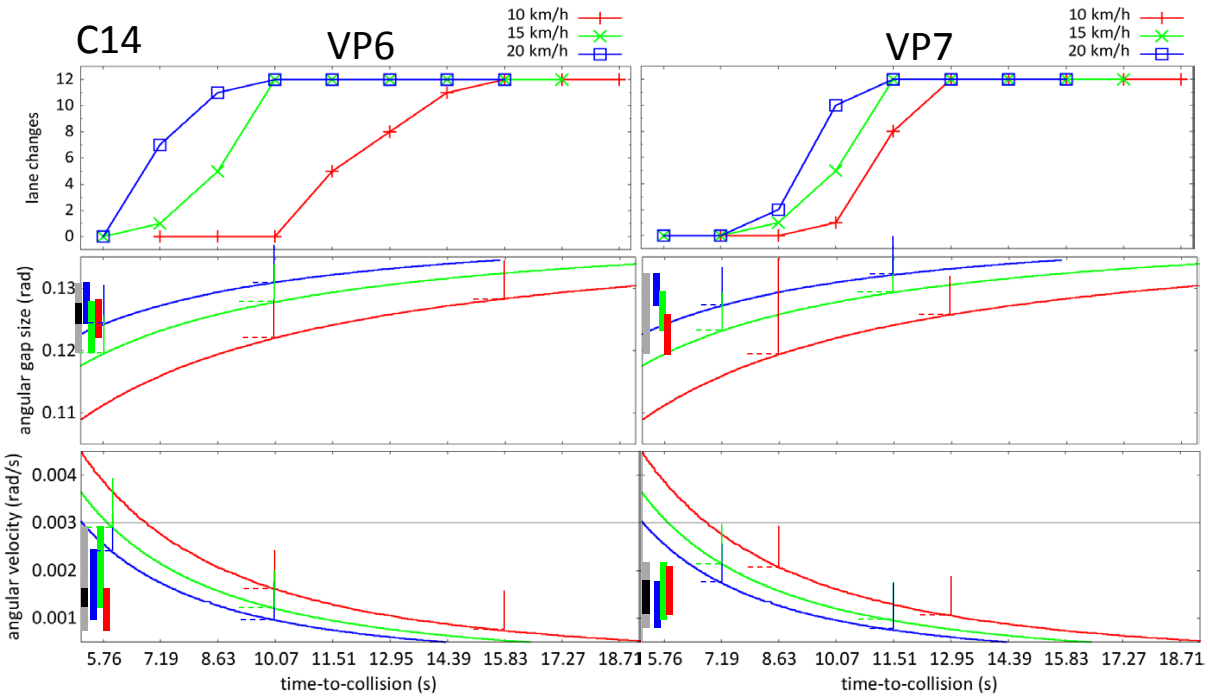

Figure 5.19: C14 sessions for VP6 and VP7.

Conclusion The concept of the transition region was introduced, which can be used to capture the variability of the lane change behavior between different the subjects of Experiment 2, but also the variability of a single subject. This variability manifests in different locations of the transition regions along the ttc_{init} conditions and a different size (how many ttc_{init} conditions a region embraces). It was concluded that both of these characteristic behavior properties have to be considered by the gap acceptance model and that an individually parameterized behavior model approach is preferred in this work.

The visual mapping approach demonstrated, how the three transition regions of an experiment session (each associated to a specific speed difference) can be mapped onto the angular measures. The mapping results in a *common value range* (overlap O) for either the angular gap size and / or the angular velocity. It was argued previously: "If these three (transition) regions can be mapped onto a similar value range of the angular gap size or its rate of change (angular velocity), such a common value range can be used as a predictor for the observed behavior with regard to all three speed differences. This angular measure can be used as input for the gap acceptance model to feed the probabilistic decision making process."

In this section it was also demonstrated, how a selection can be made between the two angular measures Θ^{gap} or Δ^{gap}. The selected variable will be used by the gap acceptance model to simulate the observed behavior of a certain subject within a specific experiment session of Experiment 2.

Going back to the IMoST model, the gap acceptance decision was made on the basis of the angular velocity Δ_{veh} (the rate of change of the angular vehicle width, see Figure 5.3, p. 110). The detailed results of Experiment 2 lead to a different finding, and subjects seem to use either a distance based or a velocity based cue for gap acceptance (Θ^{gap} or Δ^{gap}).

The implementation section 5.6.3.2 describes, how the visual mapping was implemented, to calculate $S = O/R$ for each of the 42 experiment sessions. Before the details of the model implementation are described, a final issue needs to be investigated before: the visual mapping was done for the smallest and largest ttc_{init} condition of each transition region.

These two ttc_{init} conditions describe the relation between ego and approaching vehicle at the *beginning of the trial*. If the calculated overlap O would be used by the model, it would have to make its decision right at the beginning of the trial, because O relates to the ttc_{init} condition at the start of an experiment trial.

Instead, the action response of the subjects was made after a certain *reaction time*. The modeling objectives demand that the model interacts within the Experiment 2 scenario similar to the subjects. Therefore, the reaction time needs to be considered during the calculation of $S = O/R$, too. More specifically, the point in time when the decision was made by the subjects should be approximated as good as possible.

5.5.3 Reaction Time

Figure 5.20 shows a box plot of the reaction time distribution for each subject and experiment sessions. The reaction time of the subjects was measured from the point in time where the acoustic signal occurred at the beginning of each trial (and the rear vehicle was set up), until the action was finally detected (braking or steering response). One important information is that subjects were free to decide if and *when* a braking or steering response should be done. There

was no instruction like “decide as quickly as possible“ or “decide at the latest possible moment“. In such a scenario, larger reaction time variations between the subjects can be expected and this can be observed.

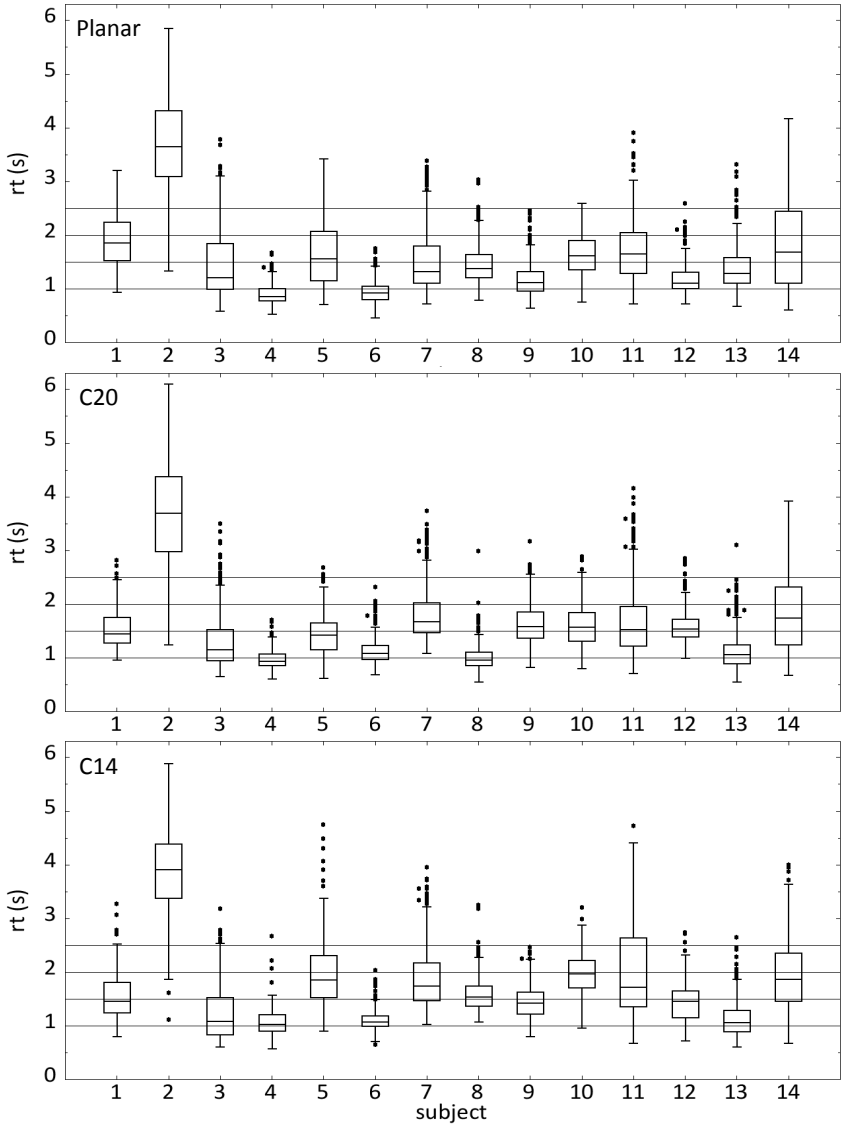

Figure 5.20: Distribution of the reaction time in seconds for each subject and experiment session; Horizontal lines added for easier comparison between subjects.

Subjects VP4 and 6 for example behaved very quickly during all three mirror sessions and their reaction time was only about a second on average. In contrast, VP2 had a noticeably longer reaction time. An additional comment that was made in the questionnaire gives a good explanation: the subject described that it is part of his driving style to restrain the approaching vehicle as less as possible, which means he first closes the gap to the lead vehicle and makes the lane change decision comparably late. This strategic approach is fully supported by the reaction time data. But the reaction time is not the best possible approximation for the point in

time when the decision was supposedly made by the subjects, because it includes the time that was necessary to execute the response action. These action response times should be subtracted from the reaction time. It should be mentioned here that steering and braking actions were not fed into the vehicle dynamics, the ego vehicle in Experiment 2 was driven by a driving automation. Steering and braking were used to record the action response according to the decision, either gap accepted (steer left), or gap rejected (brake).

For the detection of the brake action, the brake pedal had to be pressed by an amount of 20% of the total pedal range. Subjects were advised to "rest" the right foot on the brake pedal, which removed an additional time to move the foot towards the pedal and also increased the comparability between subjects. To reduce the possibility that subjects press the pedal by accident, a stronger force feedback was applied. This allowed a reliable detection of the point in time when the braking action began.

For the detection of the steer left action, the steering wheel had to be turned by 30° left until the action was recorded. The force feedback which pulls the steering wheel back to a centered location was increased, too, but over the course of a trial, subjects nevertheless held the steering wheel slightly off-centered (up to a maximum of 11 degree), and this varied from trial to trial and subject to subject. Therefore the beginning of the steer left action was determined to a steering wheel angle of 11.5 degree (to the left). Using such a unified threshold across all subjects is a trade-off between a reliable detection of all starting points for the steering action and the preciseness of the measurement. As a result, the calculated steering action times are an approximation, with a tendency to be slightly smaller than they actually were. Table 5.11 at the end of this section summarizes the mean action response times for braking and steering actions.

Lesson learned: for a more reliable detection of the reaction times, button presses would have been a better choice for the action response. When Experiment 2 was planned, the typical action responses (braking and steering) seemed to be less error prone, while pressing the wrong button by accident was a concern. But a recent simulator experiment with a similar study design showed that subjects did not report problems when using buttons on a game pad instead of using steering wheel and brake pedal. If it is generally possible to use such a device, it should be preferred in future studies.

It could be argued that the gap acceptance decision might have been done even earlier, and the action was probably "delayed". With the given experimental data and study design, there is no chance to assess such an earlier point in time, but what does such a "delayed" action mean with regard to the decision making? Assume that the decision was made previously, e.g. 500 ms earlier before the action is started. There are two alternatives: 1) if the situation would have considerably changed during the 500 ms "delay", this should have led to a revised decision which would have been recorded then. It would not be possible to track such a revised decision, but the data would nevertheless contain the final decision. In this case, the delay would not exist anymore, and the decision would have been made, based on the latest point in time before action execution. 2) If during the "delay" the decision is not revised, we would indeed use "wrong" values for the model (in this example 500 ms later). However, the decision was not revised, and the values 500 ms later should be a valid representation for the recorded decision, otherwise the decision would have changed and would end up in 1).

It is concluded that the point in time, when the action execution starts is an approximation of the point in time, when the decision was made and this time has to be considered during model development.

VP	Planar	C20	C14
1	1.9055	1.5283	1.5221
2	3.6743	3.6332	3.8625
3	1.4442	1.3261	1.2643
4	0.8963	0.9753	1.0612
5	1.6566	1.4352	1.9685
6	0.9427	1.1275	1.1080
7	1.5065	1.8461	1.8976
8	1.4425	0.9991	1.5813
9	1.1768	1.6340	1.4479
10	1.6150	1.6003	1.9481
11	1.7112	1.7100	2.0291
12	1.1768	1.5799	1.4096
13	1.3963	1.1397	1.1375
14	1.8494	1.8385	1.9355

Table 5.10: Mean reaction time in seconds for all subjects and sessions.

VP	Planar		C20		C14	
	steer	brake	steer	brake	steer	brake
1	244.97	419.29	177.68	241.12	205.02	195.78
2	297.46	158.79	282.44	178.00	269.94	179.51
3	182.72	187.29	194.01	171.01	201.20	182.61
4	238.00	107.93	311.21	134.50	194.81	114.59
5	413.74	357.58	262.12	261.06	405.79	254.17
6	251.35	183.71	220.27	202.90	300.97	279.02
7	347.40	201.46	217.86	184.05	217.47	185.22
8	421.97	228.75	280.73	183.50	498.09	273.16
9	221.15	144.44	383.90	269.17	202.25	168.71
10	160.83	136.19	162.96	167.70	214.43	191.26
11	231.27	139.14	204.95	157.57	232.92	118.73
12	217.98	193.40	217.08	209.09	199.78	172.86
13	315.57	284.57	330.01	256.87	277.15	223.69
14	377.55	140.07	279.03	191.93	393.49	157.44

Table 5.11: Mean action response times for steering and braking actions in milliseconds for all subjects

5.6 Gap Acceptance Model II: Implementation

The previous part *Gap Acceptance Model I* described the basic ideas for the gap acceptance model: the large behavioral variations that were observed in the experiment led to the decision that an individually parameterized behavior model shall be developed. On the basis of the accumulated data of all subjects it was proposed that the angular gap size Θ^{gap} and its angular velocity Δ^{gap} are the preferred input variables for the model, while τ was rejected as an explanatory variable for the effects of Experiment 2. Therefore, the visual mapping approach was used previously to illustrate how a decision can be made, which of these two measures should be used to simulate the behavior of a certain subject in a specific experiment session.

In contrast, the individual behavior analysis of VP2 revealed (see page 122) that τ might be required to adequately simulate the observed behavior of this subject. For this purpose, τ needed to be considered as a third input variable for the model, and the implementation of the visual mapping process (described in section 5.6.3.2) was extended in this regard.

This section describes in detail how the gap acceptance model was implemented. Section 5.6.1 describes, how the gap acceptance model interacts within the Experiment 2 scenario, how it behaves within each of the trials of an experiment session. The task of the subjects in Experiment 2 was used to derive an action sequence which is executed by the model. One of these actions is the perception of the three input variables, which his described in section 5.6.2. The perceived values are then used by the decision making process of the model, which is described in section 5.6.3.

5.6.1 Interaction between Simulator and Model

To describe how the gap acceptance model interacts within the scripted scenario of Experiment 2, the task of the subjects in the experiment is briefly recapped. After the simulation was started, the ego vehicle was set up on the right lane of the two-lane Autobahn. Subjects were advised to look at the lead vehicle ahead, while their own vehicle was accelerated by a cruise control to the target speed of 130 km/h. The steering was also done by an automated lane keeping assistance system, no manual car control was required. After the target speed was reached, the *scenario script* initiated the first trial. The scenario script is a submodule of the driving simulator and controls the flow of the experiment. It sets the distance and speed of the lead and rear vehicles at the beginning of a trial, generates the acoustic start signal of a trial and detects the action response of the subject (or the model in this case). As soon as the scenario script generates the acoustic cue, the subjects task was to shift the gaze towards the left exterior mirror. They had to perceive the approaching vehicle on the left lane from behind and assess the gap. If they decided that a lane change in front of the approaching vehicle was feasible, they responded with a steer left action, while they pressed the brake pedal if the gap was rejected. After the action response was recorded, the scenario script resets the trial and subjects were instructed to observe the lead vehicle ahead again, waiting for the next acoustic signal.

Based on this description, the interaction between the gap acceptance model and the scenario script can be specified. Figure 5.21 illustrates a four step action sequence, denoted by (1) - (4). This sequence was derived from the actions that were required by the subjects.

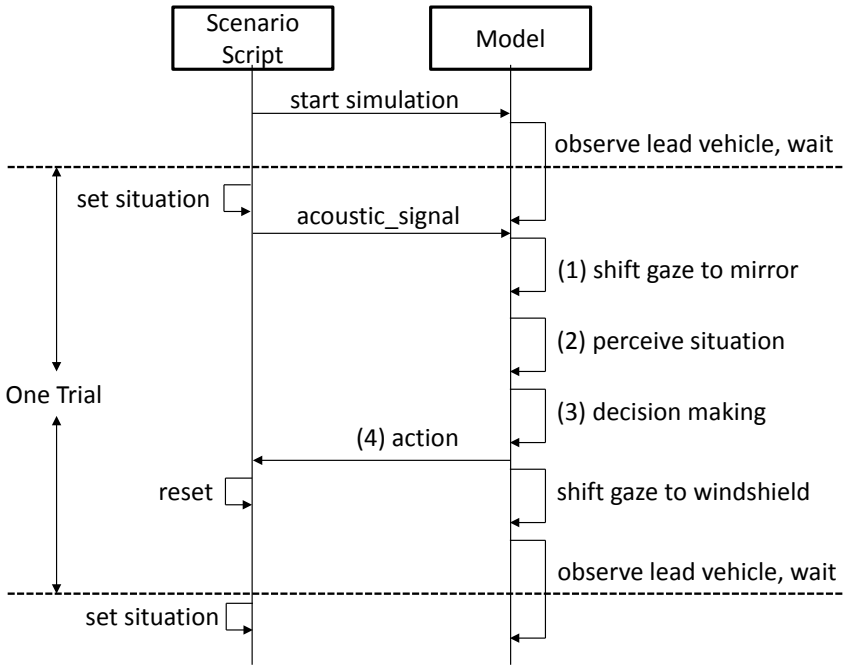

Figure 5.21: Proposed interaction between the scenario script, which controls the flow of the experiment and the gap acceptance model. Sequence (1) - (4) was derived from the task of the subjects.

Action Sequence The four sequential steps of the previous figure are realized by a state-machine (see Figure 5.22) which implements the functionality of the model (simulate the visual perception, decision making and action response). Furthermore, it times its actions with regard to the interaction with the scenario script.

The state-machine is implemented within a C++ code template that comes with the driving simulator software SILAB. The code template can be compiled and the resulting *.dll*[3] is instantiated and integrated as a plug-in module into SILAB. Such a module shares a common interface concept for the definition of input and output variables which are used to communicate information to any other module of the simulator. Each module has a callback function which is regularly triggered by SILAB (with a default frequency of 60 Hz). Within this *trigger* function the state-machine is implemented: inputs are read from other modules (e.g. the angular gap size), the execution of the state-machine progresses for the amount of time of a simulation step (considering the appropriate timing), and at the end of each trial the action response is propagated to the scenario script via the output interface (e.g. braking or steering response).

[3] dynamic link library

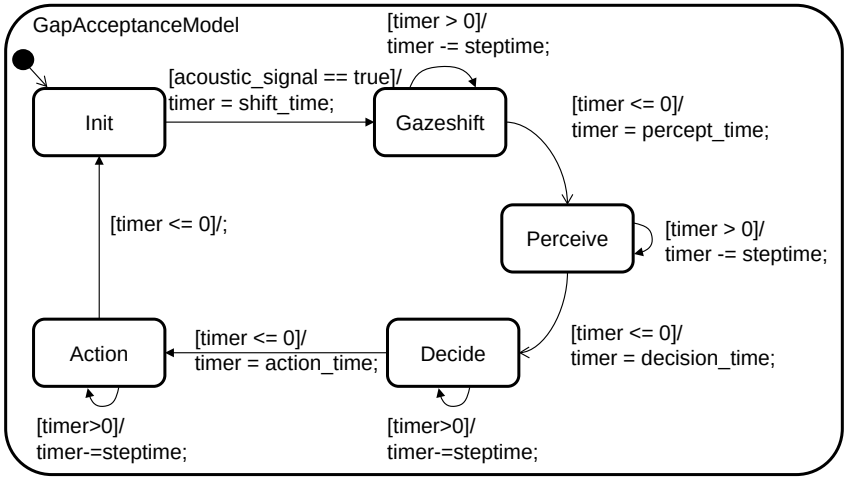

Figure 5.22: Implementation of the four main states plus an initialization state (*Init*) to wait for the acoustic cue at the start of the trial. Before entering a new state, for example *Gazeshift*, a timer is set to a configurable time in milliseconds. If the timer is expired, the state is left.

Besides the *Init* state, which waits for the occurrence of the acoustic signal, the state-machine remains in each state for a configurable amount of time, until it makes the transition to the next state. A *timer* variable is set, whenever the current state is left, e.g. when *Init* is left, the timer is set to the value of the constant parameter *shift_time*. The value of *shift_time* represents the amount of time that the model will stay in the *Gazeshift* state. Similarly the timer is set for each following state. During each simulation step, the *timer* variable is decremented by the amount of simulation time that is consumed for the current simulation step. The *steptime* is a parameter of the *trigger* function and if the simulation runs stable in real time, the value of *steptime* is 16.6 ms (60Hz). If the timer expires ($timer <= 0$), the state is finished, and the transition to the next state is taken.

At the beginning of each trial of the experiment, the state-machine starts in the *Init* state. This state is left as soon as the acoustic cue signales the beginning of a new trial (*acoustic_signal == true]*). Afterwards the *Gazeshift* state is entered, which consumes an amount of time to simulate the gaze shift from the vehicle ahead towards the mirror. The next state *Perceive* simulates the visual perception of the angular measures. The *Decide* state implements the gap acceptance decision and uses the angular measures as input. Finally, the *Action* state propagates the result of the decision making in form of a steering or braking action to the output interface of the gap acceptance module. This output is received by the scenario script which resets the current traffic situation, and the model again waits in the *Init* state, until the next trial of the experiment is signaled.

Timing The sequence of states describes how the model interacts within the Experiment 2 scenario. In addition, the interaction has to take place at an appropriate time, too and the *timer* variable has already been introduced. In section 5.5.3 the reaction time was discussed, and the mean reaction time for a trial was derived from the empirical data for each subject and session (mean reaction time data, see Table 5.10). The mean reaction time equals the time that the

model will consume for one cycle through the state machine, starting as soon as the *Init* state is left, and ending when the model again enters the *Init* state. This paragraph describes, how the mean reaction time is split between the different states.

No time is allocated to the *Init* state, because it realizes the "waiting" of the subjects between two trials, which is not part of the mean reaction time of the subjects. Therefore, the mean reaction time is split between the four states *Gazeshift*, *Perceive*, *Decide* and *Action*.

Because an eye-tracker was not available for the experiment, the time that subjects needed to shift their gaze from the vehicle ahead towards the mirror can not be extracted from the empirical data. An approximation for the gaze shifting time can be derived from published literature about combined head and eye movements. In the driving simulator, the angle between looking ahead towards the lead vehicle and the left exterior mirror is dependent on the seating position. It varies approximately between 35° - 40°, and a fixed value of 40° is used for the model. According to the literature review of [Osterloh2008] the required time $time(x)$ in seconds for a combined head and eye movements $x > 20°$ can be calculated by the following formula:

$$x = 40°, \;\; time(x) = 0.04 + \frac{min(0.31x + 13.6, 40)}{1.3x - 3} = 0.325$$

The value of 325 ms is used as default value for the model[4]. These 325 ms specify the *shift_time*, which is set by the transition that leaves the *Init* state. If an eye-tracker is used in a follow-up study this calculated time can be replaced by individual behavior data.

The next fraction of the mean reaction time that can be determined quickly is the time consumption for the *Action* state: as explained in discussion about the reaction time, the mean action response times for the braking and steering actions were extracted from the empirical data (Table 5.11, p. 5.11). For each subject and session, the average of the two mean values specifies the *action_time* which is set by the transition which leaves the *Decide* state.

With regard to the decision making state, there is no possibility to derive this time from any empirical data of the experiment. For the simulation of human behavior, cognitive architectures like ACT-R provide mechanisms to simulate rule-based decision making (section 2.2.3, p.26 provides a brief explanation on goals, rules, and the execution of these knowledge units by a production system). Within such an architecture, *condition - action* rules can be used to specify the decision making, e.g. the currently perceived value of an angular measure can be compared against the two boundaries of the transition region. The exact realization is architecture specific, and it is not the objective of this work to develop a model which is dependent on a specific architecture. Nevertheless, the comparison of the currently perceived value against the two boundaries of the transition region can be specified in the condition part of one rule. The time consumption per production system step is 50 ms (e.g. in ACT-R, CASCaS, EPIC) and rules have to be selected and executed which equals two such steps. Therefore, a value of 100 ms is assumed for the *Decide* state here.

As said before, the model will give its action response at the end of the *Action* state, after the mean reaction time is consumed (mean reaction time, Table 5.10, p. 140). Therefore, the time consumption for the last state (*Perceive*) can be calculated by subtracting the execution times of the three steps from the mean reaction time.

[4]The formula in [Osterloh2008] notes 40 instead of the 0.04, but this mistake is caused by a mix between milliseconds and seconds, 0.04 is the correct value for the formula.

As a brief summary, the model will use a fixed time of 325 ms for the *Gazeshift* state, and another fixed 100 ms for the *Decide* state. These times are not adjusted for each sessions. The time for the *Action* state instead equals the average of the mean braking and mean steering action time which is derived from the empirical data for each subject and session. The remaining difference between these three times and the mean reaction time for each subject and session is the time consumption for the *Perceive* state. Table 5.12 gives an example, how the mean reaction time, which is measured for each subject in a specific experiment session, is distributed across the four states.

State	Time
Mean RT	1898 ms
Gazeshift	325 ms (constant)
Decide	100 ms (constant)
Action	203 ms $(217.47 \text{ ms} + 185.22 \text{ms})/2$
Perceive	1270 ms $(1898 - 325 - 100 - 203)$ ms

Table 5.12: Calculation of time consumption for of each of the four states. Example for the C14 session of VP7; Mean RT taken from Table 5.10; Times for *Gazeshift, Decide* were defined as constant values; *Action*: Table 5.11 gives the mean response times for braking and steering of VP7 during the C14 sessions, average of both is used; *Perceive* is calculated by subtracting the times for *Gazeshift*, *Decide* and *Action* from Mean RT.

Remark: the resolution of the four time values is different, because the first two are given in milliseconds by either a formula or as a fixed constant in the cognitive architecture CASCaS, while the action and perception times are derived mean values from the experiment.

Functionality of the States After the action sequence of the model and the timing within the simulation have been explained, the functionality of the different states needs to be specified. The main purpose of the state *Gazeshift* is the realization of the time consumption, there is no further functionality implemented. The *Action* state generates the output value for the action response according to the outcome of the *Decide* state. For this purpose, the gap acceptance module has two outputs: one signals *braking* and another *steering*. Dependent on the outcome of the gap acceptance decision, the corresponding output is set to "1" *after* the action time has expired. Only at this point in time, the state-machine has consumed the mean reaction time that was measured for the subject in the corresponding session. The described calculation of the timing ensures, that the scenario script receives the answer of the model at the appropriate time, when the state-machine has consumed the mean reaction time of the subject. The functionalities of the *Perceive* and the *Decide* states are more complex, and each of them is explained in a separate section.

5.6.2 Perception of Angular Measures

In the previous sections of this chapter it was argued that the angular gap size Θ^{gap} and its angular velocity Δ^{gap} should be used as input variables for the gap acceptance model. Figure

5.23 depicts how and when the perception process of the angular measures takes place during the flow of each trial.

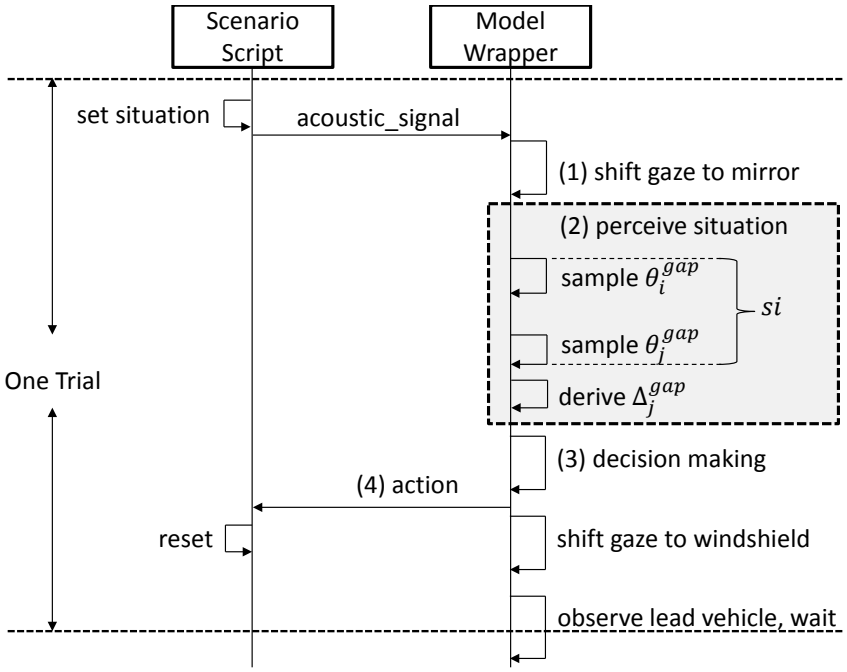

Figure 5.23: The model samples the angular gap size Θ^{gap} during the simulation and calculates the angular velocity Δ^{gap}. The sampling interval si can be adjusted.

The model perceives the angular gap size Θ^{gap} (measured in radiant) as input value from the driving simulator. Each value Θ_i^{gap} which is perceived in simulation step i is called an input *sample*. The sampling process is continuously executed, as long as the model stays in the *Perceive* state. The angular velocity Δ^{gap} is calculated by the model in the *Perceive* state, using the difference of two input samples:

$$\Delta_j^{gap} = \frac{\Theta_i^{gap} - \Theta_j^{gap}}{si}$$

- i, j represent two points in time during the simulation, with $i < j$, meaning sample Θ_i^{gap} was recorded before sample Θ_j^{gap}.
- The time interval between the two samples $\Theta_i^{gap}, \Theta_j^{gap}$ can be specified by adjusting the sampling interval parameter si in seconds.

To realize the difference calculation in the *Perceive* state, the implementation of a sampling interval si was necessary, but no information could be found in the literature with regard to the proper size of this interval. Therefore, this has to be considered an open issue of the model. But there was a practical reason, why a value of $si = 0.1$ seconds was used for the simulation: inaccuracies in calculation of the angular gap size Θ^{gap} within the simulation platform caused an oscillation effect: between two consecutive simulation steps (16 ms long), the Θ^{gap} sometimes got even smaller sometimes. The size of this effect in relation to the absolute angle is

comparably small: a maximum of 0.0005 radiant was observed, while the minimum absolute angular gap size Θ^{gap} during the experiment is 0.065. Therefore this effect causes problems especially for the difference calculation, because it changes the sign for the angular velocity Δ^{gap}. A sampling interval of 0.1 seconds removed these problems.

Remark: Instead of this very simple solution of a larger sampling interval, it would also be possible to use a moving average or a Kalman filter with the smaller sampling interval. Both of these methods are well known from signal processing with regard to noisy signals and it should be tested in future whether the simplified solution has any drawbacks.

Input Variable τ As mentioned in the introduction of this implementation section, the time-to-collision, respectively τ, needs to be considered as the third input variable for the model, because the individual behavior analysis for VP2 revealed that τ might be required to adequately simulate the observed behavior of this subject (see page 122). The perception of τ was derived from the specification used by [Lee1976]: the model perceives the *angular vehicle width* Θ^{veh} from the driving simulator. Two input samples (Θ_i^{veh}, Θ_j^{veh}) are used to calculate the angular velocity Δ_i^{veh}, and τ is calculated using the formula

$$\tau_i = \frac{\Theta_i^{veh}}{\Delta_i^{veh}}$$

In summary, the output of the perception component are three perceived variables, which are called *input variables* in the following sections. The *input variables* are fed into the decision making function of the model, which is described in the next section.

5.6.3 Decision making

This section is split into three parts, because the implementation of the decision making function is closely related to the implementation of the visual mapping approach (presented in 5.5.2).

The visual mapping was used previously to illustrate how a value $S = O/R$ can be used to decide whether the angular velocity Δ^{gap} or the angular gap size Θ^{gap} should be used as input variable by the model, to simulate the behavior of the subject. It was proposed that the angular measure which receives the highest value for S should be selected. So far, numeric values were not calculated to make a distinct decision. The implementation of this approach calculates $S = O/R$ for Θ^{gap} and Δ^{gap}, but also for the third input variable of the model, the time-to-collision, respectively τ. On the basis of these results, the decision making function is configured individually for the simulation of each experimental session.

Section 5.6.3.1 describes the implemented decision making function which is realized in the *Decide* state of the model. Afterwards, section 5.6.3.2 explains the implementation of the visual mapping, and section (5.6.3.3) summarizes the results of the calculations for $S = O/R$.

5.6.3.1 Decision Making Function

Figure 5.24 shows the implementation of the decision making function $f(x)$, which calculates a probability for a lane change $P(LC|x)$. This function is realized in the *Decide* state of the state-machine. $P(LC|x)$ is calculated once per experiment trial, using the current input value of one of the three input variables. The current values for the input variables are perceived by the perception and fed into $f(x)$.

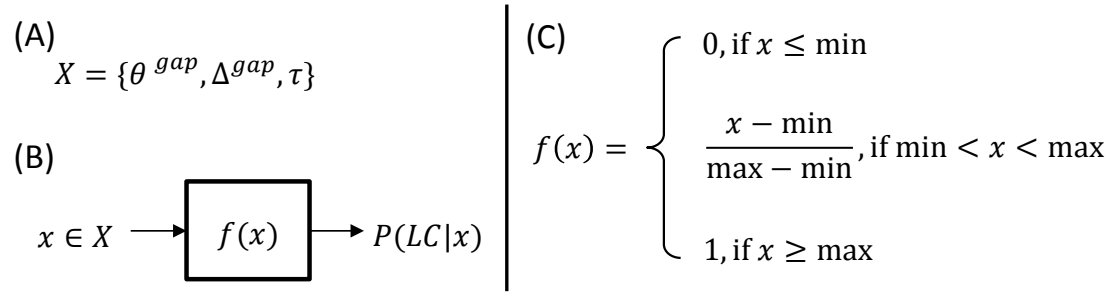

Figure 5.24: (A) X: set of input variables which can be used by the decision making process (angular gap size Θ^{gap}, angular velocity Δ^{gap}, or the time-to-collision, respectively τ; (B) For the simulation of each session, one input variable $x \in X$ is selected to feed the function $f(x)$, which calculates a probability for a lane change maneuver. (C) Implementation of $f(x)$: the probability for a lane change increases from zero to one between min and max.

The implementation of $f(x)$ as a piecewise function was derived from the concept of the transition region, which was described as a "region along the ttc_{init} conditions, where the number of lane change decisions continually rises from braking only (at a smaller ttc_{init} condition), to lane changes only (at a larger ttc_{init} condition)". The transition region concept is implemented within the value range of min and max of $f(x)$, where the probability for a lane change increases. Outside of this region (below min or above max) the model always responds with a braking action or with a lane change action.

Remark: the selection of a piecewise linear function is also discussed in the future work section 5.8.2, p. 194.

The reason, why a probabilistic decision making approach was chosen is the following: the existence of the transition region is interpreted as an indicator that gap acceptance behavior is not a precise decision making process. For each situation (ttc_{init} condition) within this region, the decision is ambiguous: sometimes subjects accept the gap and sometimes they reject it. It is assumed that this inability to clearly decide in each of these situations is probably caused by noise, which could be caused by the neural processes along the visual pathway, and further neural processes which are involved in the decision making. It is not the objective of this work, to give an explanatory hypothesis what exactly causes this noise, but it is proposed, that the outcome of this noise (the ambiguous decision making behavior) is observed for the ttc_{init} conditions of the transition regions.

Before the decision making function can be used to simulate the gap acceptance behavior of a certain experiment sessions, it has to configured: the input variable $x \in X$ has to be selected, and the values for min and max of $f(x)$ need to be adjusted. Both is done for each of the 42 sessions and for both, the results of the calculation of $S = O/R$ are used. How this is done, is explained in the next section which explains the implementation of the visual mapping to calculate $S = O/R$.

5.6.3.2 Calculation of $S = O/R$

Figure 5.25 depicts the visual mapping (section 5.5.2). The C14 session of VP7 is used as an example throughout this implementation section.

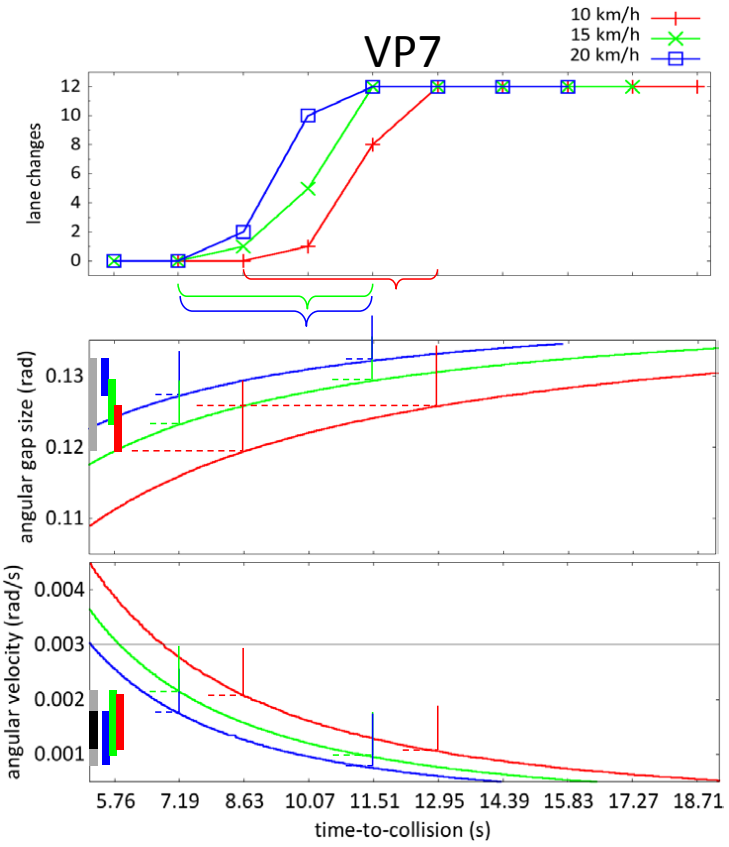

Figure 5.25: Visual mapping of the C14 session of VP7; Transition region for each speed difference is marked by a curly bracket; Transition regions are mapped onto both angular measures Θ^{gap} and Δ^{gap}; Total range R (gray bar) and overlap O (black bar) are illustrated; Larger value for $S = O/R$ indicates a better fit for the angular velocity in this session (no overlap exists for the angular gap size).

The first step is the selection of the ttc_{init} conditions which specify each of the three transition region, but this topic is deferred to the end of this implementation section. For the following explanations it is assumed that the ttc_{init} conditions are already selected for each of the three transition regions as shown in the example of Figure 5.25.

Regression Approach As illustrated in the example in Figure 5.25 above, the smallest and the largest ttc_{init} condition of each transition region are mapped onto the angular measures Θ^{gap} and Δ^{gap} (indicated by the colored vertical lines). These conditions are the boundaries of the transition region and according to the specification, they are associated to the ttc_{init} conditions where the number of lane changes is either zero or at its maximum possible number (in Experiment 2 this was 12 lane changes).

Considering all 42 sessions of Experiment 2, there are 22 of 126 transition regions (42 sessions $*$ 3 speed differences), where the maximum (12) or the minimum number of lane changes is not observed for any of the ttc_{init} conditions at a particular speed difference. These regions can be considered *incomplete*, because the lane change behavior of the subject is not fully covered by the ttc_{init} conditions of the experiment. If the largest, respectively smallest *available* ttc_{init} conditions would be used instead, the calculation of the *overlap* O and the *total range* R would rely on a varying, non-comparable range across all 42 sessions.

Figure 5.26 illustrates how this issue was solved, with the help of a linear regression approach (shown for the 20 km/h speed difference, analog for 10 and 15 km/h). The resulting linear equation $y = 3.0556x - 22.569$ the time-to-collision values for $y = 0$ lane changes and $y = 12$ lane changes can be calculated. The values are $y_0(t_0) = 7.39$ and $y_{12}(t_0) = 11.31$ seconds ttc_{init}, and t_0 denotes that the y values belong to the point in time, when an experiment trial starts. The same procedure can be applied for the transition regions of the 10 and 15 km/h speed differences and as a result three $y_0(t_0), y_{12}(t_0)$ value pairs are calculated, one for each transition region.

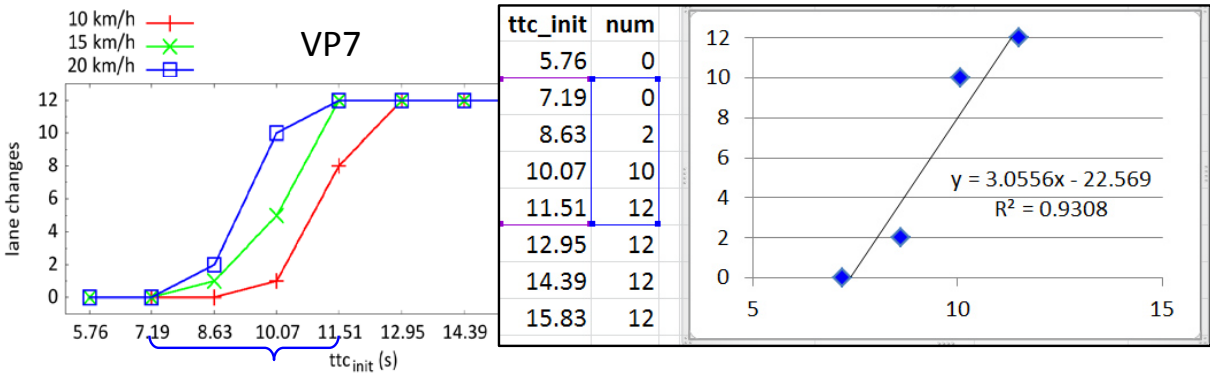

Figure 5.26: Left: lane change data for VP7, C14 mirror session; Right: Linear regression for the 20 km/h transition region: $y = 3.0556 - 22.569$.

The linear regression can also be applied for those 22 transition regions, which are incomplete. In this regard, it serves as an estimator to predict the size of the transition region. The result section 5.6.3.3 will show two example sessions, where the transition regions were incomplete, and the linear regression probably reduced the result of S.

Considering Reaction Time As mentioned above, the $y_0(t_0), y_{12}(t_0)$ values correspond to the point in time when an experiment trial starts. It was argued before (section 5.5.3) that the start of the trial is certainly not the point in time when the subjects made their decision, and

also the model will not make its decision at the beginning of the trial. The state sequence of the model was derived from the task of the subjects, and the time consumption of the states was based on the mean reaction time of the subjects. Table 5.13 was shown before to explain, how the mean reaction time is distributed between the states of the model (paragraph on "Timing", p. 143).

State	Time
Mean RT	1898 ms
Gazeshift	325 ms (constant)
Decide	100 ms (constant)
Action	203 ms $(217.47$ ms$+185.22$ms$)/2$
Perceive	1270 ms $(1898 - 325 - 100 - 203)$ ms

Table 5.13: Calculation of time consumption for of each of the four states. Example for the C14 session of VP7; Mean RT taken from Table 5.10; Times for *Gazeshift, Decide* were defined as constant values; *Action*: Table 5.11 gives the mean response times for braking and steering of VP7 during the C14 sessions, average of both is used; *Perceive* is calculated by subtracting the times for *Gazeshift*, *Decide* and *Action* from Mean RT.

The point in time, when the gap acceptance model makes its decision is reached, when the model enters the *Decide* state (see state-machine, p. 143). This is the case, after the model shifted its gaze (state *Gazeshift*), and perceived input from the environment in state *Perceive*. For the example session of VP7, the consumed time until then is 325 ms + 1270 ms = 1595 ms. This amount of time is now subtracted from each of the three $y_0(t_0), y_{12}(t_0)$ value pairs. The subtraction is necessary, because during the reaction time the traffic situation progresses, which means the time-to-collision to the rear vehicle gets smaller. For the example transition region for 20 km/h speed difference, the values are $y_0(t_{rt}) = y_0(t_0) - 1.595 = 7.39 - 1.595 = 5.795$ seconds and $y_{12}(t_{rt}) = y_{12}(t_0) - 1.595 = 11.31 - 1.595 = 9.715$ seconds.

Determining the Value Ranges After the time-to-collision values for $y_0(t_{rt}), y_{12}(t_{rt})$ are calculated, the value range can be determined for each angular measure (see Figure 5.25, the three colored bars for the three speed differences). These values were taken from look-up tables, which were built from actual simulation runs. 9 tables were necessary, one for each combination of mirror type and speed difference (three mirror types, three speed differences). Table 5.14 shows a snippet of one of these tables.

distance	ttc	Θ^{gap}	Δ^{gap}
86.79	15.61	0.13449	0.000427
86.70	15.59	0.13448	0.000428
⋮	⋮	⋮	⋮
53.89	**9.694**	0.13056	0.001028
⋮	⋮	⋮	⋮
32.21	**5.794**	0.12426	0.002528
⋮	⋮	⋮	⋮

Table 5.14: Example entries from the look-up table for the C14 mirror, and 20 km/h speed difference; Each line contains a *data sample* from one simulation step; ttc values marked bold indicate the match for the two values from the example $y_0(t_{rt}) = 5.795$ and $y_{12}(t_{rt}) = 9.715$.

The values of $y_0(t_{rt}), y_{12}(t_{rt})$ are time-to-collision values, therefore the column ttc is used as look-up key. For the two lines, where $y_0(t_{rt})$ and $y_{12}(t_{rt})$ match (bold values), the corresponding values in the columns Θ^{gap} and Δ_{gap} are used to determine the value range for these two input variables, e.g. for Θ^{gap} the value range is given by the two values $\Theta_0^{gap}(t_{rt}) = 0.12426$ and $\Theta_{12}^{gap}(t_{rt}) = 0.13056$. Because this nomenclature is very clumsy, and the value ranges are always associated to the point in time (t_{rt}), the shorter terms Θ_0, Θ_{12} are used instead, respectively Δ_0, Δ_{12} and ttc_0, ttc_{12} for the other two input variable of the model. Figure 5.27 illustrates the steps that have been explained so far for the 20 km/h transition region. The very same procedure is applied also for the 10 and 15 km/h transition regions.

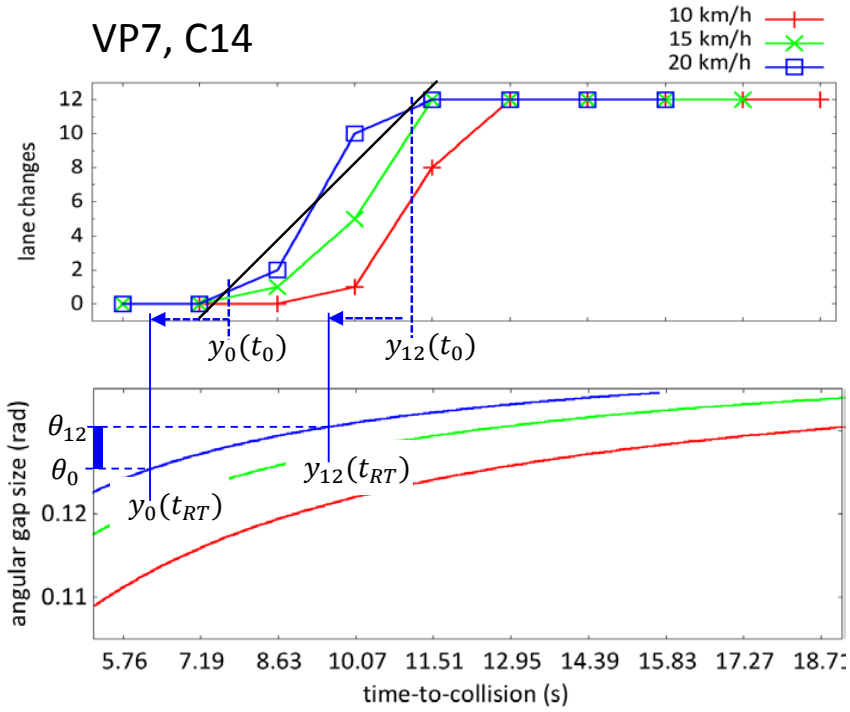

Figure 5.27: 1) black line: linear regression for the 20 km/h transition region; 2) $y_0(t_0), y_{12}(t_0)$ modified by the amount of 1.59 seconds, leading to $y_0(t_{rt}), y_{12}(t_{rt})$. 3) Look-up-table: value range for angular gap size Θ_{gap} is determined (Θ_0, Θ_{12}).

Calculation of $S = O/R$ After the value ranges for the three transition regions have been determined for each of the three input variables, the next step calculates the range R and overlap O (see illustration in Figure 5.28) which are necessary to determine the relation $S = O/R$. Considering the angular gap size Θ^{gap} first, an additional index is used to indicate that Θ_0, Θ_{12} are associated to a certain transition region, e.g. $\Theta_0^{10}, \Theta_{12}^{10}$ is used to denote the two values for the transition region for 10 km/h speed difference.

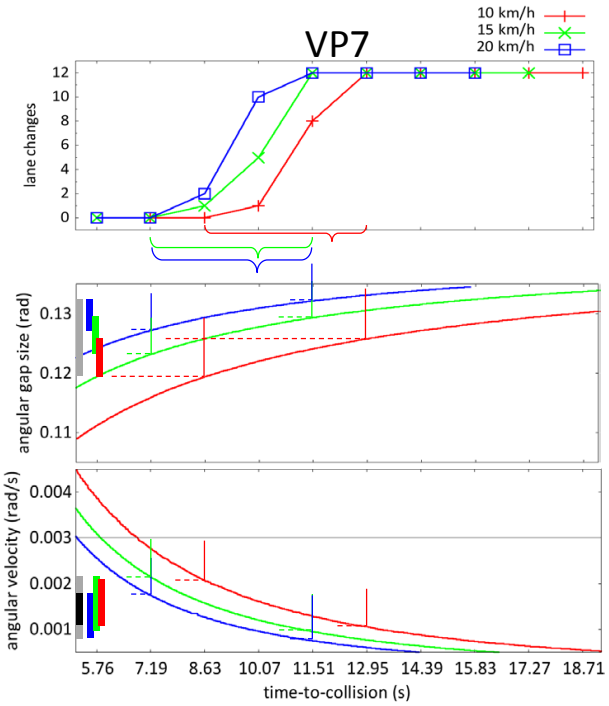

Figure 5.28: Total range R (gray bar) and overlap O (black bar) are illustrated. No overlap for Θ_{gap}.

The overlap O equals the smallest common value range which is covered by the three value ranges of the transition regions. The three values $\Theta_{12}^{10}, \Theta_{12}^{15}, \Theta_{12}^{20}$ are the upper boundaries of the three value ranges, and Θ_{min} equals the minimum upper boundary of the three value ranges. Vice versa, Θ_{max} denotes the maximum lower boundary and O is determined by their difference:

$$O = \Theta_{min} - \Theta_{max}$$

$$\Theta_{min} = Min(\Theta_{12}^{10}, \Theta_{12}^{15}, \Theta_{12}^{20})$$

$$\Theta_{max} = Max(\Theta_{0}^{10}, \Theta_{0}^{15}, \Theta_{0}^{20})$$

In the example in Figure 5.44, the calculation of O will result in a negative value, because Θ_{min} is smaller than Θ_{max}. The total value range R of all three transition regions is embraced by the maximum upper boundary and the minimum lower boundary:

$$R = Max(\Theta_{12}^{10}, \Theta_{12}^{15}, \Theta_{12}^{20}) - Min(\Theta_{0}^{10}, \Theta_{0}^{15}, \Theta_{0}^{20})$$

For the calculation of R and O for the angular velocity Δ^{gap}, a different formulation is necessary. While the vehicle approaches from behind during the course of an experiment trial, the angular gap size Θ^{gap} decreases. Instead, the angular velocity Δ^{gap} *increases*. For the angular velocity Δ^{gap}, the range R and overlap O are calculated according to:

$$O = \Delta_{min} - \Delta_{max}$$

$$\Delta_{min} = Min(\Delta_{0}^{10}, \Delta_{0}^{15}, \Delta_{0}^{20})$$

$$\Delta_{max} = Max(\Delta_{12}^{10}, \Delta_{12}^{15}, \Delta_{12}^{20})$$

$$R = Max(\Delta_{0}^{10}, \Delta_{0}^{15}, \Delta_{0}^{20}) - Min(\Delta_{12}^{10}, \Delta_{12}^{15}, \Delta_{12}^{20})$$

For the third input variable of the model (the time-to-collision, respectively τ), the range R and overlap O are calculated similar to the the the angular gap size Θ^{gap}, because Θ^{gap} and the time-to-collision behave the same way (both decrease during the approach), only the angular velocity Δ^{gap} increases.

$$O = ttc_{min} - ttc_{max}$$

$$ttc_{min} = Min(ttc_{12}^{10}, ttc_{12}^{15}, ttc_{12}^{20})$$

$$ttc_{max} = Max(ttc_{0}^{10}, ttc_{0}^{15}, ttc_{0}^{20})$$

After the values for R and O are derived for all three input variables, the value for $S = O/R$ can be calculated for each of the three input variables and each of the 42 experiment sessions. Before the results of these calculations are presented in detail in section 5.6.3.3, it is briefly explained, how the results are used to configure the decision making function $f(x)$.

Configuring $f(x)$ for the Simulation Two results of the previous calculations are used to configure the decision making function $f(x)$. The selection of the input variable $x \in X$ is made according to the results for S: for each of the 42 experiment sessions, the input variable $x \in X$ is selected which receives the highest value for $S = O/R$. For this input variable, the common value range of the three transition regions (overlap O) covers the largest portion of the total value range of all three transition regions.

It is proposed that O can be used as a predictor to simulate the observed behavior of the subject in the corresponding experiment session.

The values for min and max of the function $f(x)$, are set to the values of the upper and lower boundary of the overlap O. Dependent on the selected input variable, min and max are set to the following values:

- min=Θ_{max}, max=Θ_{min}
- min=ttc_{max}, max=ttc_{min}
- min=Δ_{min}, max=Δ_{max}, boundaries are switched, because the angular velocity Δ^{gap} increases, while the angular gap size Θ^{gap} and the time-to-collision both decrease during the approach.

At the beginning of this implementation section, the explanation how the ttc_{init} conditions for each transition region are selected, was deferred. The last paragraph of this implementation section explains the procedure that was used.

Selection of ttc_{init} Conditions This section will describe the rule-based procedure that was used to select the ttc_{init} conditions which belong to a transition region. It is admitted that this approach makes a number of assumptions, why certain ttc_{init} conditions should be included into the transition region, while others should be omitted. In the future work section 5.8.2 it is proposed to replace this rule-based approach by a segmented linear regression. This alternative approach provides a better solution to estimate the boundaries of the transition regions directly from the data, without making the assumptions that are formulated within the rule-based approach.

A basic set of selection rules was derived from the descriptive specification of the transition region: "region along the ttc_{init} conditions, where the number of lane change decisions continually rises from braking only (at a smaller ttc_{init} condition), to lane changes only (at a larger ttc_{init} condition)".

In the context of Experiment 2, "braking only" equals 0 lane changes and "lane changes only" equals 12 lane changes, but for a more general case the maximum number of lane changes can be set to n instead of 12.

Rule 1: The data of each experiment sessions is considered on its own.

Rule 2: For each session, the lane change data is separated into three sets, one for each speed difference.

Rule 3: For each of the three data sets, a transition region is specified and the following ttc_{init} conditions are included:

- **a**: Select all ttc_{init} conditions, where the number of lane changes is within the range of $[1, ..., (n-1)]$.
- **b**: Select the smallest ttc_{init} condition, where the number of lane changes is n.
- **c**: Select the largest ttc_{init} condition, where the number of lane changes is 0.

Rule 3a selects the ttc_{init} conditions, where the number of lane changes continuously increases from $[1, ..., (n-1)]$. Rule 3b and 3c select the boundaries of the transition region (n resp. 0 lane changes) and it is prevented, that all ttc_{init} conditions with n resp. 0 lane changes are selected.
The following Figure 5.29 gives two examples. The data of one session, the planar mirror session of VP14 is investigated (Requirement of Rule 1). The data is separated into the three data sets, one for each transition region (Rule 2).

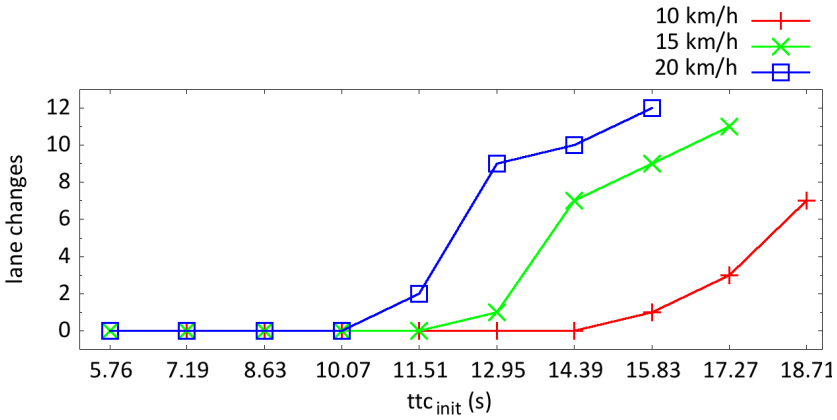

Figure 5.29: Planar mirror session of VP14;

The application of Rules 3a-3c for the example session in Figure 5.29 leads to the following result:

- Transition region 10 km/h (incomplete): Rule 3a selects ttc_{init} conditions in the range of $[15.83, ..., 18.71]$ seconds. Rule 3b does not apply, because n is not reached for any condition. Rule 3c selects $ttc_{init} = 14.39$ seconds. As a result, all ttc_{init} conditions in the range of $[14.39, ..., 18.71]$ seconds are selected.

- Transition region 15 km/h (incomplete): Rule 3a selects ttc_{init} conditions in the range of $[12.95, ..., 17.27]$ seconds. Rule 3b does not apply, because n is not reached for any condition. Rule 3c selects $ttc_{init} = 11.51$ seconds. As a result, all ttc_{init} conditions in the range of $[11.51, ..., 17.27]$ seconds are selected.

- Transition region 20km/h: Rule 3a selects ttc_{init} conditions in the range of $[11.51, ..., 14.39]$ seconds, Rule 3b selects $ttc_{init} = 15.83$ seconds, Rule 3c selects $ttc_{init} = 10.07$ seconds. As a result, all ttc_{init} conditions in the range of $[10.07, ..., 15.83]$ seconds are selected.

This first set of rules was applied to all 42 sessions of Experiment 2 and for a number of sessions, the selection of the transition regions led to a problem which is illustrated in the following Figure 5.30. If the basic selection method is applied for the 20 km/h speed difference, all ttc_{init} conditions in the range of
$[5.76, ..., 15.83]$ are selected. Considering the linear regression approach, which is applied to each transition region, the result would lead to a straight line similar to the illustration in Figure 5.30 (A).

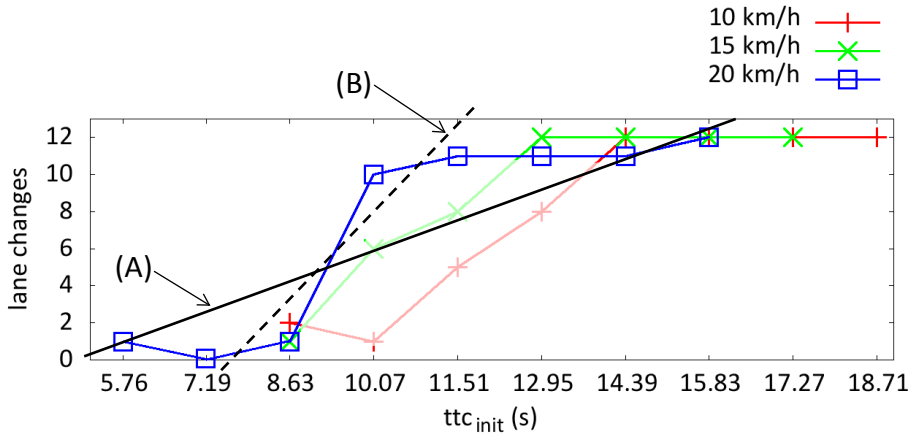

Figure 5.30: C14 session of VP2; please refer to the text below for the description.

As a consequence, the characteristic, steep gradient between the ttc_{init} conditions $[7.19, ..., 11.51]$ seconds would be lost. This is caused by two *sporadic* braking actions at the ttc_{init} conditions 12.95 and 14.39 seconds, and by one *sporadic* lane change at 5.76 seconds.

If the transition region would consist of the conditions $ttc_{init} = [7.19, ..., 11.51]$ the characteristic, steep gradient would be represented much better by the linear regression (depicted by stippled line (B)). On the other hand, the sporadic lane changes and braking actions can not be simulated then, because the corresponding ttc_{init} conditions would no longer fall into the range of the transition region, they are outside of the $y_0(t_0), y_{12}(t_0)$ value pair which is mapped onto the angular measures.

Table 5.15 below summarizes all experiment sessions and transition regions, where such sporadic actions were observed. In only three experiment sessions and four speed difference conditions a sporadic lane change action was found in the empirical data. In contrast, 19 transition regions were found, where sporadic braking actions were observed.

Mirror	Lane Changes	Braking
Planar	VP5-10, VP2-10	VP1-20, VP3-15, VP7-10
C20	-	VP1-15/20, VP2-15, VP3-10, VP4-10, VP5-10/20, VP10-15, VP12-20, VP13-10
C14	VP4-15, VP2-20	VP1-20, VP2-20, VP9-20, VP11-10/15, VP14-20

Table 5.15: Experiment sessions and speed differences where sporadic lane changes or sporadic braking actions occurred. The number after the "-" denotes the speed difference, e.g. VP5-10 denotes that a sporadic action was found for the transition region of the 10 km/h speed difference of VP5. Total number of transition regions in the experiment is 126.

Is there an explanation for this imbalance between the two categories? The sporadic braking actions occur for large ttc_{init} conditions, and a possible explanation is that subjects have probably waited too long (e.g. late reaction, lack of concentration or unsure about situation). In this case, the situation had progressed and they finally decided to brake. In contrast, the few lane changes happen at the small ttc_{init} conditions. The explanation for the braking actions can not

be transferred, because a longer reaction time increases the chances that a braking actions is done and not a lane change. Because these occurrences are very rare (4 transition regions, but each contains exactly one of these sporadic lane changes), no explanation can be given here.

It was decided to use alternative (B) which preserves the characteristic gradient, accepting that a very small number of lane changes (3) and a number of braking actions (19) can not be simulated.

The following modified selection algorithm was finally used to select the ttc_{init} conditions for all 126 transition regions of Experiment 2. Rules 1 and 2 remain unchanged, but Rules 3a-c were modified. Similar to the first algorithm, an example is given below:

Rule 1: The data of each experiment sessions is considered on its own.

Rule 2: For each session, the lane change data is separated into three sets, one for each speed difference.

Rule 3: For each of the three data sets, a transition region is specified and the following ttc_{init} conditions are included:

- **a**: Select all ttc_{init} conditions, where the number of lane changes is within the range of $[2, ..., (n-2)]$. These conditions are put into set X.
- **b**: Select all ttc_{init} conditions, where the number of lane changes is either n or $n-1$. These conditions are put into set Y.
  - **i**: The two conditions with the smallest ttc_{init} value remain in Y, the rest is removed from Y.
  - **ii**: If the smaller ttc_{init} condition in Y has n lane changes, remove the larger ttc_{init} condition from Y.
- **c**: Select all ttc_{init} conditions, where the number of lane changes is 0 or 1. These conditions are put into set Z.
  - **i**: The two conditions with the largest ttc_{init} value remain in Z, the rest is removed from Z.
  - **ii**: If the larger ttc_{init} condition in Z has 0 lane changes, remove the smaller ttc_{init} condition from Z.

  The conditions in X, Y, Z specify the transition region.

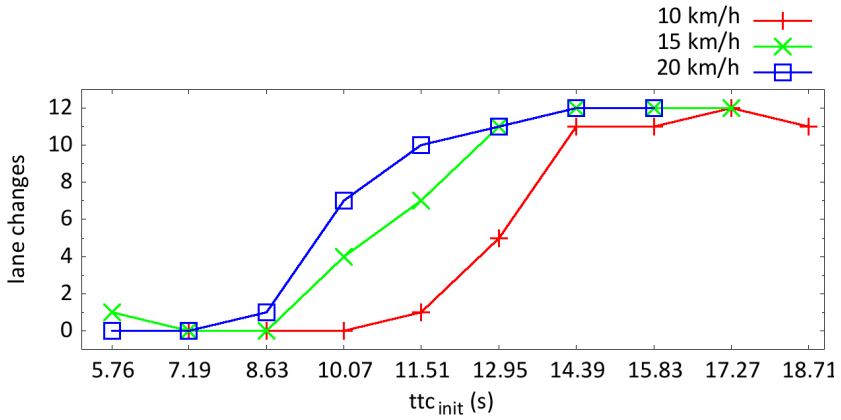

Figure 5.31: VP11, C14 mirror session; Selecting ttc_{init} conditions (Rule 3a-3c) for the transition region 10km/h:

The application of Rules 3a-3d for the example session in Figure 5.31 leads to the following result for the 10 km/h transition region:

- Rule 3a selects the condition $ttc_{init} = 12.95$ seconds and puts them into X.
- Rule 3b selects the ttc_{init} condition $[14.39, ..., 18.71]$ seconds and puts them into Y.
- Rule 3b i removes ttc_{init} conditions 17.27 and 18.71 seconds from Y and $Y = \{14.39, 15.83\}$.
- Rule 3b ii does not change Y.
- Rule 3c selects ttc_{init} conditions $[8.63, ..., 11.51]$ seconds and puts them into Z.
- Rule 3c i removes ttc_{init} condition 8.63 seconds from Z, $Z = \{10.07, 11.51\}$
- Rule 3c ii does not change Z.
- Rule 3d $Z = \{10.07, 11.51\}, X = \{12.95\}, Y = \{14.39, 15.83\}$, the transition region contains the ttc_{init} conditions in the range of $[10.07, ..., 15.83]$ specify the transition region for the 10 km/ speed difference.

5.6.3.3 Calculation of $S = O/R$: Results

Table 5.16 contains the calculated S values for Θ^{gap} and Δ^{gap} for each of the 42 sessions. The results with regard to the third input variable (the time-to-collision) are presented later in this section.

	$S = O/R$					
VP	Planar		C20		C14	
	$S_{\Theta^{gap}}$	$S_{\Delta^{gap}}$	$S_{\Theta^{gap}}$	$S_{\Delta^{gap}}$	$S_{\Theta^{gap}}$	$S_{\Delta^{gap}}$
6	0.6928	0.1797	0.6678	0.1193	0.6993	0.2407
1	0.6601	0.1870	0.6764	0.0574	0.5761	0.2509
4	0.6692	0.2023	0.6269	0.2448	0.7233	0.2376
9	0.6738	0.4233	0.6756	0.1865	0.4457	0.4140
7	0.2275	0.4944	-0.1160	0.6528	-0.0184	0.6955
10	0.1984	0.4471	0.0986	0.5433	0.2676	0.7601
14	0.2769	0.5501	0.2539	0.7218	0.1219	0.5568
2	0.1828	0.5977	0.3533	0.4364	0.4240	0.7046
8	0.1743	0.2487	0.7015	0.2392	0.0627	0.4399
13	0.2413	0.3098	0.3324	0.1220	0.2451	0.2635
11	0.3341	0.3059	0.3171	0.2125	0.2938	0.5276
3	0.3877	0.2159	0.3631	0.1644	0.2280	0.5753
12	0.7500	0.1326	0.2512	0.4515	-0.0061	0.2665
5	0.2091	0.6155	0.5388	0.1790	0.4205	0.3780

Table 5.16: Calculated values for S for angular gap size Θ^{gap} (denoted by $S_{\Theta^{gap}}$) and the angular velocity Δ^{gap} (denoted by $S_{\Delta^{gap}}$) for all 42 experiment sessions, Highest value for S for each session is highlighted; yellow color indicates that both values are separated by less then 0.1, or their absolute values is below 0.3;

The behavior of subjects VP6 and VP7 was used in example of the visual mapping (section 5.5.2, p .133) and the calculated values for S underpin the result with numbers: for VP6 the angular gap size Θ^{gap} has the highest value for S in all three experiment sessions. For VP7, Δ^{gap} has a higher value for S in all three experiment sessions.

There were three more subjects where Θ^{gap} received the highest value for S for all three experiment sessions (Subjects VP1/4/9). Similarly, three more subjects were also found, where Δ^{gap} received the highest value for S for all three experiment sessions (Subjects VP10/14/2). For the other six subjects, not all three experiment sessions received the highest value for S for the same measure[5].

It is not possible to discuss all the 42 sessions here, but there are a number of sessions marked in yellow, where the difference between values for S for Θ^{gap} and Δ^{gap} is rather small (< 0.1), or where the absolute value of S is rather small (< 0.3). In the following paragraphs, these sessions are investigated in more detail. The sessions of VP2 and VP12 are discussed at the end of this section, because for these two subjects the third input variable (the time-to-collision) needs to be considered.

[5]Within these three groups, there is no specific ordering in Table 5.16

VP9 C14 session, $S_{\Theta^{gap}} = 0.4457$, $S_{\Delta^{gap}} = 0.4140$.
Figure 5.32 shows, that the transition region for the 10 km/h speed difference is incomplete: the maximum number of lane changes is not reached. Considering the small number of lane changes even for the largest ttc_{init} conditions, it can be assumed, that a flat linear regression line is calculated for this transition region. An inspection of the $y_0(t_{rt}), y_{12}(t_{rt})$ value pairs showed this: the difference between these two values for the 15 and 20 km/h transition region is 5.76 seconds, respectively 5.58 seconds, but for the 10 km/h transition region the difference is 19.2 seconds.

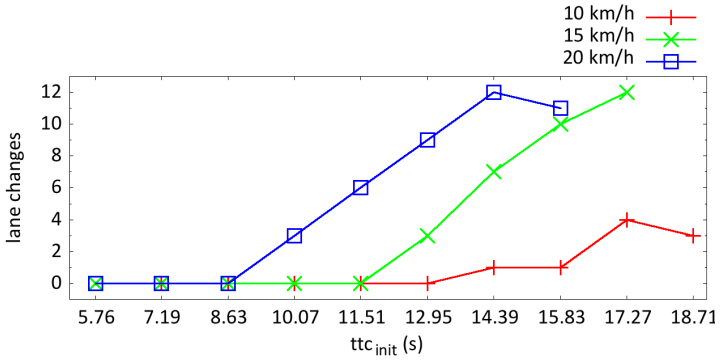

Figure 5.32: VP9, number of lane changes.

As a consequence, there is a large value range for the 10 km/h transition region, while the other two are comparably small. Considering the calculation of overlap O, each of the small regions can only cover a small part of the large region. Naturally, the overlap O between all the three mapped value ranges is reduced. This observation of one large / two small transition regions, or vice versa one small / two large transition regions was found multiple times. This affects the calculation of S of both angular measures (Θ^{gap} and Δ^{gap}) and the value for S is reduced for both of them.

VP8, VP13 Planar mirror session VP8 $S_{\Theta^{gap}} = 0.1743$, $S_{\Delta^{gap}} = 0.2487$, planar mirror session VP13 $S_{\Theta^{gap}} = 0.2413$, $S_{\Delta^{gap}} = 0.3098$.

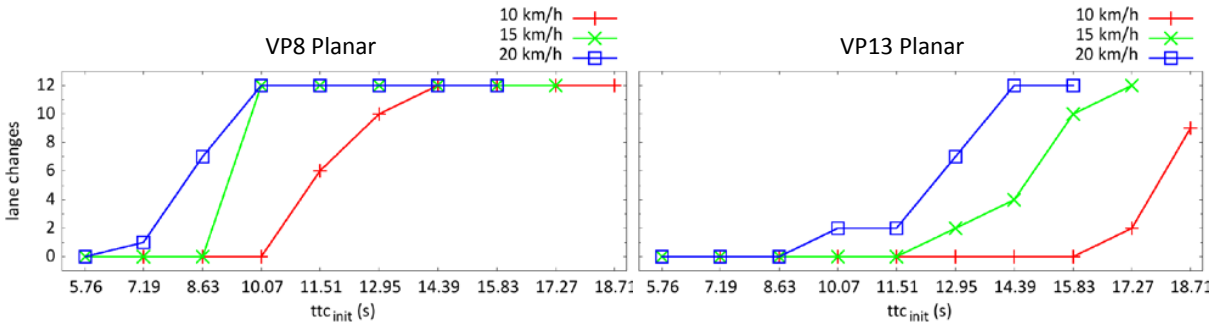

Figure 5.33: VP8 and VP13, number of lane changes.

Generally, the same effect that was previously described for VP9 is observed for the two experiment sessions of these two subjects. A difference is that one smaller and two larger transition regions are found here while the opposite was observed for VP9. For VP13: 20 km/h (small) vs. 10, 15 km/h (large). Similar to VP9, one transition region is incomplete. For VP8: 15 km/h (small) vs. 10, 20 km/h (large) and in contrast to VP9, all three transition regions are completely covered by the ttc_{init} conditions. Therefore the occurrence of the effect is not linked to the interpolation of the regression approach, it is already part of the recorded behavior data.

VP11 Planar mirror session: $S_{\Theta^{gap}} = 0.3341, S_{\Delta^{gap}} = 0.3059$ and C20 mirror session: $S_{\Theta^{gap}} = 0.3171, S_{\Delta^{gap}} = 0.2125$.
It was argued in section 5.5.2, that a larger difference in the number of lane changes with increasing speed difference (larger effect size of Hypothesis 2.2) leads to a better value for S for the angular gap size Θ^{gap}, while a smaller effect size of Hypothesis 2.2 leads to a higher value for S for the angular velocity Δ^{gap}.

The planar mirror session in Figure 5.34 shows, that the difference in the number of lane changes is small between the 15 and 20 km/h speed difference. Such a smaller effect size of Hypothesis 2.2 fits better with the angular velocity Δ^{gap}. Instead, the much larger difference between 10 and 15 km/h fits better with the angular gap size Θ^{gap}. It is assumed, that these two opposing effects lead to a similar value for S and also their absolute values are reduced because of that.

This changes for the C20 experiment session, where the difference with regard to the number of lane changes between the 15 and 20 km/h speed differences increases slightly. Overall, the effect of Hypothesis 2.2 improves, which is reflected in the two values for S: although both remain on a comparably small level, the difference between the two values increases compared to the planar mirror session.

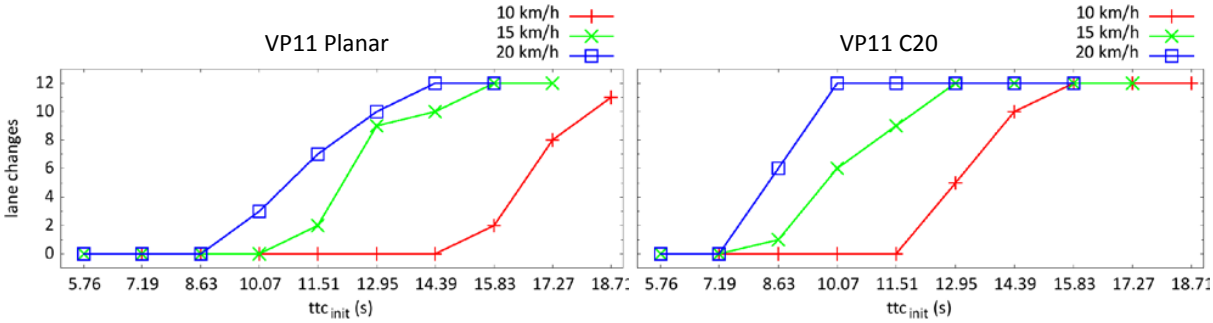

Figure 5.34: VP11, number of lane changes.

VP5 C14 mirror session $S_{\Theta^{gap}} = 0.4205, S_{\Delta^{gap}} = 0.3780$.
Similar to the planar mirror session of VP11 before, the difference in the number of lane changes between the 10 km/h speed difference and the two speed differences 15 and 20 km/h, leads to a larger effect size of Hypothesis 2.2, therefore the angular gap size Θ^{gap} receives a higher value for S. Instead, the 15 and 20 km/h speed differences are very similar and this reduces the overall value of both S values.

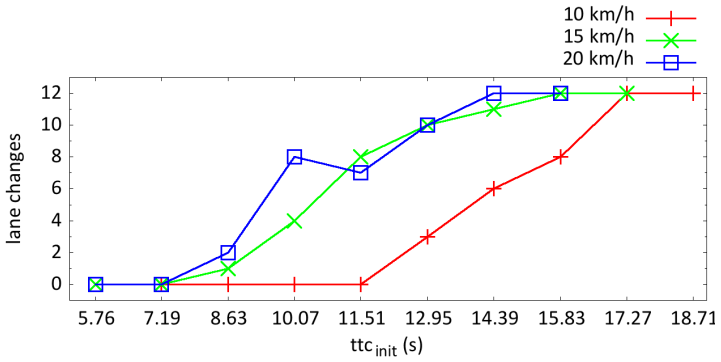

Figure 5.35: VP5, number of lane changes.

VP2 In the individual behavior analysis section (5.4.2) it was mentioned that the behavior of VP2 indicates, that the time-to-collision (ttc) should be considered as a third input variable for the decision making function. Table 5.17 contains the results for S for all three input variables for VP2.

VP	Planar			C20			C14		
	$S_{\Theta^{gap}}$	$S_{\Delta^{gap}}$	S_{ttc}	$S_{\Theta^{gap}}$	$S_{\Delta^{gap}}$	S_{ttc}	$S_{\Theta^{gap}}$	$S_{\Delta^{gap}}$	S_{ttc}
2	0.1828	0.5977	0.7120	0.3533	0.4364	0.6002	0.4240	0.7046	0.4493

Table 5.17: Calculated values for S for VP2 and all three input variables.

Figure 5.36 shows the number of lane changes for VP2 and all three experiment sessions. Considering the planar mirror session first, the number of lane changes is almost identical for all three speed differences. This observation is reflected in the values for S in Table 5.17, where the time-to-collision received the highest value for S for the planar mirror session (0.7120). Because the three speed differences are almost identical with regard to the number of lane changes, the effect size of Hypothesis 2.2 is reduced to a minimum (Hypothesis 2.2 postulated an increased number of lane changes with increasing speed difference). It was also proposed in section 5.5.2 that the angular velocity Δ^{gap} predicts a small effect size for Hypothesis 2.2, while the angular gap size Θ^{gap} predicts a larger effect size of Hypothesis 2.2. This is also supported by the values of S, because the angular velocity Δ^{gap} receives the second best value for S, while the angular gap size Θ^{gap} receives the smallest value for S.

For the C20 mirror session, the situation changes and their is a bigger difference in the number of lane changes between the three speed differences. But the difference is not large enough and the value for S is still smaller for the angular velocity Δ^{gap} compared to the time-to-collision.

In contrast, for the C14 session, a small effect size of Hypothesis 2.2 is observed for the ttc_{init} conditions $[10.07, ..., 12.95]$ and this is now reflected by the values for S and the highest value is calculated for the angular velocity Δ^{gap}.

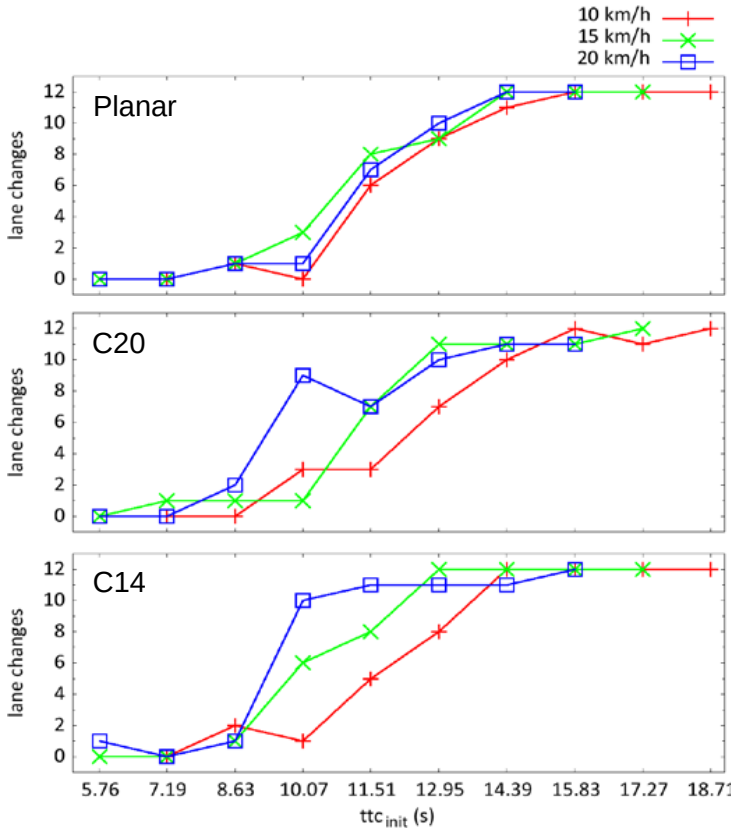

Figure 5.36: VP2, number of lane changes for all three sessions.

The calculation of S for the time-to-collision was done for all 42 experiment sessions. The results can be seen in Table 5.18. Besides the two sessions for VP2 (planar, C20), the time-to-collision received the highest value S value in only one additional session (VP12, C14 session). In 19 sessions, a negative S was even observed, which indicates that no overlap O exists.

The results in Table 5.18 support the assumption of the individual behavior analysis, and the time-to-collision received the highest value for S in three sessions. Nevertheless, these are only 3 out of 42 experiment sessions, and it can be concluded, that the time-to-collision did not play a central role in this experiment.

	$S = O/R$					
VP	Planar		C20		C14	
	$S_{\Delta^{gap}}$	S_{ttc}	$S_{\Delta^{gap}}$	S_{ttc}	$S_{\Delta^{gap}}$	S_{ttc}
6	0.1797	-0.1083	0.1193	-0.1442	0.2407	0.0055
1	0.1870	-0.1158	0.0574	-0.2702	0.2509	-0.0152
4	0.2023	-0.0859	0.2448	-0.0704	0.2376	-0.0528
9	0.4233	0.0418	0.1865	-0.1307	0.4140	0.0611
7	0.4944	0.2098	0.6528	0.1939	0.6955	0.3967
10	0.4471	-0.0054	0.5433	0.3368	0.7601	0.2371
14	0.5501	0.0436	0.7218	0.2881	0.5568	0.3287
2	0.5977	**0.7120**	0.4364	**0.6002**	0.7046	0.4493
8	0.2487	0.0444	0.2392	0.0943	0.4399	0.0627
13	0.3098	-0.0805	0.1220	-0.1861	0.2635	-0.1817
11	0.3059	-0.0440	0.2125	-0.1468	0.5276	0.3655
3	0.2159	-0.1896	0.1644	-0.0991	0.5753	0.0736
12	0.1326	-0.1417	0.4515	0.3246	0.2665	**0.2925**
5	0.6155	0.0479	0.1790	-0.1595	0.3780	0.1617

Table 5.18: Values for S for angular velocity Δ^{gap} and time-to-collision (ttc). Negative values: No overlap O. Bold values: ttc received the highest value for S.

VP12 C14 mirror session $S_{\Theta^{gap}} = -0.0061, S_{\Delta^{gap}} = 0.2665, S_{ttc} = 0.2925$.
Although values for S for the two angular measures allow a decision for the angular velocity Δ^{gap}, the absolute values for S are on a rather low level here. Again, the effect of one smaller (10 km/h) and two larger transition regions (15, 20 km/h) is observed here.

With regard to the C14 session of VP12 (Figure 5.37 below), the absolute value of S for the angular velocity Δ^{gap} and angular gap size Θ^{gap} are rather small. It was explained earlier, that one smaller transition region (here 10 km/h) and two larger transition regions (here 15, 20 km/h) cause such overall reduced values for S. The time-to-collision receives a higher value for S here, because the transition regions for 15 and 20 km/h span across the same ttc_{init} values $[5.76, ..., 10.07]$.

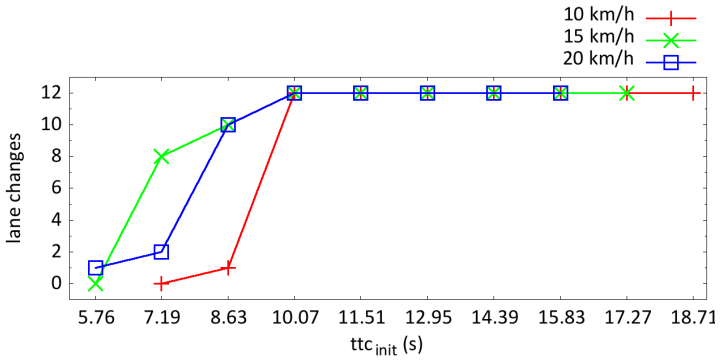

Figure 5.37: C14 mirror sessions for VP12.

Conclusion For 21 of 42 sessions, the angular gap size Θ^{gap} received higher values for S compared to the angular velocity Δ^{gap}. For 18 sessions, the angular velocity Δ^{gap} received the highest values for S, while the time-to-collision was favored in the remaining 3 sessions.

The proposal that all three variables should be considered is also in line with previous findings by [Regan1993, Regan1995, Hoffmann1994]. It was reported that the visual pathway has the capabilities to respond to each of the three measures and it was furthermore proposed that distinct processing channels exist in the visual pathway.

Section 5.5.2 presented the basic ideas for the development of the gap acceptance model, and one observation of the visual mapping approach was that the angular gap size Θ^{gap} receives higher values for S if the effect size of Hypothesis 2.2 is large and in case of a small effect size, the angular velocity Δ^{gap} receives a higher value for S (see Figure 5.19, p. 136). After the values for S are calculated for all sessions and each of the three input variables, it can also be concluded that the time-to-collision is selected, whenever there is no effect size of Hypothesis 2.2 (see VP2 above).

The "order" of the three variables with regard to the effect size of Hypothesis 2.2 is also supported by the following observation: in those sessions, where Δ^{gap} received smaller values for S compared to the angular gap size Θ^{gap} (these are the sessions, where Δ^{gap} is not marked in Table 5.18), the time-to-collision received even smaller values for S. In contrast, for the three sessions where the time-to-collision received the highest value for S, the angular velocity Δ^{gap} received the second highest value S and the angular gap size Θ^{gap} received the lowest value for S.

5.7 Simulation of Experiment 2

Before the simulation of each of the 42 experiment sessions can be done, the gap acceptance model needs to be configured. With regard to the decision making function $f(x)$ (p. 155, "Configuring $f(x)$ for the Simulation"), the input variable $x \in X$ is selected which receives the highest value for S. The results were presented in the previous section (Tables 5.16 and 5.18). The values for min and max of the function $f(x)$ are set to the values of the upper and lower boundary of the overlap O. Dependent on the selected input variable, min and max are set to the following values:

- min=Θ_{max}, max=Θ_{min}
- min=ttc_{max}, max=ttc_{min}
- min=Δ_{min}, max=Δ_{max}, boundaries are switched (compare indices), because the angular velocity Δ^{gap} increases, while the angular gap size Θ^{gap} and the time-to-collision both decrease during the approach.

These values are found in Table 7.1 in the Annex, p. 219. Additionally to the configuration of $f(x)$, the timing of the state-machine of the gap acceptance model has to be configured, because four of five states consume a certain amount of the time (section 5.6.1 on the time consumption of the states):

- *Gazeshift*: 325ms (constant)
- *Decide*: 100 ms (constant)
- *Action*: average value of the mean braking and steering times (Table 5.11, p. 140) measured for the subject in the experiment session.
- *Percept*: difference between the mean reaction of the subject (Table 5.10, p. 140) in the experiment session and the time consumption of the previous three states.

After these parameters are configured for a session, the simulation is started. Because the model is integrated as a plug-in module in the driving simulator software SILAB, there is no additional effort needed to start or synchronize a separate executable model program. It is only necessary to start the simulator software, load the workspace for Experiment 2 and start the simulation. Once this is done, the scenario script (see Figure 5.21, p. 142) processes all 312 trials of one experiment session.

From the interaction point of view, the driver model behaves in the same way as the subjects did in the experiment (details, section 5.6.1, p. 141): the model perceives the current value of the selected input variable via its visual perception component in real-time, and gives its action response after the mean reaction time of the subject in that session was consumed by the model. This action response is propagated to the simulator software. No changes are required with regard to the control flow of the experiment. Another advantage of this tight integration is that the data recording module from the experiment can be reused and also all data analysis scripts.

But there is one major drawback of the simulation: the driving simulator software does not allow to use an accelerated simulation time and the platform is bound to real-time. Because the time-consumption of the model for each trial equals the mean reaction time of the subject, the model needs a very similar amount of time for the simulation of a complete session. Some modification were possible to the overall flow of the experiment to cut down the simulation time: the training phase and two small pauses could be removed. Additionally, there was a small pause between each of the trials which could be eliminated. Nevertheless, the average simulation time for each session was approximately 30 minutes. In case of subject VP2 (the subject with the extraordinary long reaction time per trial) the simulation needed 40-45 minutes per session.

Another important question for the simulation is, whether a single repetition of the experiment (each of the 42 sessions simulated once) is already sufficient to evaluate the model? The answer is no, because a random number is drawn during decision making, and a certain amount of variability is part of the behavior of the model. Because their was no experience with the developed model, it was also not known, how much variation will actually be seen. Therefore an incremental approach was chosen, and the experiment was repeated three times to receive an initial database. A quick analysis was done and each of the three simulated experiment repetitions was assessed against the empirical data of Experiment 2 with the help of a scatter plot and a linear regression. The explained variation (R^2 values of the linear regression) was high (see next section), and also the difference between the R^2 values between the three comparisons was

rather small. A second set with three additional simulated experiment repetitions was generated to extend the database.

The next subsection (5.7.1) describes the results of the six experiment repetitions on the level of the accumulated data of all 42 sessions (the results of the empirical study were analyzed at the same level in experiment chapter 4.2). The question of interest in this section is, how well the results of the experiment are reproduced by the simulation in each of the six simulated experiment repetitions.

Afterwards, the second subsection 5.7.2 takes a more detailed look at the simulation results of the individual sessions (this approach will be called session-based analysis in the following). The question of interest here is, how well the behavior of the 14 individual subjects is reproduced by the individually parameterized gap acceptance model. For this session-based analysis, average values can only be calculated for the six repetitions of each session. This results in much smaller data sets compared to the first analysis which uses all 42 sessions and a higher variation in the simulated number of lane changes is expected in the session-based analysis.

A summary of the simulation results as well as a brief discussion of open issues for future work is given in the last subsection 5.8.

5.7.1 Experiment 2 Hypotheses

As mentioned in the introduction, the simulation was done in two iterations, each of them consisted of three experiment repetitions and a quick assessment of the results was done in between the iterations. Nevertheless, this section will not make a difference between the six repetitions and summarizes the results of all of them. The six simulated repetitions of the experiment will be called *Model Run 1-6*, in the following.

Similar to the experiment chapter, the analysis starts with a visual inspection of the data. The following figures shows a comparison of the number of lane changes of Experiment 2 (graphics were already shown in the experiment chapter), against the number of lane changes of a model run. The comparisons for Model Run 1 and 4 are used as examples for the discussion here, similar figures for the other four model runs can be found in the Annex at p. 217.

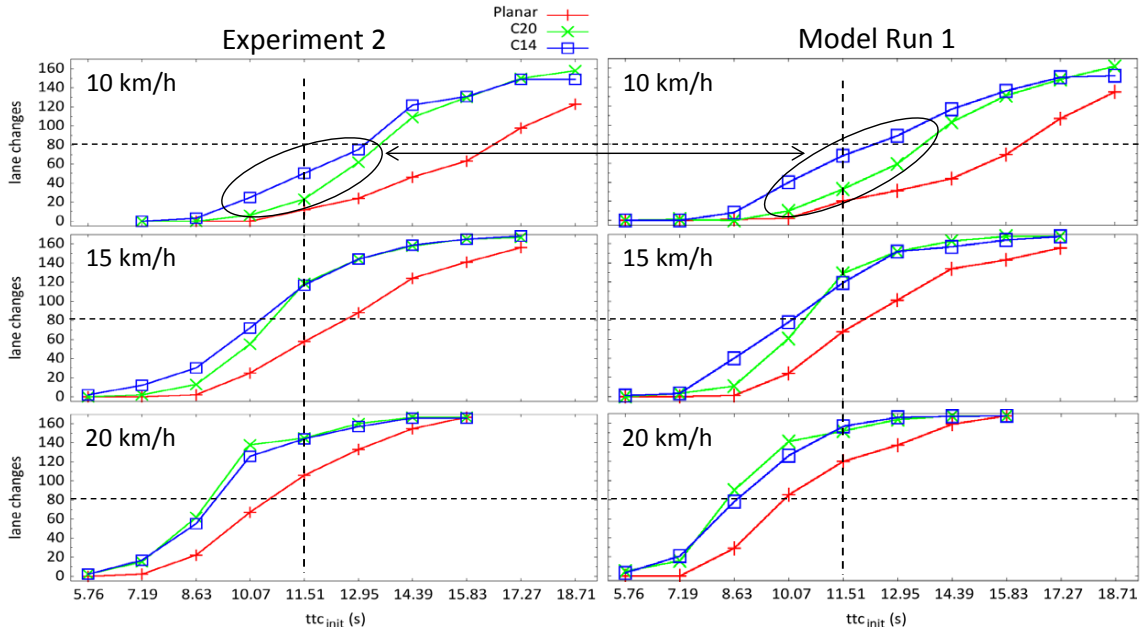

Figure 5.38: Number of lane changes of Experiment 2 (left) and Model Run 1. Differences exist, but a closer look is necessary. The marked difference at 10 km/h is one of the more obvious ones, cmp. also with Figure 5.39 below.

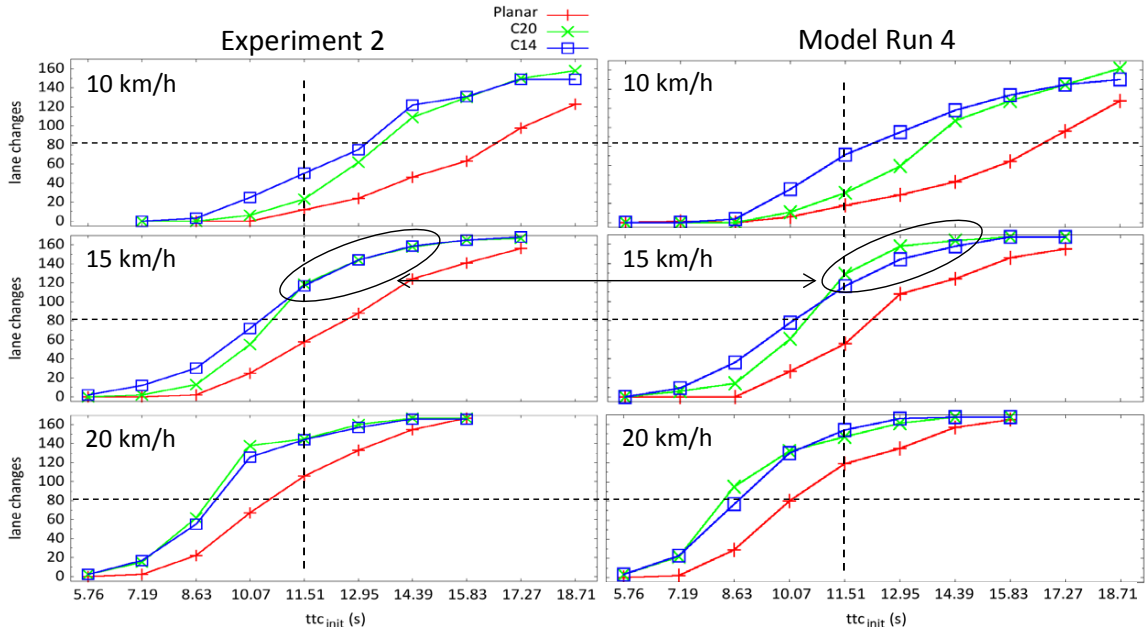

Figure 5.39: Number of lane changes of Experiment 2 (left) and Model Run 4. Marked difference at 15 km/h: overestimation of the number of lane changes for the C20 in relation to the C14 which is not observed in the experiment. Compare also with Figure 5.38 above, where this local overestimation is not observed.

The visual comparison of simulation and experiment shows that the results of Experiment 2 with regard to Hypothesis 2.2 are well represented in both simulation runs:

1) The planar mirror has the fewest number of lane changes, and the significant difference between planar and both curved mirrors is well preserved in both model runs.

2) In the experiment, the number of lane changes was not significantly different between the two curved mirrors C20 and C14. This is also observed for the model runs, although in Model Run 1 the marked area shows a bigger separation between these mirrors compared to the experiment data.

3) Despite the non significant result for the curved mirrors, it was nevertheless observed that there is difference between these mirrors for the 10 km/h speed difference ($ttc_{init} = [10.07 - 14.39]$ seconds). With increasing speed difference, this difference is reduced, and at 20 km/h the C14 has even fewer lane changes, e.g. for $ttc_{init} = 8.63, 10.07]$. The model runs also reproduce this effect.

4) The effect reported in 3) can also be observed between the planar mirror and the two curved mirrors and this is also preserved in the model runs.

This rough overview on the two of six simulation runs looks promising, because the visual inspection does not immediately show obvious errors in the results. But there are differences between simulation and experiment and there is variation between the six model runs, two examples are marked in the figures.

A difference which is not visible at the first glance is that the simulated model runs overestimate the total number of lane changes. This can be seen when the stippled lines in both figures are used to compare the experiment data with the two model runs. This observation is supported by the numeric data in the following tables 5.19 and 5.20

	Total Number of Lane Changes							
Mirror	Experiment 2	Run 1	Run 2	Run 3	Run 4	Run 5	Run 6	Mean 1-6
Planar	1612	1734	1731	1724	1688	1709	1722	1718
C20	2317	2406	2407	2421	2407	2419	2413	2412
C14	2406	2528	2568	2523	2518	2536	2533	2534

Table 5.19: Model *Runs 1-6* produce more lane changes compared to the experiment data of the subjects; Column *Mean 1-6*: average number of lane changes for *Run 1-6*.

	Overestimation of the Number of Lane Changes (%)						
Mirror	Run 1	Run 2	Run 3	Run 4	Run 5	Run 6	Mean 1-6
Planar	**+7.57**	+7.38	+6.95	**+4.71**	+6.02	+6.82	+6.57
C20	**+3.75**	+3.79	**+4.40**	+3.79	+4.31	+4.05	+4.10
C14	+4.90	**+6.56**	+4.69	**+4.48**	+5.23	+5.10	+5.28

Table 5.20: Simulated experiment runs lead to an overestimation of the number of lane changes compared to the experiment. Minimum and maximum amount of overestimation across the six runs are marked for each mirror type.

Table 5.19 shows for each mirror type and simulated experiment run, that the total number of lane changes is higher compared to the Experiment 2 results. The amount of overestimation in

percent is given in Table 5.20, and the average across all six simulated experiment runs is given in the column *Mean 1-6*. Although there is a considerable amount of overestimation on average (6.57%, 4.1% and 5.28% for the three mirrors), the relative difference between the mirrors is only slightly changed, because the overestimation is found consistently for each mirror. This is the reason, why the effect of Hypothesis 2.1 is well preserved.

Considering the total amount of overestimation, it was assumed that a relation between amount of overestimation and speed difference Δv_{CA} might be found: the main parameter of the model (overlap O) is derived from the specification of three transition regions (one for each speed difference). It is possible that the mapping of these regions could lead to a systematic error which fosters an overestimation at a certain speed difference.

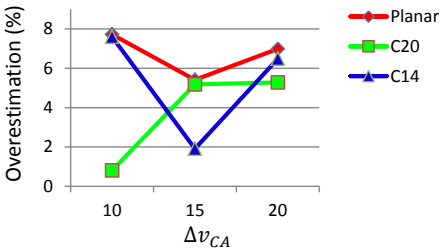

Overestimation (%)			
Δv_{CA}	10 km/h	15 km/h	20 km/h
Planar	7.72	5.42	6.99
C20	0.81	5.18	5.28
C14	7.60	1.91	6.49

Figure 5.40: Average overestimation per speed difference, averaged over model run 1-6.

Figure 5.40 shows the average amount of overestimation across all six simulated experiment runs, separated according to the mirror type and speed difference Δv_{CA}. For the planar mirror and the C14, the overestimation is the smallest for the 15 km/h speed difference, but the reduction from 10 km/h to 15 km/h is much stronger for the C14. Instead for the C20, the overestimation is very small for the 10 km/h speed difference, while it is almost equally high for 15 and 20 km/h. A common pattern across all three mirrors is not observed and it is concluded that a systematic relation between overestimation and the speed difference can not be found. This discussion about the overestimation will be resumed in the next section, when the more detailed view on the 42 individual sessions is presented.

The example figures from the beginning of the section (Figure 5.38, 5.39) visualized the number of lane changes for all 26 experiment conditions for the two model runs 1 and 4. To calculate how well the simulated number of lane changes fits with the empirical data of the experiment, a direct comparison can be made across all 26 experiment conditions (see Table 5.1, p. 107). For this purpose, three scatter plots were drawn which compare the number of lane changes between the empirical data and the six model runs. One plot was drawn for each mirror type and for each of them, a linear regression was calculated.

Figure 5.41 shows the three scatter plots and the linear regressions for the two model runs 1 and 4. Table 5.21 summarizes the R^2 values of all 18 linear regressions for all six model runs.

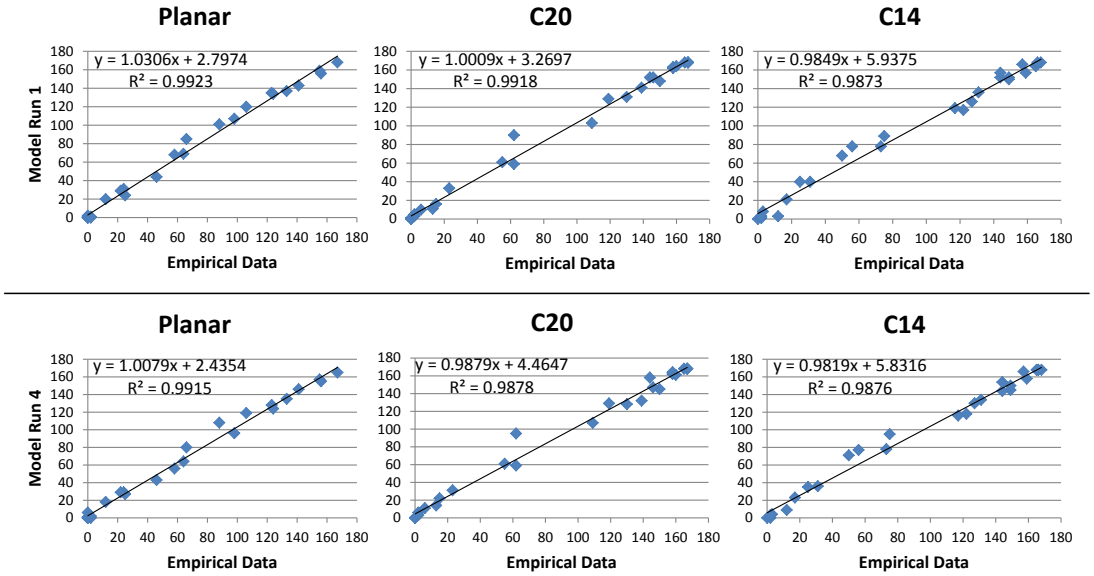

Figure 5.41: Comparison of the number of lane changes for all 26 experiment conditions (Table 5.1, p. 107); Scatterplots were drawn and a linear regression was calculated. Top: simulated experiment run 1; Bottom: simulated experiment run 2.

	R^2 values derived from scatter plots						
Mirror	Run 1	Run 2	Run 3	Run 4	Run 5	Run 6	Diff 1-6
Planar	**0.9923**	**0.9869**	0.9912	0.9915	0.9886	0.9893	0.0054
C20	**0.9918**	0.9888	**0.9854**	0.9878	0.9879	0.9863	0.0064
C14	0.9873	0.9887	**0.9805**	0.9876	**0.9928**	0.9856	0.0123

Table 5.21: The largest and smallest R^2 values for each mirror are marked bold. Column *Diff 1-6* gives the difference between the minimum and maximum R^2 values of the six runs.

The high R^2 values support the results of the visual comparison: the six model runs reproduce the characteristic properties of the empirical data and the explained variation (indicated by R^2) is very high. Furthermore, the variability of the R^2 values between the six model runs is < 0.01 for the planar and the C20 mirrors. This value is doubled for the C14, but still < 0.02. This observation indicates that the number of lane changes of Experiment 2 are reproduced in all six simulated experiment repetitions with a small margin of error. But it has to be considered that the overestimation is not well represented in this R^2 value, because it is distributed across multiple of the 26 experimental conditions. This can be seen in Figure 5.42, which shows the scatter plots for each of the six model runs, but here the data of all three mirrors is considered at once.

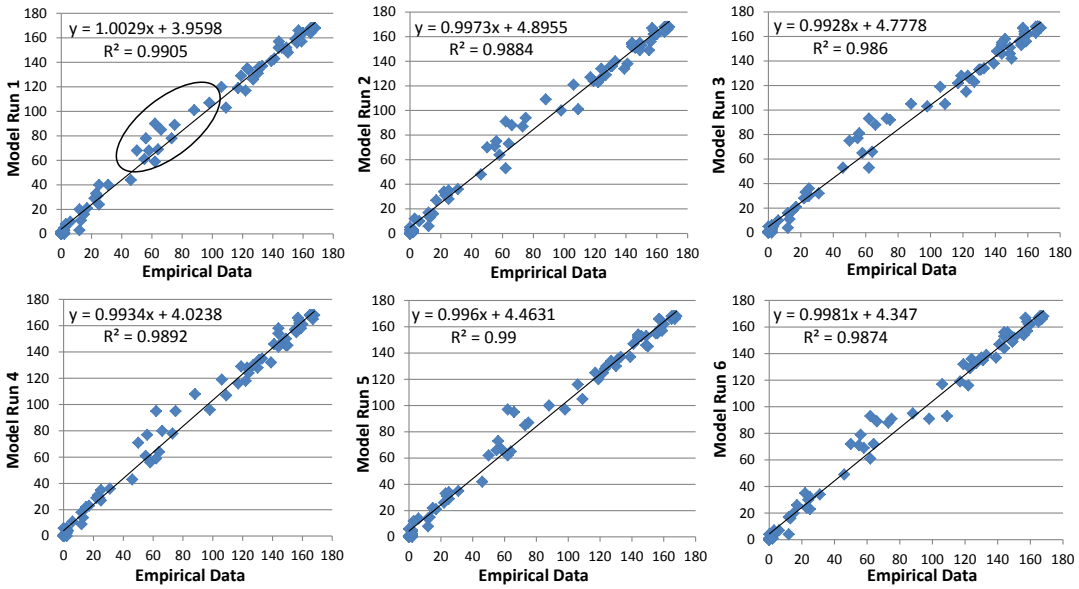

Figure 5.42: Scatter plots for the full data of all six model runs. The marked region in model run 1 shows where the strongest overestimation is observed (compare over all six model runs).

To complete this section, the last comparison of the experiment data and the model runs on this level (accumulated data across all 42 sessions) revisits a table of the Experiment 2 chapter. The data in the columns 2-4 of Table 5.22 was previously used in the experiment chapter to analyze the hypotheses (see p. 93).

	Number of Lane Changes					
	Experiment 2			Model Run 1-6		
Δv_{CA} (km/h)	+10	+15	+20	+10	+15	+20
planar	146	438	651	167.5	471.3	696.5
C20	330	656	856	334.7	697.5	899.3
C14	406	701	833	458.3	719.2	887.0

Table 5.22: Total number of lane changes. Columns 2-4 taken from Experiment 2 chapter, Table 4.5. Columns 5-7 shows the average number of lane changes across the six model runs. This data set was used for the hypothesis testing in the experiment chapter.

It has to be considered that this table contains the data of the experiment conditions $ttc_{init} = [7.19 - 15.83]$ seconds, because only those were available for all three speed differences and allowed a comparison with regard to Hypothesis 2.2. For this purpose, the same data range was also extracted from each of the six model runs and the average values are presented in the columns 5-7. Similar to the experiment data, the average number of lane changes for the six simulated experiment runs increases with increasing speed difference for each mirror type and the scatter plots shows that the average of the six model runs very well fits the data ($R^2 = 0.9967$). Similar high R^2 values were calculated for each of the six individual runs (Table 5.23).

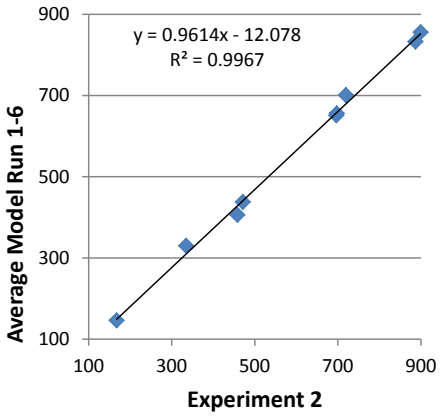

Figure 5.43: Number of lane changes: scatter plot for the data of Table 5.22.

R^2 values derived from scatter plots					
Run 1	Run 2	Run 3	Run 4	Run 5	Run 6
0.9963	0.9957	0.9965	0.996	0.9983	0.9944

Table 5.23: R^2 values for the comparisons of the six model runs against the experiment data presented in Table 5.22.

Do these results already allow an assessment of the quality of the implemented decision making process of the model? Only in a limited way, because the number of lane changes was investigated on the basis of the accumulation of all 42 sessions of each of the six simulated experiment runs. It is possible that the simulation of specific subject sessions contains stronger overestimations or underestimations of the number of lane changes, and these different effects might not be visible in the accumulated data. Even if they do not harm the results at this accumulated data level, it is necessary to do a more detailed analysis.

The next section will investigate the simulation of the 42 experiment sessions, and assess the quality of the decision making process with regard to its ability to reproduce the individual behavior data. An important part of this investigation is to explore potential reasons for the observed overestimation of the number of lane changes.

5.7.2 Simulation Results per Subject and Session

The question of interest for this section is how well each of the 42 simulated experiment sessions of a model run reproduces the number of lane changes of its corresponding subject session of Experiment 2. It was mentioned before, that the whole experiment was simulated six times, therefore each of the 42 experiment sessions of the subjects can be compared against a set of six corresponding simulated sessions of the model (resulting in 42*6 = 252 comparisons). Because the model uses a probabilistic decision making process, the number of lane changes for a simulated session is not deterministic. Some of these variations have been seen in the accumulated data in the previous section (the variations between the six runs), but it is expected that stronger variations will be observed for the individual sessions.

Before the comparison is done, it needs to be decided whether the lane change data of all 26 experiment conditions[6] should be compared, or a specific subset is better suited for this analysis. Figure 5.44 can be consulted to investigate which data is best suited for this analysis.

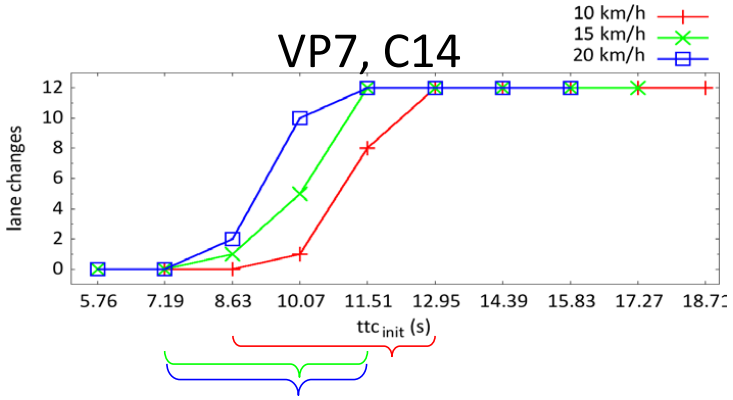

Figure 5.44: C14 session of VP7; Transition regions for each speed difference are marked by a curly bracket; Section 5.6.3.2 explains, how the ttc_{init} conditions are selected for each region.

It was argued that the existence of the three transition regions in each experiment session can be interpreted as the noise along all neural pathways which are involved in the perception and decision making of the subject. Therefore, a probabilistic decision making process was implemented (for full argumentation, see section 5.6.3.1, p.148). For those ttc_{init} conditions which do not belong to the transition regions, the decision making of the subjects can be considered *deterministic*. Deterministic means, subjects always respond with a braking or steering action in these ttc_{init} conditions (a small number of *sporadic* braking and lane change actions was not considered in the model, Table 5.15, p. 158).

The evaluation of the *deterministic part* of the model is not of much interest here, and its inclusion into the comparison has a severe consequence: this part artificially increases the fit between experiment session and simulated session, because the simulation and the experimental session always produce a very good match with regard to the number of lane changes (apart from the sporadic braking and lane change actions). Certainly, this reduces the expressiveness of the comparison with regard to the variation of the model that is caused by the non-deterministic part. It is expected, that the high R^2 values from the analysis in the previous section carry this artifact.

Result Overview The lane change data for the three transition regions was extracted from each of the 42 experiment sessions, and the same data range was extracted from each of the corresponding six simulated experiment sessions. Scatter plots were drawn for each comparison, and a linear regression was calculated. Overall 252 comparisons were done, which are separated according to the three mirror types in the following. This leads to 84 comparisons per mirror (14 subject sessions, each compared against 6 simulated sessions). The three tables below summarize the results of all these 252 comparisons.

[6] see Table 5.1 p. 107

Planar Mirror Sessions								
	R^2							
VP	Run 1	Run 2	Run 3	Run 4	Run 5	Run 6	Mean 1-6	Diff 1-6
1	0.838	0.821	0.908	0.816	0.801	0.846	0.838	0.106
2	0.889	0.874	0.853	0.880	0.898	0.819	0.869	0.079
3	0.674	0.705	0.828	0.715	0.668	0.761	**0.725**	**0.160**
4	0.910	0.882	0.893	0.917	0.897	0.899	0.899	**0.034**
5	0.750	0.704	0.862	0.762	0.865	0.823	0.794	**0.160**
6	0.875	0.924	0.865	0.804	0.898	0.917	0.880	0.119
7	0.875	0.893	0.922	0.901	0.871	0.924	0.898	0.053
8	0.892	0.955	0.955	0.883	0.944	0.931	**0.927**	0.072
9	0.962	0.916	0.922	0.814	0.912	0.889	0.903	0.148
10	0.906	0.925	0.895	0.932	0.901	0.942	0.917	0.047
11	0.857	0.789	0.789	0.792	0.806	0.716	0.791	0.140
12	0.853	0.837	0.860	0.888	0.811	0.851	0.850	0.077
13	0.841	0.924	0.894	0.824	0.900	0.900	0.880	0.100
14	0.927	0.840	0.815	0.815	0.860	0.852	0.851	0.112
Mean	0.860	0.856	**0.876**	**0.838**	0.859	0.862	0.859	0.101

Table 5.24: Six simulated experiment sessions (Run 1-6) compared against their corresponding subject session (subject VP1-14); Scatter plots were drawn and a linear regression through the plot was used to calculate R^2; Column Mean 1-6: mean value of the six R^2 values of Run 1-6, minimum VP3 (0.725), maximum VP8 (0.927); Column *Diff 1-6*: difference between maximum and minimum R^2 value observed for Run 1-6.

C20 Mirror Sessions								
	R^2							
VP	Run 1	Run 2	Run 3	Run 4	Run 5	Run 6	Mean 1-6	Diff 1-6
1	0.873	0.816	0.864	0.927	0.714	0.874	0.844	**0.212**
2	0.649	0.584	0.652	0.645	0.557	0.717	**0.634**	0.160
3	0.827	0.753	0.754	0.822	0.747	0.860	0.794	0.113
4	0.816	0.925	0.898	0.796	0.857	0.896	0.865	0.129
5	0.857	0.899	0.799	0.871	0.784	0.849	0.843	0.115
6	0.961	0.976	0.981	0.959	0.956	0.968	**0.967**	**0.025**
7	0.798	0.905	0.924	0.881	0.978	0.893	0.896	0.180
8	0.892	0.928	0.860	0.848	0.889	0.896	0.885	0.080
9	0.875	0.924	0.865	0.851	0.881	0.882	0.880	0.073
10	0.842	0.776	0.779	0.816	0.905	0.877	0.832	0.129
11	0.787	0.735	0.794	0.777	0.752	0.733	0.763	0.061
12	0.944	0.962	0.924	0.903	0.862	0.904	0.917	0.100
13	0.868	0.875	0.878	0.900	0.878	0.818	0.869	0.082
14	0.803	0.913	0.894	0.789	0.849	0.781	0.838	0.132
Mean	0.842	**0.855**	0.847	0.842	**0.829**	0.853	0.845	0.114

Table 5.25: R^2 values for all simulated C20 sessions; Description, see Table 5.24 above.

C14 Mirror Sessions								
	R^2							
VP	Run 1	Run 2	Run 3	Run 4	Run 5	Run 6	Mean 1-6	Diff 1-6
1	0.816	0.884	0.934	0.894	0.843	0.906	0.879	0.118
2	0.735	0.823	0.759	0.794	0.866	0.898	0.812	0.164
3	0.951	0.736	0.717	0.850	0.953	0.701	0.818	0.252
4	0.974	0.866	0.922	0.862	0.972	0.894	0.914	0.112
5	0.853	0.869	0.843	0.815	0.840	0.879	0.850	0.064
6	0.917	0.967	0.937	0.931	0.862	0.915	0.922	0.105
7	0.817	0.800	0.788	0.887	0.879	0.848	0.836	0.099
8	0.859	0.735	0.942	0.936	0.756	0.888	0.853	0.206
9	0.927	0.915	0.888	0.884	0.900	0.924	0.906	**0.043**
10	0.823	0.911	0.927	0.884	0.838	0.898	0.880	0.104
11	0.877	0.942	0.978	0.932	0.936	0.941	**0.934**	0.101
12	0.624	0.726	0.907	0.861	0.694	0.659	0.745	**0.283**
13	0.790	0.645	0.649	0.688	0.644	0.650	**0.678**	0.146
14	0.767	0.799	0.655	0.846	0.846	0.854	0.794	0.199
Mean	0.838	**0.830**	0.846	**0.862**	0.845	0.847	0.844	0.143

Table 5.26: R^2 values for all simulated C20 sessions; Description, see Table 5.24 above.

The last row of each of the three tables contain the mean value across the 14 individual R^2 values of a column. This mean value is not an R^2 value derived from a linear regression, but the mean values in the columns *Run 1 - 6* can be used as an indicator, how well the 14 subject sessions are reproduced on average in each simulation run. For a better overview, these mean values are summarized below (Table 5.27).

	Mean values of Tables 5.24 - 5.26							
	Run 1	Run 2	Run 3	Run 4	Run 5	Run 6	Mean 1-6	Diff 1-6
Planar	0.860	0.856	**0.876**	**0.838**	0.859	0.862	0.859	0.101
C20	0.842	**0.855**	0.847	0.842	**0.829**	0.853	0.845	0.114
C14	0.838	**0.830**	0.846	**0.862**	0.845	0.847	0.844	0.143

Table 5.27: Mean R^2 values for the six experiment runs; Column Mean 1-6: mean value of the six R^2 values of Run 1-6; Column *Diff 1-6*: difference between maximum and minimum R^2 value observed for Run 1-6.

	R^2 from analysis of full experiment data						
Mirror	Run 1	Run 2	Run 3	Run 4	Run 5	Run 6	Diff 1-6
Planar	**0.9923**	**0.9869**	0.9912	0.9915	0.9886	0.9893	0.0054
C20	**0.9918**	0.9888	**0.9854**	0.9878	0.9879	0.9863	0.0064
C14	0.9873	0.9887	**0.9805**	0.9876	**0.9928**	0.9856	0.0123

Table 5.28: Reprint of Table 5.21 from the previous section.

Both tables above are used to compare the two different analysis approaches. The R^2 values from the analysis of the full experiment data were very high (Table 5.28), even the smallest R^2

value is 0.9805 (Run 3 and the C14 mirror). Considering the mean values of the session-based analysis (Table 5.27) these are much smaller: 0.876 is the largest value here (Run 3, planar mirror).

Besides the absolute R^2 values, a further difference between the two analysis approaches is observed for the difference between the minimum and maximum R^2 values over the six simulated runs. For this purpose the *Diff 1-6* columns are considered. Comparing the values between the two tables above, the difference is much larger for the session-based analysis, which means there is a larger variability between the six model runs found here.

The reason for both of these differences between the two analysis approaches is caused by the reduced database for the session-based analysis. As assumed in the introduction of this section, the comparison of the transition region on the basis of the transition region data (without the deterministic part of each session) provides a better assessment of the probabilistic decision making process.

Individual Session Results After the overview tables were shown with all 252 session results, and a comparison between the two analysis approaches was done, this section addresses the question how well the behavior of the 14 subjects is reproduced by each of the six simulated sessions. It is not possible to discuss the six simulated sessions for all 42 subject sessions, instead, a subset of six subject sessions can be used as reference. From each of the three main result tables (5.24 - 5.26) two subject sessions are selected: the session where the six simulated sessions received the lowest R^2 value on average (value in column *Mean 1-6*) and the subject session where the highest R^2 was observed. These six subject sessions are summarized in Table 5.29.

		R^2							
	VP	Run 1	Run 2	Run 3	Run 4	Run 5	Run 6	Mean 1-6	Diff 1-6
Planar	3	0.674	0.705	0.828	0.715	0.668	0.761	0.725	0.160
	8	0.892	0.955	0.955	0.883	0.944	0.931	0.927	0.072
C20	2	0.649	0.584	0.652	0.645	0.557	0.717	0.634	0.160
	6	0.961	0.976	0.981	0.959	0.956	0.968	0.967	0.025
C14	13	0.790	0.645	0.649	0.688	0.644	0.650	0.678	0.146
	11	0.877	0.942	0.978	0.932	0.936	0.941	0.934	0.101

Table 5.29: Subject sessions where the six simulated sessions received the highest or lowest R^2 value on average (column *Mean 1-6*).

Considering the column *Mean 1-6*, there is a noticeable difference between minimum and maximum R^2 values for each pair of subjects: 0.202 between VP3 and VP8, 0.333 between VP2 and VP6 and 0.256 between VP11 and VP13. A second observation is made for the last column *Diff 1-6*: the 3 subjects with the smaller *Mean 1-6* value have a larger value here, which means the variability between the six repetitions with regard to the R^2 value is larger. Both of these observations indicate that the individually parameterized model does not perform equally well for all subject sessions, and the rest of this section will explore potential reasons for this observation.

The result of the calculation $S = O/R$ was used to decide which of the three input variables (Θ^{gap}, Δ^{gap} or the ttc) is selected for the simulation of the subject's session. The first question

that is investigated is whether the absolute value of S for the selected input variable is linearly correlated to the mean value of the six R^2 values for the simulated sessions (*Mean1-6*). In other words: "Does a lower value for S always lead to a worse performance (with regard to R^2) of the simulation"? Table 5.30 shows the results for S and the planar mirror sessions.

Planar Mirror		Results $S = O/R$	
VP	Mean 1-6	$S_{\Theta^{gap}}$	$S_{\Delta^{gap}}$
1	0.838	0.6601	0.1870
2	0.869	$^*S_{ttc} = 0.7120$	
3	**0.725**	0.3877	0.2159
4	0.899	0.6692	0.2023
5	0.794	0.2091	0.6155
6	0.880	0.6928	0.1797
7	0.898	0.2275	0.4944
8	**0.927**	0.1743	0.2487
9	0.903	0.6738	0.4233
10	0.917	0.1984	0.4471
11	0.791	0.3341	0.3059
12	0.850	0.7500	0.1326
13	0.880	0.2413	0.3098
14	0.851	0.2769	0.5501

Table 5.30: *Mean 1-6* from Table 5.24; Values for S taken from Table 5.16, $^*ttc$ received highest value for S.

For each session, the input variable which received the highest value for S is selected and used for the simulation. The session of VP3 received a higher value $S_{\Theta^{gap}} = 0.3877$ compared to session of VP8 who received a value of $S_{\Delta^{gap}} = 0.2487$. This is the opposite of the assumed dependency between S and expected performance of the simulation: the session of VP3 has a larger value for S, but the performance of the simulation (with regard to the R^2) was worse compared to VP8. Another counter example can be found for the subjects VP11 vs. VP13: again, the simulation performed better for the subject who had the smaller value for S (VP13).

After a couple of counter examples was already found, a scatter plot was drawn for the values of S and the values in column *Mean1-6*. This was done for the 14 sessions of each of the three mirror types and a linear regression was calculated. The results can be seen in Figure 5.45. The very low R^2 for the planar and C20 mirrors reject a linear dependency between S and the values of *Mean1-6*. The R^2 value of 0.35 for the C14 indicate a weak correlation, but considering the values for all three mirror types, it is concluded that a larger absolute value of S can not be directly used as an indicator how well the performance of the simulation will be.

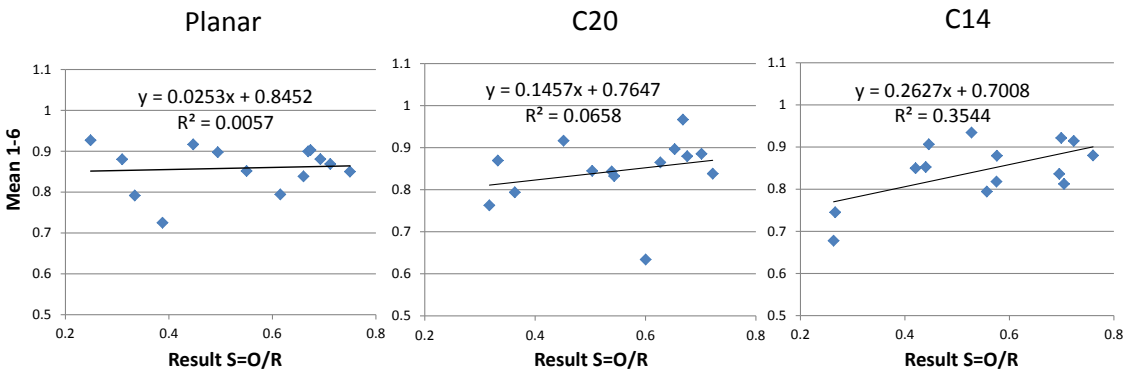

Figure 5.45: No linear correlation between the value of S and the average of the R^2 values for the six simulated sessions (column *Mean1-6* in Table 5.30).

The next analysis takes a closer look at the simulated planar mirror sessions of VP3 and VP8, and whether another explanation can be found why the simulation performs weaker (VP3) or better (VP8) for certain subjects. Figure 5.46 shows the number of lane changes for the planar mirror session of subject VP3 and two of the six simulated sessions with the largest $R^2 = 0.828$ (Run 3) and the smallest $R^2 = 0.668$ (Run 5).

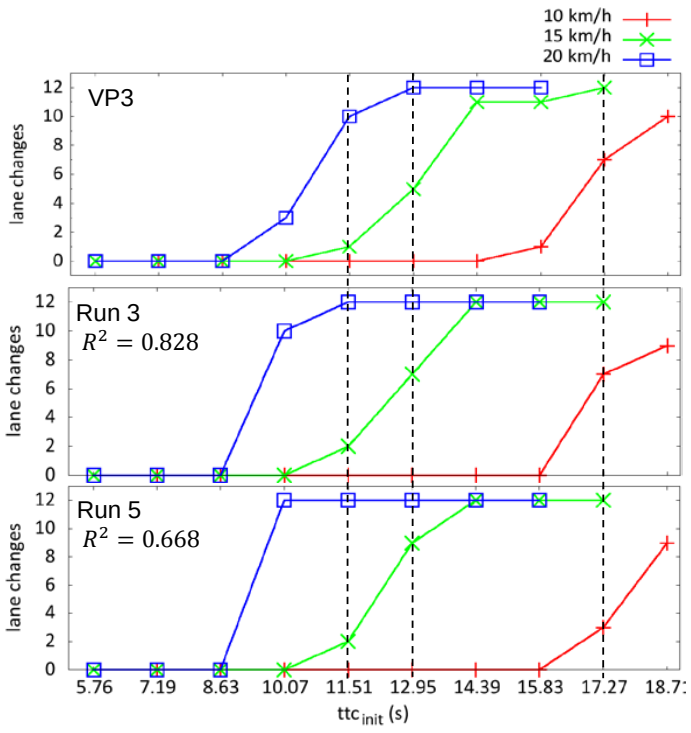

Figure 5.46: Planar mirror session of VP3 (top diagram) and two of the six simulated sessions below.

For the simulation of the planar mirror session of VP3, the angular gap size Θ^{gap} is selected as input variable according to the value of S (see Table 5.30). It was argued earlier in this work

that the angular gap size Θ^{gap} is selected as input variable if a larger effect size of Hypothesis 2.2 is observed in the subject data (Hypothesis 2.2: the number of lane changes increases with increasing speed difference). In contrast, a small effect size of Hypothesis 2.2 leads to a selection of the angular velocity Δ^{gap} (see "Conclusion", p.167, or section 5.5.2, p. 133).

Because the angular gap size Θ^{gap} is used for the simulation of the VP3 session, the Hypothesis 2.2 effect is clearly visible for both of the simulated sessions in the Figure 5.46. But if the vertical lines are used to compare both simulated sessions against the empirical session of the subject, it can be seen that the effect of Hypothesis 2.2 is *overestimated* by the model in both of the simulated sessions. Comparing the number of lane changes for each of the three speed differences of Run 3 first: the simulated number of lane changes is underestimated by 2 for 10 km/h, but it is overestimated by 4 for 15 km/h and by 9 for the 20 km/h speed difference. The overestimation for the full session is 11 lane changes $(-2 + 4 + 9)$. The exact same amount of overestimation is observed for Run 5, too: -6 for 10 km/h, +6 for 15 km/h, +11 for 20 km/h. In contrast, if the absolute difference in the number of lane changes is considered, Run 3 has an *error* of 15 (2+4+9) lane changes while Run 5 has an error of 23 lane changes (6+6+11).

Before overestimation and error are investigated in more detail, two simulated sessions of VP8 are quickly presented. Figure 5.47 shows the number of lane changes for the planar mirror session of subject VP8.

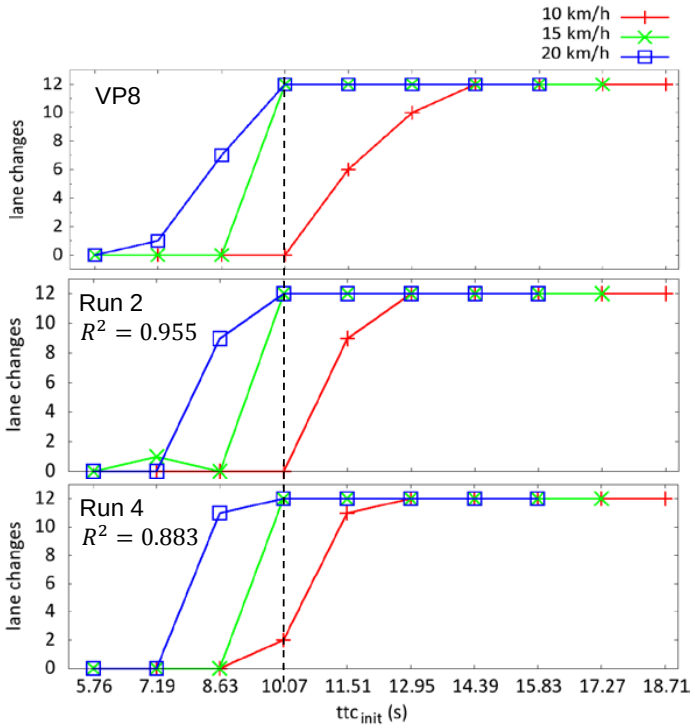

Figure 5.47: Planar mirror session of VP8 and two simulated sessions (Run 2 and Run 4).

The selected input variable for the simulation of the planar mirror session of VP8 is Δ^{gap} (see Table 5.30). In contrast to VP3, the selection of Δ^{gap} is an indicator for a smaller effect size of Hypothesis 2.2. A comparison of the sessions between VP3 and VP8 in the two figures shows

that the difference in the number of lane changes between the three speed differences is much smaller for VP8. But similar to VP3, an overestimation of the number of lane changes is also found in both simulated sessions here. For Run 2, the overestimation is 6 (+5 for 10 km/h, +1 for 20 km/h) and the error is 8 (5 for 10 km/h, 3 for 20 km/h). For Run 4 the overestimation is 12 (+9 for 10 km/h, +3 for 20 km/h) and the error is 14 (9 for 10 km/h, 5 for 20 km/h). Compared to VP3, the error in the number of lane changes is smaller, which leads to a better R^2 value for both sessions, but also the overestimation is smaller.

Similar to the example sessions of VP3 and VP8, the calculation of overestimation and error was done for all 252 sessions. The average overestimation and the average error across the six simulated sessions for each of the 42 subject sessions are summarized in Table 5.31 below. Three additional tables with the detailed results for each of the 252 sessions are found in the Annex (Tables 7.2 - 7.4, p. 220).

Number of Lane changes: Overestimation(+) or Underestimation(-) / Error						
	Absolute			**Relative%**		
VP	Planar	C20	C14	Planar	C20	C14
1	18.7 / 23.7	5.0 / 15.0	8.2 / 16.2	21.5 / 27.2	6.9 / 20.6	11.2 / 22.2
2	-13.0 / 24.3	-11.3 / 32.7	16.2 / 24.8	-12.6 / 23.6	-10.8 / 31.1	21.0 / 32.3
3	**15.2 / 22.8**	-3.8 / 17.2	5.8 / 17.5	**25.3 / 38.1**	-5.0 / 22.3	7.8 / 23.3
4	3.0 / 16.0	1.7 / 14.0	0.7 / 12.7	4.0 / 21.3	2.7 / 22.2	0.8 / 16.0
5	16.8 / 19.8	9.0 / 19.0	8.3 / 24.3	35.8 / 42.2	11.5 / 24.4	7.3 / 21.4
6	-1.7 / 15.7	2.0 / 8.7	3.3 / 12.3	-2.2 / 20.9	2.4 / 10.2	4.0 / 14.7
7	6.2 / 16.5	9.8 / 13.2	17.5 / 18.8	7.9 / 21.2	14.3 / 19.1	27.8 / 29.9
8	**8.3 / 10.0**	12.0 / 17.7	-5.5 / 13.2	**12.3 / 14.7**	12.2 / 18.0	-7.3 / 17.3
9	-3.5 / 4.8	14.7 / 17.0	5.0 / 15.0	-19.4 / 26.9	23.7 / 27.4	7.0 / 21.1
10	-3.2 / 11.0	7.0 / 21.3	19.3 / 22.0	-5.7 / 17.2	6.8 / 20.9	17.7 / 20.2
11	12.2 / 24.2	-0.2 / 19.5	7.8 / 13.5	14.2 / 28.1	-0.2 / 26.7	7.6 / 13.1
12	0.0 / 18.7	2.0 / 10.0	3.7 / 18.0	0.0 / 20.5	3.0 / 15.2	5.4 / 26.5
13	-10.2 / 15.5	11.5 / 15.8	18.3 / 21.7	-16.4 / 25.0	15.8 / 21.7	23.5 / 27.8
14	9.0 / 18.7	18.8 / 23.5	13.5 / 21.5	14.5 / 30.1	20.5 / 25.5	20.5 / 32.6
Mean	4.1 / 17.26	5.58/ 17.46	8.72/ 17.96	5.6 / 25.5	7.4 / 21.8	11.0 / 22.7

Table 5.31: First value in each cell is either overestimation (positive values) or underestimation (negative values), second value after '/' is the error which is always positive. Columns 2-4 contain the overestimation / error in absolute values for the number of lane changes across the six simulated sessions. Last three columns contain the relative overestimation and relative error in %.

With regard to the planar mirror sessions of the subjects VP3 and VP8 (marked bold in Table 5.31), the findings that were made for the 4 example runs are supported also by the average values: the average of the six simulated planar sessions of VP8 have a smaller average error (10.0 vs. 22.8), as well as a smaller amount of overestimation (8.3 vs 15.2). As explained above, a difference between the subjects is the selected input variable for the model (angular gap size Θ^{gap} for VP3 angular velocity Δ^{gap} for VP8). It was also tested whether the simulations where Θ^{gap} is used lead a larger error and / or overestimation, compared to the simulations where Δ^{gap} is used. For this purpose, the data of Table 5.31 was split into two groups and the average

overestimation and error was calculated for both groups. The results are summarized in Table 5.32 below.

	Planar		C20		C14		All Mirrors	
	#	Overest. / Error	#	Overest. / Error	#	Overest. / Error	#	Overest. / Error
Θ^{gap} used	7	6.26 / 17.98	9	5.76 / 15.98	5	5.10 / 16.10	21	5.71 / 16.69
Δ^{gap} used	6	4.42 / 15.25	4	9.42 / 17.00	8	11.63 / 19.13	18	8.49 / 17.13
Θ^{gap} - Δ^{gap}		+1.84 / +2.73		-3.66 / -1.01		-6.53 / -3.03		**-2.78 / -0.44**

Table 5.32: Number of lane changes: overestimation and error averaged across all simulated sessions, where either Θ^{gap} or Δ^{gap} is used as input variable for the model. #: number of subject sessions where Θ^{gap} or Δ^{gap} is used.

Considering the group of sessions where Θ^{gap} is used (first line in Table 5.32), the overestimation reduces slightly from planar to C20 to C14, while the error reduces from planar to C20, but again increases slightly from C20 to C14. In contrast, for the group of sessions where Δ^{gap} is used (second line in Table 5.32), both values increase from planar to C20 to C14, and the magnitude of the increase is much stronger here compared to the Θ^{gap} group. Considering the difference between the two groups (last line in Table 5.32), for the planar mirror sessions, overestimation and error are larger for the Θ^{gap} group. For the C20 and C14 mirror, overestimation and error are larger if Δ^{gap} is used. For the average across all 252 sessions (last column in the table), the sessions which are simulated with Δ^{gap} lead to higher overestimation (8.49 vs. 5.71) and a slightly higher error (16.69 vs. 17.13). With regard to the initial assumption, if the overestimation and / or error are always larger for one of the two groups, no definitive answer can be given, because this changes between the mirror types.

But the results in Table 5.32 suggest, that the overestimation for the Δ^{gap} group rises with increasing mirror curvature (from planar to C20 to C14). It was supposed that a systematic error might be caused by the sampling mechanism of the perception component (section 5.6.2) which is illustrated in Figure 5.48.

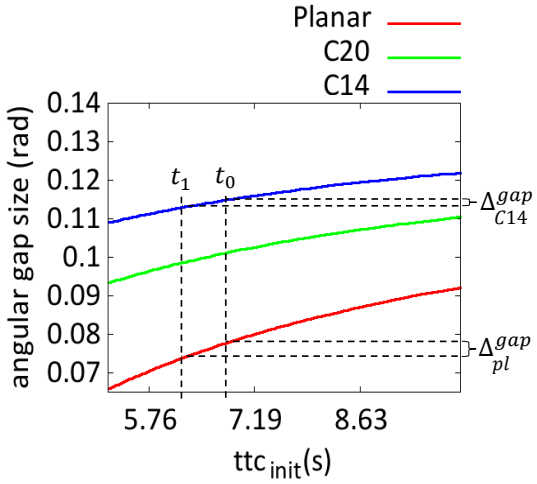

Figure 5.48: Perception of angular gap size Θ^{gap} and sampling of Δ^{gap}. Original sampling interval between t_0, t_1 is 100ms, increased for illustration purposes.

The figure depicts how the angular velocity Δ^{gap} is calculated by the percept component as the difference of two input samples of Θ^{gap}. During the simulation the vehicle approaches and the time-to-collision is reduced, therefore the subsequent samples are recorded at simulation times t_0 and t_1. t_1 is the point in time when the perception is finished and the resulting angular velocity is calculated as the difference of both samples. The real speed at the point in time t_1 is always underestimated (perceived slower than real value) because of the sampling. This underestimation is stronger for the planar mirror (and $\Delta_p^{gap}l$), because the non-linear curvature is stronger here. As a consequence, a stronger underestimation of the angular velocity for the planar mirror, compared to the C14, would lead to more lane changes for the planar and less for the C14. But the overestimation of the number of lane changes increases from planar to C20 to C14, which is the opposite. Therefore, the sampling itself can not be the reason for the increased overestimation with increasing mirror curvature.

While this problem was investigated, a small implementation error was discovered which could be a cause for at least a portion of the general overestimation of the model: the point in time when the decision is made by the model equals the time t_1 in the figure plus a fixed amount of 100ms for the decision making step. This point in time is also used for the mapping of the transition regions and the calculation of the overlap O. Because the sampling generally underestimates the speed, this should be considered in the calculation of the overlap O. Therefore the decision making point in time should be slightly corrected to $t_1 - si/2 + 100$ ms for the mapping process. This would lead to a slightly changed value range for the overlap O which reduces the underestimation of the velocity that is induced by the sampling. As a consequence, the overestimation of the number of lane changes would be reduced which was observed consistently across all mirror types. Unfortunately, it was not possible anymore to test this revised implementation, therefore the benefit of this change can not be assessed here anymore. This is part of the future improvements of the model.

5.8 Summary and Future Work

The development of the gap acceptance model was guided by four modeling objectives and the results with regard to each of the objectives are summarized in this section. Objectives 2-4 required the implementation of specific model capabilities, and they are presented first. Objective 1 required that the model shall be able to simulate the observed findings of Experiment 2 with regard to the experiment hypotheses. After the results with regard to the objectives are presented, section 5.8.2 discusses known issues of the model and proposes alternative approaches, which can be addressed by further modeling efforts and additional empirical studies in the future.

5.8.1 Summary with regard to Modeling Objectives

Objective 4 This objective required that the gap acceptance model "shall interact within the Experiment 2 scenario similar to the human participants." To fulfill this objective, a sequence of four behavioral steps was derived from the task description that subjects received as instruction for Experiment 2: 1) shift gaze from the lead vehicle towards the mirror, 2) perceive the

situation with the help of the mirror, 3) conduct the gap acceptance decision and 4) give the appropriated actions response, either braking or steer left.

Because the model interacts in real-time within the driving simulator and the Experiment 2 scenario, each of these four steps has to consume a certain amount of time. For this purpose, the mean reaction time of the subjects was calculated for each of the 42 experiment sessions (section 5.5.3). This period of time was split and small portions were assigned to each of the four steps. The action response (steer left or braking) is always given after the mean reaction time is fully consumed by the model. Section 5.6.1 describes the state machine implementation of the task model as well as the timing behavior.

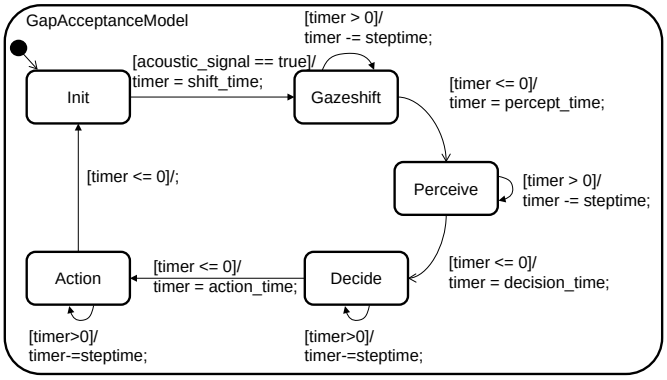

Figure 5.49: Implementation of the four main states plus an initialization state (*Init*) waiting for the start of the trial. Before entering a new state, a timer is set to a configurable time in milliseconds. If the timer is expired, the state is left.

Objective 2 tackled the visual perception of the gap acceptance model, which is implemented in step two of the four behavior steps of the model. It was required that the model "shall perceive its visual input via the implemented mirror simulation (described in section 3.3 realizing the "look into the mirror", from a first-person driver perspective."

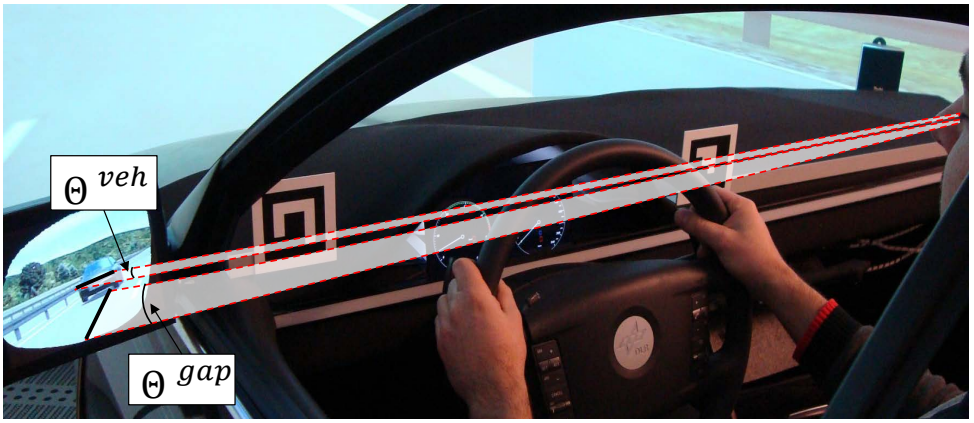

Figure 5.50: *Angular gap size* Θ^{gap} and *angular vehicle width* Θ^{veh} of the approaching rear vehicle. For each angle the rate of change can be calculated: Δ^{gap}, respectively Δ^{veh}. The time-to-collision can be perceived by the driver according to the τ theory of [Lee1976]: $\tau = \frac{\Theta^{veh}}{\Delta^{veh}}$.

Section 5.3 discussed different categories of model variables. It was argued that the angular gap size Θ^{gap} and its angular velocity Δ^{gap} are the preferred model variables (Figure 5.50). Additionally, the analysis of the individual behavior in section 5.4 concluded that the time-to-collision, respectively τ should be considered as a third model variable.

At runtime of the simulation, the values of the angular gap size Θ^{gap} and Θ^{veh} are calculated by the mirror simulation, and both are received by the visual perception component of the model (within the *Perceive* state). The angular velocity Δ^{gap} as well as τ are calculated within the perception component (section 5.6.2). The output of the perception component are three variables (Θ^{gap}, Δ^{gap} and τ), which are then used by decision making process of the model (Objective 3). These variables are called the *input variables* of the model.

Objective 3 This objective required that the model "needs a decision making process to solve the gap acceptance task of the subjects in Experiment 2. The threshold concepts of the IMoST model shall be evaluated with regard to its appropriateness and, if necessary, revisions shall be done." Apart from a safety distance check for the blind-spot region, the gap acceptance decision in the IMoST model was made on the basis of the angular velocity Δ^{veh} of the approaching rear vehicle. Its value was compared against a fixed decision making threshold.

Section 5.5.1 discussed the appropriateness of this single threshold concept and presented the basic model ideas which were implemented in this thesis. It was argued that a fixed decision making threshold is not sufficient to reproduce the individually different gap acceptance behavior observed in Experiment 2. The concept of a transition region was introduced: "there is a certain region along the ttc_{init} conditions (x-axis in the figure), where the number of lane change decisions continually rises, from braking only (at a smaller ttc_{init} condition), towards lane changes only (at a larger ttc_{init} condition)". Figure 5.51 sketches two examples (marked by curly brackets, for VP8 and VP9).

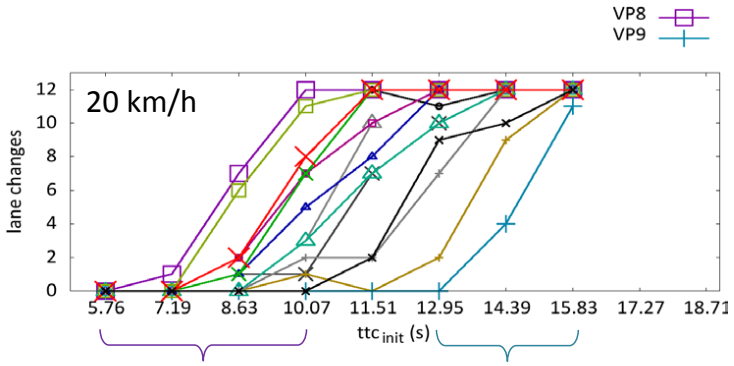

Figure 5.51: Planar mirror sessions, 20 km/h speed difference. Lane change behavior of the 14 subjects. Two transition regions are marked (VP8, 9). Full figure at p.132

The transition regions vary from subject to subject with regard to two characteristic properties: 1) their location along the x-axis in the figure (region of VP9 is located at smaller ttc_{init} condition compared to VP8), and 2) also their size (how many ttc_{init} conditions are embraced).

The transition region concept was used in an illustrative approach (called visual mapping, section 5.5.2) which demonstrated that Θ^{gap} and Δ^{gap} can explain behavioral differences with regard to the strength of the effect that is postulated by Hypothesis 2.2: "With increasing speed difference Δv_{CA}, the number of accepted gaps for situations with equal ttc_{init} will increase." The implementation of the visual mapping (section 5.6.3.2, 5.6.3.3) led to the result sketched in Figure 5.52 and described below.

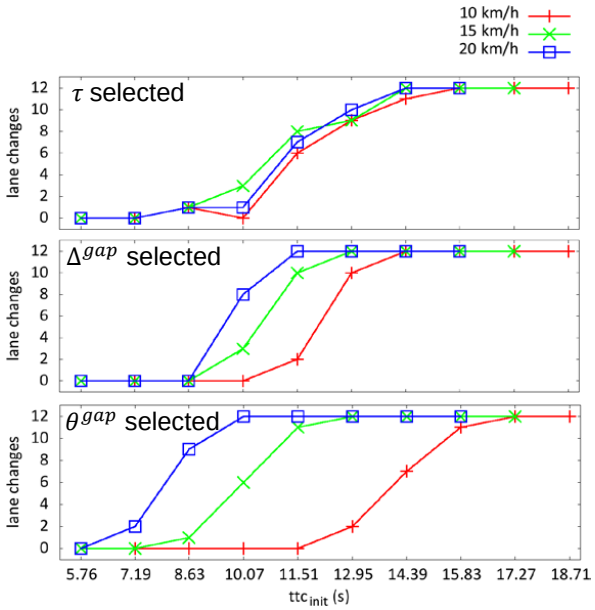

Figure 5.52: Three different Experiment 2 sessions: different input variable selected, dependent on the strength of the effect postulated by Hypothesis 2.2.

1) if no effect size for Hypothesis 2.2 was observed in an experiment session, the time-to-collision was selected. This occurred for 3 out of 42 sessions. 2) if a small effect size for

Hypothesis 2.2 was observed, the angular velocity Δ^{gap} was selected (18 sessions). 3) For the remaining 21 sessions the angular gap size Θ^{gap} was selected, and in these sessions, a large effect size was observed for Hypothesis 2.2.

The transition region concept also motivated the implementation of the decision making function of the gap acceptance model as a piecewise function (Figure 5.53). During the simulation, this function is executed in the *Decide* step of the model. It receives the current value of the selected input variable $x \in X$ from the perception and calculates the probability for a lane change $P(LC|x)$.

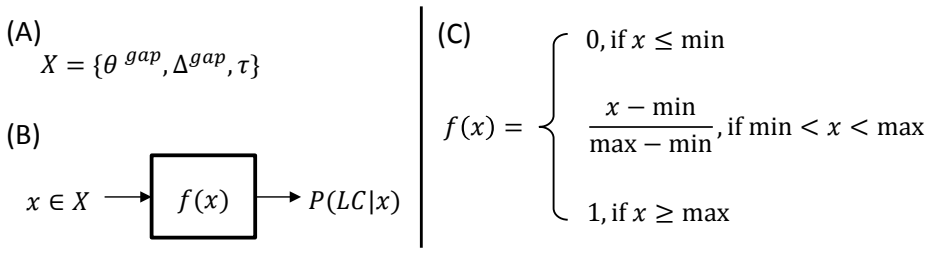

Figure 5.53: Implementation of the decision making function $f(x)$

The adjustment of min and max of function $f(x)$ was derived from the empirical data for each of the 42 experiment sessions (see beginning of section 5.7, p.167). The assessment of the quality of the implemented model with regard to modeling Objective 3 (quality of the decision making) as well as modeling Objective 1 (model shall be able to simulate the findings of Experiment 2 with regard to Hypothesis 2.1 and 2.2) is summarized in the next paragraph.

With regard to the fulfillment of Objective 3: compared to the IMoST model, the gap acceptance decision is no longer made using the angular velocity Δ^{veh} and a single decision making threshold. Instead, different behaviors with regard to Hypothesis 2.2 can be simulated now, by selecting one of the three input variables for the decision making process. The configuration of min and max of the decision making function $f(x)$ realizes two characteristic properties of the transition region mentioned above, which are important to capture the individual behavior differences. As a result, this work led to a revised model concept which is able to capture individual behavioral differences. Furthermore, the underlying database (Experiment 2) allowed to investigate gap acceptance behavior in much more detail as it was possible for the IMoST model.

Objective 1 This objective required, that "the model shall be able to simulate the observed findings of Experiment 2 with regard to the experiment hypotheses". The model was integrated into the driving simulation platform and interacted within the Experiment 2 scenario similar to the participants of the experiment (Objective 4). The model was configured for each of the 42 sessions and afterwards the session was simulated. This procedure leads to the simulation of the complete Experiment 2. Six repetitions of the experiment were simulated to inspect the quality of the probabilistic decision making function.

All six experiment runs were first investigated on the basis of the accumulated data of all 42 sessions (section 5.7.1). The following results were observed: the linear correlation between

simulated number of lane changes and the empirical number of lane changes led to a high $R^2 > 0.95$ for all six simulated experiment repetitions. The difference between the smallest and the largest R^2 for a simulated experiment run was < 0.02, which can be used as an indicator with regard to reproducibility, in other words, how much variability is observed between the six experiment repetitions. The main findings for Hypothesis 2.2 as well as Hypothesis 2.1 of Experiment 2 are preserved in the simulation: the significant difference in the number of lane changes between planar and both curved mirrors is reproduced, and also the non-significant difference between C20 and C14 was preserved in the simulated experiment runs (Hypothesis 2.1). Additionally, the significant increase of the number of lane changes with increasing speed difference is observed in each simulation run (Hypothesis 2.2).

It has to be considered that Hypothesis 2.1 was not explicitly considered during the development of the model, instead the model development focused on the effect of Hypothesis 2.2. Nevertheless, the simulation of each of the sessions and the reproduction of the behavior was good enough to reproduce the results with with regard to Hypothesis 2.1 also. In this regard, the main modeling *Objective 1* was fulfilled.

In a second analysis step, it was investigated how well the simulation was able to reproduce the number of lane changes for each of the 42 subject sessions of Experiment 2. For this purpose, only the reproducibility with regard to the transition regions was investigated, which excluded those ttc_{init} conditions, where the model decides deterministically for a braking maneuver or a lane change (see $f(x)$, p. 189: $x \leq$ min or $x \geq$ max).

Compared to the analysis which was done with regard to the experiment hypotheses, the R^2 values of this second analysis dropped considerably. For the simulation of the planar mirrors sessions the average of the R^2 values was 0.859, for the C20 it was 0.845 and for the C14 it was 0.844. Across all 252 simulated sessions the smallest R^2 value was 0.584 (simulation run 2 for the C20 mirror session of VP2) and the best R^2 value was 0.962 (simulation run 1 for the C14 mirror session of VP9). The variation between the six repetitions for each of the 42 sessions was also higher: the average difference between smallest and largest R^2 for each of the six simulated sessions was < 0.12 across all 42 sessions, but for the simulation of certain sessions this difference went up to 0.180 (simulation of the C20 mirror session of VP7).

Although the effects of both experiment hypotheses were preserved in the simulation, the total number of lane changes was also considerably overestimated by the model in each of the six simulated experiment repetitions. The investigation of the overestimation was considered an important step with regard to modeling *Objective 3* and the assessment of the quality of the decision making process.

For each of the three mirror types, the average overestimation across all six simulated experiment repetitions is 6.57% (planar), 4.1% (C20) and 5.28% (C14). Several observation were made with regard to the overestimation:

1. A (linear) dependency between increasing speed difference and the amount of overestimation was not found across all three mirror types, overestimation is found in all speed difference conditions.

2. An average amount of overestimation of 5.71% was found for the simulated sessions where the angular gap size Θ^{gap} was used as input variable for the decision making func-

tion $f(x)$. There was a slight tendency that the overestimation decreased with increasing mirror curvature (planar: 6.26%, C20: 5.76%, C14: 5.10%).

3. An average amount of overestimation of 8.49% was found for the simulated sessions where the angular velocity Δ^{gap} was used as input variable for $f(x)$. For these simulations, the overestimation increased with increasing mirror curvature (planar: 4.42%, C20: 9.42% C14: 11.63%), and this effect was considerably stronger compared to the reduction that was observed for the simulated sessions where Θ^{gap} was used. It was assumed that a small error with regard to the internal calculation of Δ^{gap} in the visual perception could cause this effect, but this was rejected.

4. With regard to the calculation of Δ^{gap}, a slight timing error was discovered in the model implementation (approximately 50 ms), which contributes to the amount of overestimation (see Figure 5.48 and text below). It was not possible anymore to conduct further simulations with a revised model version, therefore it can not be answered, by how much the overestimation will be reduced with this model improvement.

This second, more detailed analysis showed that the model is not able to reproduce the behavior of each of the 42 experiment sessions with equal quality: across all 252 simulated sessions (42 experiment sessions, 6 repetitions), the smallest R^2 value for a single simulated sessions was 0.584, the best R^2 was 0.962, the average R^2 across all 6 repetitions was: 0.859 (for all 84 simulated planar mirror sessions), 0.845 (C20), 0.844 (C14). All values are found in the tables 5.24 - 5.26, p. 177.

Conclusion The model interacts within the Experiment 2 scenario similar to the human participants. It simulates the task of the subjects and times its actions according to the mean reaction time of the subjects (Objective 4). A first person perspective was implemented and the model simulates the look into the mirror. It does not use an artificial variable mirror type, instead it perceives three input variables which are based on the concept of visual angles. In this regard, the result of the minification effect of the curved mirrors is implicitly perceived by the model (Objective 2). With the results of Experiment 2 it was possible to revise the decision making process of the IMoST gap acceptance model (Objective 3). The model development was focused on the effect of Hypothesis 2.2 and is able to simulate different behavioral characteristics with regard to the effect strength of this hypothesis. With regard to Hypothesis 2.1, the model is able to reproduce these effects, but a prediction is not possible so far, because the data of Experiment 2 did not allow to separate behavioral differences from the effect size that was expected for Hypothesis 2.1 (the difference between the mirrors, details in section 5.4.3).

Finally, there are still a number of open issues, especially with regard to the implemented decision making process, and the implemented procedure that selects the input variables. The next section explains these issues and presents alternative solutions that can be implemented and tested in future work.

5.8.2 Future Work

So far, the model development and simulation was based solely on the data of one experiment, namely Experiment 2. The data was used for the development and the analysis of the six simulated experiment repetitions assesses the quality of the approach with regard to the question how well each experiment session is *reproduced*. For a validation of the model it is certainly necessary to compare the model behavior against another empirical study, but this could not be done anymore. Further steps with regard to model validation are discussed in the next paragraph and afterwards modifications to the current model are discussed.

Model Validation One possible next step with regard to model validation would be, to use the empirical data of only two speed differences (e.g. 10 and 15 km/h) to build the model. Afterwards, the model is used to simulate (predict) the lane change behavior for the third speed difference (20 km/h). This process can be repeated three times to predict the lane change behavior for each speed difference. Afterwards the number of lane changes of the simulation can be compared against the empirical data of the subjects. This can be done on an accumulated data level, but also for each session individually.

At the end of the individual behavior analysis in section 5.4.3 it was concluded, that the design of Experiment 2 was not optimal. Because each mirror was tested only once per subject, the variability in the behavior from session to session interferes with the effect of Hypothesis 2.1 (the differences between the mirrors). It was argued, that this likely caused the fail of Hypothesis 2.1 with regard to a difference in the number of lane changes between the C20 and the C14. It was proposed, that the same experiment should be repeated, but this time each mirror should be used in multiple experiment sessions, again on different days. This allows to assess the individual behavior variability of across multiple days for each mirror type. Afterwards, the variability between the different mirror types can be assessed.

In this new experiment, one of the three speed differences should be changed, too, e.g. 10, 20 and 30 km/h could be used. Reusing two speed differences (10 and 20 km/h) would allow to compare both experiments (Experiment 2 and this new one). If the difference between both experiment is not significant, the currently developed individual behavior models could be used to predict the lane change data for the 30 km/h speed difference. Afterwards the accumulated data of all simulation runs is compared against the empirical data.

As a second step, it would be possible to validate at least some of the existing individual behavior models, too. For this purpose, the lane change data of the 10 and 20 km/h speed differences of each subject of the new experiment can be correlated with the simulated data of the already existing individual behavior models. For those individual behavior models, where a high correlation is found for these two speed differences, the data of the 30 km/h speed difference can be compared against the subjects data.

In advance to these validation steps, there are a couple of issues with regard to the implementation of the model. Alternative solutions are sketched in the next paragraphs, and these changes should probably be implemented first. The revised model can be used to produce a new set of simulation runs to test the improvements. The validation with a new experiment should be done as the last step.

Replacing the Calculation of S and O Section 5.6.3.2 described the implementation of the visual mapping approach (see section 5.5.2) which delivered the numerical results for $S = O/R$. These calculations were done for each of the three input variables of the model and each of the 42 experiment sessions. The input variable which received the highest value for S was used as input variable for the decision making process. It was also described that the minimum and maximum values of the overlap O were used to configure the min and max values of the decision making function $f(x)$. The calculation of S and O is a specific development, which was derived from the visual mapping approach. Using such a specific approach, instead of a more standardized and well known one, makes the model vulnerable, because the procedure is not well known. But there is an alternative, which can replace the calculation of S and O, and does not require to change the rest of the model implementation.

The current approach uses three linear regressions to calculate three value pairs $y_0(t_0), y_{12}(t_0)$, one for each of the three transition regions. The values were modified by the reaction time $(y_0(t_{rt}), y_{12}(t_{rt}))$ and mapped onto the angular measures using lookup tables. Subsequent steps calculated S and O (please see section 5.6.3.2 for the description of this approach). One alternative solution is the following: after the ttc_{init} conditions are selected for each transition region, all of these values are modified by the amount of the reaction time (not only $y_0(t_0), y_{12}(t_0)$). Afterwards, all values are mapped onto each of the input variables (Θ^{gap}, Δ^{gap}, time-to-collision, respectively τ) using the look-up tables. For each input variable, a linear regression is calculated for the mapped values. Instead of using the value of S to select the input variable for $f(x)$, the decision can be made using the R^2 values of the regression. Furthermore, the linear equation of the regression can be used to calculate the min and max values for the decision making function $f(x)$: the y values for $x = 0$ (the minimum number of lane changes per ttc_{init} condition) and $x = 12$ maximum the number of lane changes (the maximum number of lane changes per ttc_{init} condition).

This alternative approach replaces the calculation of S and O, but the selection of the ttc_{init} conditions for each transition region still relies on the selection rules, described in section 5.6.3.2, p. 156. The next paragraph extends this approach and not only replaces S and O but also the selection rules.

Transition Region: Segmented Linear Regression Section 5.6.3.2 described a set of rules, which was used to select the ttc_{init} conditions for the transition regions. This approach made certain assumptions which ttc_{init} condition should be included and which should be excluded. Brief explanations were given why it was decided to include / exclude a certain ttc_{init} condition, but the selection of the ttc_{init} conditions is not based on a standardized, data driven estimation procedure.

Fitting a piecewise linear function with two break-points β_1, β_2 as illustrated in Figure 5.54 could be used as a replacement for the selection rules.

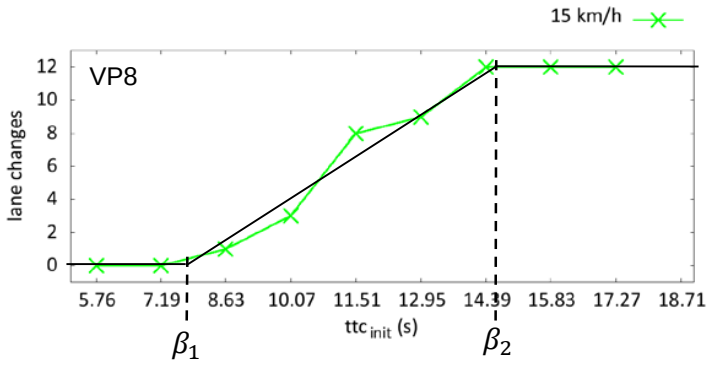

Figure 5.54: Illustration of a piecewise linear function with two break points β_1, β_2.

[Muggeo2008] presents a segmented linear regression, which fits piecewise linear functions. This method is able to calculate the locations of multiple unknown break-points (β_1, β_2 in Figure 5.54)[7]. The calculated values for the two break-points already specify the time-to-collision values for $y_0(t_0), y_{12}(t_0)$. In this regard, this approach not only replaces the selection rules, but it already includes the linear regression of the current implementation (p. 150).

The segmented linear regression can be applied for the transition regions of each speed difference, and the three $y_0(t_0), y_{12}(t_0)$ pairs are modified by the reaction time (see p. 150). Afterwards, the three $y_0(t_{rt}), y_{12}(t_{rt})$ pairs are mapped onto each angular measures using the look-up tables. A linear regression is calculated for the mapped values for each angular measure, and as explained in the alternative approach, the R^2 value of this regression can be used to decide which angular measure is is as input variable for $f(x)$. Similarly, the linear equation can be used to calculate the min and max values for the decision making function $f(x)$.

A comparison of this alternative approach with the existing implementation is of interest in a number of ways: 1) Does this approach lead to the same selection with regard to the input variables? 2) Are the calculated values for min and max of the decision making function $f(x)$ different? 3) Does this approach lead to a better result with regard to the simulation of the individual behavior? 4) Is the overestimation effect reduced?

Further Approaches In this work a piecewise linear approach was used to model the probability of a lane change. The modifications in the two paragraphs above should be considered as necessary improvements, but even with those changes the linear approach has some drawbacks: a small number of sporadic braking and lane change actions were not considered so far (see Table 5.15, p.158). The nature of these actions was not discussed in detail, but at least the four lane changes at small time-to-collision values might be critical events with regard to driving safety. The probability for a lane change was set to zero for those situations that had a smaller time-to-collision below the lower boundary of the transition region.

At this point it becomes obvious, that an s-shaped function would be the better choice. The *logistic regression* was originally proposed by [Cox1958] to model the probability of a binary decision which depends on one or multiple continuous independent variables. The logistic regression assumes that errors / noise is distributed according to the logistic distribution function.

[7] According to [Muggeo2008], this algorithm is implemented in the R statistic software package *segmented*

Instead, the probit regression should be used if the noise is normally distributed. The shape of both of these cumulative distribution functions is very similar, and without applying both of these approaches it can not be answered right away which one would fit better. With regard to modeling noise in human behavior, the cognitive architecture ACT-R uses the logistic distribution (act-r-noise command) to model noise for memory retrieval times, but ACT-R also uses uniform noise distributions (act-r-random) for example in the utility module (see ACT-R Reference Manual [Bothell2017]. The manual also states that the logistic distribution is an „*approximation of a normal distribution*“ which could be interpreted as an indicator, that normally distributed noise should be used but the approximation was used for some reason.

Two things should also be considered if these approaches are applied to the data: 1) each of the ttc_{init} conditions was repeated twelve times and a distinct decision which of the two approaches is better suited can probably not be done unless more repetitions (new experimental data) become available. For the same reason even the segmented linear regression might perform equally well, especially if the three segments are specified by three different linear equations (so far only the transition region itself was specified by a linear equation, while the upper and lower segments were set to constant values either one respectively zero). But in this case the smaller number of parameters should clearly favor the logit or probit model over the segmented linear model.

Reaction Time The point in time when the model executes its braking or steering action was not varied during the simulation. Instead, the action response was always given when the mean reaction time of the subject that was measured in an experiment session expired (summary section above, modeling Objective 4). A more detailed investigation of the reaction time according to the different ttc_{init} conditions was not considered so far, but could be a topic for a further improvement of the model.

Figure 5.55 visualizes the mean reaction time across all subjects, separated into situations where either a braking or a steering action was done. In those cases where a braking response was given, the reaction time increases with increasing ttc_{init}. This is observed across all three speed differences.

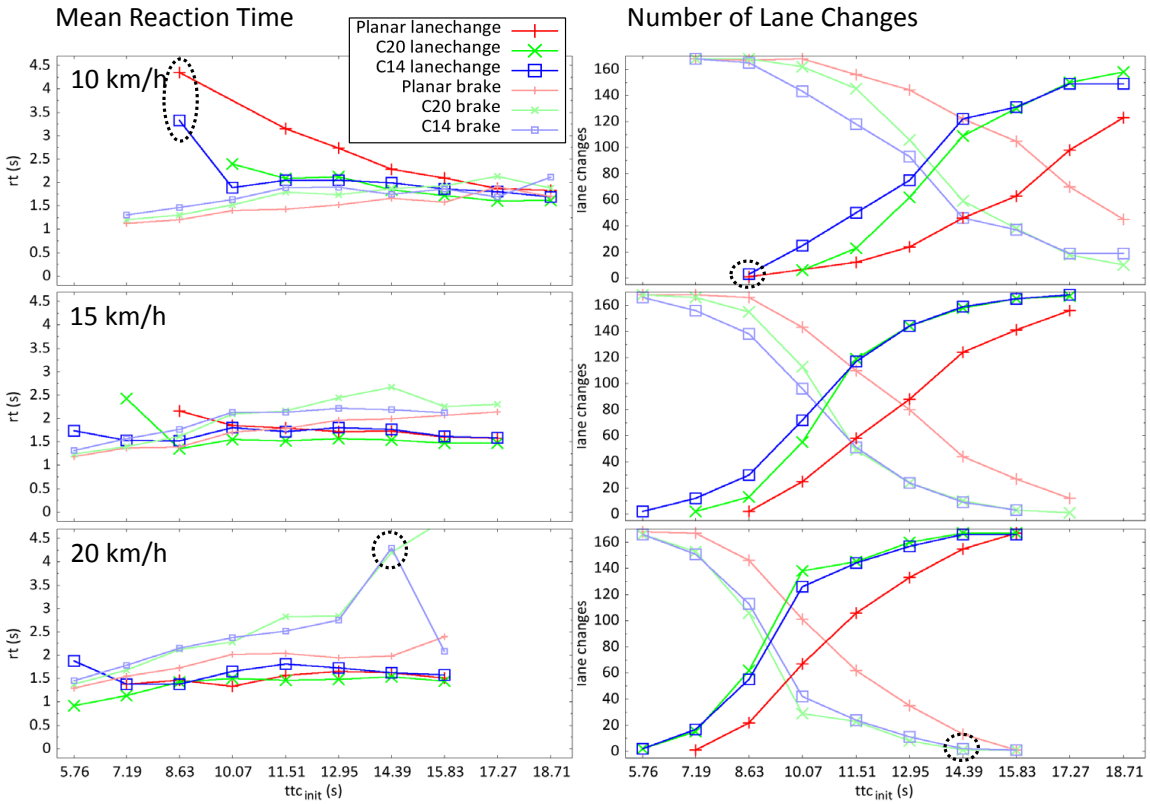

Figure 5.55: Left: mean reaction time of all subjects separated according to braking actions (pale colors) and lane changes. Right: number of braking actions and lane changes. Marked mean reaction time values are caused by only very few late lane changes (10 km/h), or very few late braking actions (20 km/h).

The following hypothetical explanation can be given: for the smallest ttc_{init} conditions, drivers quickly reject the gap, because a quick glance is already sufficient to assess that the angular gap size Θ^{gap} is too small, or the angular velocity Θ^{gap} is too high. With increasing ttc_{init}, the angular gap size Θ^{gap} increases successively, and the angular velocity Θ^{gap} successively decreases. In these situations the driver probably uses more time to assess the situation, and to decide whether a lane change is possible or not. There are a few rejected gaps at the largest ttc_{init} conditions, and it can be hypothesized that subjects might have waited too long, or they were uncertain, and the gap was finally not large enough anymore to accept it. In these situations, the braking actions are executed comparably late.

On an individual behavior level, these observations could not be made, because the 12 repetitions of each ttc_{init} condition in one experiment session was to small, and no stable reaction time values could be calculated. This problem increased, because the small amount of repetitions had to be divided into braking and lane change actions. Because no sufficient data was available to improve the model on an individual behavior level, this effect was not investigated any further and could not be integrated into the model. A further experiment would be necessary where the number of repetitions per ttc_{init} conditions is increased. This would allow to assess the reaction time of the subjects individually, and could be used to improve the existing

model.

To consider the reaction time on a more detailed level, some modifications to the implementation are also needed. Currently, all $y_0(t_0), y_{12}(t_0)$ values are modified by the mean reaction time. In a first revision, the mean reaction time per ttc_{init} condition can be considered, and each $y_0(t_0), y_{12}(t_0)$ value pair is modified by an individual amount of time. As a consequence, the model behavior at run time also needs to be adjusted, meaning the four steps of the state-machine have to consume a different amount of time. It would be beneficial to first estimate a function which captures the relation between reaction time and ttc_{init} conditions and use these function for the modification of the $y_0(t_0), y_{12}(t_0)$ values. Furthermore, this function can be used at runtime, to modify the time consumption of the model for each of the 26 experiment conditions.

6 Results of this Thesis

In the introduction of this work, the following two objectives were defined.

Objective 1: "This work will investigate the impact of different types of rear view mirrors (driver-side only) with regard to their influence on the driver's gap acceptance behavior. The scenario of interest is the lane change left maneuver on a two-lane freeway (German Autobahn)."

Objective 2: "A behavior simulation model will be developed which is able to simulate the findings with regard to Objective 1. A previously developed and published gap acceptance model [Weber2013] will be reviewed, and if necessary, modifications will be implemented."

The results of the reviewed gap acceptance studies (section 2.3.3) were limited with regard to the level of detail. Different studies investigated traffic situations, but as a result, single characteristic number were reported only, e.g. an average reduction of the time-gap, or an increased number of accepted gaps for a certain mirror type. For the development of the gap acceptance model, it was necessary to gather a sufficient empirical database, which allowed to investigate the impact of different rear view mirrors on gap acceptance behavior in more detail. Field studies could not be done, because this would have required an adequate (closed) road section and real vehicles. Instead, the driving simulator of the C.v.O. University Oldenburg was the preferred option.

Before any driving simulator studies could be conducted, it was necessary to develop a simulation for the different types of rear view mirrors. The results with regard to the mirror simulation are summarized in the first section below. Afterwards, the developed mirror simulation was validated. For this purpose, a distance estimation experiment was conducted in the driving simulator (Experiment 1). The study setting was derived from previous field studies, e.g. [Flannagan1996, Carstengerdes2005]. The objective was to show that the simulator study can reproduce the findings of the field studies with regard to distance estimation with the different mirror types. Afterwards, a lane change study was designed and performed (Experiment 2), and the results served as database for the development of the gap acceptance model.

6.1 Mirror Simulation, Chapter 3

Generally, three different types of driver side mirrors are mounted on real vehicles: planar mirrors, spheric (convex) mirrors and aspheric mirror types. For this work, a simulation for a planar mirror and two different spheric mirror types, C20 and the C14, were used. The surface of a planar mirror is flat, objects are reflected with their true size and no image distortion occurs. This mirror has the smallest field of view of all mirror types. In contrast to the planar mirror,

spheric mirror types have a constantly curved mirror surface which leads to a larger overall field of view. The drawback of this mirror type is that the image is minified and objects are no longer reflected with their true size. The short name C20 means, the curvature of the mirror equals a circle with 2000mm radius. For the C14, this curvature is 1400 mm and the minification effect is even stronger. The implementation of the different mirror types (planar, C20, C14) within the driving simulator was done by adjusting different parameters of the OpenGL visualization of the driving simulator software:

1) The horizontal field of view of the OpenGL view was adjusted to 15.33° for the planar mirror (section 3.3.1). For the C20 and the C14 the field of view was adjusted to 23.6°, respectively 30.9° (section 3.4). These settings lead to a minification factor of 0.58 for the C20 and 0.49 for the C14, which is comparable to the measurements for real C20 and C14 mirrors, published in [NHTSA2008, p. 44].

2) The horizontal and vertical adjustment for the planar mirror type was done according to an empirical procedure, which was derived from the Directive 2003/97/EG from the European Commission [EC2003], (section 3.3.1). The horizontal adjustment of the C20 and C14 was done by adjusting the height of the horizon to the same level as it was shown by the planar. With regard to the vertical adjustment of the curved mirrors, both curved mirrors were turned towards the outside, until the visible portion of the ego vehicle was the same compared to the planar mirror.

The adjustment of the mirrors was done carefully, because [Meyer2013] reported that different mirror adjustments impact the perception of distances. Before the two empirical studies were done, it was also necessary to modify the physical mockup of the driving simulator. Participants of previous studies reported problems to assess the exact position of their own vehicle on the road. To reduce the risk that these problems have a negative impact on the results of the distance estimation study (Experiment 1) as well as the lane change study (Experiment 2), a number of modification were made to improve the simulator and make its appearance more realistic (see section 3.1).

Finally, the calculation of visual angles was implemented in the driving simulator software SILAB (Figure 6.1), because such angles were later on used by the gap acceptance model (details in section 3.6).

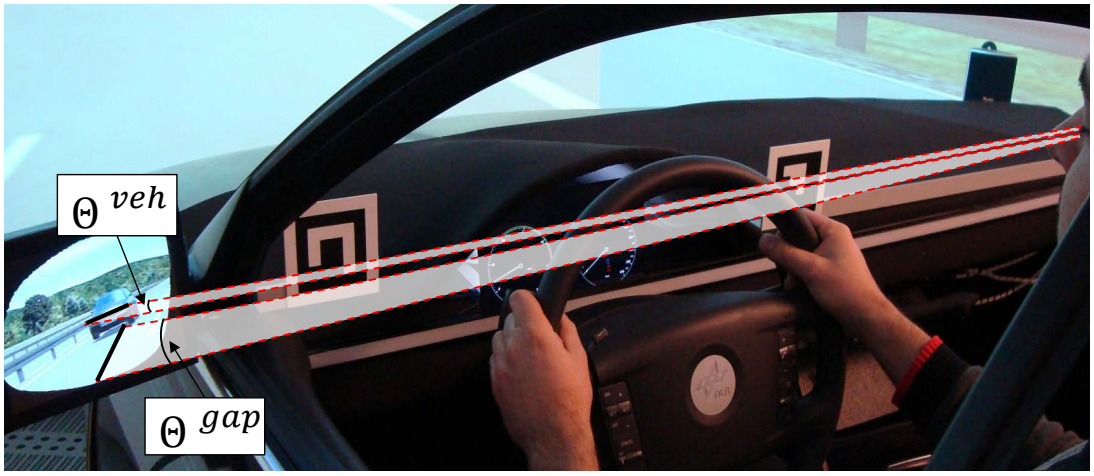

Figure 6.1: Calculation of visual angles: thick, black lines illustrate the *visible gap size* between ego car and rear car, and the *visible vehicle width*, measured across the front width of the rear vehicle. Pixel information about both is available in the simulator, and transformed into a length in millimeter using the pixel resolution of the mirror display. The length in millimeter is used to calculate the corresponding angles: *angular gap size* Θ^{gap} and *angular vehicle width* Θ^{veh}.

6.2 Experiment 1, Chapter 4.1

Figure 6.2 illustrates the scenario of the distance estimation experiment.

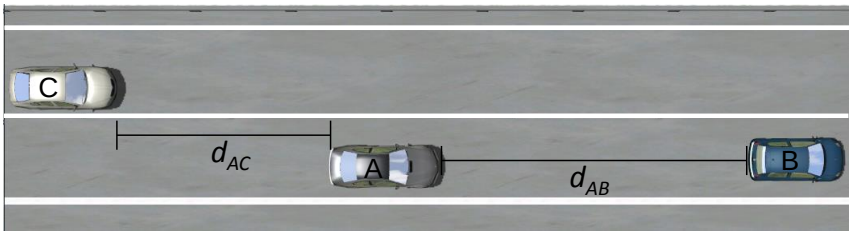

Figure 6.2: Ego vehicle (A), with a lead car (B) located at different distances $d_{AB} = 20$, 40 or 60 meter; The rear vehicle (C) which was set up at one of five relative distances $d_{AC} = d_{AB} * \{70, 85, 100, 115, 130\}\%$. None of the vehicles was moving.

The task of the participants was to estimate the rear car distance d_{AC} in relation to the lead car distance d_{AB}. Estimations had to be given in percent, e.g. 100%, if they thought distances were equal. If it appeared to them that $d_{AC} < d_{AB}$, estimations should be $< 100\%$. Vice versa, if d_{AC} appeared to be larger than d_{AB}, estimations should be $> 100\%$. The magnitude of the percent estimations should equal the perceived difference between the distances, e.g. if d_{AC} appeared to be at half the distance of d_{AB}, the answer should be 50%.

Figure 6.3 shows the experiment scenery as it was seen from the perspective of the participants.

Figure 6.3: Experiment 1 scenario from the perspective of the subjects.

Three hypotheses were tested in this experiment, Hypothesis 1 & 2 were derived from the study of [Carstengerdes2005]. The systematic variation of the lead car distance d_{AB} was not found in the literature and Hypothesis 3 tested its impact on the amount of underestimation.

Hypothesis 1: Drivers underestimate the distance of the rear vehicle (C) when using a simulated, planar mirror.

Hypothesis 2: Increasing the field of view of the simulated mirrors (from Planar to C20 to C14) successively reduces the amount of underestimation compared to the planar mirror.

Hypothesis 3: Increasing the distance of the reference / lead vehicle (d_{AB}) and the dependent rear car distances (d_{AC}) reduces the amount of underestimation.

Table 6.1 shows the result with regard to Hypothesis 1 & 2. The largest amount of underestimation was observed for the planar mirror (25.48%). With increasing mirror curvature, the amount of underestimation successively reduced. For the C14, there was almost no underestimation effect found anymore (0.04%). An ANOVA and a pairwise t-test showed that the differences between each pair of mirrors was significant, Hypothesis 1 & 2 were accepted.

Estimation (%)			
Mirror	Planar	C20	C14
Mean	74.52	91.82	99.96
St.-dev.	23.94	19.03	17.13

Table 6.1: Mean distance estimations accumulated over all subjects.

A quantitative comparison of the amount of underestimation with the study of [Carstengerdes2005] was possible only on the basis of a visual comparison (Figure 4.7, p. 88), but results were comparable. In a similar study setting, [Flannagan1996] reported an underestimation of 35% for the planar mirror. The effect of reduced underestimation with increasing mirror curvature was also found in that study, but the curvature of the convex mirror was 1000 mm, and a quantitative comparison was not possible with the C20 and the C14.

Hypothesis 3 was also accepted, and the amount of underestimation reduced significantly with increasing lead distance. Figure 6.4 shows the mean values of the distance estimations, for all three mirror types, each of the three lead car distances d_{AB} (m) and the five relative rear car distances d_{AC} (%).

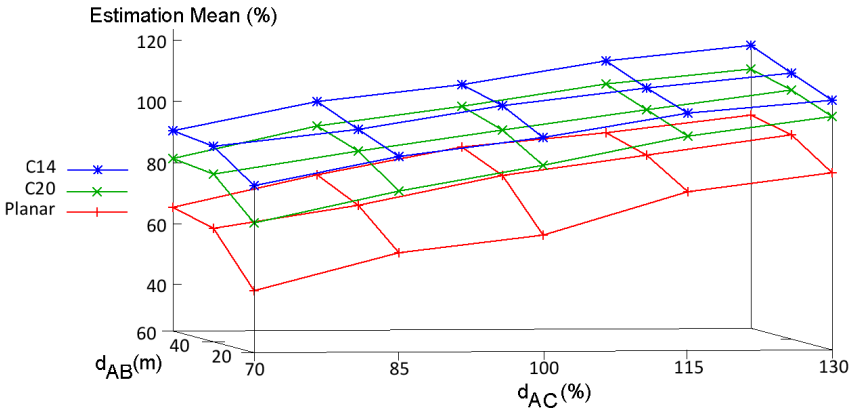

Figure 6.4: Visualization of the mean values from Table 4.2

The effects postulated by the three hypotheses can be seen: with the planar mirror the largest distance underestimation is observed for all 15 combination of d_{AB}, d_{AC}. All mean estimations for the C20 are larger compared to the planar mirror, and similarly all mean estimation for the C14 are larger compared to the C20. With increasing lead car distance d_{AV}, the amount of underestimation also reduces for all rear car distances d_{AC}.

The relative differences between the mirrors with regard to the estimation of distances replicated the published findings in the literature and it could be concluded that the simulated mirrors are comparable to the real mirrors. Unfortunately, a comparison of the quantitative effect was only partially possible, because scenario details vary between all published studies. In this regard, a further field study with the equivalent real mirrors and the same distance combinations would be useful to further validate the mirror simulation. With regard to Hypothesis 3, no comparable literature was found, therefore the significant effect is considered a contribution to the state of the art.

6.3 Experiment 2, Chapter 4.2

The second driving simulator experiment investigated the gap acceptance decision of drivers during a simulated lane change scenario on a two-lane German Autobahn. The scenario is illustrated in Figure 6.5 and the 26 experimental conditions are listed in Table 6.2.

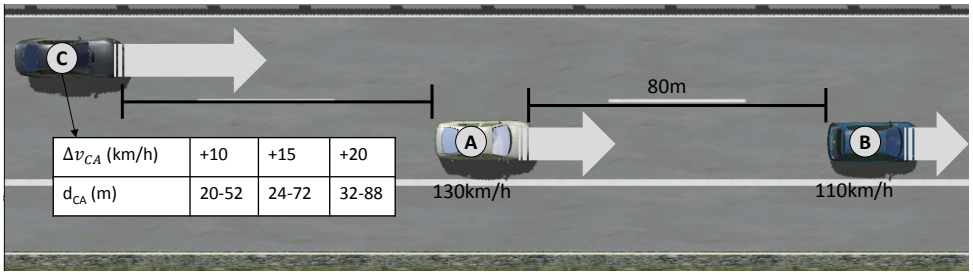

Figure 6.5: Different scenario configurations at each trial start; Ego / subject vehicle (A); slower lead car (B) located 80 meter ahead; faster rear vehicle (C) set up with a higher speed difference Δv_{CA} = {+10, +15, +20} km/h. For each speed difference, (C) was set up at different distances d_{CA} (see Table 6.2.

Δv_{CA} (km/h)	+10	+15	+20
ttc_{init} (s)	d_{CA} (m)		
5.76	-	24	32
7.19	20	30	40
8.63	24	36	48
10.07	38	42	56
11.51	32	48	64
12.95	36	54	72
14.39	40	60	80
15.83	44	66	88
17.27	48	72	-
18.71	52	-	-

Table 6.2: Overview on the 26 experimental conditions for the approaching vehicle C. Distance d_{CA} in meter, which results from the combination of ttc_{init} and speed difference Δv_{CA}.

The 26 experimental conditions were repeated 12 times in one experiment sessions, and each of the 14 participants was invited for three sessions, using a different mirror type each time. The following two hypotheses were tested:

Hypothesis 2.1: The planar mirror leads to the smallest number of lane changes. Increasing the field of view of the simulated mirrors (from Planar to C20 to C14) leads to an increased number of lane changes.

Hypothesis 2.2: With increasing speed difference Δv_{CA}, the number of accepted gaps for situations with equal ttc_{init} will increase.

Hypothesis 2.1 was derived from the results of the first experiment: if the distance is used as gap acceptance cue, a larger underestimation should lead to fewer lane changes for the planar mirror and to successively more lane changes with the curved mirrors.

Hypothesis 2.2 was motivated by the following idea: if the subjects would rely on the time-to-collision to make their lane change decision, the number of accepted gaps should be the same for situations with equal ttc_{init} (a row in Table 6.2). But if ttc_{init} is held constant, the

increasing speed difference automatically leads to an increased distance, because the time-to-collision is calculated by $d_{CA}/\Delta v_{CA}$. It is proposed, that the effect of Hypothesis 2.2 is caused by the increasing distance, which is coupled with the increasing speed. This proposal was based on the findings of [Carstengerdes2005], who tested the impact of different mirror types on the perception of the time-to-collision. He manipulated speed and distance and found that the distance had a stronger influence compared to the speed (independent of the mirror type).

Figure 6.6 shows the accumulated number of lane changes of all 14 participants, for all 26 experiment conditions and all three mirror types.

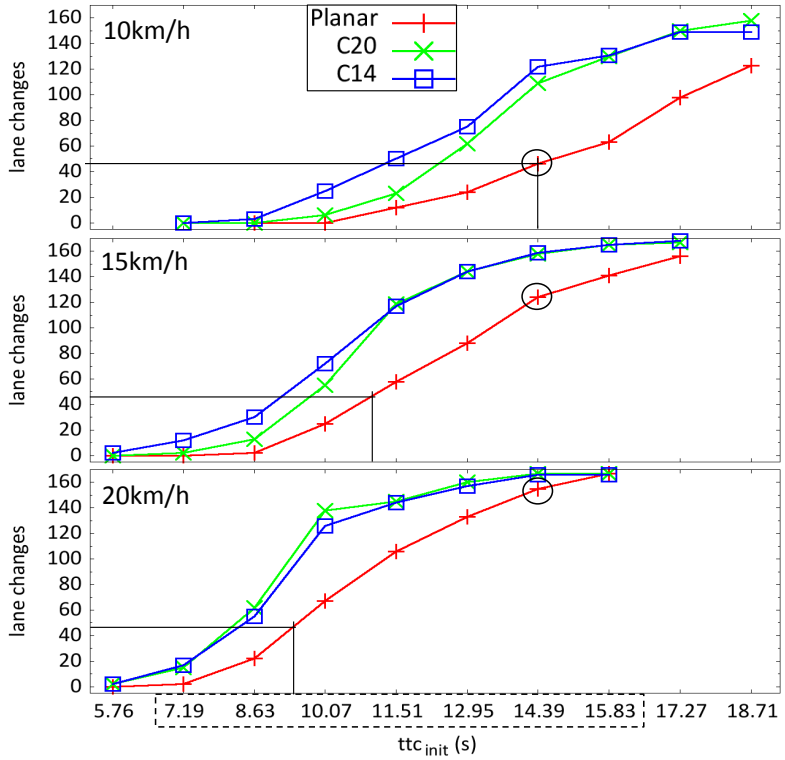

Figure 6.6: Number of lane changes for all three Δv_{CA}; Effect of Hypothesis 2.2 is illustrated at $ttc_{init} = 14.39$ seconds (small circles).

With regard to Hypothesis 2.1, the planar mirror led to the fewest number of lane changes and both curved mirrors led to more lane changes. The results of the ANOVA and t-test analysis were the following: a significant difference in the number of lane changes was found for the two mirror combinations planar - C20 and planar - C14. The two curved mirrors were not significantly different with regard to the number of lane changes. As a result Hypothesis 2.1 was only partially accepted. Hypothesis 2.2 instead was fully accepted for all three speed differences and was found across all mirror types.

A detailed analysis why Hypothesis 2.1 failed partially was done with the following conclusion (section 5.4.2): 1) the difference between C20 and C14 with regard to the characteristic properties field of view and strength of minification is much smaller, compared to the difference between planar vs. C20 and planar vs. C14. 2) Individual behavior differences between the different experiment sessions (one mirror was used in each of the three sessions) were strong

enough to cause multiple violations against Hypothesis 2.1, which reduced the proposed effect between the two mirrors C20 - C14. A follow-up study was proposed, which should allow to separate the individual behavior differences from the effect postulated by Hypothesis 2.1 (conclusion section 5.4.3).

Although Hypothesis 2.1 was only partially accepted, the significant difference between the planar mirror and both curved mirrors supported observations from a previous field study by [deVos2000], who observed a significant reduction of the accepted time-gap for curved mirrors. Previous studies were done exclusively with real mirrors in field studies. Although these studies use the real mirrors, a drawback is that the systematic variation and reproduction of such lane change situations is complex and very time-consuming. The driving simulator offered the possibility to investigate the differences between the mirrors in much more detail, using 26 experiment conditions and 12 repetitions. This database was necessary for the development of the gap acceptance model.

6.4 Gap Acceptance Modeling, Chapter 5

The developed gap acceptance model is able to interact in real-time within the 26 different traffic situations of Experiment 2, similar to the participants. It simulates the gap acceptance behavior of each of the 14 subjects and all 42 experiment sessions (Three sessions per subject, each with a different mirror type). The implementation of the model is based on a first-person viewing perspective, which means it perceives visual information from the perspective of the participants in the experiment (The model "sits" in driver's seat). The simulation of the participant's behavior is realized by a state-machine, and a sequence of four states, which was derived from the task of the participants: 1) Shift gaze from the lead vehicle towards the mirror. 2) Perceive the situation by simulating the "look into the mirror". 3) Make a decision to either accept or reject the gap. 4) Give the appropriate action response by either steering left or braking.

The most important states of the model are the perception state (2) and the decision making state (3). Within the percept state, the model perceives different input variables, and on the basis of the current input value of the variables, the decision making function of the model either accepts or rejects the gap.

The implementation of the first-person perspective suggested that *visual angles*, also called angular measures here, could be used as model variables. Section 5.3 discusses different types of model variables in detail. Three model variables were finally used: 1) the angular gap size Θ^{gap}, 2) its rate of change, the angular velocity Δ^{gap}, and 3) the time-to-collision, specified as $\tau = \frac{\Theta^{veh}}{\Delta^{veh}}$, according to [Lee1976].

With the help of an informal, visual illustration (section 5.5.2), an algorithm was derived (section 5.6.3.2) which matches the observed behavior of each subject and experiment session against each of the three model variables. The variable which receives the highest match is selected as input variable for the model's decision making function. During the simulation of the experiment session, the selected input variable is perceived by the model, and the values are used by the decision making process, which is shown in Figure 6.7.

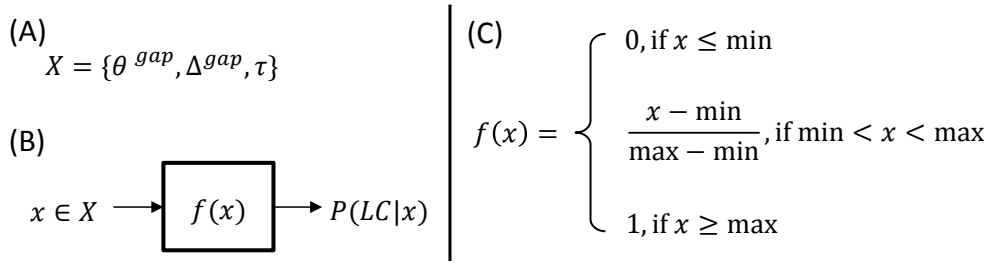

Figure 6.7: (A) X: set of input variables which can be used by the decision making process (angular gap size Θ^{gap}, angular velocity Δ^{gap}, or the time-to-collision, respectively τ; (B) For the simulation of each session, one input variable $x \in X$ is selected to feed the function $f(x)$, which calculates a probability for a lane change maneuver. (C) Implementation of $f(x)$: the probability for a lane change increases from zero to one between min and max.

The selection of the input variable and the configuration of the decision making function $f(x)$ is one part of the model (description, section 5.6.3.2). Another important aspect is the timing behavior of the model, because it interacts in real-time with the Experiment 2 scenario, and the perceived values continuously change. For this purpose, the mean reaction time was derived from the experiment data for each subject and experiment session (reaction time: time measured from the starting point of each trial, until the action response was recorded; mean reaction time: reaction time averaged across all trials of one experiment session). The model gives its action response (braking or steer left) exactly after the mean reaction time expires. Section 5.6.1 describes the state-machine of the model and the timing behavior in more detail.

During the model development, the data of Experiment 2 was utilized from the perspective of Hypothesis 2.2: "With increasing speed difference Δv_{CA}, the number of accepted gaps for situations with equal ttc_{init} will increase". The following results were obtained with regard to the selection of the variables: 1) if no effect size for Hypothesis 2.2 was observed in an experiment session, the time-to-collision was selected. This occurred for 3 out of 42 sessions. 2) if a small effect size for Hypothesis 2.2 was observed, the angular velocity Δ^{gap} was selected (18 sessions). 3) For the remaining 21 sessions the angular gap size Θ^{gap} was selected, and in these sessions, a large effect size was observed for Hypothesis 2.2. Figure 6.8 illustrates the relation between selected variable and the effect size of Hypothesis 2.2.

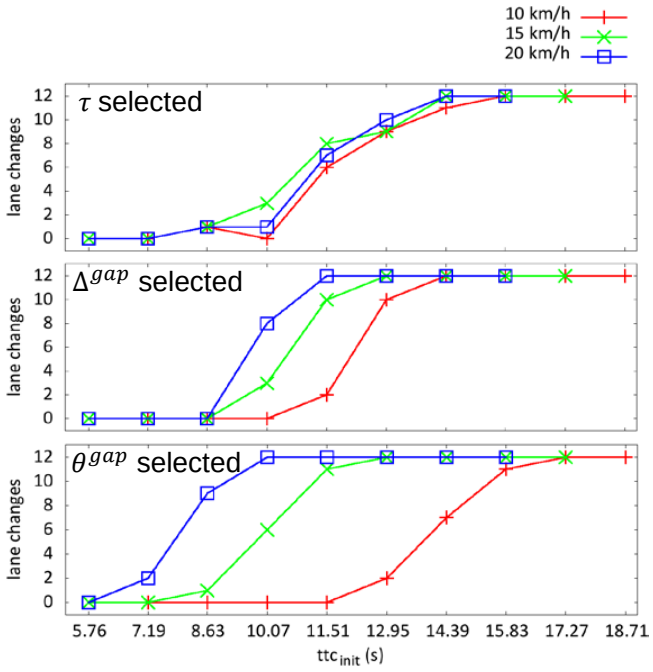

Figure 6.8: Number of lane changes of three experiment sessions: different outcome for the selection of the input variable, dependent on the strength of the Hypothesis 2.2 effect.

Furthermore, the adjustment of the min and max values of the decision making function $f(x)$ realizes two characteristic behavioral properties, which were motivated with the help of the transition region concept (Figure 6.9): "there is a certain region along the ttc_{init} conditions (x-axis in the figure), where the number of lane change decisions continually rises, from braking only (at a smaller ttc_{init} condition) towards lane changes only (at a larger ttc_{init} condition)".

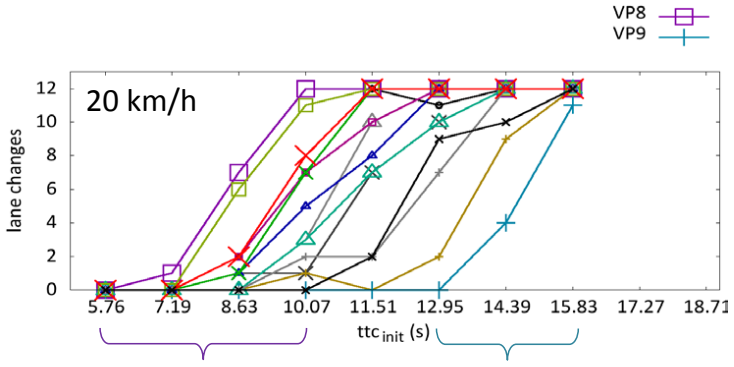

Figure 6.9: Planar mirror sessions, 20 km/h speed difference. Lane change behavior of the 14 subjects. Two transition regions are marked (curly brackets for VP8, VP9). Full figure at p.132

Figure 6.9 shows that the transition regions vary with regard to: 1) their location along the time-to-collision axis (region for VP9 is located at smaller ttc_{init} conditions compared to VP8). 2) their size (how many ttc_{init} conditions are embraced). These properties are derived from

the data and they are used to configure min and max of $f(x)$. In this regard they represent an important part of the individual gap acceptance behavior.

Simulation Results The model was used to simulate six repetitions of Experiment 2 and the simulated number of lane changes was compared against the empirical data of the subjects. Figure 6.10 shows the number of lane changes of one of the six simulated experiment runs in comparison to the data of Experiment 2.

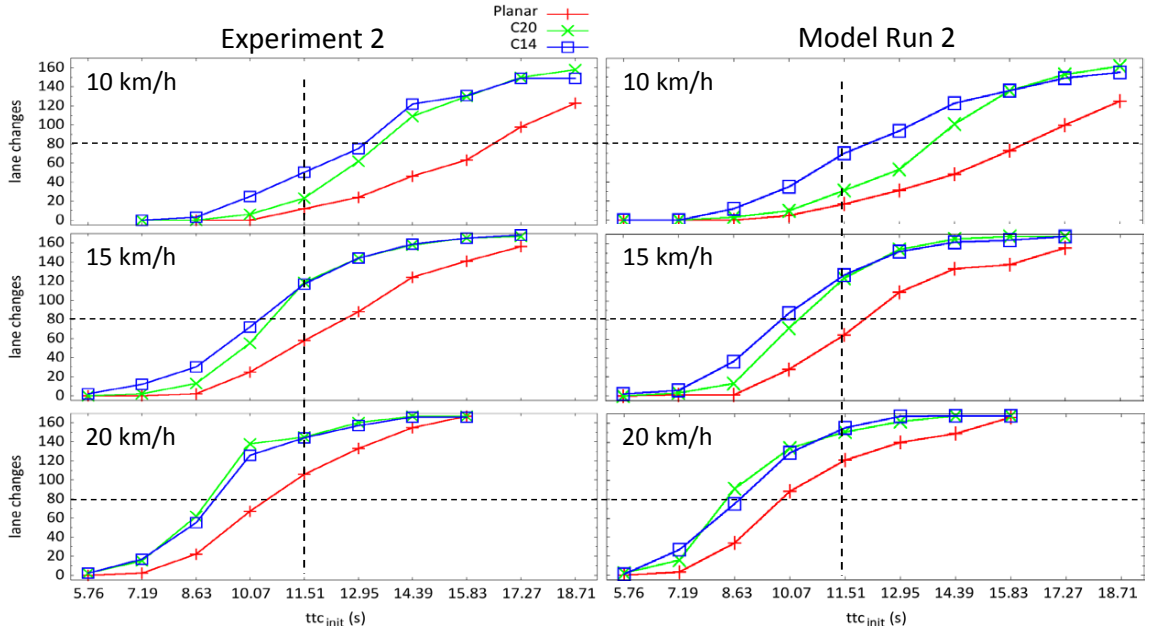

Figure 6.10: Number of lane changes of Experiment 2 (left) and Model Run 2. Comparison is done on the basis of all 42 experiment sessions by the subjects and the corresponding 42 simulated sessions of the model.

The results of Experiment 2 with regard to Hypothesis 2.1 as well as Hypothesis 2.2 are reproduced by model. For each of the six model runs (Run 1 - Run 6) a scatter plot was drawn for each mirror type which compared the empirical data against the simulation results of the model. A linear regression was fitted and the results can be seen in Table 6.3.

	R^2 values derived from scatter plots					
Mirror	Run 1	Run 2	Run 3	Run 4	Run 5	Run 6
Planar	**0.9923**	**0.9869**	0.9912	0.9915	0.9886	0.9893
C20	**0.9918**	0.9888	**0.9854**	0.9878	0.9879	0.9863
C14	0.9873	0.9887	**0.9805**	0.9876	**0.9928**	0.9856

Table 6.3: The largest and smallest R^2 values for each mirror are marked bold.

Although the R^2 values are high, the model overestimated the number of lane changes: 6.57% more lane changes for the planar mirror sessions, 4.1% for the C20 and 5.28% for the C14. Because overestimation was found for all mirrors the relative difference between the

mirrors was only slightly changed, therefore the overestimation did not impact the simulation of the effects of Hypothesis 2.1.

Several potential reasons for the overestimation were investigated, and a slight timing error was discovered in the perception component (approximately 50 ms), which leads to overestimation. Future tests with a revised model implementation have to show how much this already reduces the overestimation. Apart from this implementation bug, further reasons were investigated: overestimation was found for all speed differences, but there were no indications that overestimation increases with increasing speed difference. Overestimation was found for sessions where the angular gap size Θ^{gap} was used by the model, but also for those where the angular velocity Δ^{gap} was used. For the latter ones, the overestimation increased with increasing mirror curvature. In this case, a systematic error with regard to the sampling of Δ^{gap} in the perception component could be excluded

It is possible that the algorithm which estimates the model parameters (especially min, max of $f(x)$) is responsible for the overestimation (description, section 5.6.3.2). A couple of changes to this algorithm were already sketched in the future work section 5.8.2. Although it needs to be tested whether these changes solve the problem of overestimation, they should be implemented anyways, because they replace parts of the algorithm which were already identified as known issues.

Besides the analysis of the results with regard to the two hypotheses of Experiment 2, the simulation of each individual session was analyzed. For this purpose, only the reproducibility with regard to the transition regions was investigated, which excluded those ttc_{init} conditions, where the model decides deterministically for a braking maneuver or a lane change (see $f(x)$, p. 207: $x \leq$ min or $x \geq$ max). The detailed results of the analysis of all 252 simulated sessions (42 experiment sessions, 6 simulated repetitions) are presented in section 5.7.2. The overview table below shows that the R^2 values are considerably lower for this analysis method, but for an assessment of the quality of the probabilistic decision making function the method is more appropriate.

	Mean values of Tables 5.24 - 5.26					
	Run 1	Run 2	Run 3	Run 4	Run 5	Run 6
Planar	0.860	0.856	**0.876**	**0.838**	0.859	0.862
C20	0.842	**0.855**	0.847	0.842	**0.829**	0.853
C14	0.838	**0.830**	0.846	**0.862**	0.845	0.847

Table 6.4: Mean R^2 values for the six experiment runs, compare with Table 6.3 above

For the simulation of the planar mirrors sessions the average R^2 value was 0.859, for the C20 it was 0.845 and for the C14 it was 0.844. Across all 252 simulated sessions, the smallest R^2 value for a single simulated session was 0.584 and the best R^2 value was 0.962.

Comparison with other Models The literature review about driver modeling revealed that the majority of the executable driver models (simulation models) is either dedicated to the driving maneuvers lane-following and car-following, or to the vehicle control abilities of drivers (longitudinal / lateral control behavior). In contrast, the number of executable driver models which is dedicated to the lane change maneuver is comparably small. With regard to lane change decisions and gap acceptance, several models were found in the traffic flow

simulation domain (section 2.2.2), but these models do not focus on individual driver behavior, instead they are used to simulate macroscopic traffic flow effects. They also rely on measures like distance in meter or speed in km/h. Section 5.3 explained, why these measures were not preferred in this thesis.

In the domain of cognitive driver modeling, [Salvucci2002, Salvucci2006] described the development of an executable driver behavior model which interacts within a driving simulator, similar to the model developed in this work. In contrast to this work, their focus was not on gap acceptance. With regard to a lane change left maneuver, their model used a fixed distance threshold for gap acceptance, which was set to 40 m according to [Salvucci2006]. Authors mentioned that the model used a rear-view mirror to observe the traffic from behind, but no specific details about the implementation were given. Because their model used a fixed distance in meter as decision making criterion, it can be assumed that mirror view implementation is different from the approach in this work. Additionally, this work investigated changes to the gap acceptance behavior if different mirror types are used and this was not considered by any model before.

The gap acceptance model in this work was inspired by the idea of the first-person perspective of the driver, which in turn was the motivation to investigate the three variables Θ^{gap}, Δ^{gap} and τ. The decision to investigate all three of these variables was based on the findings of Experiment 2 and an individual behavior analysis (sections 5.3 and 5.4). The published work of [Regan1993, Regan1995] was important for this decision, too, because they reported that the visual pathway is sensitive to the angular size of objects, as well as the angular velocity and also τ.

The finding that individual behavior differences, which were observed in Experiment 2, can be matched onto these variables, indicates that different subjects probably rely on these different situational cues. However, these results should be considered with care, because the number of subjects in Experiment 2 was selected to test the two hypotheses on the basis of the accumulated data of all subjects. Further experiments are necessary to increase the database, and clearly identify individual driver behavior "strategies" amongst a larger driver population. But there is already some support that such behavioral differences can be found in gap acceptance behavior: [Gray2005] reported that drivers rely on different gap acceptance strategies during overtaking on rural roads with oncoming traffic. They investigated three strategies: a distance-based strategy, a strategy according to the rate of expansion (angular velocity) of the opposing vehicle, and a temporal margin strategy (details on this study, see p. 49 and Figure 2.12). Their results showed that each of these strategies was used by a number of subjects.

Finally, the a conclusion is drawn with regard to the two main objectives of this work:

Objective 1: "This work will investigate the impact of different types of rear view mirrors (driver-side only) with regard to their influence on the driver's gap acceptance behavior. The scenario of interest is the lane change left maneuver on a two-lane freeway (German Autobahn)."

Objective 2: "A behavior simulation model will be developed which is able to simulate the findings with regard to Objective 1. A previously developed and published gap acceptance model [Weber2013] will be reviewed, and if necessary, modifications will be implemented."

Objective 1 was tackled by the implementation of the mirror simulation and the two driving simulator studies. The results of Experiment 2 fulfilled the requirement to "investigate the impact of different types of rear view mirrors (driver-side only) with regard to their influence on the driver's gap acceptance behavior".

An executable driver behavior model was developed, which was able to simulate the observed behavioral findings of Experiment 2 with regard to both hypotheses. Before this thesis was started, I was involved in the development of another executable driver model (section 5.1, [Weber2013]). That model drew its decision on the basis of the angular velocity Δ^{veh} (see Figure 6.1), and a single decision making threshold. The model developed in this thesis is able to simulate individual behavior differences with regard to the effect strength of Hypothesis 2.2 by selecting one of the three input variables. It also realizes the behavioral differences that were explained with the help of the transition region (see Figure 6.9 above). In this regard, the concepts of the previously developed model were reviewed and revised and Objective 2 was fulfilled.

However, the implementation of the model, and especially the implementation of the decision making function including the parameter estimation procedure (section 5.6.3.1) has some known issues. Alternative solutions were proposed in the future work section (5.8.2), and it is expected that their implementation improves the estimation of the transition region boundaries and leads to a better performance of the model.

7 Annex

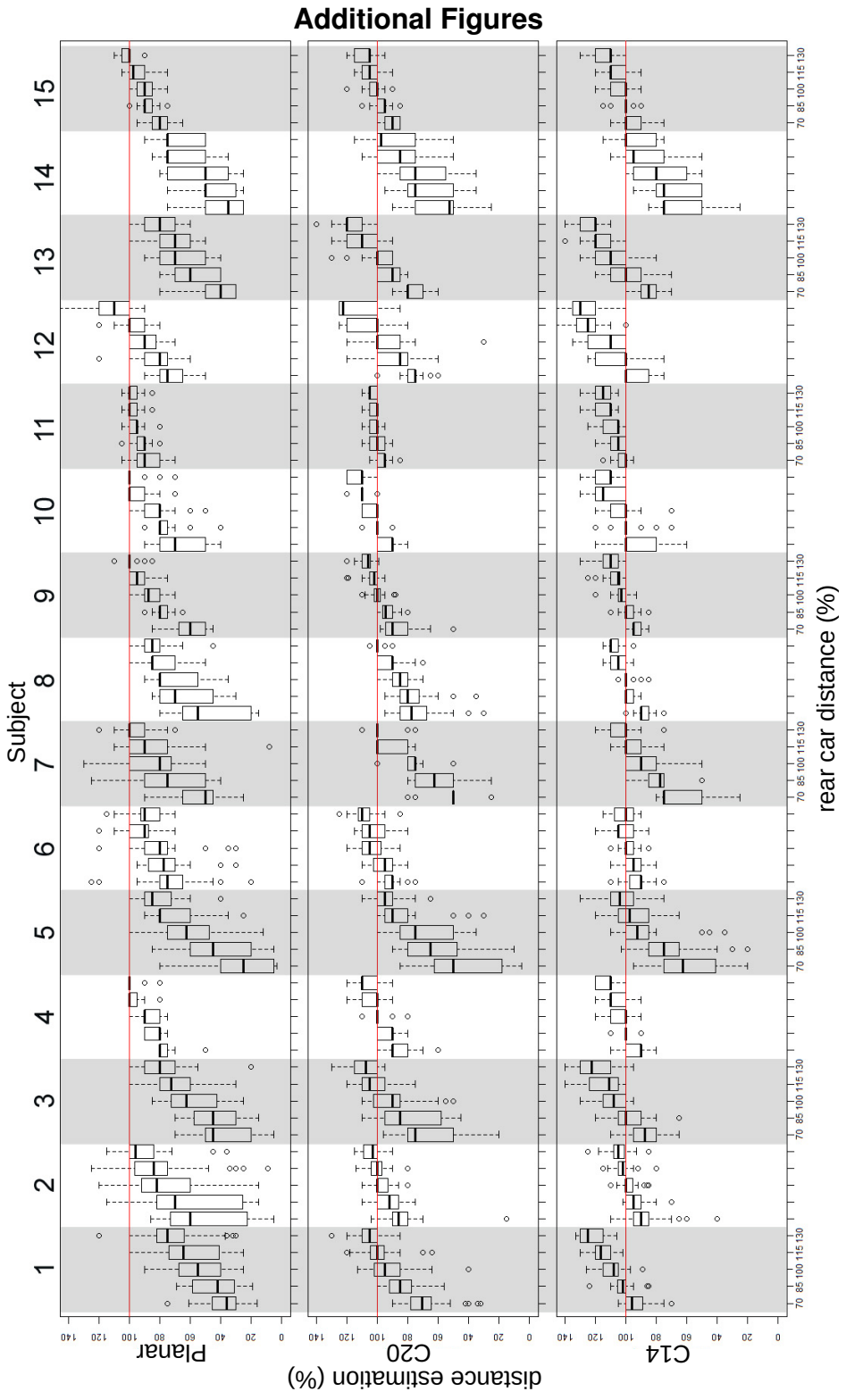

Figure 7.1: Large version of Figure 4.4, p. 80

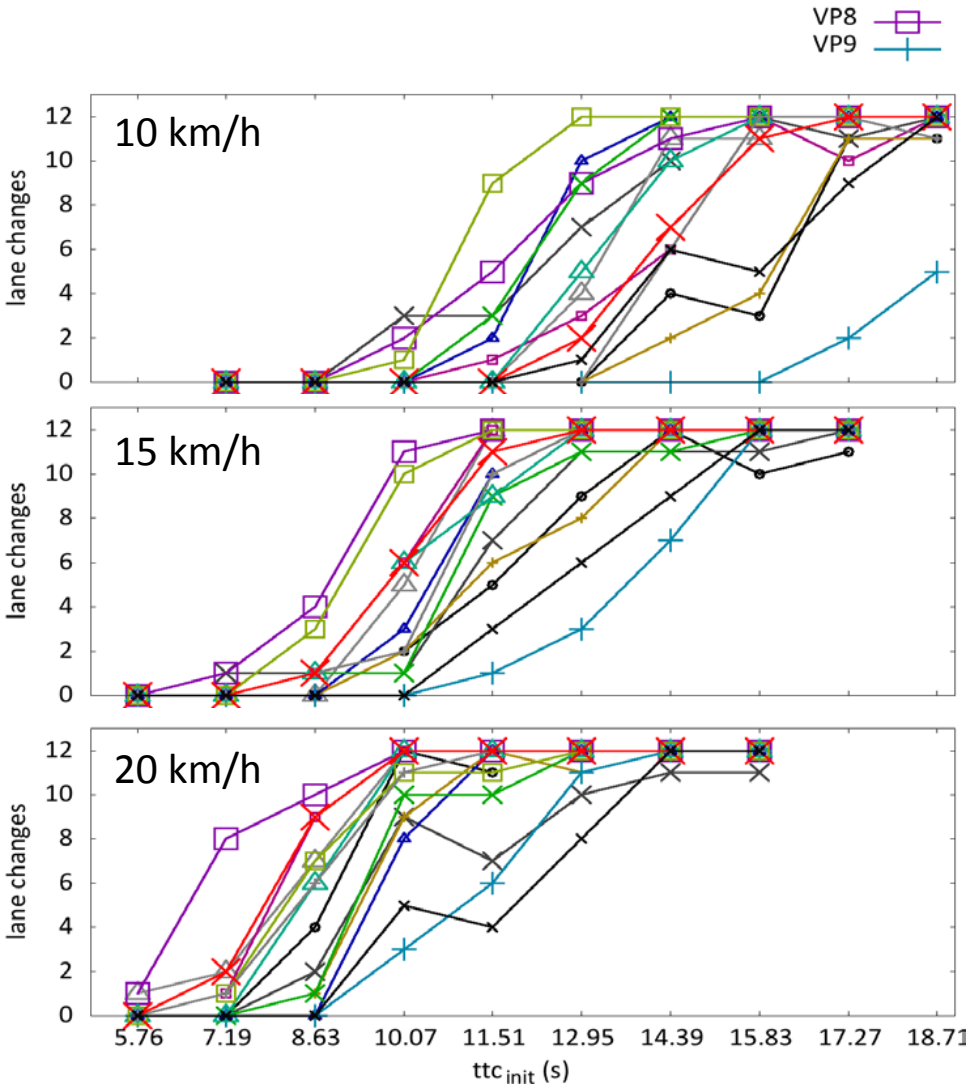

Figure 7.2: C20 mirror data per subject. Explanation can be found in section 5.4, p. 115

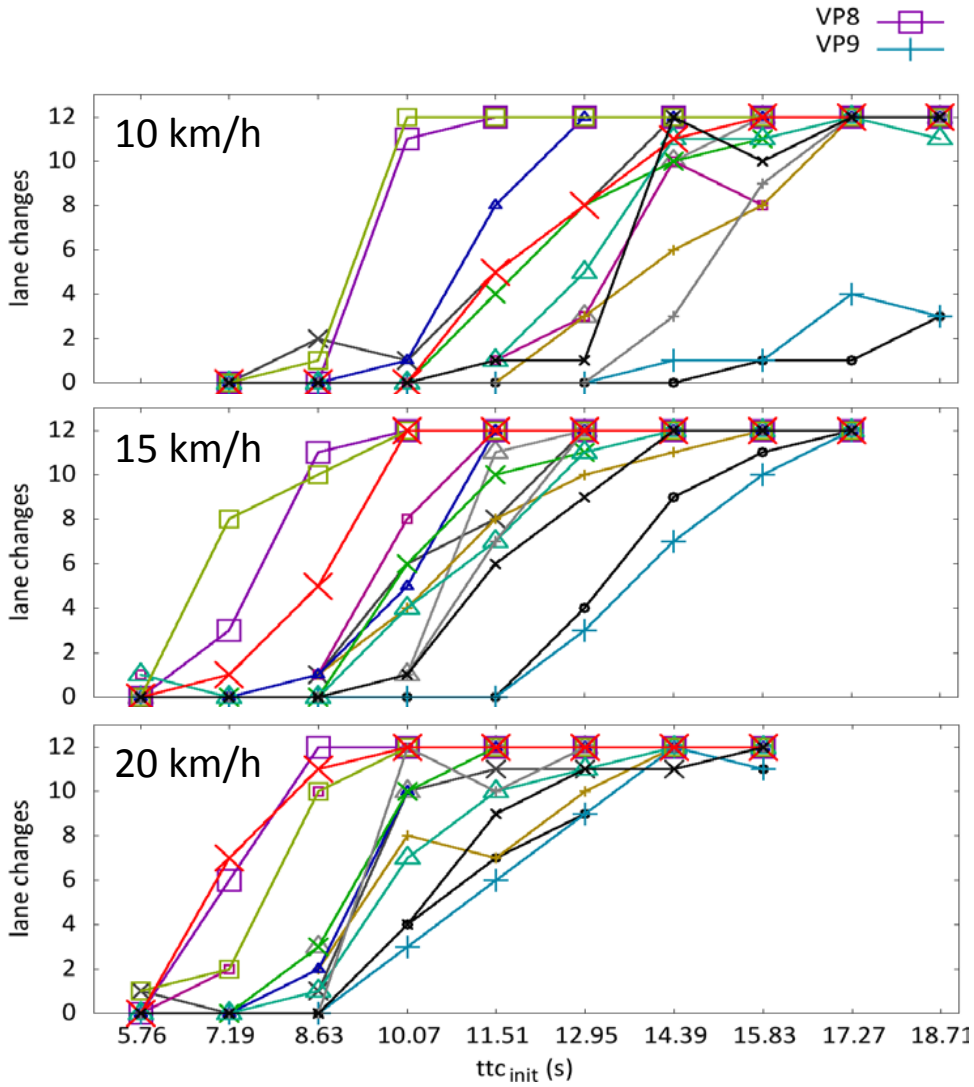

Figure 7.3: C14 mirror data per subject. Explanation can be found in section 5.4, p. 115

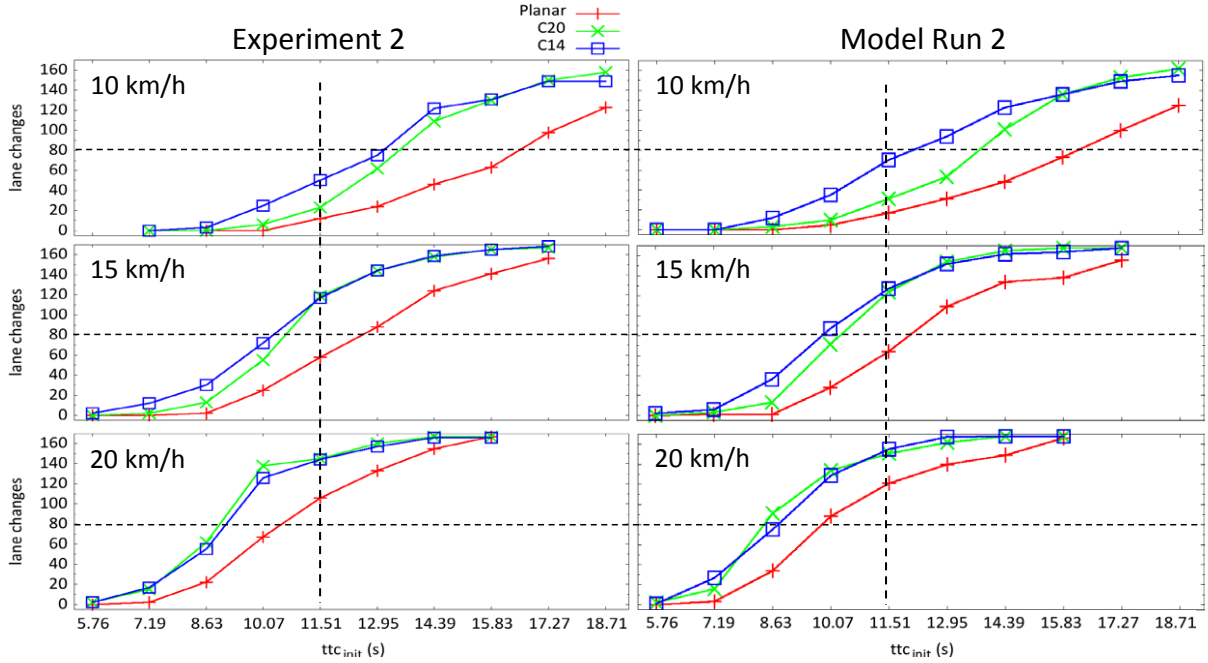

Figure 7.4: Number of lane changes of Experiment 2 (left) and Model Run 2.

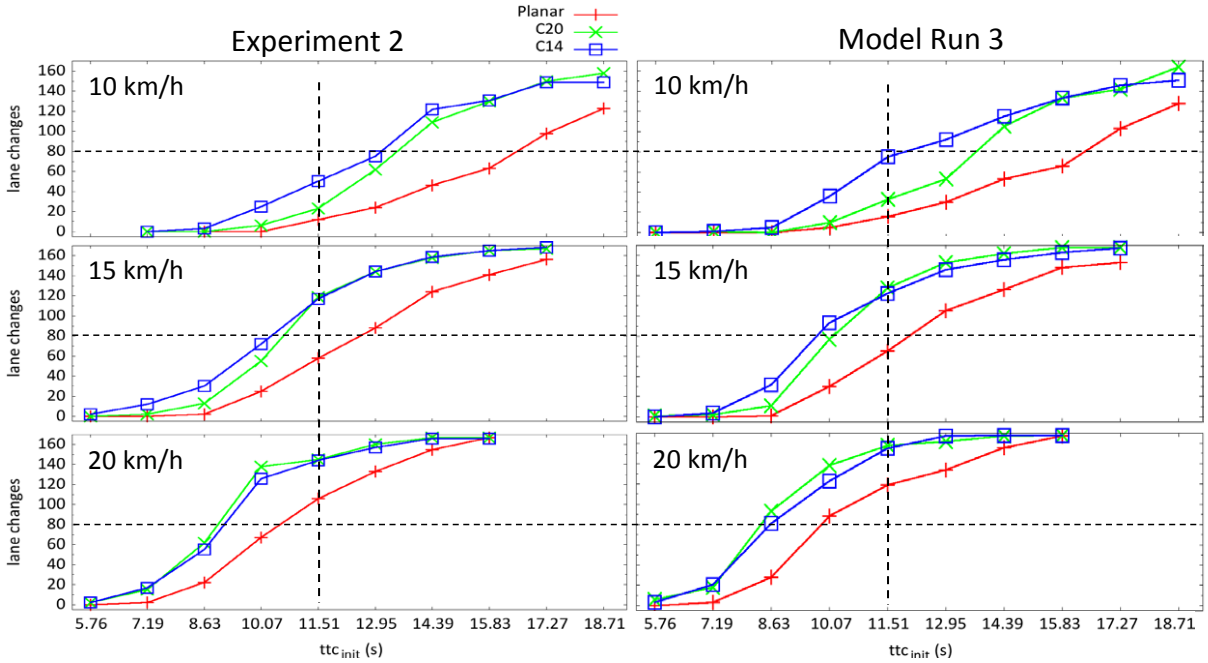

Figure 7.5: Number of lane changes of Experiment 2 (left) and Model Run 3.

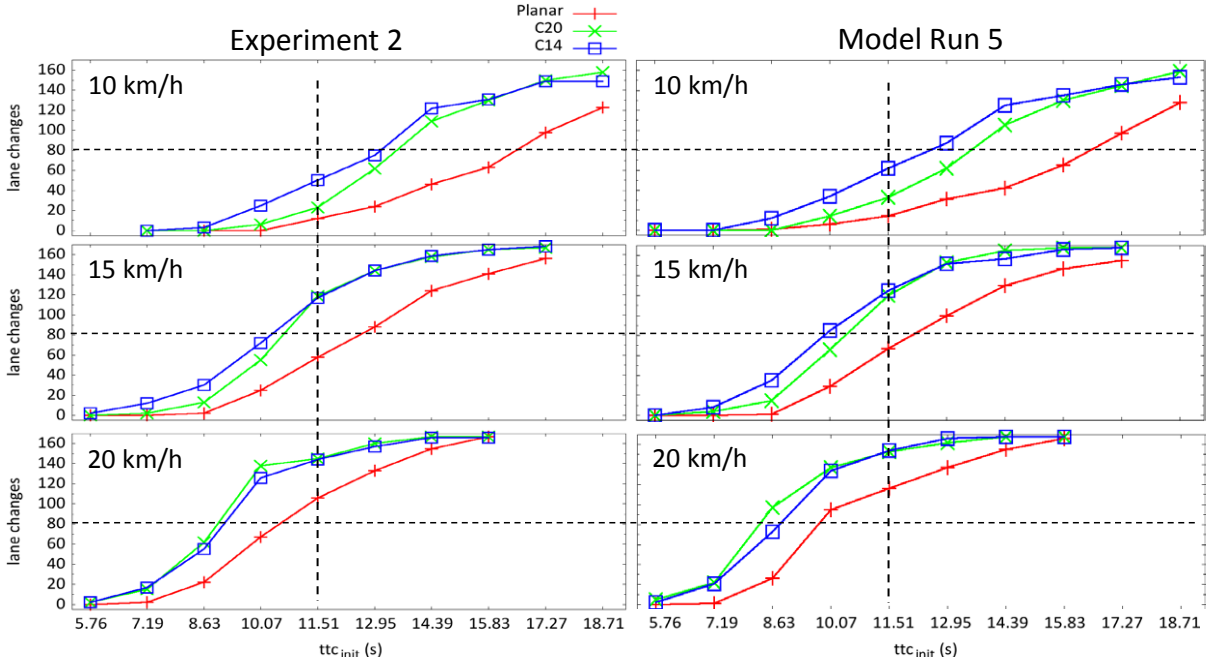

Figure 7.6: Number of lane changes of Experiment 2 (left) and Model Run 5.

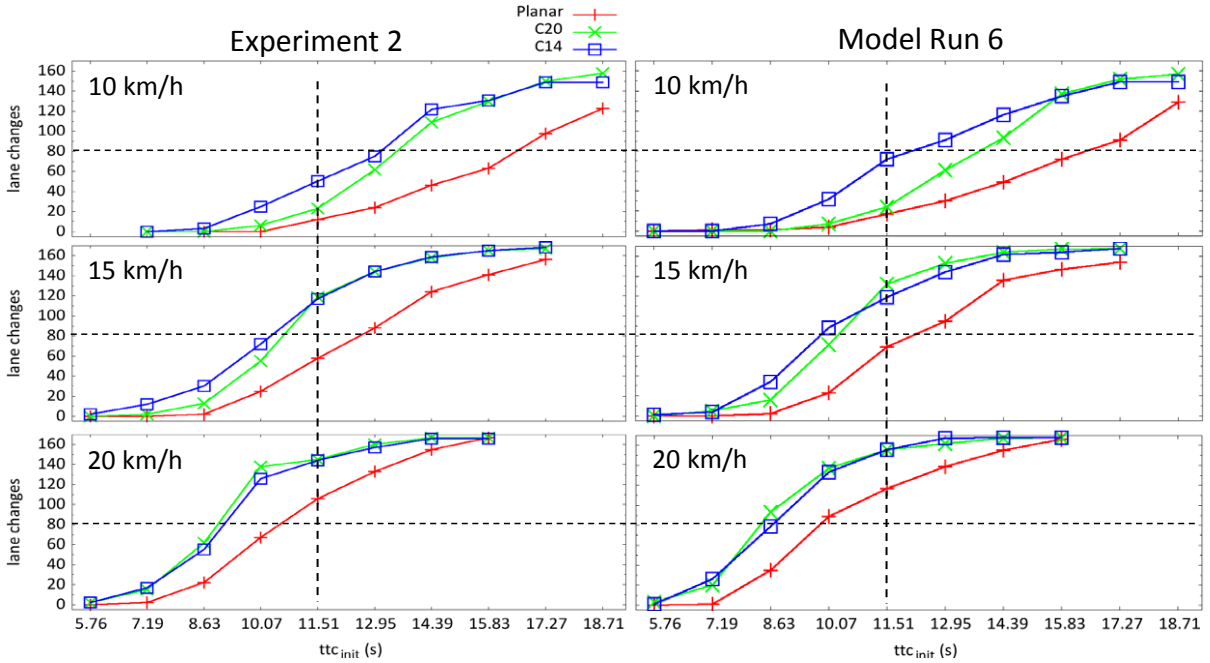

Figure 7.7: Number of lane changes of Experiment 2 (left) and Model Run 6.

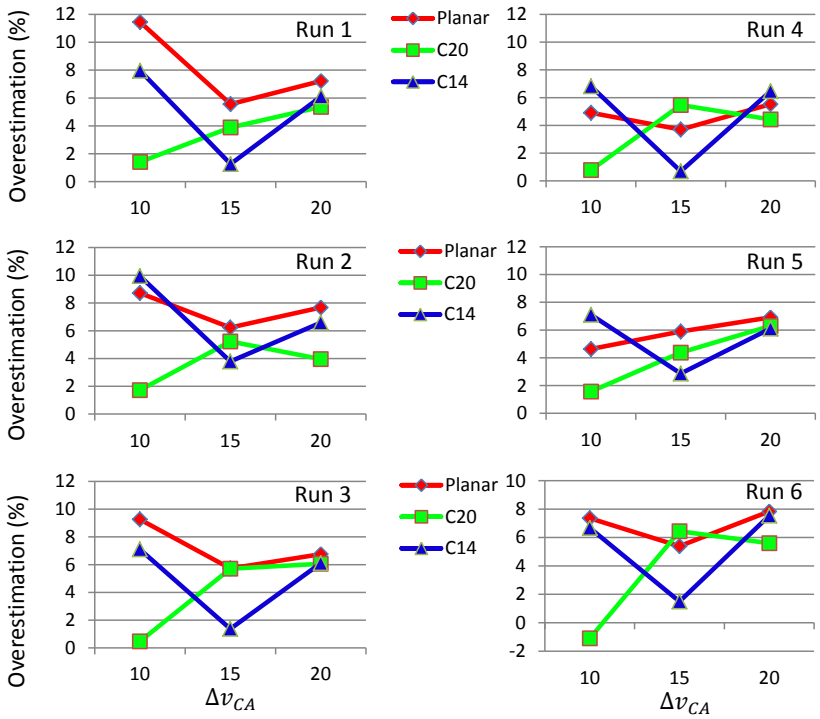

Figure 7.8: Overestimation per simulation run separated according to mirror type and speed difference Δv_{CA}. Especially the results of Run 1,2,3 and 6 are similar to each other.

Supplementary Tables

	Overlap O, used to configure min, max of $f(x)$					
VP	Planar		C20		C14	
	$[\Theta_{max} - \Theta_{min}]$	$[\Delta_{min} - \Delta_{max}]$	$[\Theta_{max} - \Theta_{min}]$	$[\Delta_{min} - \Delta_{max}]$	$[\Theta_{max} - \Theta_{min}]$	$[\Delta_{min} - \Delta_{max}]$
6	$[0.101 - 0.112]$		$[0.111 - 0.119]$		$[0.119 - 0.127]$	
1	$[0.098 - 0.108]$		$[0.115 - 0.119]$		$[0.127 - 0.132]$	
4	$[0.102 - 0.111]$		$[0.112 - 0.119]$		$[0.122 - 0.129]$	
9	$[0.113 - 0.117]$		$[0.117 - 0.123]$		$[0.128 - 0.132]$	
7		$[0.0014 - 0.0032]$		$[0.0015 - 0.0025]$		$[0.0013 - 0.0025]$
10		$[0.0019 - 0.0031]$		$[0.0014 - 0.0027]$		$[0.0015 - 0.0025]$
14		$[0.0011 - 0.0020]$		$[0.0008 - 0.0020]$		$[0.0010 - 0.0026]$
2	*ttc [5.82-11.10] (sec)		*ttc [5.40-11.00] (sec)			$[0.0013 - 0.0044]$
8		$[0.0029 - 0.0039]$	$[0.106 - 0.116]$			$[0.0016 - 0.0027]$
13		$[0.0011 - 0.0016]$	$[0.114 - 0.118]$			$[0.0009 - 0.0011]$
11	$[0.102 - 0.108]$		$[0.113 - 0.117]$			$[0.0009 - 0.0021]$
3	$[0.104 - 0.109]$		$[0.113 - 0.118]$			$[0.0009 - 0.0017]$
12	$[0.098 - 0.109]$			$[0.0016 - 0.0033]$		$[0.0019 - 0.0033]$
5		$[0.0010 - 0.0018]$	$[0.116 - 0.121]$		*ttc [6.45-8.10] (sec)	

Table 7.1: Values for overlap O for the measure which received the highest value for S; *time-to-collision received the highest value for S. For configuration purposes, 1.19s have to be added, because τ has a constant offset (see Remark below Figure 5.4, p. 111).

Planar	**Overestimation, Error**						
VP	Run 1	Run 2	Run 3	Run 4	Run 5	Run 6	Mean 1-6
1	15, 21	23, 25	22, 24	16, 24	15, 25	21, 23	18.7, 23.7
2	-11, 21	-16, 24	-13, 27	-15, 23	-4, 22	-19, 29	-13.0, 24.3
3	32, 32	23, 27	11, 15	7, 21	11, 23	7, 19	15.2, 22.8
4	13, 17	-1, 15	-1, 21	0, 12	5, 17	2, 14	3.0, 16.0
5	19, 23	16, 24	14, 16	19, 21	16, 16	17, 19	16.8, 19.8
6	-9, 17	4, 18	3, 15	-1, 19	-4, 14	-3, 11	-1.7, 15.7
7	6, 16	9, 17	10, 18	-1, 17	8, 18	5, 13	6.2, 16.5
8	8, 10	6, 8	6, 8	12, 14	8, 10	10, 10	8.3, 10.0
9	-1, 3	-6, 6	-3, 3	-3, 7	-5, 5	-3, 5	-3.5, 4.8
10	-7, 13	0, 10	-6, 12	-1, 9	-8, 12	0, 10	-3.2, 11.0
11	-3, 23	16, 24	12, 24	16, 26	14, 20	18, 28	12.2, 24.2
12	1, 17	-4, 18	3, 19	-5,15	4, 22	1, 21	0.0, 18.7
13	-10, 18	-9, 13	-12, 14	-16, 22	-7, 13	-7, 13	-10.2, 15.5
14	12, 14	9, 17	10, 20	5, 23	8, 20	10, 18	9.0, 18.7
						Mean	4.1, 17.26

Table 7.2: Comparison of the 84 simulated planar mirror sessions (Run 1-6) against the corresponding subject experiment session (VP1-14). Overestimation (+) and underestimation (-) of the number of lane changes.

C20	**Overestimation, Error**						
VP	Run 1	Run 2	Run 3	Run 4	Run 5	Run 6	Mean 1-6
1	6, 14	7, 17	6, 14	7, 11	-5, 19	9, 15	5.0, 15.0
2	-14, 34	-13, 37	-6, 28	-17, 31	-8, 40	-10, 26	-11.3, 32.7
3	-4, 18	-10, 16	-3, 19	-2, 16	0, 20	-4, 14	-3.8, 17.2
4	-1, 11	0, 10	3, 15	7, 17	-2, 16	3, 15	1.7, 14.0
5	11, 21	9, 15	8, 20	9, 17	9, 23	8, 18	9.0, 19.0
6	1, 9	-3, 7	5, 7	-3, 9	10, 12	2, 8	2.0, 8.7
7	16, 18	9, 13	8, 12	10, 14	7, 7	9, 15	9.8, 13.2
8	9, 17	6, 14	13, 19	17, 21	12, 16	15, 19	12.0, 17.7
9	15, 17	14, 14	17, 19	16, 20	14, 16	12, 16	14.7, 17.0
10	4, 20	2, 26	15, 25	10, 22	7, 15	4, 20	7.0, 21.3
11	-1, 19	-2, 20	2, 18	-1, 19	-1, 19	2, 22	-0.2, 19.5
12	0, 8	5, 9	0, 10	3, 11	6, 12	-2, 10	2.0, 10.0
13	12, 16	13, 17	8, 14	10, 14	14, 16	12, 18	11.5, 15.8
14	21, 27	21, 21	15, 17	12, 24	24, 28	20, 24	18.8, 23.5
						Mean	5.58, 17.46

Table 7.3: Comparison of the 84 simulated C20 mirror sessions (Run 1-6) against the corresponding subject experiment session (VP1-14). Overestimation (+) and underestimation (-) of the number of lane changes.

C14	**Overestimation, Error**						
VP	Run 1	Run 2	Run 3	Run 4	Run 5	Run 6	Mean 1-6
1	10, 20	10, 16	7, 11	2, 16	15, 21	13, 5	8.2, 16.2
2	20, 30	20, 26	19, 27	13, 25	11, 21	20, 14	16.2, 24.8
3	3, 9	10, 24	7, 23	7, 17	0, 10	22, 8	5.8, 17.5
4	-1, 7	10, 16	-1, 13	-4, 18	0, 8	14, 0	0.7, 12.7
5	5, 23	12, 26	16, 24	-1, 25	7, 25	23, 11	8.3, 24.3
6	5, 13	-2 , 8	1 , 11	2, 12	9, 17	13, 5	3.3, 12.3
7	21, 21	20, 20	18, 22	16, 16	13, 15	19, 17	17.5, 18.8
8	-10, 16	-5, 17	-2, 8	-1, 9	-6, 16	13, -9	-5.5, 13.2
9	5 , 13	8 , 16	0, 16	8, 20	2, 12	13, 7	5.0, 15
10	18, 26	17, 17	19, 19	22, 24	19, 25	21, 21	19.3, 22
11	9 , 19	9 , 15	6, 8	6, 14	11, 13	12, 6	7.8, 13.5
12	2 , 22	10, 20	-3, 11	7, 13	2, 20	22, 4	3.7, 18
13	19, 19	17, 21	13, 23	21, 21	22, 22	24, 18	18.3, 21.7
14	7 , 19	22, 26	8, 24	12, 20	18, 22	18, 14	13.5, 21.5
						Mean	8.72, 17.96

Table 7.4: Comparison of the 84 simulated C14 mirror sessions (Run 1-6) against the corresponding subject experiment session (VP1-14). Overestimation (+) and underestimation (-) of the number of lane changes.

Empirical Procedure to Create an Aspheric Mirror Type Simulation As explained in the main part of this work, I originally planned to use an aspherical mirror type also. Although the driving simulation software SILAB allowed to implement the visual characteristics of such a mirror (explained below), the visual distortion effects for the aspheric mirror portion were calculated on the graphics card. The 3D object coordinates of the vehicles were not transformed and the calculation of the visual angles was not correct. Nevertheless, the procedure how this mirror was implemented is presented here.

The adjustment of the field of view of the OpenGL window is not sufficient to simulate the visual characteristics of an aspheric mirror. SILAB offers the possibility to manipulate / distort an OpenGL view with a bezier curved patch which has a $5*5$ control point matrix. The question was: "How to adjust the patch to simulate the distortion effects of the aspheric mirror portion ?"

A set of photos was made in a real car from the drivers perspective and a number of reference objects was located in the vicinity of the vehicle to make the distortion visible. These photos were then used to adjust the bezier matrix accordingly.

Figure 7.9 shows the basic setting: a $3 * 3$ field of small pylons was positioned behind a real vehicle. The pylons were located at consecutive 5 m distances longitudinal and 2m lateral. A camera was mounted at the drivers' seat and oriented towards the mirror. Figure 7.10 shows a reference object which is used to visualize the horizontal distortion of the aspheric mirror. The mirror view at the bottom right was used as reference to build the simulated mirror in SILAB.

Figure 7.9: *Top*: Positioning of the test vehicle. The pylons are located in 5m distances backwards and 2m distances sidewards *Middle*: Positioning of the camera in the test vehicle. *Bottom*: The mirror was adjusted horizontally until the first row of the pylons just disappeared from the bottom of the mirror.

Figure 7.10: *Top*: Positioning of the reference object in 75 cm distance to the mirror. The height was adjusted to equal the center of the mirror. *Bottom*: The photo taken from the drivers perspective from the exact same position as in Figure 7.9

In the upper part of Figure 7.11 two photos (taken from the exact same position) were merged: one with and one without the reference object. This was necessary, because the tripod of the reference object covered one of the pylons. Furthermore, each 5th bar of the reference object was elongated using an image manipulation tool.

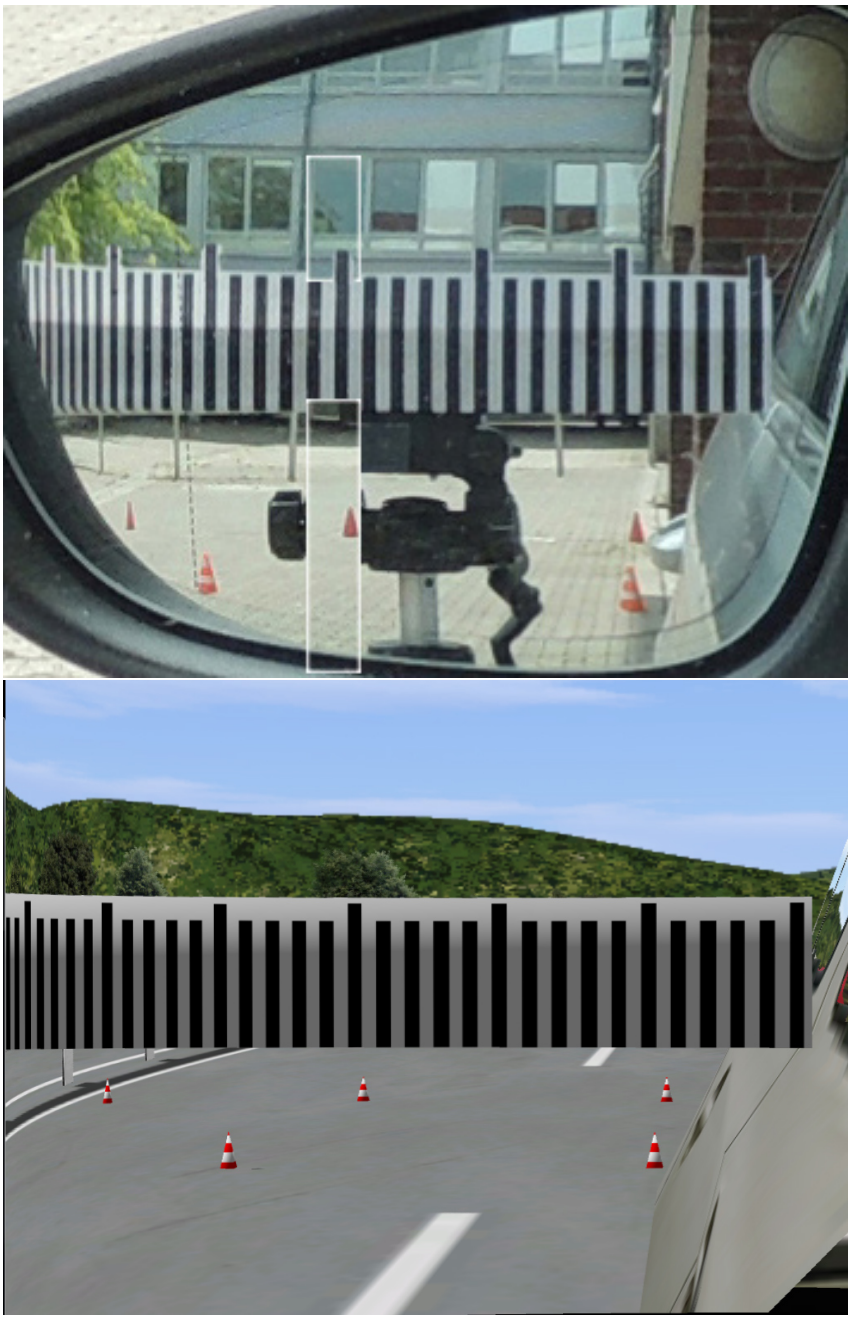

Figure 7.11: *Top*: Pylons and the reference object are combined into one image. *Bottom*: Simulated aspheric mirror in driving simulator software SILAB. Remark: the display is covered and only the shape of the mirror is visible, not the full rectangular view as seen here. Degree of similarity can be compared by putting a rules across the two figures.

The bottom part of Figure 7.11 shows the simulated aspheric mirror in SILAB. It was realized using a 5*5 Bezier Distortion Matrix to create the spheric and aspheric portion of the mirror. The effect is visible at the outer 12-15 bars.

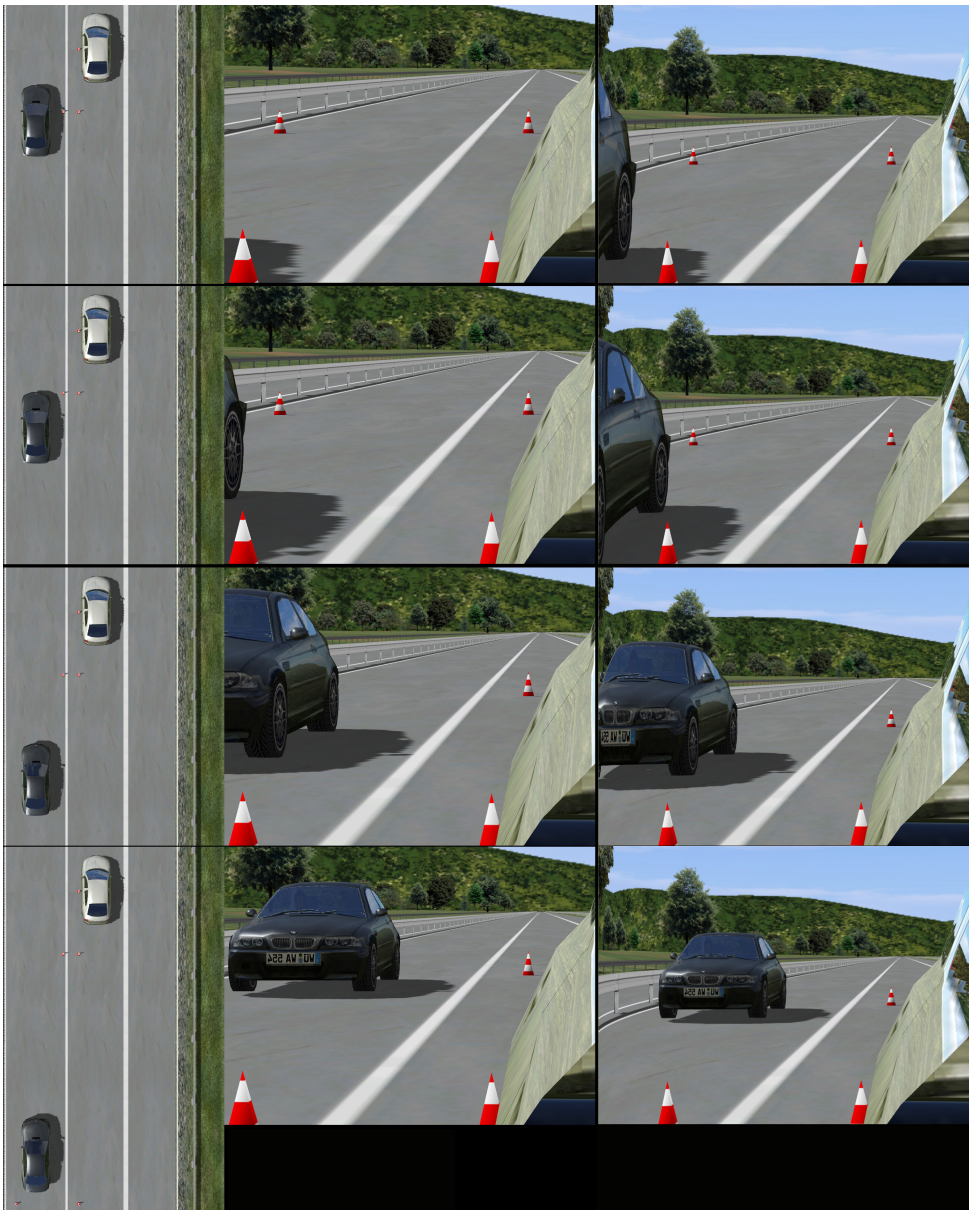

Figure 7.12: Comparison of the planar mirror (middle column) and the distortion of the aspheric mirror model (right column). Due to the convex inner part the fov is increased also in comparison to the planar mirror (compare horizontal position of lower left pylon). The left column shows the bird's eye view on the scenery. From top to bottom the four bumper to bumper distances between ego and rear car are shown: 0, 1.6, 6 and 12 meter

.

8 Bibliography

[Aasman1995] Jannes Aasman. *Modelling Driver Behaviour in Soar*. PhD thesis, Rijksuniveriteit Groningen, May 1995.

[Ahmed1999] Kazi Iftekhar Ahmed. *Modeling Drivers' Acceleration and Lane Changing Behavior*. PhD thesis, MIT, 1999.

[Albers2010] A Albers, T. Düser, O. Sander, C. Roth, and J. Henning. X-in-the-Loop- Framework für Fahrzeuge, Steuergeräte und Kommunikationssysteme. *ATZ elektronik*, 5(5):60–65, 2010.

[Anderson2004] J. R. Anderson, D. Bothell, M. D. Byrne, S. Douglass, C. Lebiere, and Y. Qin. An integrated theory of the mind. *Psychological Review*, 11:1036–1060, 2004.

[Anderson2007] G.J. Anderson and C.W. Sauer. Optical information for car following: The driving by visual angle (dva) model. *Human Factors*, 49:878 – 896, 2007.

[Anderson2009] J.R. Anderson and N.A. Taatgen. The past, present and future of cognitive architectures. *Topics in Cognitive Science*, 2(4):1–12, 2009.

[Bach2006] P. Bach, G. Rüter, N. Carstengerdes, Wender K.F., and D. Otte. Untersuchung von Verkehrssicherheitsaspekten durch die Verwendung asphärischer Aussenspiegel. Technical report, bast, 2006.

[Baumann2009] M.R.K. Baumann and J.F. Krems. A comprehension based cognitive model of situation awareness. In *Digital Human Modeling: HCI 2009*. Springer, 2009.

[Baumann2010] M. Baumann, R. Steenken, A. Kassner, L. Weber, and A. Lüdtke. Effects of situational characteristics on drivers' merging into freeway traffic. In *Human Modelling in Assisted Transportation*. Springer, 2010.

[Bellet1999] T. Bellet and H. Tattegrain-Veste. A framework for representing driving knowledge. *International Journal of cognitive ergonomics*, 3:37 – 49, 1999.

[Bellet2011] T. Bellet, P. Mayenove, J.C. Bornard, J.C. Paris, D. Gruyer, and B. Claverie. *Human modelling in assisted transportation: models, tools and risk methods*, chapter Human driver modeling and simulation into a virtual road environment, pages 251 – 262. Milan, Springer, 2011.

[Bi2009] L.-Z. Bi and Liu Y. Modeling driver car-following based on the queuing network cognitive architecture. In *Proceedings of the eighth internaction conference on machine learning and cybernetics*, 2009.

[Boer1998] E.R. Boer and M. Hoedemaeker. Modeling driver behavior with different degrees of automation: aa hierarchical decision framework of interacting mental models. In *Conference on human decision making and manual control*, 1998.

[Bothell2017] D. Bothell. *ACT-R 6.0 Reference Manual (Working Draft)*, 2017.

[Brackstone1999] M. Brackstone and M. Mcdonald. Car-following: a historical review. *Transportation Research Part F*, 2:181 – 196, 1999.

[Bruce2003] V. Bruce, P.R. Green, and M.A. Georgeson. *Visual Perception: physiology, psychology and ecology*. Psychological Press, Tylor & Francis Group, 4th edition, 2003.

[Brumby2007] D.P. Brumby, D.D. Salvucci, W. Mankowski, and A. Howes. A cognitive constraint model of the effects of portable music-player use on driver performance. In *Proceedings of the Human Factors and Ergonomics Society 51st Annual Meeting (HFES 2007)*, 2007.

[Brumby2009] D.P. Brumby, D.D. Salvucci, and Howes A. Focus on driving: how cognitive constraints shape the adaptation of strategy when dialing while driving. In *CHI 2009 Studying cell phone use*, 2009.

[Burton1945] H.E. Burton. The optics of Euclid. *Journal of the optical society of America*, 35(5):357–372, 1945.

[Caird1992] J.K. Caird and P.A. Hancock. The perception of arrival time for different oncoming vehicle at an intersection. *Ecological Psychology*, 6:83 – 109, 1992.

[Carstengerdes2005] N. Carstengerdes. *Im Rückblick ist alles anders - Experimentelle Untersuchungen zu Distanzschätzungen mit Spiegeln*. PhD thesis, Universität Trier, 2005.

[CoP2006] Response 3 Project. Annexes to the Code of Practice for the Design and Evaluation of ADAS. Technical report, Response 3 a PReVENT Project, 2006.

[Corker1990] K. Corker, N.L. Cramer, and E.H. Henry. Methodology for evaluation of automation impacts on command control c2 systems: Implementation. BBN Report No.7242, Armstrong Laboratory, Logistics Research Division, 1990.

[Cox1958] D.R. Cox. The Regression Analysis of Binary Sequences. *Journal of the Royal Statistical Society. Series B(Methodological)*, 20:215 – 242, 1958.

[Crossman1968] E.R.F.W. Crossman and H. Szostak. Man-machine models for car steering. In *4th NASA University Conference on Manual Control*, pages 171 – 195, 1968. NASA SP-192.

[Cutting1995] J.E. Cutting and P.M. Vishton. *Handbook of Perception and cognition*, chapter Perceiving layout and knowing distances: the integration, relative potency, and contextual use of different information about depth, pages 69 – 117. San Diego, CA: Academic Press, 1995.

[DESTATIS2015] DESTATIS. Verkehr: Verkehrsunfälle, Fachserie 8, Reihe 7. Technical report, Statistisches Bundesamt, 2015.

[Donges1978] E. Donges. A two-level model of driver steering behavior. *Human Factors*, 20(6):691–707, December 1978.

[EC2003] EC. Directive 2003/97/eg of the European Parliament and of the Council. Technical report, European Commission, 2003.

[Eilers2010] M. Eilers and C. Möbus. Learning of a Bayesian Autonomous Driver Mixture-of-Behaviors (BAD-MoB) Model. In *1st International Conference on Digital Human Modeling*, 2010.

[Eilers2011] M. Eilers and C. Möbus. Learning the human longitudinal control behavior with a modular hierarchical bayesian mixture-of-behaviors model. In *IEEE Intelligent Vehicle Symposium*, 2011.

[Eilers2014] M. Eilers and C. Möbus. Discriminative Learning of Relevant Percepts for a Bayesian Autonomous Driver Model. In *Proceedings of the Sixth International Conference on Advanced Cognitive Technologies and Applications, COGNITIVE 2014*, pages 19–25, 2014.

[Emmert1881] E. Emmert. Größenverhältnisse der Nachbilder. *Klinische Monatsblätter für Augenheilkunde und für augenärztliche Fortbildung*, 19:443–450, 1881.

[Endsley1995] M.R. Endsley. Toward a theory of situation awareness in dynamic systems. *Human Factors*, 37(1):32 – 64, 1995.

[Epstein1961] W. Epstein, J. Park, and Casey A. The current status of the size-distance hypthesis. *Psychological Bulletin*, 58:491 – 514, 1961.

[Feyen2002] R.G. Feyen. *Modeling human performance using the queuing network-model human processor (qn-mhp)*. PhD thesis, University of Michigan, Ann Arbor, 2002.

[Fincham1945] W.H.A. Fincham and M. H. Freeman. *Optics*. Hatton Press Ltd, 1945.

[Fischer2008] R. Fischer, T. Butz, M. Ehmann, and M. Irmscher. Fahrermodellierung für Fahrdynamik und Verbrauchsberechnungen. In *Fortschrittsbericht des VDI*, volume 22 of *Berliner Fachtagung Fahrermodellierung*, 2008.

[Fischer2011] R. Fischer, T. Butz, M. Ehmann, and M. Vockenhuber. Fahrermodell zur virtuellen Regelsystementwicklung. *ATZ*, 12:4, 2011.

[Flannagan1996] M.J. Flannagan, M. Sivak, and E.C. Traube. Driver perceptual adaptation to nonplanar rearview mirrors. Technical Report UMTRI-96-4, University of Michigan, Transportation Research Institute, 1996.

[Flannagan1997] M.J. Flannagan, M. Sivak, J. Schumann, S. Kojima, and E.C. Traube. Distance perception in driver-side and passenger-side convex rearview mirrors: objects in mirror are more complicated than they appear. Technical Report UMTRI-97-32, University of Michigan, Transportation Research Institute, 1997.

[Flannagan1998] M.J. Flannagan, M. Sivak, S. Kojima, and E.C. Traube. A field study of distance perception with large-radius convex rearview mirrors. *SAE Technical Paper Series*, 980916:8, 1998.

[Flannagan2003] M.J. Flannagan. Distance perception with a camera-based rear vision system in actual driving. In *Third International Driving Symposium on Humand Factors in Driving Assessment, Training and Vehicle Design*, pages 58 – 65, 2003.

[Fuller1984] R. Fuller. A conceptualization of driver behavior as thread avoidance. *Ergonomics*, 27:1139 – 1155, 1984.

[Fuller2010] H.J.A. Fuller. *The virtual driver: integrating physical and cognitive human models to simulate driving with a secondary in-vehicle task*. PhD thesis, University of Michigan, 2010.

[Gilinsky1951] S. Gilinsky, A. Perceived size and distance in visual space. *Psychological Review*, 58:460–482, 1951.

[Girden1992] E.R. Girden. Anova: Repeated measures. *Sage University Paper Series. Quantitative applications in the social science*, 07(84), 1992.

[Gogel1964] W.C. Gogel. Size cues and the adjacency principle. Technical report, FAA Medical Service, Civil Aeromedical Research Institute, Oklahoma City, 1964.

[Gogel1997] W.C. Gogel and Eby D.W. Measures of perceived linear size, sagittal motion and visual angle from optical expansions and contractions. *Perception & Psychophysics*, 59:783 – 806, 1997.

[Goldstein1997] E.B. Goldstein. *Wahrnehmungspsychologie. Eine Einführung*. Spektrum Akademischer Verlag, 1997.

[Gray1998] R. Gray and D. Regan. Accuracy of estimating time to collision using binocular and monocular information. *Vision Research*, 38:499 – 512, 1998.

[Gray1999] Rob. Gray and D. Regan. Do monocular time-to-collision estimates necessarily involve perceived distance. *Perception*, 28:1257 – 1264, 1999.

[Gray2005] R. Gray and D. Regan. Perceptual processes used by drivers during overtaking in a driving simulator. *Human Factors*, 47:394 – 417, 2005.

[Groeger1988] J.A. Groeger and I.D. Brown. *Vision in vvehicle - II*, chapter Motion perception is not direct with indirect viewing systems, pages 27 – 34. Gale, A.G. and Freeman, M.H. and Haslegrave, C.M. and Smith, P. and Taylor S.P., 1988.

[Gunzelmann2011] G. Gunzelmann, L.R. Moore Jr., D.D. Salvuccci, and K.A. Gluck. Sleep loss and driver performance: quantitative predictions with zero free parameters. *Cognitive Systems Research*, 12:154 – 163, 2011.

[Hecht2004] H. Hecht and G.J.P Savelsbergh, editors. *Time-to-contact*. Elsevier Science, 2004.

[Hoffmann1994] E. R. Hoffmann and R.G. Mortimer. Drivers' estimates of time to collision. *Accident Analysis and Prevention*, 26(4):511–520, 1994.

[Holway1941] A.H. Holway and Boring E.G. Determinants of apparent visual size with distance variant. *The American Journal of Psychology*, 54(1):21 – 37, 1941.

[IPG2010] IPG. *IPGDriver User Manual*. IPG Automotive GmbH, 6.1 edition, 2010.

[Juergensohn1997] T. Jürgensohn. *Hybride Fahrermodelle*, volume Band 4 of *ZMMS Spektrum*. Pro Universitate Verlag, 1997.

[Kaufman2006] L. Kaufman, R. Kaufman, J.H. andNoble, S. Edlund, S. Bai, and T. King. Perceptual distance and the constancy of size and stereoscopic depth. *Spatial Vision*, 19:439 – 457, 2006.

[Kesting2007] A. Kesting, M. Treiber, and D. Helbing. Mobil: General lane-changing model for car-following models. *Transportation Research Record*, 1999:86 – 94, 2007.

[Kilpatrick1953] F.P. Kilpatrick and W.H. Ittelson. The size-distance invariance hypothesis. *Psychological Review*, 60:223–231, 1953.

[Krylov1930] N.M. Krylov and N. Bogoliubov. *Introduction to Nonlinear Mechanics*. Princeton University Press, US, 1930.

[Laird2012] J.E. Laird. The Soar Cognitive Architecture. *AISB Quarterly*, 134:1 – 4, 2012.

[Laird2015] J.E. Laird and C.B. Congdon. The Soar User's Manual. Technical report, University of Michigan: Computer Science and Engineering Department, 2015.

[Land1994] M.F. Land and D.N. Lee. Where we look when we steer. *Nature Science*, 369:742 – 744, 1994.

[Langley2009] P. Langley, J.E. Laird, and S. Rogers. Cognitive architectures: Research issues and challenges. *Cognitive Systems Research*, 10:141–160, 2009.

[Lee1976] D.N. Lee. A theory of visual control of braking based on information about time-to-collision. *Perception*, 5:437 – 459, 1976.

[Levison1989] W.H. Levison. *Applications of Human Performance models to system design*, chapter The Optimal Control Model for Manually Controlled Systems, pages 185 – 198. Springer US, 1989.

[Levison1995] W.H. Levison and N.L. Cramer. Description of the integrated driver model. Technical report, Federal Highway Association, Office of Safety and Traffic Operations R & D, 1995.

[Liu1996] Y. Liu. Queueing network modeling of elementary mental processes. *Psychological Review*, 103:116 – 136, 1996.

[Mayne1951] R. Mayne. Some engineering aspects of the mechanism of body cotnrol. *Electrical Engineering*, 70:207 – 212, 1951.

[McKee1992] P.S. McKee and L. Welch. The precision of size constancy. *Vision Research*, 8:1447–1460, 1992.

[McRuer1957] D.T. McRuer and E.S. Krendel. Dynamic response of human operators. Technical report, Wright Air Development Center, OH Air Material Command, 1957.

[McRuer1965] D. McRuer, D. Graham, E. Krendel, and W. Reisener. Human pilot dynamics in compensatory systems. Technical report, U.S. Air Force Research Program AF 33 (616)-7501, 1965.

[McRuer1967] D.T. McRuer and H.R. Jex. A review of quasi-linear pilot models. *IEEE Transaction on humand factors in electronics*, 8:231 – 249, 1967.

[McRuer1969] D. McRuer and D.H. Weir. Theory of manual vehicular control. *IEEE Transaction on Man-Machine Systems*, 10:257 – 291, 1969.

[McRuer1977] D.T. McRuer, R.W. Allen, D.H. Weir, and R.H. Klein. New results in driver steering control models. *Human Factors*, 19:381 – 397, 1977.

[Meyer1999] D.E. Meyer and D.E. Kieras. Precis to a Practical Unified Theory of Cognition and Action: Some Lessons from EPIC Computational Models of Human Multiple-Task Performance. *Attention and Performance*, XVIII:17–88, 1999.

[Meyer2013] L. Meyer and E.-M. Skottke. Wahrnehmungsfehler bei der Abstandsschätzung im Strassenverkehr aufgrund verschiedener Spiegeleinstellungen. *Fahrermodellierung in Wissenschaft und Wirtschaft, 4. Berliner Fachtagung Fahrermodellierung*, 35:96–108, 2013.

[Michaels1963] R.M. Michaels. Perceptual factors in car following. In *Proceedings of the second international symposium on the theory of traffic flow*, pages 44–59, 1963.

[Michon1985] J.A. Michon. *A critical view of driver behavior models: what do we know, what should we do?*, chapter 4, pages 485 – 520. Springer US, 1985.

[Moebus2009] C. Möbus and M. Eilers. Further steps towards driver modeling according to the bayesian programming approach. In *Digital Human Modeling*, 2009.

[Muggeo2008] V.M.R. Muggeo. segmented: An R Package to Fit Regression Models with Broken-Line Relationships. *R-News*, 8:20 – 25, 2008.

[Murray2006] S.O. Murray, H. Boyaci, and D. Kersten. The representation of perceived angular size in human primary visual cortex. *nature neuroscience*, 9:429 – 434, 2006.

[NHTSA2008] NHTSA. Study of Driver Performance / Acceptance Using Aspheric Mirrors in Light Vehicle Applications, Final Report. Technical report, NHTSA, 2008.

[Naeaetaenen1974] R. Näätänen and H. Summala. A model for the role of motivation factors in drivers' decision making. *Accident Analysis Prevention*, 6:243 – 261, 1974.

[Newell1972] A. Newell and H.A. Simon. *Human Problem Solving*. Prentice-Hall, 1972.

[Noguchi1981] K. Noguchi and K. Taya. A Neglected Problem: Kinetic Size Constancy. *Acta Psychologica*, 48:187 – 194, 1981.

[Osterloh2008] J.P. Osterloh and A. Lüdtke. Analyzing the Ergonomics of Aircraft Cockpits using Cognitive Models. In *Proceedings of the 2nd International Conference on Applied Humand Factors and Ergonomic (AHFE)*, 2008.

[Platzer1995] G. Platzer. The geometry of automotive rearview mirrors - why blind zones exist and strategies to overcome them. *Human factors in vehicle design: lighting, seating, and advanced electronics*, 950601:143 – 156, 1995.

[Rasmussen1983] J. Rasmussen. Skills, rules and knowledge; signals, signs and symbols and other distinctions in human performance models. *IEEE Transaction on systems, man, and cybernetics*, 13(3):257 – 266, 1983.

[Regan1986] D. Regan, C.J. Erkelens, and H. Collewijn. Necessary condition for the perception of motion in depth. *Investigative Ophtalmologie & visual science*, 27(4):584 – 597, 1986.

[Regan1993] D. Regan and S.J. Hamstra. Dissociation of Discrimination Thresholds for Time to Contact and for Rate of Angular Expansion. *Vision Research*, 33(4):447 – 462, 1993.

[Regan1995] D. Regan and A. Vincent. Visual Processing of Looming and Time to Contact Throughout the Visual Field. *Vision Research*, 33:1845 – 1857, 1995.

[Riedel1990] A. Riedel. IPG-DRIVER - EIN MODELL DES REALEN FAHRERS FUER DEN EINSATZ IN FAHRDYNAMIK-SIMULATIONSMODELLEN. *Automobil-Industrie*, 35(6):655 – 662, 1990.

[Rock1968] I Rock, A.L. Hill, and M. Fineman. Speed constancy as a function of size constancy. *Perception & Psychophysics*, 4:37 – 40, 1968.

[Salvucci2001] D.D. Salvucci, E.R. Boer, and A. Liu. Toward an integrated model of driver behavior in a cognitive architecture. *Transportation Research Record*, 1779(1779):9 – 16, 2001.

[Salvucci2002] D.D. Salvucci and A. Liu. The time course of a lane change: Driver control and eye-movement behavior. *Transportation Research Part F*, 5:123–132, 2002.

[Salvucci2002a] D.D. Salvucci and K.L. Macuga. Predicting the effects of cellular-phone dialing on driver performance. *Cognitive Systems Research*, 3:95 – 102, 2002.

[Salvucci2005] D.D. Salvucci, M. Zuber, E. Beregovaia, and D. Markley. Distract-R: Rapid prototyping and evaluation of in-vehicle interfaces. In *CHI*, 2005.

[Salvucci2006] D.D. Salvucci. Modeling Driver Behavior in a Cognitive Architecture. *Human Factors*, 48:362 – 380, 2006.

[Salvucci2007] D.D. Salvucci, H.M. Mandalia, N. Kuge, and T. Yamamura. Lane-change detection using a computational driver model. *Human Factors*, 49:532 – 542, 2007.

[Salvucci2008] D.D. Salvucci and J. Beltowska. Effects of memory rehearsal on driver performance: experiment and theoretical account. *Human Factors*, 50:834 – 844, 2008.

[Salvucci2009] D.D. Salvucci. Rapid Prototyping and Evaluation of In-Vehicle Interfaces. *ACM Transactions on Computer-Human Interaction*, 16(9):33, 2009.

[Schick2007] B. Schick, R. Buüttner, K. Baltruschat, and J. Meier. TÜV SÜD Automotive GmbH: Bewertung von Funktion und Güte von Fahrerassistenzsystemen be aktivem Bremseingriff. *ATZ*, 109(5):414–425, May 2007.

[Schick2008] B. Schick, J. Henning, E. Wurster, and B. Klein-Rider. SIMULATION METHODS TO EVALUATE AND VERIFY FUNCTIONS, QUALITY AND SAFETY OF DRIVER ASSISTANCE SYSTEMS IN THE CONTINUOUS MIL, SIL, AND HIL PROCESS. In *3. Taguing Aktive Sicherheit durch Fahrerassistenz*, 2008.

[Schwarzkopf2013] D.S. Schwarzkopf and G. Rees. Subjective size perception depends on central visual cortical magnitication in human v1. *PLOSOne*, 8:12, 2013.

[Simon1959] H.A. Simon. Theories of decision-making in economics and behavioral science. *The American Economic Review*, 49(3):253 – 283, 1959.

[Steenken2011] R. Steenken, F. Lethaus, M. Baumann, and L. Weber. Schätzung der TTC des rückwärtigen Verkehrs beim Einfädeln auf die Autobahn. In K. Bittrich, S. Blankenberger, and J. Lukas, editors, *Beiträge zur 53. Tagung experimentell arbeitender Psychologen*. Lengerich: Pabst Science Publishers, 2011.

[Steenken2014] R Steenken, L. Weber, H. Colonius, and A. Diederich. Designing Driver Assistance Systems with Crossmodal Signals: Multisensory Integration Rules for Saccadic Reaction Times Apply. *PLOSone*, 9:12, 2014.

[Thouless1931] R.H. Thouless. Phenomenal regression to the real object. *Britisch Journal of Psychology*, 21(4):339–359, 1931.

[Toledo2003] T. Toledo. *Integrated Driving Behavior Modeling*. PhD thesis, Massachusetts Institute of Technology, 2003.

[Treiber2002] M. Treiber and D. Helbing. Realistische Mikrosimulation von Strassenverkehr mit einem einfachen Modell. In *Simulationstechnik ASIM 2002*, 2002.

[Tsimhoni2003] O. Tsimhoni and Liu Y. Modeling steering using the queuing network- model human processor (qn-mhp). In *Annual Conference of the Humand Factors and Ergonomics Society*, 2003.

[Ungerleider1982] L.G. Ungerleider and M. Mishkin. *Analysis of visual behavior*, chapter Two cortical visual systems. MIT Press: Cambridge, MA., 1982.

[UnitedNations2011] United Nations. Consolidated resolution on the construction of vehicles (r.e.3) revision 2. Resolution Revision 2, United Nations Economic and Social Council - Economic Commision for Europe, Inland Transport Committee, June 2011.

[Walraven1969] P.L. Walraven and J.A. Michon. The influence of some side mirror parameters on the decisions of drivers. In *International Automotive Engineering Congress, Detroit Mich.*, 1969.

[Weber2013] L. Weber, R. Steenken, and A. Lüdtke. Integrated Modeling for Safe Transportation (IMoST2) - Driver Modeling & Simulation. *Fahrermodellierung in Wissenschaft und Wirtschaft, 4. Berliner Fachtagung Fahrermodellierung*, 35:26–40, 2013.

[Weir1973] D.H. Weir and D.T. McRuer. Measurement and interpretation of driver / vehicle system dynamic response. *Human Factors*, 15:367 – 387, 1973.

[Wickens1988] C.D. Wickens and Y. Liu. Codes and modalities in multiple resources: A success and a qualification. *Human Factors*, 30(5):599–616, 1988.

[Wilde1982] G.J.S. Wilde. The theory of risk homeostasis: implications for safety and health. *Risk Analysis*, 2(4):209 – 225, 1982.

[Wist1976] E.R. Wist, H.C. Diener, and J. Dichgans. Motion constancy dependent upon perceived distance and the spatial frequency of the stimulus pattern. *Perception & Psychophysics*, 6:485 – 491, 1976.

[Wu2007] C. Wu and Y. Liu. Queuing Network Modeling of Driver Workload and Performance. *IEEE Transactions on intelligent transportation systems*, 8:528 – 537, 2007.

[Wurster2010] U. Wurster and B. Schick. Substantial progress of virtual driver skills in interaction with advanced control systems to meet the new challenges of vehicle dynamics simulation. In *AVEC 2010: 10th International Symposium on Advanced Vehicle Control*, 2010.

[Yan2015] Fei Yan, Lars Weber, and Andreas Luedtke. Classifying driver's uncertainty about the distance gap at lane changing for developing trustworthy assistance systems. In *Intelligent Vehicles Symposium (IV), 2015 IEEE*, pages 1276–1281. IEEE, 2015.

[Zhao2013] S. Zhao, D.P Brumby, M. Chignell, D.D. Salvucci, and S. Goyal. Shared input multimodal mobile interfaces: interaction modality effects on menu selection in single-task and dual-task environments. *Interacting with computers*, 25(15):386–403, 2013.

[deVos2000] A.P. deVos. Non-planar driver's side rearview mirrors: a survey of mirrory types and european driver experience and a driver behavior study on the influence of experience and driver age on gap acceptance and vehicle detection. Technical Report DOT HS 809 149, NHTSA, 2000.